THE DESIGN AND SYNTHESIS OF RUBBER TOUGHENED THERMOPLASTICS

Michael Morris B.Sc.

This Thesis is submitted in partial fulfilment of the requirements for the Degree of PhD of the Council for National Academic Awards.

The collaborating establishment was :-

I.C.I. plc. (Plastics and Petrochemicals Division),

Wilton Centre, Wilton, Middlesbrough, TS6 8JE.

Department of Metals and Materials Engineering,

Sheffield City Polytechnic,

Pond Street,

Sheffield, S1 1WB.

February 1988

THE DESIGN AND SYNTHESIS OF RUBBER TOUGHENED THERMOPLASTICS

Michael Morris B.Sc.

This thesis is based upon an investigation carried out mainly at Sheffield City Polytechnic, but also in part at I.C.I. plc. (Plastics and Petrochemicals Division), Wilton, during the period October 1981 to September 1984, under the supervision of Dr. D.W. Clegg and Dr. A.A. Collyer of Sheffield City Polytechnic and Dr. M.K. Cox and Dr. D.G. Parker of I.C.I. (Wilton).

The thesis is submitted to the Council for National Academic Awards in partial fulfilment of the requirements for the Degree of Doctor of Philosophy, in February 1988. The collaborating establishment in the work reported was I.C.I. plc. (Plastics and Petrochemicals Division), Wilton.

The candidate has not, during the period of registration for the CNAA degree of PhD, been a registered candidate for any other CNAA award or for any University degree.

The results presented in the thesis are, to the best of my knowledge, original except where reference and acknowledgement has been made to other authors. No part of this thesis has been submitted for a degree at any other University or College.

As part of the course structure a number of additional subjects were studied, these are outlined below.

Sheffield City Polytechnic, M.Sc. in Metallurgical Process Management:-

Module 1:
- Process Metallurgy
- Mechanical Metallurgy
- Applied Thermodynamics

Module 2:
- Numerical Methods and Programming
- Economic Analysis
- Financial Control

Module 3: Advanced Studies
- High Strength Alloys
- Metals and Competitive Materials
- Stainless Steels
- Heat Treatment and Transformations
- Quality Assurance
- Refractories

Module 4: Case Studies
- i) Materials Selection for Submersibles.
- ii) An assessment of the energy savings attainable on using Ceramic Fibre insulation in Heat Treatment Furnaces.
- iii) Investment in machinery for the recycling of I.C.I. APC-2 composite material - An Economic Assessment (see Appendix 1).

The study programme was subject to assessment: this involved an open book examination of Module 1, a case-study examination and continuous assessment of other parts of the course.

In addition the candidate presented a paper entitled 'The Impact Modification of Polyethersulphone' at a conference on Polyethersulphone held at the Department of Materials and Energy Science, Coventry (Lanchester) Polytechnic, on 18th July 1983.

The candidate has also co-authored two papers containing results from this study these are:-

1) 'Rheology of Poly(ethersulphone)/Poly(dimethylsiloxane) Blends', Collyer, A.A., Clegg, D.W., France, G.H., Morris, M., Blake, K., Groves, D.J., Cox, M.K.; IXth Int. Congress Rheol., Acapulco, Oct. 8-13, 1984, 3, 543-550, Elsevier Applied Science (1985) (see Appendix 2).

2) 'The Rheological Behaviour of Engineering Thermoplastics and Silicone Rubber Blends', France, G.H., Collyer, A.A., Blackmore, D.L., Blake, K., Clegg, D.W., Morris, M., Groves, D.J., Bootsma, J.P.C., Kampschreur, J.H.; Proc. Xth Int. Congress Rheol., 1988, Sydney, Aug. 14-19 (see Appendix 3).

THE DESIGN AND SYNTHESIS OF RUBBER TOUGHENED THERMOPLASTICS

M. Morris, Dept. of Metals and Materials Engineering,
Sheffield City Polytechnic.

ABSTRACT

Objective.

To produce an impact toughened grade of 'Victrex' Polyethersulphone by blending with $(A\text{-}B)_n$ type Polyethersulphone/ Poly(dimethylsiloxane) [P.E.S./P.D.M.S.] block copolymers.

Progress.

A number of novel $(A\text{-}B)_n$ type P.E.S./P.D.M.S. block copolymers of varying block molecular weights have been synthesised and characterised.

These have been melt blended with pure 4800P grade P.E.S. to yield a series of 'impact modified' P.E.S./P.E.S.-co-P.D.M.S. blends.

Standard Izod and Tensile test pieces have been injection moulded from these blends, and these test pieces used in a study of the physical, chemical and mechanical properties of the blends.

The melt shear viscosity of P.E.S. has been found to be substantially reduced by the presence of P.E.S./P.D.M.S. copolymers. This is believed due, at least in part, to the migration of the P.D.M.S. bearing copolymer to the surface of the blend during processing.

Improvements in sharp notch impact strength of up to 43% have been observed in P.E.S./P.E.S.-co-P.D.M.S. blends containing as little as 2.5% copolymerised P.D.M.S. These improvements have been achieved at the expense of more modest reductions (no more than 24%) in tensile strengths.

Examination of impact fracture surfaces has revealed that the copolymers promote localised plastic deformation in sharply notched P.E.S., the copolymer particles themselves undergoing cavitation during crack propagation.

It has also been shown, however, that the copolymers suppress the gross plastic deformation usually observed in unnotched or bluntly notched P.E.S. The additive particles promote crack initiation in such specimens, and although they also facilitate localised plastic deformation, the overall result is usually a decrease in P.E.S. impact strength.

Significantly, blends containing P.E.S. and P.E.S./P.D.M.S. copolymers do not appear to perform any better under impact than simple physical blends of P.E.S. and linear P.D.M.S. This is believed to be due to migration of the P.D.M.S. domains to the surface of the P.E.S./P.D.M.S. copolymers. Once at the surface, they inhibit the formation of the desired adhesive bond between the P.E.S. matrix and the P.E.S. domains in the copolymer.

The presence of the copolymers does not appear to have any significant effect on the mechanical performance of P.E.S. as tested after immersion in a range of organic and inorganic reagents at room temperature.

ACKNOWLEDGEMENTS

The author wishes to thank Dr. D.W. Clegg and Dr. A.A. Collyer for their advice and guidance during the period of this work.

He is also indebted to all the members of the Department of Metals and Materials Engineering, Sheffield City Polytechnic, associated with the project, and in particular to Miss M. Watson for her patient assistance during the Electron Microscopy investigations.

The author wishes also to thank the staff at I.C.I. Plastics and Petrochemicals Division, Wilton, and in particular Dr. M.K. Cox and Dr. D.G. Parker for their technical and material support.

CONTENTS

1. INTRODUCTION AND AIMS OF THE INVESTIGATION.

Poly(oxy-1,4-phenylenesulphonyl-1,4-phenylene), repeat unit $(-O-C_6H_4-SO_2-C_6H_4-)_n$ is marketed commercially by Imperial Chemical Industries p.l.c. under the trade name 'Victrex' PES. It is a high temperature engineering thermoplastic, and is available in four unfilled injection mouldable grades, 3600P, 4100P, 4800P and 5200P, all of which possess good thermal stability and dimensional stability at high temperatures.

'Victrex' PES exhibits good resistance to X-rays, beta-rays, and gamma-rays along with good electrical properties and low flammability. It is, however, degraded by ultraviolet light. Furthermore, although tough, 'Victrex' PES is notch sensitive, exhibiting brittle fracture behaviour when a sharp notch is present.

The problem of U.V. degradation is, to some extent, overcome by the use of pigments such as carbon black where outdoor applications are required.

The problem of poor notched impact strength, however, is one which has yet to be satisfactorily overcome, and one which inhibits 'Victrex' PES from making further inroads into important markets e.g. the aerospace industry. Here a demand exists for a toughened grade which also possesses the excellent thermal stability and low toxic gas and smoke emission properties of pure 'Victrex' PES.

The investigation undertaken here explores methods of producing such an impact resistant grade of poly(oxy-1,4-phenylenesulphonyl-1,4-phenylene) (referred to hereafter as polyethersulphone or P.E.S.) without sacrificing its

high temperature mechanical properties, chemical stability, solvent resistance or processability.

It has already been demonstrated that the impact strength of sulphone polymers may be improved by the incorporation of additional groups into the polymer backbone (1). It is, however, extremely likely that significant and undesirable changes in other properties would result from such modification.

Initial work involving the addition of impact modifiers such as polyethylene (2), polysiloxane (2,3) and fluoropolymer (3) rubbers to a P.E.S. matrix has also resulted in an improvement in impact strength. Problems have been encountered with this route however, the poor adhesion of modifier particles to the matrix resulting in delamination of mouldings at additive levels >3%.

Another impact modification route available to the technologist is that of introducing to the matrix an additive in which the impact modifier is chemically bonded to some agent which, in turn, is 'compatible' with the matrix. By doing this it should be possible to greatly improve the dispersity of, and adhesion between the modifier and the matrix itself, thus resulting in a superior product. It is a detailed examination of this particular type of system that forms the basis of this study.

Well characterised oligomers have been used to synthesise a series of novel alternating block copolymers containing P.E.S. and a rubber phase.

These copolymers have been thoroughly characterised prior to being blended with pure 4800P P.E.S. to yield 'impact modified' P.E.S. grades.

A detailed examination of the properties of these blends has been performed, with particular attention being paid to understanding the toughening mechanisms operating in the modification procedure. Theories relating to the procedure have also been reviewed and developed.

2. LITERATURE REVIEW.

2.1 BLENDING AS A ROUTE TO THE IMPACT MODIFICATION OF POLYMERS.

With the cost of research and development into new polymers becoming prohibitively high, attention has now turned to modifying existing commercial polymers in order that they may fulfil set requirements. Thus the concept of physically blending two or more existing polymers to obtain new products is now attracting widespread interest and commercial application.

Many of the commercially available thermoplastics lack toughness to such an extent as to exclude them from many applications. However, it has been found that this deficiency can be eliminated by blending these glassy polymers with small amounts of suitable rubbery polymers.

2.1.1 Toughening Mechanisms.

Various theories have been proposed to explain the toughening of polymers with rubber particles including energy absorption by rubber (4,5), stress relief by cavitation around rubber particles (6), crack branching induced by rubber particles (7), crack termination at rubber particles (8), matrix crazing (8-15), shear yielding (16-21) and combined crazing and yielding (8,9,13). These theories have been formulated mainly using inferential evidence obtained by optical and electron microscopy, or by volumetric strain measurements.

It is fair to say that none of these theories can be considered as adequate in providing a total theory of rubber toughening. Indeed, the relative role of each mechanism can be expected to vary with the particular system and test conditions

under investigation. For instance, Kinloch et al (22) could find no evidence for the presence of crazing on examining epoxy resin modified with a carbonyl-terminated random copolymer of butadiene and acrylonitrile. They proposed a toughening mechanism in which the deformation processes were (a) localised cavitation in the rubber, or at the particle/matrix interface, and (b) plastic shear yielding in the epoxy matrix; the latter being the main source of energy dissipation.

Petrich (23) too, after studying P.V.C. modified with methacrylate-butadiene-styrene copolymer, concluded that crazing could not be involved in the reinforcing mechanism and that in these systems the rubber particles lower the yield stress, facilitating cold drawing and thereby increasing energy absorption as manifested by enhanced impact resistance.

Recent work by Wu (24) on rubber - toughened nylon attempts to examine toughening mechanisms quantitively. He analysed the impact fracture mechanisms of rubber toughened nylon by measuring the energy dissipated in several different processes during notched fracture. In this way he established an energy balance for the impact fracture. The stress whitened zone was shown to be the energy dissipation zone, and he found that 25% of the impact energy was dissipated by matrix crazing while the remaining 75% was dissipated as heat by matrix yielding.

A certain amount of information on the fracture behaviour of P.E.S. is available. Hine and co-workers (25) studied unmodified P.E.S. using fracture toughness measurements and optical examination. They proposed a mixed mode fracture model in which

the total strain energy release rate contains a plane strain term from crazing and a plane stress term from shear lip formation.

2.1.2 Structure-Property Relationships.

It is well known that the size of the included rubbery particles influences greatly the efficiency of impact modification and there is a minimum particle size below which no significant toughening occurs (26).

Attempts to understand the role of the rubber particles and why an optimum size exists have focussed primarily on their ability to initiate crazes and/or shear bands (8, 11-13, 27, 28).

It has been suggested (13) that in high impact polystyrene (H.I.P.S.) the smallest particles (<1μm) are able to nucleate crazes readily but are not effective at terminating them. Thus poor termination efficiency is supposed to lead to long crazes which fail at relatively low strains.

It has been pointed out recently, however, that this explanation is based on two assumptions whose validity must be questioned (29). Firstly, if a rubber particle acts as a stress concentrator to initiate crazes it cannot also be a craze terminator, and secondly, the model assumes that a large craze is a weak craze. It has been demonstrated that this is not the case, at least for those polymers in which crazes thicken by surface drawing (30). Growth studies with an optical microsceope have shown little indication that crazes are terminated by rubber particles of any size in this system (31), and it appears that an alternative explanation of the low contribution to toughness of small particles in H.I.P.S. is necessary. The observation that

solid rubber particles in H.I.P.S. are less able to accommodate large deformation without voids forming at the craze-rubber interface than particles containing a large number of sub-inclusions (32), suggests that the particle-size effect may be at least partially due to the different internal structure of particles.

One point which does emerge from the literature is that critical particle sizes, below which rubber toughening ceases to be effective, are not the same for all systems. The best available estimates are 0.8 μm for H.I.P.S., 0.4 μm for A.B.S., and 0.2 μm for toughened P.V.C. These results, which are further supported by the experiments performed by Bucknall et al on H.I.P.S./P.S./P.P.O. blends (13) indicate that the critical particle size for toughening decreases with increasing ductility of the matrix polymer.

One explanation of this phenomenon is that in relatively ductile polymers craze growth is inhibited by shear yielding, the rubber particles being too small to control crazing directly, but large enough to control it indirectly by initiating shear bands.

Apart from particle size, the number of rubber particles present is also important since this determines the number of potential sites available for energy dissipation on impact. This is affected by both the level of rubber added and the degree of dispersion.

The rubber-matrix adhesion is also crucial in the impact modification of plastics. If the rubber is not well bound to the matrix, any crazes formed may not be effectively terminated and

the propagation of a catastrophic crack through the sample becomes a probability (33). In addition, a poorly bound rubber particle can be deformed readily during processing forming a lamellar structure which delaminates on injection moulding and impact testing. This can usually be prevented by increasing the stability of the particles by grafting and crosslinking (34).

In a recent study, Wu (35) stressed that rubber particle size and rubber-matrix adhesion are inter-related i.e. changing one will change the other.

He studied the effects of rubber particle size and rubber-matrix adhesion on the notched impact toughness of nylon-rubber blends. A sharp tough brittle transition was found to occur at a critical particle size when the rubber volume fraction and rubber-matrix adhesion were held constant. The critical particle size was found to increase with increasing rubber volume fraction according to the equation:-

$$d_c = T_c \left[(\pi/6\Phi_r)^{\frac{1}{3}} - 1\right]^{-1}$$

where d_c is the critical particle diameter

T_c is the critical interparticle distance

Φ_r is the rubber volume fraction

The critical interparticle distance is a material property of the matrix, independent of rubber volume fraction and particle size. Thus the general condition for toughening is that the interparticle distance must be smaller than the critical value.

Wu suggests that this toughening criterion should be valid for all polymer blends which are toughened by increased shear yielding of the matrix.

2.1.3 Thermodynamic considerations in Polymer-Polymer Miscibility.

In a few instances the blending procedure results in the formation of a 'compatible' single phase blend, but generally the formation of a two-phase system of rubbery particles in a rigid matrix is observed. The formation of this two-phase system is crucial to the rubber toughening of polymers and some insight into which systems are likely to display this phenomenon is required.

Miscible mixtures will occur whenever the free energy of mixing is negative as given by:-

$$\Delta G_{mix} = \Delta H_{mix} - T\Delta S_{mix}$$

Scott (36) when applying the Flory-Huggins equation to mixtures of dissimilar polymers 1 and 2 obtained the following expressions for the enthalpy and entropy of mixing:-

$$\Delta H_{mix} = BV\phi_1\phi_2$$

and

$$\Delta S_{mix} = \left(-\frac{RV}{Vr}\left(\frac{\phi_1 \ln\phi_1}{X_1} + \frac{\phi_2 \ln\phi_2}{X_2}\right)\right)$$

where Vr is the volume per monomer repeat unit.

V is the volume of the system.

X_i is the degree of polymerisation of species i.

ϕ_i is the volume fraction of i in the binary.

B is the interaction energy density characteristic of the polymer-polymer segmental interactions in the blend.

These equations clearly show that ΔS_{mix} is a function of molecular size and tends toward zero with increasing molecular weight. On the other hand ΔH_{mix} depends primarily on the energy

change associated with changes in nearest neighbour contacts during mixing (37) and is much less dependent on molecular lengths. It can be seen therefore that ΔG_{mix} is primarily influenced by the sign and magnitude of ΔH_{mix} for high molecular weight mixtures.

For weakly interacting materials ΔH_{mix} is predicted to be positive and dependent on the difference in pure component solubility parameters, δ_i (38) via the equation:-

$$\Delta H_{mix} = V(\delta_1 - \delta_2)^2$$

This relationship between $(\delta_1-\delta_2)^2$ and ΔH_{mix} has been used to predict whether a specific rubber would be a good toughening additive for a specific brittle polymer.

It has already been stated that two prime requirements for good rubber toughening are the formation of two phases and good adhesion between phases. Stehling et al (39) attempted to place these two requirements on a more quantitative basis. They observed that phase separation would only occur if the absolute value $|\delta_1-\delta_2|$ is sufficiently large. Following Krause (40) and assuming a molecular weight of 10^5 for each component, they calculated that the critical value of the solubility parameter difference $|\delta_1-\delta_2|_{cr}$ which must be exceeded for phase separation to occur is 0.4 $(J/cm^3)^{0.5}$ for rubber contents of 5-10% at 25°C.

They considered adhesion between polymer pairs with the aid of Helfand's theory for the thickness of the interface between two polymer phases (41). This theory states that the interfacial thickness increases as $|\delta_1-\delta_2|$ decreases.

Stehling et al introduced the hypothesis that good adhesion requires physical entanglement between the two kinds of molecules in the interface. Taking the number of chain bonds between entanglement points (42) to be typically 500, a bond distance of 0.15nm, and assuming freely jointed bonds they calculated the root-mean-square distance between entanglements to be $0.15 \times 500^{0.5}$ nm i.e. 3.3nm. This approach leads to the conclusion that the interfacial thickness should be greater than 3nm for good adhesion. This requires that $|\delta_1 - \delta_2| < \sim 0.8$ $(J/cm^3)^{0.5}$.

Experimental results on P.V.C. toughened with poly(butadiene -co-acrylonitrile), ethylene-propylene copolymers and poly(styrene-co-butadiene) were found to be in satisfactory agreement with the predictions of this model.

Thermodynamics does not limit us to systems which mix endothermically however; if the heat of mixing is exothermic then the above-mentioned restrictions to polymer-polymer miscibility no longer apply since the negative contributions to ΔG_{mix} are not restricted to the rather small help to be expected from a positive combinatorial ΔS_{mix} .

Since enthalpic interactions result from short-range forces between adjacent centres, a reasonable test of the necessity of exothermic interactions for the formation of miscible blends would be to compare the observed miscibility of the polymer pairs with the calorimetrically observed heats of mixing of their low molecular weight analogues. Work carried out by Cruz (43) seems to support this contention.

Important studies related to polymer-polymer solubility such as the two-component solubility parameter approach by Shaw (44), the adaptation of Flory's equation of state thermodynamics by McMaster (45) and the solvent probe techniques discussed by Kwei (46) and Olabisi (47) are considered major advances.

A number of techniques have been introduced which hopefully will provide additional insight into the polymer-polymer interactions that lead to blend miscibility. These include pulsed nuclear magnetic resonance (46), small angle neutron scattering (48, 49), nonradiative energy transfer (50) and excimer fluorescence (51).

2.1.4 The Polymer-Polymer Interface and Compatibilisation Concepts.

As has been stated previously, immiscibility is generally the result when polymers are physically mixed. Good mixing, however, is dependent on the magnitude of the interfacial tension between the two components, and in the solid state, good mechanical behaviour necessitates adhesion at the interface for efficient transfer of stress between the component phases. Wu (52) has recently reviewed this area but as yet not enough is known about the polymer-polymer interface. More often than not polymers do not adhere to each other well and poor mechanical properties e.g. tensile strength, elongation and impact strength are the result.

Often there are reasons for blending two polymers even though the two do not adhere adequately and thus methods for improving this situation are of great interest.

Probably the best approach to improving adhesion is to employ an additive within the blend. Thus the development of 'compatibilisers' has increased in importance over recent years (53). Suitably chosen chemically bonded hybrids e.g. block and graft copolymers are ideal for this application. These copolymers can act as interfacial agents between two immiscible phases as illustrated below.

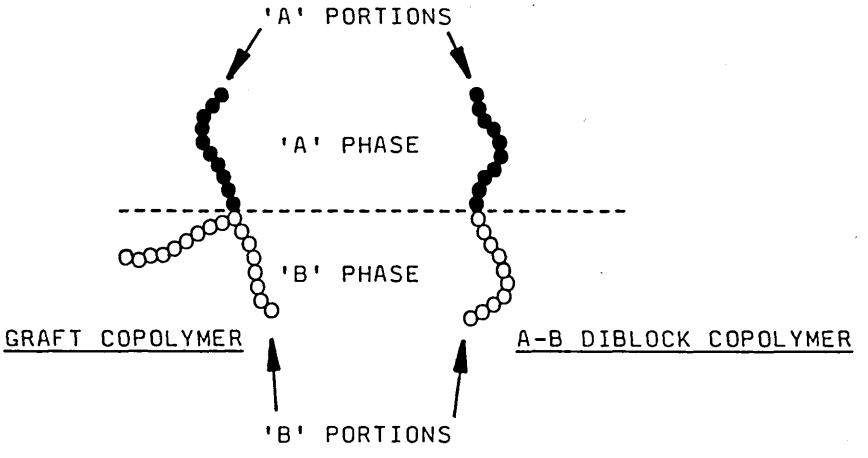

This is similar to the solubilising effect of detergents for oil and water phases. The physical affinity of the 'A' portion of the copolymer for the 'A' phase and the 'B' portion of the copolymer for the 'B' phase serves to locate the copolymer at the interface and connect physically the two phases through the covalent bonds in the copolymer backbone. The net result of this improved adhesion is often a great improvement in the ultimate mechanical properties, elongation and tensile strength and a finer dispersion of the minor component.

Conformational restraints are important in this system and because of this a block copolymer would be expected to be superior to a graft copolymer for this purpose (54). A graft with multiple branches would restrict the opportunities for the backbone to penetrate its homopolymer phase. For the same reason A-B diblock copolymers should be more effective than A-B-A triblocks (54).

For the block or graft copolymer to locate at the blend interface it should have the propensity to segregate into two phases. This tendency depends on the interactions between the two segments and on their molecular weights. The theories relating to the polymer-polymer interface and microphase separation in copolymers will be considered later.

A further requirement for the effective compatibilisation of a polymer blend by a block or graft copolymer is that the block or graft should not be miscible as a whole molecule in one of the homopolymer phases. This tendency also depends on segmental interactions and molecular weights.

An example of the compatibilising effect of copolymers in blends of corresponding homopolymers is provided by the work of Del Giudice et al (55).

They obtained a high molecular weight polymer mixture from a sequential Ziegler-Natta polymerisation of styrene and propylene. After removing unwanted homopolymers from the reaction product, the resultant diblock copolymer of isotactic polystyrene and isotactic polypropylene was incorporated into blends of isotactic polystyrene and isotactic polypropylene. At low copolymer concentrations the diblock functioned as a dispersing agent, significantly reducing the size of domains in the heterogenous blends. At higher copolymer concentrations a dramatic improvement in the adhesion across the domain boundaries was also observed. This resulted in the attainment of enhanced mechanical properties.

Commercially, extensive use is made of copolymers as interfacial agents in the impact modification of polymers; for instance, the impact modification of polystyrene is achieved by producing a reactor-generated blend with a diene rubber. In this instance, rubber is dissolved in the styrene monomer which is subsequently polymerised. It has been shown that chain transfer processes accompany polymerisation and result in a certain amount of graft polymer formation simultaneous with polystyrene homopolymer. This graft is believed to play an interfacial role in the blend to provide the necessary adhesion between phase domains (53).

P.V.C. is also impact modified by blending with rubbery particles. In this process the two polymers are made separately and subsequently blended. The preformed rubber particles used in this blend usually contain some grafted material at the surface which is believed to act as an interfacial agent.

The above concepts are also employed in the manufacture of compounds in the A.B.S. family. Here the base polymer is typically a glassy copolymer of styrene and acrylonitrile while the dispersed rubbery particles are generally composed of copolymers of butadiene and acrylonitrile. Once again some graft material is generally involved to provide the interfacial adhesion.

2.2 THE ROLE OF COPOLYMERS IN THE IMPACT MODIFICATION OF HOMOPOLYMERS.

It has already been shown that block and graft copolymers can play an important role as 'compatibilisers' in the rubber modification of polymers. Recently, however, increasing attention has been paid to the role that copolymers themselves can play as impact modifiers when blended with homopolymers (56). This blending procedure can, if carefully controlled, produce a fine dispersion of the 'foreign' segment in the homopolymer matrix (an important requirement for good impact modification).

In this section the criteria for the successful application of copolymers as impact modifiers are reviewed and reference is made to specific examples of impact modification achieved via this route.

2.2.1 Theories relating to Phase Separation in Block Copolymers and Blends of Copolymers with Homopolymers.

We have already seen how the blending of two polymers usually results in macrophase separation. In block copolymers, however, incompatible polymers are linked to each other via a covalent bond. This bond inhibits macroscopic phase separation and instead these systems often exhibit separation on a micro-scale.

From a thermodynamic viewpoint, there is a positive surface free energy associated with the interface between A and B domains in block copolymers. This serves as a driving force toward growth of the domains. As a result of the tendency of the block joints to stay in the interfacial region there is a loss of entropy in two ways. One is attributable to the confinement of the joints to the interface. The other has its origin maintaining the virtually constant overall polymer density by the suppression of a vast number of polymer conformations. The equilibrium domain size and shape are a result of the balance of these three free-energy terms.

Much attention has been paid to theories relating to domain formation and the state of the interface in block copolymers with Meier (57-59), Helfand (41, 60-67), Krause (68-70), Leary and Williams (71-73), Soen et al (74) and LeGrand (75) being the principle workers in this area.

Meier, on studying A-B and A-B-A copolymers established the thermodynamic criteria for domain formation and calculated that higher block molecular weights were required for phase separation in a copolymer than in simple homopolymer blends (59).

This theory relies heavily on Flory's interaction parameter (X_{AB}) (37) and hence is somewhat limited to nonpolar polymer systems where only dispersive interactions are important. Further work by Meier (58) allowed a quantitive estimate of the size of the interfacial zone between segments of A and B in an A-B diblock copolymer to be calculated as a fraction of the system volume.

To a first approximation this was estimated to be a function only of the product of the copolymer molecular weight (M) and a measure of the segmental interactions estimated by the solubility parameter difference for the two segment types $|\delta_A - \delta_B|$. When the volume of the interfacial zone between A and B segments of the copolymer is near zero, a sharp interface exists. This requires a high molecular weight or a large segmental repulsion such that the function $M(\delta_A - \delta_B)^2$ is very large. If the interfacial volume fraction is near unity, there will be no segregation into domains. This occurs at very low molecular weights or with very small segmental interactions e.g. when $\delta_A \sim \delta_B$.

The first workers to realise that the interphase between dissimilar segments was diffuse and had a finite thickness were Leary and Williams (71, 72). They calculated the Gibb's free energy of demixing by estimating separately the enthalpic and entropic contributions. The enthalpy of demixing was based on the Scatchard-Hildebrand regular solution theory. For a triblock copolymer A-B-A, it reads:-

$$\Delta H_m = -V_m \Phi_A \Phi_B (\delta_A - \delta_B)^2 + f V_m \overline{\Phi_A' \Phi_B'} (\delta_A - \delta_B)$$

where the first term represents complete demixing and the second term corrects for the presence of a mixed interphase region. $\overline{\phi_A' \phi_B'}$ is the volume averaged product of the volume fractions of A and B in the mixed region. Values of f are dependent on the geometry of the domains (spheres, cylinders or lamellae). V_m is the molar volume and δ_i is the solubility parameter of component i.

The entropic term consists of three contributions:-

$$\Delta S_{total} = \Delta S_1 + \Delta S_A + \Delta S_B$$

ΔS_1 is the entropy change resulting from the requirement that one of the junctions of the A-B blocks must be placed in the mixed region. ΔS_A is associated with the stipulation that one end of the A chain must be in the mixed region and the other in the A region, while ΔS_B is due to the fact that both ends of the B chain in the triblock copolymer must be in the mixed region. By minimising the free energy obtained from these respective contributions, Leary and Williams were able to predict the favoured morphology for triblock copolymers.

The Leary-Williams model for the microphase thermodynamics of triblock A-B-A copolymers has recently been modified to accommodate deviations from homogeneous random-coil configurations in the B chain dimensions as well as those in the A chains and has also been extended to cover the case of diblock A-B copolymers (76).

The more recent papers by Helfand et al (41, 60-67) use a mean field approach to inhomogeneous systems. For a diblock copolymer with a high degree of polymerisation they obtained the following free energy expression (63):-

$$\frac{G}{NkT} = \frac{(2\gamma)}{(kT)}\left(\frac{x_A}{\rho_A} + \frac{x_B}{\rho_B}\right)\left(\frac{1}{d}\right) + \log\left(\frac{d}{2a_j}\right)$$

$$+ 0.141 d^{2.5}\left(\frac{(x_A^{0.5}/b_A\rho_A)^{2.5} + (x_B^{0.5}/b_B\rho_B)^{2.5}}{[(x_A/\rho_A) + (x_B/\rho_B)]^{2.5}}\right) - \frac{\alpha(x_A/\rho_A)(x_B/\rho_B)}{(x_A/\rho_A) + (x_B/\rho_B)}$$

where γ is the interfacial tension

x is the degree of polymerisation

ρ is the density of pure A or B

d is the domain repeat distance

a_j is the width of the interfacial region

α is a measure of the repulsion between A and B blocks

Their predictions of domain sizes as a function of molecular weight agree well with the data of Douy et al. The calculated interfacial thicknesses also compare favourably with S.A.X.S. results by Hashimoto et al (78).

Soen et al (74) treated the problem from the point of view of micelle formation. As the solvent evaporates, a critical micelle concentration is reached, at which the domains are formed and are assumed not to change upon further drying. Minimum free energies for an AB type of block copolymer were computed in this way. At low weight fractions of A (below ~ 0.12) the spherical morphology is favoured. Between 0.12 and 0.38 weight fractions of A rods or cylinders are expected to form. As the equimolar relationship is approached the lamellar morphology is the equilibrium structure.

LeGrand (75) has developed a model to account for domain formation and stability based on the change in free energy which occurs between a random mixture of block polymer and a micellar domain structure. The model also considers contributions to the free energy of the domain morphology resulting from the interfacial boundary between phases and elastic deformation of the domains.

A different approach to determining microphase separation in copolymers, which is strictly thermodynamic and not concerned with morphology, was developed by Krause (68-70). This model predicts that phase separation becomes more difficult as the number of blocks increase in a copolymer molecule of given length. It predicts easier phase separation when the molecular weight of the block copolymer increases at fixed copolymer composition and number of blocks per molecule. Furthermore, phase separation occurs readily for a system having a 1:1 ratio of components (by volume) when the molecular chain length and number of blocks are kept constant. Phase separation is also improved by an increasing Flory-Huggins interaction parameter (X_{AB}) for the copolymer.

Krause's theory is based on the calculation of the critical interaction parameter $(X_{AB})_{cr}$ using the equation:-

$$(X_{AB})_{cr} = \frac{zVr}{(z-2)V_A v_B^c n_A^c} \left\{ -\ln(v_A^c)^{v_A^c}(v_B^c)^{v_B^c} + 2(m-1)\left(\frac{\Delta S_{dis}}{R}\right) - \ln(m-1) \right\}$$

Where Vr = volume of a lattice site

z = co-ordination number of the lattice

v_A^c = vol fraction of monomer A in the copolymer molecule

v_B^c = vol fraction of monomer B in the copolymer molecule

m = number of blocks in each block copolymer molecule

V_A = amorphous volume of a repeat unit of A

n_A^c = number of A units in each copolymer molecule

$\Delta S_{dis}/R$ = disorient^n. entropy change gain on fusion per segment

When this equation is used to make predictions about phase separation in block copolymers it is convenient to let $Vr=V_A=V_B$ and to set a convenient value for z, possibly 6 or 8 & $(\Delta S_{dis}/R)$ possibly 1.0

In order to use the above equation it is necessary to first calculate X_{AB} . This interaction parameter is often calculated from Hildebrand's solubility parameters (38):-

$$X_{AB} = \frac{Vr}{RT}(\delta_A-\delta_B)^2$$

The theory predicts that polymers should not phase separate until $(X_{AB})_{cr} \leqslant X_{AB}$.

A feature of both Meier's and Krause's work is the use of Hildebrand's solubility parameter. Studies conducted by McGrath et al (79) have served to illustrate both the importance of the differential solubility parameter $|\delta_1-\delta_2|$ or Δ and the chemical bond between the segments on the microphase separation in block copolymers.

Theoretical approaches have also been made on more complex inhomogenous multicomponent systems (e.g. blends of homopolymers with copolymers).

Krause (70) developed an equation predicting the conditions necessary for microphase separation in mixtures of block copolymers with one of the corresponding homopolymers:-

$$(\chi_{AB})_{cr} = \frac{zVr}{(z-2)V_B v_A^m n_B^c}\left(-\ln(v_A^m)^{v_A^c}(v_B^m)^{v_B^c} - \frac{N_{HA}}{N_c}\ln v_A^m + 2(m-1)\left(\frac{\Delta S_{dis}}{R}\right) - \ln(m-1)\right)$$

where v_A^m = vol frac of monomer repeat unit A in the total mixture

v_B^m = vol frac of monomer repeat unit B in the total mixture

N_{HA} = number of homopolymer A molecules in the system

N_c = total number of copolymer molecules in the system

This equation was derived using essentially an approach suitable for a one component system, although a mixture of homopolymer with block copolymer is, of course a two component system. This approach is possible because it is assumed that the homopolymer HA does not mix with microphase B after microphase separation i.e. the system is not allowed to act as an ordinary two-component system.

Meier (80) in an extension of his theory concerning microphase separation in block copolymers calculated that only about 5% (w/w) of a homopolymer can be solubilised by a copolymer at equilibrium if they have the same molecular weight. This limited solubility can be attributed to the unfavourable entropy for accommodating both unrestrained and restrained polymer chains in the same domain, in spite of their chemical identity.

More recently Hong and Noolandi (81) developed a theory of inhomogeneous multicomponent systems starting from the functional integral representation of the partition function. This theory can be used to determine the interfacial properties and microdomain structures of a combination of homopolymers, block copolymers, monomers and solvents, and has been used to study the emulsifying effect of block copolymers in immiscible homopolymer blends (82). It has recently been used in the evaluation of the free energy of an inhomogeneous diblock copolymer-homopolymer blend (83).

2.2.2 Morphological considerations in systems containing Block Copolymers.

Five fundamental domain structures are possible for block copolymers consisting of two types of blocks. At compositions with approximately equal proportions of the two components a lamellar structure is favoured. As the proportion of one component increases at the expense of the other, cylindrical morphologies will result with the matrix phase being composed of the component in greater abundance. On increasing the proportion of one component further, the morphology of spherical domains of minor component in a matrix of the other component results. These structures have been observed by Inoue et al (84) in diblock copolymers of isoprene and styrene cast from toluene.

The morphology of a block copolymer can also be modified by changing the casting solvent while keeping the composition of the block copolymer fixed. The work performed by Inoue et al (84) on a 40/60 styrene/isoprene copolymer serves to illustrate the point. The domain structure of the sample cast from toluene was shown to exhibit an alternating lamellar arrangement whilst that cast from methyl ethyl ketone displayed considerable interconnections between the styrene domains. The films cast from cyclohexane, carbon tetrachloride, n-hexane and n-heptane, however, all appeared as polystyrene domains dispersed in a polyisoprene matrix.

These different domain structures are not necessarily equilibrated ones, and can sometimes be changed to the equilibrated ones by thermal treatment (73).

In the case of blends of block copolymers and homopolymers, a more complicated situation arises. Many early studies (85, 86) suggest that homopolymer chains can be considerably solubilised in the domains of the like blocks of the copolymer provided the molecular weight of the former is not larger than that of the latter. Nevertheless, there were some reports (87, 88) concerning the presence of some large supramolecular features with different interior structures from the bulk sample in certain copolymer-homopolymer blends. These features were regarded as 'unusual structures' but no reasonable explanation for their formation was given.

More recently Eastmond et al (89, 90) have presented a series of morphological studies on blends of so-called non-linear block copolymers or AB crosslinked copolymers (ABCP's) with their corresponding homopolymers. In order to explain the formation of the 'unusual structures' which were inevitably found to appear in these blends under suitable combinations of molecular species and processing conditions, they suggested that the homopolymer chains are incompatible with the like blocks of copolymers at equilibrium, and the discrete regions found in the blends are virtually the copolymer-rich phase. The unusual morphologies are formed by a combination of macrophase separation between the homopolymer and the block copolymer and microphase separation in the block copolymer itself. This view is supported by Meier's theoretical calculations (80).

2.2.3 Block vs Graft Copolymer.

In this chapter we have concerned ourselves solely with theories and morphologies associated with block copolymers. Why such emphasis should be placed on these copolymers rather than graft copolymers requires some explanation.

It is important to recognise that a high degree of structural control and integrity is necessary in order to achieve the ultimate properties inherent in microphase separated systems. It is in this respect that block copolymers offer a clear advantage over graft copolymers. Because of the greater reliability and predictability of block copolymer synthetic techniques, it is possible to achieve desired structures more precisely.

This results in much better control of important parameters such as sequence architecture, segment length and spacing, polydispersity and contamination by homopolymer or undesired copolymer architectures. These factors lead to a higher degree of morphological perfection in block copolymers than in graft copolymers, which, in turn, is reflected in superior physical properties.

The degree to which the above structural control is achieved can only be ascertained through the use of effective characterisation tools. The characterisation techniques traditionally used to analyse homopolymers can also be used in elucidating copolymer structures. Although block copolymers can be difficult to characterise because of the inevitable presence of some contaminating homopolymer and also the need to be able to determine the copolymer architecture (e.g. A-B vs A-B-A), graft copolymers present additional obstacles to accurate structural characterisation. These macromolecules are even more complex than block copolymers for several reasons. While the number of segments can be deduced with some certainty from the synthetic route adopted, this is rarely possible with graft copolymers due to the multifunctional nature of the backbone and to the questionable efficiency with which these functionalities participate in the grafting reaction. The length of the graft segments and their polydispersity are also more difficult to determine for the same reasons. An important further complication is the unanswered question of the spacing of the graft junction points along the backbone.

In block copolymers this parameter is more accessible. In A-B and A-B-A block copolymers there are by definition one or two junction points respectively. In $(A-B)_n$ block copolymers the distance between intersegment linkages can be deduced from a knowledge of the block molecular weight.

It may be concluded that although block copolymer synthesis can be more demanding than graft copolymer synthesis, the additional effort is usually more than rewarded by the excellent structural control obtained and the greater ease with which the structure may be characterised.

2.2.4 Architectural Considerations in Block Copolymers.

In the previous section it was ascertained that block copolymers had distinct advantages over graft copolymers as impact modifiers for homopolymers. Because of the expectancy of a superior product resulting from impact modification via block copolymers, future discussion will consider only this particular species of polymer hybrid.

There are three basic architectural forms of block copolymer, A-B, A-B-A, and $(A-B)_n$. The A-B or diblock structure is composed of one segment of 'A' repeat units and one segment of 'B' repeat units. The second form is the triblock structure consisting of a single segment of 'B' repeat units located between two segments of 'A' repeat units. The third basic type is the multiblock containing many alternating 'A' and 'B' blocks.

Mention has already been made of the likelihood of the A-B diblock structure being the most suitable when copolymers are used as compatibilisers in blends of two immiscible homopolymers.

It would be presumptious, however, to expect the A-B structure to also be the peferred copolymer structure when one homopolymer is modified by the simple addition of a copolymer.

While a number of copolymer properties are independent of architecture e.g. thermal transition behaviour, chemical resistance etc., other properties are significantly affected. These include elastomeric behaviour, melt rheology and toughness in rigid materials.

The unique elastomeric behaviour observed only with A-B-A and $(A-B)_n$ block copolymers is responsible for the development of an important technology i.e. thermoplastic elastomers. These are characterised by a combination of features previously considered to be mutually exclusive i.e. thermoplasticity together with rubberlike behaviour.

The key requirement for achieving thermoplastic-elastomeric behaviour is the ability to form a two-phase physical network. In this system there must be a major fraction of a soft block (Tg < room temperature) and a minor fraction of a hard block (Tg > room temperature). The hard blocks associate to form small morphological domains that serve as physical crosslinking and reinforcement sites. These sites are thermally reversible i.e. melt processability is possible at temperatures above the hard block Tg or Tm.

It is important that the volume fraction of the hard block is sufficiently high ($\geq$20%) to provide an adequate level of thermally labile crosslinking for good recovery properties. If the volume fraction of hard material is too high however, the rigid domains may change from spherical, particular regions to an extended form in which elastic recovery is restricted (91). A-B diblock copolymers are incapable of producing network structures since only one end of the soft block is chemically linked to a domain or hard segments.

Because of their ability to form physical network systems, A-B-A and $(A-B)_n$ architectures exert an adverse effect on melt rheology. Depending on specific chemical structure and block length, these networks can even persist in the block copolymer melt. This results in exceptionally high melt viscosities and elasticities. In contrast, A-B architectures, which do not produce network structures, display better melt processability.

Thermoplastic elastomers based on $(A-B)_n$ rather than A-B-A structures could be expected to display enhanced recovery properties due to the presence of a greater number of physical junction sites per polymer chain. For the same reason it could be argued that network disruption due to degradation or to the presence of physical network imperfections should be less extensive for $(A-B)_n$ rather than for A-B-A structures. From a melt rheology viewpoint, consideration should be given to the possibility that $(A-B)_n$ thermoplastic elastomers are more likely to have block molecular weights shorter than their characteristic entanglement molecular weights than their A-B-A counterparts.

Finally, observations indicate that A-B structures develop a coarser morphology than A-B-A structures. Extrapolation of this trend suggests that $(A-B)_n$ copolymers should produce the finest morphology and therefore result in materials with the greatest optical clarity.

2.2.5 Selected Examples of the Impact Modification of Polymer Systems with Block Copolymers.

A number of examples are available in the literature which relate to the impact modification of homopolymers with block copolymers. For instance, considerable interest has been shown in this particular route as a means to improving the impact resistance of polystyrene.

Riess et al (92) studied the ternary system polystyrene-polyisoprene-styrene/isoprene diblock copolymer. They found that they could obtain impact resistant compositions both with binary and ternary blends. Their best results were obtained with a binary blend of polystyrene and a block copolymer of high molecular weight containing about 40% styrene. In order to achieve significant improvements over the homopolymer blends, however, rather large amounts of block copolymer (>25%) were required.

Childers et al (93, 94) blended different styrene-butadiene block copolymers with polystyrene both with and without dicumyl peroxide to crosslink the rubbery domains. Block copolymer structures investigated were SB, SBS, $(SB)_n$ and S:BS (a diblock polymer containing a random copolymer sequence and a pure polystyrene block).

Signficantly, when block copolymers of 25% styrene were blended with polystyrene in a 1:3 ratio a much greater improvement in impact strength was observed than when polybutadiene or a random copolymer of styrene and butadiene were likewise blended with polystyrene. By crosslinking the rubber phase, further increases in impact strength and tensile strength were observed. This was particularly noticeable in the block copolymer blends. In experiments where the styrene block length in the copolymers was reduced from 18,000 to ~9,000 a significant loss in impact strength was observed. This suggests that the styrene blocks chemically bonded to the rubbery domains act as anchors to the polystyrene matrix, performing the role of the grafts in conventional impact polystyrene or A.B.S. In order to perform this function effectively it appears necessary that the polystyrene blocks must be of a certain minimum size.

Further work by Durst et al (95) on similar systems resulted in the formation of excellent compositions without the use of peroxide. Polystyrene was blended in solution with SBS type styrene-butadiene block copolymers of various compositions to give a series of H.I.P.S. polymers all containing 20% by weight of polybutadiene. In a second experiment polybutadiene was also added, again keeping the total polybutadiene concentration at 20%. The results show a number of interesting features. Impact strengths are low when the styrene content of the block copolymer is low. This can be attributed to the interfacial adhesion between the rubber and matrix being poor. Increasing the styrene-butadiene ratio in the block copolymer dramatically increases the impact strength which reaches 500J/m when the ratio is 50:50.

At higher styrene contents, the block copolymer becomes much less effective because the surfactant properties of the block copolymer lead to a reduction in particle size below the critical level for toughening. Addition of polybutadiene to form a ternary blend increases the particle size. In order to obtain high impact strengths in melt-blended mixtures, it is found necessary to use block copolymers of high molecular weight, otherwise the rubber particle size is reduced below 1μm during melt blending and toughness is lost.

The impact strengths obtained by Durst et al in the best of the block copolymer blends were five times higher than those usually obtained in H.I.P.S. although the volume fraction of the rubber phase is comparable with, and sometimes lower than the volume fraction in commercial H.I.P.S.

The compounding of SBS triblock copolymers with graft polymer H.I.P.S. is also interesting. Blends of polystyrene and the thermoplastic rubber show worthwhile impact strength increases only when the elastomer is present at a volume fraction >25%, but when the thermoplastic rubber is added to H.I.P.S. which already has about 25% by volume rubber, the result is a product with superhigh impact strength (96).

Although the major current applications of block copolymers in blends involve styrene-diene polymers, other block copolymers have been found to be useful.

It has been found that impact resistant blends resembling A.B.S. can be produced by melt-blending styrene/acrylonitrile copolymers with rubbery styrene/butadiene/ -caprolactone triblock copolymers and an organic peroxide (97).

Without doubt the most significant work yet performed which bears direct relevance to the aims of this investigation is that performed by Noshay et al (91, 98-111). They reported block copolymers of the $(A\text{-}B)_n$ type containing high molecular weight segments of polysulphone:-

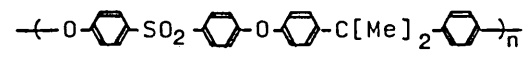

and poly(dimethylsiloxane):-

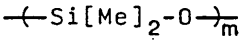

These were synthesised by the interaction of preformed dihydroxyl-terminated polysulphone oligomers and bis(dimethylamine)-terminated poly(dimethylsiloxane) oligomers in chlorobenzene solution.

The block copolymer structures produced were well defined and strictly controlled, the oligomers being mutually reactive. As a result the structures of the segments in the copolymers were essentially identical to those of the oligomer starting materials.

The morphology of these block copolymers can be controlled by varying the molecular weight of the oligomers. At a constant polysulphone $\bar{M}n$ of 4,700, poly(dimethylsiloxane) (P.D.M.S.) oligomers of $\bar{M}n$ 1,700 gave single phase copolymers while $\geq$5,000 $\bar{M}n$ P.D.M.S. oligomers produced two-microphase systems due to domain formation. The latter copolymers displayed two Tg's (one at -120°C due to the P.D.M.S. phase and another at +160°C due to the polysulphone domains.

The extensive phase separation displayed by these systems at such low block $\bar{M}n$ levels is unusual. This phenomenon is considered to be due to the high degree of incompatibility of polysulphone with P.D.M.S. [δ for polysulphone is 21.7 $(J/cm^3)^{0.5}$ and δ for P.D.M.S. is 14.9 $(J/cm^3)^{0.5}$].

Mechanical properties of polysulphone/P.D.M.S. block copolymers vary widely with composition. The copolymers obtained ranged from rigid low elongation materials to flexible, high elongation compositions with thermoplastic elastomer characteristics.

Polysulphone/P.D.M.S. block copolymers containing segments $\geq$5,000 $\bar{M}n$ were found to display astonishingly poor melt processability. Compression moulding gave poor quality films and extrusion at 340°C (180°C above the Tg of the polysulphone phase) produced a powdery extrudate. This behaviour is due to extremely high melt viscosity and extensive melt fracture. This, in turn, is believed to be caused by a significant degree of retention of the physical network structure even in the melt. Improved melt processability was observed in copolymers containing shorter polysulphone segments ($\bar{M}n$ = 2,000), however, this phenomenon, which is probably due to reduced chain entanglement and greater phase blending, results in a 20°C sacrifice in the Tg of the polysulphone phase.

Matzner et al (105) attributed the high degree of physical network retention in the melt to the large difference in the solubility parameters of the polysulphone and P.D.M.S. segments. These workers evaluated the melt processability of a series of organosiloxane block copolymers containing organic segments of varying structure (and therefore varying solubility parameter). They concluded that the differential solubility parameter (Δ) between the segments should be $\leqslant 2$ $(J/cm^3)^{0.5}$ in order to obtain good melt processability.

The polysulphone/P.D.M.S. block copolymers were found to be particularly effective as impact modifiers for polysulphone homopolymers (109, 110). The optimum effect was obtained with copolymers containing 5,000 $\overline{Mn}$ polysulphone and P.D.M.S. blocks at block copolymer concentrations of 5% by weight and with blending conditions that produce a polysulphone/P.D.M.S. maximum particle size of 0.5-3.0μm. Under these conditions good quality injection moulded parts can be produced with notched Izod impact strengths as high as 1174 J/m compared with 69.4 J/m for unmodified polysulphone. Significantly the other properties of polysulphone were found to be affected to only a minor extent by this modification. This unique behaviour is believed to result from two important characteristics of the block copolymer - compatibility and rheology. The borderline compatibility of the block copolymer with the polysulphone matrix, which is due to the presence of the polysulphone segment in the copolymer, results in efficient dispersion and good interphase adhesion.

The unusual rheological behaviour of the copolymer, which prevents it from being melt processable on its own, serves an important beneficial function in the blend i.e. it discourages excessive particle breakdown during shear blending and melt fabrication operations. In this respect, the block copolymer resembles the behaviour of the styrene-diene graft systems formed in situ in impact modified polystyrene systems, with the important exception that it is not crosslinked.

2.3 Selection of Route and Materials for the Impact Modification of Polyethersulphone.

2.3.1 Selection of Route.

In this report a number of routes to the impact modification of polymers have been discussed. Of these, one of the most interesting and effective routes was that adopted by Noshay et al (91, 98-111). They found that by adding as little as 5% of an $(A\text{-}B)_n$ type block copolymer to a polysulphone matrix they could improve the notched impact strength of the matrix twentyfold. Significantly the addition of this low level of copolymer had little effect on the other properties of the polysulphone matrix.

Further investigations into this route were considered necessary in order to gain a more complete understanding of the toughening mechanisms operating. With this in mind, the decision was made that attempts to improve the notched impact strength of polyethersulphone (P.E.S.) should proceed via the blending of a copolymer of P.E.S. and a suitable elastomer with P.E.S. homopolymer.

2.3.2 Selection of Block Copolymer Architecture.

All basic block copolymer architectures (A-B, A-B-A, and $(A-B)_n$) can be expected to yield copolymers which will adhere well to P.E.S. homopolymers provided one of the components is compatible with the P.E.S. homopolymer. This of course can be facilitated by using P.E.S. itself as one of the copolymer constituents.

Only two of the architectures, however, are capable of forming what are termed thermoplastic elastomers. Both A-B-A and $(A-B)_n$ structures can form two-phase physical networks where the hard blocks form small morphological domains that serve as physical crosslinking and reinforcement sites. As a consequence of this there is no requirement for chemical crosslinking of the elastomeric segments in the block copolymer in order for it to be processed by modern rapid thermoplastics processing techniques such as injection moulding.

Copolymers exhibiting thermoplastic elastomeric behaviour are considered to be an important advancement in polymer technology, and because of their interesting properties, the inclusion of such copolymers in this investigation was considered to be desirable.

The expected properties of A-B-A and $(A-B)_n$ structures have been compared critically in an earlier section. In that review it was noted that the $(A-B)_n$ structure was expected to have a number of advantages over the A-B-A structure i.e. enhanced recovery properties, less extensive network disruption, better melt processability and finer morphology.

On the basis of this, the decision was made that the $(A\text{-}B)_n$ copolymer structure would be the one employed in this investigation.

2.3.3 Selection of Elastomer for inclusion in the Copolymer Structure.

The choice of elastomer to be used in the $(A\text{-}B)_n$ block copolymer is severely restricted by the requirements of the system into which it is to be incorporated. Polyethersulphone finds commercial applications because of its excellent high temperature properties. Another important feature of this polymer is its low flammability. In order that these properties be maintained after impact modification, it is necessary that the elastomer employed in the copolymer possesses similar properties.

Probably the most suitable elastomers available with the required properties are those based on the siloxane polymer repeat unit -(Si[RR']-O)-. Indeed poly(dimethylsiloxane) $-(Si[Me]_2\text{-}O)_n-$, apart from possessing excellent high temperature properties, also displays good low temperature characteristics (Tg = -123°C, M.Pt. -55°C). These properties along with its low toxicity and flammability have made P.D.M.S. a popular choice as the elastomer in copolymerisation with thermoplastics.

A number of workers apart from Noshay et al have recognised the desirable attributes of P.D.M.S., and outstanding strength and toughness has been reported in block copolymers of P.D.M.S. with poly(bisphenol-A carbonate) (112), polystyrene (113, 114) and polyα-methylstyrene (115). Block copolymers containing P.D.M.S. have been thoroughly reviewed elsewhere (91).

The simple linear P.D.M.S. homopolymer $-(Si[Me]_2-O)_n-$ was considered to be a suitable elastomer for investigations into copolymerisation with P.E.S. not only because of its above mentioned properties, but also because the large difference in solubility parameters between the two homopolymers [P.E.S. δ = 25.2 $(J/cm^3)^{0.5}$, P.D.M.S. δ = 14.9 $(J/cm^3)^{0.5}$] should ensure microphase separation in the copolymer at very low block molecular weights.

2.4 THE SYNTHESIS AND CHARACTERISATION OF $(A-B)_n$ TYPE COPOLYMERS.

2.4.1 Synthesis Techniques.

The synthetic techniques available for copolymer production are often restricted to a considerable extent by the block copolymer architecture that is desired. Whilst A-B and A-B-A block copolymers are primarily synthesised by anionic living polymerisation techniques, $(A-B)_n$ structures are most often prepared via step growth (condensation) methods. The reason for this is the high probability of premature chain termination (caused by the adventitious impurities encountered during repeated sequential monomer addition cycles) which inhibits the production of well defined $(A-B)_n$ structures via living addition techniques.

Both living addition polymerisation and step growth polymerisation methods have three desirable features. Firstly, the location and concentration of active sites are known. Secondly, homopolymer contamination is minimal. This results from the absence of terminating side reactions in living systems and from stoichiometry control in the step-growth systems. Finally

segment length and placement are controlled. This is accomplished by sequential monomer addition techniques in the living polymerisations and by the judicious selection of oligomer end groups and oligomer molecular weight in the step-growth case.

Although long block lengths and narrow molecular weight distributions are more readily achieved in living systems than in step-growth processes, the latter offer the advantage of a much wider selection of polymer types, and are much less sensitive to reactive impurities than the living polymerisations.

Taking all these factors into consideration, the decision was made that attempts to produce the desired $(A\text{-}B)_n$ structures should proceed via the step-growth polymerisation process. This decision is supported by the evidence of a number of workers who, over recent years, have been successful in producing block copolymers of this type by the interaction of functionally terminated oligomers.

Vaughn (112) and Kambour (116) reported the synthesis of a group of randomly alternating block copolymers of bisphenol-A-polycarbonate and P.D.M.S. by the in situ polymerisation of dichloro-terminated siloxane oligomers and bisphenol-A and phosgene. Pyridine was used as an acid acceptor. Merritt (117) reported an improvement on this process whereby an alkali metal hydroxide was used as an acid acceptor in the phosgenation rather than pyridine.

Noshay et al have also been active in this area. In a previous discussion mention was made of their route to the synthesis of polysulphone/P.D.M.S. block copolymers via the

silylamine-hydroxyl reaction (103). Further work (118) resulted in the production of poly(α-methylstyrene)/P.D.M.S. via the condensation of dihydroxyl-terminated poly(α-methylstyrene) oligomers and bisdimethylamino-terminated P.D.M.S.

More recently Tang et al (119) prepared a series of perfectly alternating block copolymers of bisphenol-A polycarbonate and P.D.M.S. by the silylamine-hydroxyl reaction. In this reaction slightly less than the stoichiometric quantity of siloxane oligomers was incrementally added to a hydrated solution of the polycarbonate in refluxing chlorobenzene.

Pittman et al carried out the preparation of alternating poly(arylenesiloxane) by the heterofunctional condensation of bis-silanols with bis-aminosilanes to obtain highly viscous silicone oils having functional groups (120). Furthermore O'Malley et al (121) studied the synthesis and characterisation of alternate poly(hexamethylene sebacate)/P.D.M.S. $(A\text{-}B)_n$ type block copolymers by the coupling reactions of the terminal hydroxyl groups of hexamethylene sebacate and either of the chlorosilyl or dimethylaminosilyl terminal groups on P.D.M.S. In a similar manner Nagase et al (122) synthesised $(A\text{-}B)_n$ type tetramethyl-p-silphenylene siloxane (T.M.P.S.)/P.D.M.S. copolymers by the polycondensation of silanol terminated T.M.P.S. oligomers and dimethylamino-terminated P.D.M.S. oligomers.

The available evidence suggests that it should be possible to tailor the silylamine-hydroxyl reaction to produce perfectly alternating $(A\text{-}B)_n$ type block copolymers of P.E.S. and P.D.M.S. in which the block sizes of each component are strictly

controlled. The preparation and characterisation of a series of such copolymers was considered to be the essential first step in this investigation.

2.4.2 Techniques for the Characterisation of the Reacting Oligomers and Block Copolymers.

No one particular analytical technique is capable of presenting a complete picture of the nature of a polymer. A combination of techniques must be employed in elucidating the structure of such a compound. Generally all the tools used for the characterisation of homopolymers may be used in identifying block copolymers, however, additional complexities over and above those inherent in the characterisation of homopolymers are encountered by the analyst when these molecules are considered. For instance, there are specific uncertainties associated with block copolymers such as the length, sequential placement, polydispersity and compositional heterogeneity of the component segments. Although some of these problems can be alleviated by knowledge of the synthetic procedure employed, important issues such as knowledge of whether a given reaction product is, in fact, a block copolymer, a random copolymer, a blend of homopolymers or, indeed, a complex mixture of two or more of these remain unresolved.

In the following discussion an attempt is made to review briefly, some of the important techniques used in the characterisation of both the reacting oligomers and the resulting block copolymers. It is not the intention here to enter into detailed discussion on the theory behind the techniques, for this

information can be obtained from standard texts and reviews. Instead it is intended to point out, in some instances with reference to specific examples, techniques that can best yield useful information on the polymers under consideration.

Let us first consider the reaction product. Obviously the first thing we require to know is if it is truly the block copolymer we desire or whether it is simply a mixture of the two starting materials. The property most commonly relied upon to answer this question is solubility behaviour. If we have a simple mixture of dissimilar homopolymers then sequential extraction with solvents selective for each of the components results in complete dissolution of the blend leaving no insoluble residue. When this procedure is performed on a block copolymer, the chemical link to the insoluble segment inhibits the dissolution of the soluble segment in its selective solvent and a residue results.

Another method of differentiating between simple mixtures and block copolymers is film clarity. Unless the two homopolymers in a simple mixture have similar refractive indices, films cast from this mixture will appear very opaque due to phase separation on a macro-scale. In contrast, block copolymers should produce reasonably transparent films since phase separation in these compounds is usually on a micro-scale.

Gel Permeation Chromatography (G.P.C.), a method commonly used for molecular weight determinations, can also be employed in solving this problem. Essentially, a block copolymer should give rise to a single peak on the chromatogram, whereas a simple blend should give rise to a peak for each of the two components. These

two peaks, however, will only be resolved if there is an appreciable difference in the molecular weights of the two homopolymers.

Assuming that we have positively identified the product as a block copolymer, then the next task is to determine its macromolecular structural characteristics e.g. molecular weight and molecular weight distribution. This can be done using the same instrumentation as applied to homopolymers, but their determination requires more complicated experimental procedures and/or data treatments, except for that of $\bar{M}n$ by osmometry.

Dumelow et al have recently reported a procedure for the determination of the molecular weight and compositional heterogeneity of block copolymers using combined G.P.C. and low-angle laser light scattering (123). They defined a compositional heterogeneity parameter whose variation with molecular weight could be measured. This procedure was applied to copolymers and blends of polystyrene and P.D.M.S.

In addition to characterising the block copolymer as a whole, it is also important to be aware of the molecular structure of the segments themselves. The particular synthesis technique employed in the formation of copolymers in this investigation i.e. the interaction of mutually reactive oligomers, makes this possible.

The reacting oligomers can be characterised before use, and because of their mutual reactivity, their molecular structure by definition will not change upon incorporation into the block copolymer. In addition to the usual homopolymer characterisation techniques, the reactive oligomers may be characterised by

chemical or physical methods such as end-group analysis or nuclear magnetic resonance spectroscopy (N.M.R.).

Recent developments in end-group analysis include a new spectrophotometric method (124) and potentiometric method (125) for the analysis of phenolic end-groups in polymers.

Van Houwelingen in his review of functional group analysis (126) describes the determination of hydroxyl and amino groups in polymers by a variety of techniques.

The value of N.M.R. spectroscopy in elucidating polymer molecular structures is highlighted in the work performed by Williams et al (127). They presented a method for the complete analysis of bisphenol-A polycarbonate/P.D.M.S. block copolymers by ^{29}Si and ^{13}C N.M.R. This analysis included number average block length determinations of both bisphenol-A (B.P.A.) polycarbonate and silicone blocks, total polymer composition (percent silicone and B.P.A. carbonate), and an analysis of the fraction of isolated B.P.A. units incorporated into the polymer by virtue of the synthetic technique.

Having performed the previously described characterisation measurements, it then remains for the architecture of the block copolymer to be confirmed and the purity of this architectural form to be assessed.

The number of tools available to define architecture is extremely limited, but in certain circumstances a differentiation between architectural forms can be made.

Elastomeric A-B structures will display poor elastic recovery properties compared to A-B-A and $(A-B)_n$ structures which, of course, are capable of displaying thermoplastic

elastomeric behaviour.

Rheological properties can also be used to distinguish an A-B structure from A-B-A or $(A-B)_n$ structures, for the latter two types generally display high melt viscosities.

Knowledge of the polymerisation technique operating in the formation of a block copolymer does ease the situation and allows impurities in the main product to be identified.

Provided there is a sufficiently large difference between the molecular weight of the required product - say an $(A-B)_n$ type copolymer - and the molecular weight of possible impurities i.e. A-B or A-B-A type copolymers or even A and B homopolymers, then G.P.C. may be used to assess the impurity levels in the final product.

In contrast to the molecular characteristics, block copolymers quite often display behaviour attributable to supermolecular structures. As we have seen, these structures result from the aggregation of segmented polymers to form complex morphological systems. These systems are comprised of two normally incompatible phases forced to co-exist with each other, which produces microheterogeneous structures of colloidal dimensions.

The criteria for microphase separation in block copolymers have been discussed in a previous section and will not be considered here. Instead, the techniques most commonly used to examine supermolecular structures in block copolymers will be reviewed.

There are several techniques that can be used to investigate supermolecular structures and the effect of parameters such as

block molecular weight on domain size.

Thermal analysis, such as modulus-temperature relationships, differential scanning calorimetry (D.S.C.) and rheological properties can detect the presence of supermolecular structures, but cannot readily distinguish between morphological types. For instance, modulus-temperature and D.S.C. data can reveal the presence of two phase morphology by identifying the presence of multiple glass transition and/or melting behaviour.

Transmission and scanning electron microscopy may reveal the shape and size of domains in block copolymer specimens. Examination of specimens cut at different angles can yield additional information on the shape of the domains.

Quite often, achieving sufficient phase contrast can be a problem and selective staining procedures have to be adopted. In certain systems, however, this is not necessary.

Saam et al (113), working on polystyrene/P.D.M.S. block copolymers, obtained good contrast between the two phases because of the difference in electron absorption and scattering of the polystyrene and P.D.M.S. blocks.

Other useful tools for investigating the morphology of amorphous block copolymers are small-angle X-ray scattering (S.A.X.S.) and small-angle neutron scattering (S.A.N.S.). These techniques afford information on subsurface morphological characteristics and are the most useful tools for investigating interdomain spacing and the nature of the interfacial region (128, 129).

3 EXPERIMENTAL AND RESULTS.

The experimental work presented here describes the synthesis and characterisation of a series of hydroxyl-terminated P.E.S. oligomers of differing molecular weight.

The characterisation and modification of a series of hydroxyl-terminated P.D.M.S. oligomers, again of differing molecular weight, is also detailed.

These well characterised oligomers have been used to synthesise a series of $(A\text{-}B)_n$ type P.E.S./P.D.M.S. block copolymers of varying block molecular weights, designed to exhibit behaviour ranging from thermoplastic to thermoplastic-elastomeric.

After extensive characterisation, these copolymers have been added in carefully controlled amounts to pure 4800P grade P.E.S. to yield a series of 'impact modified' P.E.S./P.E.S.-co-P.D.M.S. blends.

Standard Izod and Tensile test pieces have been injection moulded from these blends, and these test pieces used in a study of the physical, chemical and mechanical properties of the blends.

Test pieces of pure 4800P P.E.S. and a simple physical blend of linear P.D.M.S. and 4800P P.E.S. have been prepared in an identical manner and used as reference materials.

3.1 PREPARATION OF COPOLYMERS.

The first stage in the preparation of the desired copolymers involves the synthesis of the reacting oligomers i.e. hydroxyl-terminated P.E.S. and dimethylamino-terminated P.D.M.S. The

routes to, and characterisation of these oligomers are discussed here.

3.1.1 Synthesis of Hydroxyl-terminated P.E.S. Oligomers.

A number of synthesis routes to poly(arylene-ether sulphones) have been described in the literature. These include (a) the self-condensation of certain dinuclear arylsulphonyl chlorides catalysed by ferric chloride (130), (b) the polycondensation of 4,4'-dihalogenodiphenyl sulphones with bisphenoxides (131), (c) the polycondensation of halogenophenylsulphonyl phenoxides (132), (d) the polycondensation of compounds containing halogenophenylsulphonyl and hydroxyphenyl groups in the presence of potassium fluoride (132), (e) the polycondensation of silylated bisphenols with 4,4'-dichlorodiphenyl sulphone and 4,4'-difluorodiphenyl sulphone (133) and (f) the nucleophilic aromatic substitution of 4,4'-dihalogenodiphenyl sulphones with bisphenols using potassium carbonate/dimethylacetamide as base and aprotic dipolar solvent respectively (134).

The route recommended by I.C.I. (135) and used here to prepare three P.E.S. oligomers of differing molecular weights proceeds as follows :-

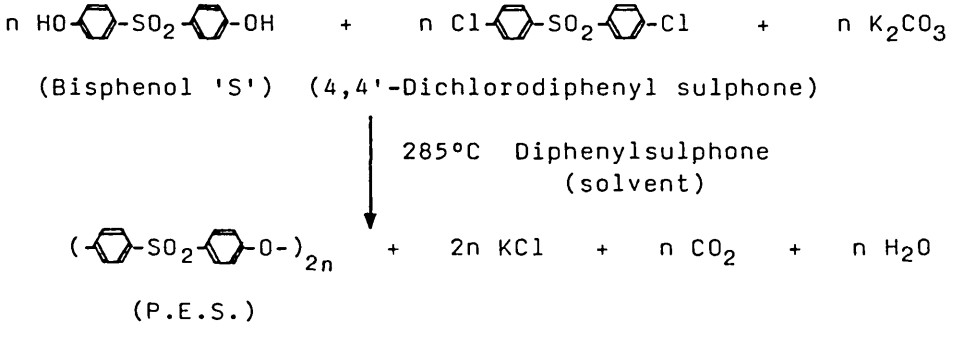

In this reaction Bisphenol 'S' is used in excess to ensure the resulting P.E.S. polymer is hydroxyl-terminated.

The molecular weight of the end product is controlled by judicious manipulation of this Bisphenol 'S' excess in accordance with the simple relationship for condensation reactions :-

$$(\bar{DP})_{max} = 1+r/1-r$$

where $(\bar{DP})_{max}$ = maximum degree of polymerisation in end product.

r = ratio of reactant molar concentrations.

The procedure for the preparation of one such P.E.S. oligomer with a $(\bar{DP})_{max} \sim 27$ is described here in detail.

Reagents

	Weight (g)	Molar Excess (%)
Bisphenol 'S' (99.7% pure)	270.35 (1.08M)	8
Dichlorodiphenyl sulphone (99.7% pure)	287.15 (1.00M)	-
Potassium carbonate (Analar*)	152.05 (1.10M)	10
Diphenyl sulphone	503.50 (2.33M)	-

* The potassium carbonate was sieved to ⩽300 micron prior to use.

Procedure

The reactants were charged to a 2 litre, 3-necked, round-bottomed flask fitted with a nitrogen inlet, mechanical stirrer, and outlet to a 250ml round-bottomed flask (to collect evolved water). The contents were dry mixed under a steady stream of nitrogen. The flask was then placed in a heating mantle and the contents heated to 175°C. This temperature was maintained until the contents were molten whereupon the stirrer was started. The flask was then heated at 225°C for 2 hours and then at 285°C for 3 hours. Then, while still molten, the product was poured into an aluminium tray and allowed to cool.

In the reaction, carbon dioxide and water are evolved, and the latter was seen to condense in the 250ml flask.

The product at the end of the reaction was P.E.S. containing diphenyl sulphone and potassium salt impurities which had to be removed by washing. This was done by grinding the product to a fine powder and then stirring in a series of solvents using a solvent/solids ratio of 4:1. The washing sequence was as follows :-

(a) 8 one hour methanol washes at 50°C.

(b) 1 one hour water/10% acetic acid wash at 80°C.

(c) 2 one hour water washes at 80°C.

The resulting 'pure' P.E.S. oligomer was characterised using a variety of analytical techniques.

Two further P.E.S. oligomers with $(\overline{DP})_{max}$s of 5 and 108 were prepared and characterised in a similar manner.

3.1.2 Characterisation of Hydroxyl-terminated P.E.S. Oligomers.

3.1.2.1 Molecular Structure.

The molecular structure of the three P.E.S. oligomers was verified using infrared and nuclear magnetic resonance techniques.

Films of the oligomers cast from dichloromethane solution were analysed on a Pye-Unicam SP-200 Infrared Spectrophotometer. The resultant absorption spectra (figs 1-3) were examined, and specific bond stretching and vibrational modes assigned to the observed absorption peaks. These are summarised in TABLE 1.

Of particular interest in the I.R. spectra of these P.E.S. oligomers is the strong peak at 1240cm^{-1} due to the 'aryl-O' bond

(assym. C-O-C str.). The presence of this bond is proof of the formation of P.E.S. since it occurs only in the polymer and not in either of the original reactants (Bisphenol 'S' and Dichlorodiphenyl sulphone) or, indeed, the solvent (Diphenyl sulphone). It is also worth noting the intensity of the O-H str. peak at ~3,400cm^{-1} on each of the three spectra. This intensity decreases on moving from the P.E.S. oligomer with a low degree of polymerisation to the oligomer with a high degree of polymerisation. This reflects the decrease in number of reactive O-H terminations present on moving to higher polymer molecular weights.

Nuclear magnetic resonance provides further confirmation of the structure of the P.E.S. oligomers. The ^{1}H N.M.R. spectra of all three oligomers display essentially the same features (figs 4-6). The strong peaks at 10τ are attributable to the calibration standard tetramethylsilane (T.M.S.) incorporated into the system, while the peaks at chemical shift 7.50τ are attributable to the presence of residual protons in the deuterated dimethylsulphoxide used as a solvent for the P.E.S. oligomers. The presence of moisture in the system manifests itself as peaks between 6 and 7τ.

If we now consider the structure of P.E.S. :-

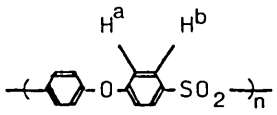

The ^{1}H N.M.R. spectra obtained for all three oligomers are consistent with the above structure. A normal AB quartet is observed indicating repeat units containing only two non-equivalent types of proton (chemical shifts 1.98τ for H^b and

2.72τ for H^a). Non-equivalent protons are positioned ortho to each other as shown by the typical coupling constant (J value) of 8c/s.

A much smaller AB quartet (particularly evident on the ^1H N.M.R. spectrum of the P.E.S. oligomer with a $(\overline{DP})_{max}$ of 5, (fig 4) can be attributed to the presence of impurities. Reference to the ^1H N.M.R. spectra of the starting materials - bisphenol 'S', dichlorodiphenyl sulphone and diphenyl sulphone (figs 7-9) suggests that this impurity is, in fact, unreacted bisphenol 'S'.

3.1.2.2 Molecular Weight.

Three different analytical techniques were employed in the determination of the molecular weight of the three P.E.S. oligomers.

(a) Gel Permeation Chromatography Analysis.

Samples submitted to the Rubber and Plastics Research Association (R.A.P.R.A.) were analysed using Gel Permeation Chromatography (G.P.C.). The operating conditions employed were as follows:-

Column 1 P.L. gel mixed bed - 5 micron bead.

Flow Rate 0.5ml/min.

Solvent Dimethylformamide.

Temperature 80°C.

Calibration The system was calibrated with poly(ethylene oxide) and poly(ethylene glycol) calibrants, and all molecular weight values are expressed as calibration polymer 'equivalents'.

The values obtained are summarised in TABLE 2.*

* M_W/M_N VALUE DISREGARDED DUE TO ABNORMALLY HIGH VALUE

(b) Viscometry Analysis.

The number average molecular weight of the three oligomers was determined using a viscometric method developed by I.C.I. In this method 0.5g of dry polymer is weighed into a clean, dry 50ml standard volumetric flask. Approximately 30ml of dimethylformamide (D.M.F.) is added and the flask shaken until the polymer has dissolved. When made up to the mark with D.M.F. and shaken, the flask contains a 1% w/v solution of P.E.S. in D.M.F.

A clean dry standard U-tube viscometer is placed in a thermostat bath at 25°C + 0.1°C and D.M.F. added. The time for the solvent to flow between the two indicated levels (A seconds) is recorded with a stopwatch. The flow time is measured a further two times, after which the viscometer is drained and rinsed with the polymer solution. The required volume of polymer solution is then added and the flow time for this solution (B seconds) measured in triplicate. The reduced viscosity (R.V.) of the polymer (for a 1% solution) is calculated as follows :-

$$\text{R.V.} = \frac{\text{average flow time of solution in seconds}}{\text{average flow time of solvent in seconds}} - 1 = \frac{B}{A} - 1$$

The value of reduced viscosity may be converted to a value for the number average molecular weight ($\bar{M}n$) using the following relationships :-

$$\text{Degree of Polymerisation (D.P.)} = 292 \times \text{R.V.}^{1.508}$$

and

$$\bar{M}n = M_o \times \text{D.P.}$$

where M_o = molecular weight of the polymer repeat unit (232.25 for P.E.S.).

The values of $\bar{M}n$ obtained for the P.E.S. oligomers using

this method are contained in TABLE 3.

(c) Potentiometric Titrations.

The number average molecular weight of certain polymers can be determined rapidly and easily by potentiometric titration.

Phenolic compounds are usually so weakly acidic that they cannot be titrated in water; however, in basic non-aqueous solvents such as ethylenediamine, D.M.F., pyridine and dimethylsulphoxide, phenols can be titrated as very weak acids.

Deal and Wyld (136) have described a potentiometric method of titrating phenols, dihydroxy phenols and polyphenolic compounds in D.M.F. and ethylenediamine solvents utilising a glass-calomel electrode system. Alcoholic solutions of potassium hydroxide and tetrabutylammonium hydroxide (TBAOH) were investigated as titrants. In these studies, the titrations carried out in D.M.F. using TBAOH as titrant were found to be superior to those employing other solvent-base combinations.

More recently Wnuk et al (125) determined the $\bar{M}n$ of hydroxyl-terminated poly(aryl ether) sulphone oligomers (including P.E.S.) by potentiometric titration using a glass-calomel electrode system. Dimethylacetamide and tetraethylammonium hydroxide were used as solvent and titrant respectively.

In the present work, the D.M.F./TBAOH solvent-titrant system used successfully by Deal and Wyld on phenolic compounds is employed in the potentiometric titration of bisphenol 'S' and the three P.E.S. oligomers.

Apparatus.

A Pye Unicam 290 pH meter was used in conjunction with a combined glass-calomel electrode. A 60mm diameter x 60mm high glass vial equipped with a screw-on bakelite top served as a titration vessel. Holes in the cap to permit passage of the electrode, burette nozzle and a nitrogen inlet were carefully sized so as to retain a tight seal. The titrant (0.1N TBAOH in a solvent of 9:1 toluene/methanol) was dispensed using a 2ml burette and the solution mixed via a small P.T.F.E.-coated stirring bar/magnetic stirrer system. A schematic diagram of the apparatus is given in figure 10.

Prior to use, the nitrogen was passed through a U-tube containing soda-asbestos (a carbon dioxide absorbant) and the glass-calomel electrode was conditioned in D.M.F. for two days.

Procedure.

Immediately before commencing the molecular weight determinations, a blank titration of the solvent (25ml) was made employing the same procedures as followed for the polymers. The electrode was then rinsed with clean D.M.F. prior to further use.

A sample of bisphenol 'S' was accurately weighed into the titration vessel and dissolved in D.M.F. (25ml) with stirring, while dry, CO_2-free nitrogen was passed over the solution. After complete dissolution, the electrode was immersed in the solution and the burette lowered such that the tip just pierced the surface. The cell potential was then measured as a function of volume of TBAOH added until such time as the potential ceased to change upon further additions of titrant. This procedure was repeated for the three P.E.S. oligomers.

Titration curves were prepared for the four materials (fig 11), and the end points taken as the inflection points on these curves.

Calculations.

In the reaction between TBAOH and hydroxyl-terminated P.E.S., the P.E.S. behaves as an acid thus :-

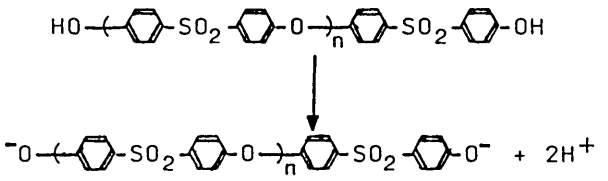

The TBAOH behaves as a base thus :-

$$(Bu)_4N\text{-}OH \longrightarrow (Bu)_4N^+ + OH^-$$

The reaction may be represented by the equation :-

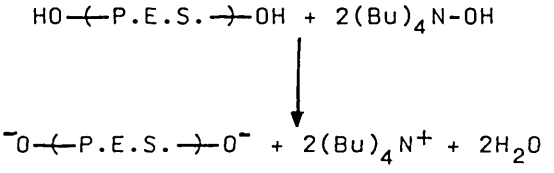

Thus :-

1 mole P.E.S. = 2 moles TBAOH.

The relationship between $\bar{M}n$ for the sample and the volume and concentration of titrant used is therefore given by the expression :-

$$\bar{M}n = 2(W)/(V)(C)$$

where W = weight of sample in grams, V = volume of titrant in litres (corrected for the blank) and C = concentration of titrant in moles per litre.

Taking a value of 0.01ml as the volume of 0.1M (0.1N) TBAOH used in the blank determination, the results summarised in TABLE 4 were obtained.

A comparison between the values of $\bar{M}n$ obtained for the

P.E.S. using the three different evaluation methods is shown in TABLE 5.

The spread of results may be attributed partly to the presence of impurities e.g. residual bisphenol 'S', dichlorodiphenyl sulphone and diphenyl sulphone in the P.E.S. oligomers. These impurities could affect the potentiometric titration and viscometry results in different ways; for instance, the presence of any of these low molecular weight residues would reduce the viscosity of the polymers and hence reduce the value of $\bar{M}n$ obtained by this method. On the other hand, the presence of dichlorodiphenyl sulphone and diphenyl sulphone would reduce the weight fraction of reactive hydroxyl groups present in the sample. This reduction would result in a smaller volume of TBAOH being required in the potentiometric titrations and hence a higher calculated value for $\bar{M}n$ being obtained. The presence of bisphenol 'S' would, of course, have the opposite effect.

With regard to the G.P.C. results, the unavailability of Mark-Houwink constants for P.E.S. prevented conversion of the results via universal calibration. Consequently, the results obtained are expressed as 'polyethylene glycol/polyethylene oxide equivalents' only.

3.1.2.3 Thermal Characteristics.

The glass transition temperatures (Tg s) of commercial 4800P grade Victrex and the three P.E.S. oligomers were determined using differential scanning calorimetry (D.S.C.)*. A Mettler DSC 30 measuring cell was employed and the results processed using a Mettler TC 10 TA microprocessor. The samples were heated

* using DTA to simulate true D.S.C. as used in Mettler instrument

in standard aluminium pans at a rate of 10°C/min and the resultant curves recorded (fig 12).

The Mettler system yields three different values for each Tg evaluation. In order to be consistent and unambiguous, only the second of these values has been considered in each case. This value is defined as the temperature at which an extrapolation of the base line prior to any specific heat capacity (Cp) change intercepts the tangent to the curve at the point where half the Cp change has occurred. TABLE 6 summarises the Tg values obtained.

The value obtained for the high molecular weight 4800P grade Victrex is in good agreement with the expected value of 223°C.

The values for the P.E.S. oligomers, however, are somewhat lower than this value. This was not unexpected since the general trend in polymeric materials is for the Tg to decrease with decreasing molecular weight.

One interesting feature which conflicts with the argument, however, is the apparent increase in Tg on moving from the oligomer P.E.S.$(\overline{DP})_{max}$ 27 to the oligomer with the lowest molecular weight i.e. P.E.S.$(\overline{DP})_{max}$ 5. This may be attributed to the presence of a certain degree of crosslinking within the low molecular weight polymer (137).

The thermal stability of 4800P grade Victrex and the three P.E.S. oligomers was assessed using thermogravimetric analysis (T.G.A.). The instrumentation employed in this study comprised a Du Pont 950 Thermogravimetric Analyser coupled to a Du Pont 900 Differential Thermal Analyser. The samples were heated at a rate of 15°C/min in a steady stream (250ml/min) of nitrogen.

The relationships between sample weight loss and temperature for these materials are represented graphically in figure 13.

Immediately evident from this information is the excellent thermal stability of 4800P grade Victrex. No appreciable weight loss was observed in this material until temperatures >450°C had been attained. Also of interest from these curves is the apparent dependence of thermal stability on polymer molecular weight. The general trend is for thermal stability to decrease with decreasing molecular weight. Once again, however, it can be seen that the P.E.S. oligomer with $(\overline{DP})_{max}$ 5 defies convention. Its superior high temperature stability over the oligomer with $(\overline{DP})_{max}$ 27 may, once again, be attributed to the presence of crosslinking.

Despite the effects of oligomer molecular weight on thermal stability, it is worth noting that very little weight loss is observed in any of the polymers below 350°C.

The results are consistent with the findings of Crossland et al (138) who, in their study of the thermal stability and mechanism of degradation of Poly(arylene sulphones), found the degradation of P.E.S. in nitrogen to be a single stage reaction, coupled with the formation of a fairly stable char comprising 30-40% of the starting weight.

3.1.3 Characterisation of Hydroxyl-terminated P.D.M.S. Oligomers.

Five hydroxyl-terminated P.D.M.S. oligomers were provided by I.C.I. for use in this investigation. These samples required characterising before they could be considered for conversion to

dimethylamino-terminated P.D.M.S. and reacted with hydroxyl-terminated P.E.S.

Similar characterisation techniques were employed on these oligomers as were employed on the P.E.S. oligomers.

3.1.3.1 Molecular Weight.

Gel Permeation Chromatography and Viscometry were employed in the determination of oligomer molecular weight.

The G.P.C. was performed by R.A.P.R.A. using the following instrumental parameters :-

Columns Four columns containing 100, 10, 1 and 0.1 micron pore diameter P.L. particles.

Flow Rate 1.0ml/min.

Solvent Tetrachloroethylene.

Temperature 80°C.

Concentration 0.3%.

Calibration The calibration standard employed was polystyrene, but as the Mark-Houwink constants were not known, universal calibration could not be applied. The molecular weight averages obtained were therefore expressed as 'polystyrene equivalents'. The values obtained are summarised in TABLE 7.

Solution viscometry was also employed for the determination of P.D.M.S. oligomer molecular weight. The procedure described here was applied to each of the five oligomers in turn.

A series of solutions of the oligomer in toluene was prepared. Each solution was made to contain a different oligomer concentration. The relative viscosity of each solution was then determined by measuring the time taken for the solution to flow through an Ostwald Viscometer (Type BS/U B) at 25°C and comparing

it with the time taken for pure solvent to flow at the same temperature.

The information obtained allows the calculation of $\bar{M}v$ for a particular oligomer according to the theory outlined below :-

$$\eta_r \text{ (relative viscosity)} = \eta/\eta_o = t/t_o$$

where t = time taken for polymer solution to flow.

t_o = time taken for solvent only.

From η_r, η_{sp} (specific viscosity) can be obtained from the relationship :-

$$\eta_{sp} = \eta-\eta_o/\eta_o = \eta_r-1$$

A linear relationship of the reduced viscosity (η_{sp}/c) to polymer concentration is usually found when η_r <2. This linear dependence is described well by the expression :-

$$\eta_{sp}/c = [\eta] + k'[\eta]^2c$$

where $[\eta]$ = intrinsic viscosity.

Intrinsic viscosity is obtained by extrapolation of a graph of reduced viscosity vs concentration of solution to zero concentration of polymer :-

$$[\eta] = \lim_{c \to 0}(\eta_{sp}/c)$$

The Mark-Houwink equation :-

$$[\eta]_i = KM_i^a$$

gives the molecular weight of a sample provided $[\eta]_i$ and K and a (the Mark-Houwink constants) are known.

It should be mentioned that this equation applies strictly to well fractionated samples.

For an unfractionated polymer :-

$$[\eta] = K(\bar{M}v)^a$$

where $\bar{M}v$ = viscosity average molecular weight.

Thus, $\bar{M}v$ can be obtained for a particular oligomer if $[\eta]$ is determined and the Mark-Houwink constants, K and a, are known for that oligomer in a particular solvent at a fixed temperature.

For P.D.M.S. in toluene at 25°C, $K = 0.738 \times 10^{-2}$ and $a = 0.72$ (139).

Using these values of K and a and intrinsic viscosities obtained from plots of η_{sp}/c vs c for the five oligomers (figs 14,15) values of $\bar{M}v$ were calculated. These values are recorded in TABLE 8.

For the samples where $\bar{M}v$ was determined by both G.P.C. and viscometry, good agreement was observed in the values obtained. This serves to validate the 'polystyrene equivalents' obtained by G.P.C. as reasonable approximations for the P.D.M.S. oligomer molecular weights.

Because of the high molecular weight and hence very low level of reactive end-groups in samples 11 38/71/4-5, these polymers were considered unsuitable for use in copolymerisation with P.E.S. via a condensation type reaction. For this reason most of the future discussion relates only to samples 11 38/71/1-3.

3.1.3.2 Molecular Structure.

All three samples (labelled 11 38/71/1-3) yielded similar spectra when analysed on a Pye-Unicam S.P.1200 Infrared Spectrophotometer (figs 16-21). Potassium bromide plates were employed in the analysis in order to facilitate the observation of sample absorption at wavenumbers below $600cm^{-1}$. TABLE 9 summarises the peak inference for these spectra.

Of interest in these spectra is the relative intensity of the broad band at 3,700-3,100cm^{-1} relating to the terminating Si-OH bonds. As expected, this intensity decreases on moving from the low molecular weight oligomer to that with the highest molecular weight.

The ^{1}H N.M.R. spectra of the three P.D.M.S. oligomers are very simple (figs 22-24). The six equivalent protons in the P.D.M.S. give rise to a singlet which appears at a chemical shift of 10.0τ. The spectra are calibrated using an external T.M.S. standard owing to the proximity of the P.D.M.S. chemical shift to that for the T.M.S. (10.0τ).

3.1.3.3 Thermal Characteristics.

D.S.C. curves were obtained for the three hydroxyl-terminated P.D.M.S. oligomers (fig 25). The same instrumentation and evaluation procedures were employed as for the P.E.S. oligomers discussed earlier.

All three P.D.M.S. oligomers were found to have a Tg value of -123°C. These results are consistent with the findings of Lee et al (140). They obtained a P.D.M.S. Tg value of -123°C at infinite molecular weight and found that the molecular weight of the polymer had a negligible effect on Tg if the molecular weight exceeded 3,000.

The work performed here suggests that the molecular weight effect is negligible at even lower polymer molecular weights than 3,000.

Other interesting features of the D.S.C. curves for the P.D.M.S. oligomers are the exothermic cold crystallisation peaks

observed between -70°C and -90°C, and the endothermic melting peaks observed around -40°C. These peaks too were observed by Lee et al.

The presence of the cold crystallisation peak indicates that during cooling a portion of the polymer remained uncrystallised giving rise to cold crystallisation on heating. This peak becomes smaller as the cooling rate decreases and eventually disappears at cooling rates less than ~4°C/min.

The P.D.M.S. melting peaks may appear as a singlet or doublet depending on the rate of cooling and the rate of heating of the sample.

Thermogravimetric analysis performed on a series of hydroxyl-terminated P.D.M.S. oligomers showed there to be a strong relationship between thermal stability and oligomer molecular weight (fig 26).

Employing the same apparatus and operating conditions as for the P.E.S. oligomers it was shown that sample 11 38/71/1 (a volatile oligomer with a $\bar{M}n \sim 600$) commenced losing weight even at room temperature. Sample 11 38/71/2 ($\bar{M}n \sim 5,000$) remained thermally stable up to 250°C, whilst a P.D.M.S. oligomer of high molecular weight - sample 11 38/71/4 ($\bar{M}n \sim 53,000$), and a sample of crosslinked P.D.M.S. remained thermally stable up to~400°C.

3.1.4 Preparation of Dimethylamino-terminated P.D.M.S.

Before copolymerisation with hydroxyl-terminated P.E.S., the P.D.M.S. oligomers characterised in the previous section required modification such that the hydroxyl terminal groups were replaced by dimethylamino groups. This was considered to be best achieved

by the adoption of the method described by Nagase et al in their recent paper (122). This two-stage process proceeds as follows :-

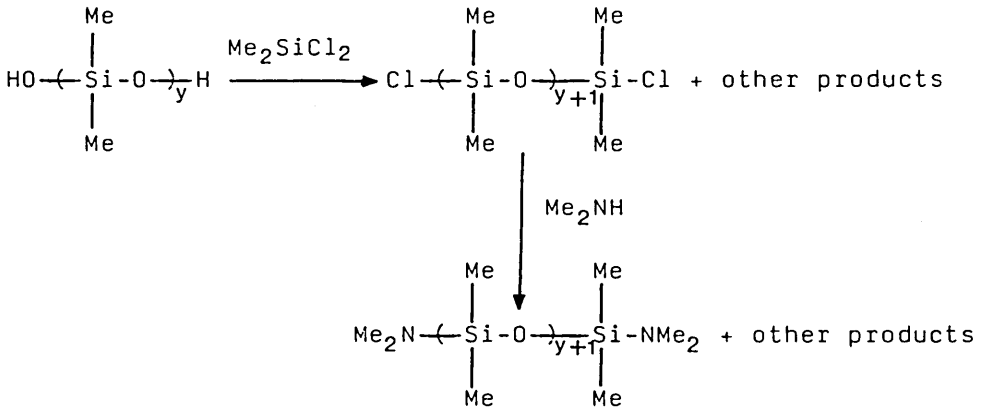

Outlined here are the experimental details relating to the conversion of sample 11 38/71/2 from hydroxyl-terminated to dimethylamino-terminated P.D.M.S.

3.1.4.1 Chlorination of Hydroxyl-terminated P.D.M.S.

A 500ml three-necked flask was equipped with a nitrogen inlet, mechanical stirrer and reflux condenser (fig 27). Dichlorodimethylsilane (100ml) was placed in this flask and a solution of hydroxyl-terminated P.D.M.S. (107.0g) in 100ml toluene (sodium dried and freshly distilled over CaH_2) added dropwise over 90 minutes in a dry nitrogen atmosphere and with vigorous agitation. The solution was allowed to react for a further hour after which excess dichlorodimethylsilane and toluene were removed by gentle heating under vacuo. The residue (chloro-terminated P.D.M.S.), which had a viscosity similar to the starting material, was stored under dry nitrogen as a precaution against hydrolysis.

3.1.4.2 Amination of Chloro-terminated P.D.M.S.

Using similar apparatus to that employed in the chlorination process, dimethylamino end-groups were attached to the P.D.M.S. oligomer.

To a solution of dimethylamine (15ml) in freshly distilled ether (200ml) was added dropwise chloro-terminated P.D.M.S. (100g) under dry nitrogen and with vigorous agitation. Upon completion of the addition (1 hour) the mixture was refluxed for a further hour after which the precipitated dimethylamine hydrochloride was removed by filtration in a dry box. The filtrate was evaporated under vacuo to remove ether and unreacted dimethylamine. Again the end product was stored under nitrogen to prevent hydrolysis.

A similar procedure was adopted in order to attach dimethylamino end-groups to sample ll 38/71/3. However, the high volatility of sample ll 38/71/1 necessitated the utilisation of a solvent with a lower boiling point than toluene (b. pt. 111°C) for the chlorination process. For this reason, benzene (b. pt. 80°C), which had been freshly distilled over CaH_2, was employed. This modification apart, the procedure employed for sample ll 38/71/1 was the same as that utilised for the other two samples.

3.1.5 Characterisation of Dimethylamino-terminated P.D.M.S. Oligomers.

3.1.5.1 Molecular Structure.

Infrared spectra were recorded for all three P.D.M.S. oligomers after both the chlorination and amination stages (figs 28-39).

There are two features of particular interest on the spectra recorded after the chlorination process. These are highlighted by reference to the spectra of sample ll 38/71/1 before chlorination (figs 16,17), and after chlorination (figs 28,29). The disappearance in figs 28 and 29 of the Si-OH peak at 3,700-3,100cm^{-1} and the appearance of a peak at 465cm^{-1} attributable to the Si-Cl assym. str. mode provide strong evidence that the hydroxyl end-groups have been successfully replaced by chloro end-groups.

Examination of the spectra obtained after amination of the samples (figs 34-39) reveals little evidence for the presence of either the Si-OH or the Si-Cl bond. This provides inferential evidence for the presence of dimethylamino end-groups.

3.1.5.2 Molecular Weight.

Intrinsic viscosities and hence viscosity average molecular weights were determined for all three P.D.M.S. samples after amination.

By employing a procedure similar to that previously described for the hydroxyl-terminated samples, the results summarised in TABLE 10 were obtained.

By referring to TABLES 8 and 10 it can be seen that very little increase in molecular weight was observed for samples 11 38/71/1-2 on conversion to dimethylamino-terminated P.D.M.S.

The viscosity of sample 11 38/71/3, however, increased substantially on modification giving a $\bar{M}v$ of 91,684 compared with a $\bar{M}v$ of 53,392 for the hydroxyl-terminated oligomer. This viscosity average molecular weight was equated to a number average molecular weight by reference to fig 40. This curve was constructed by relating $\bar{M}v$ (obtained viscometrically) to $\bar{M}n$ (obtained by G.P.C.) for all the hydroxyl-terminated P.D.M.S. oligomers where both values were quoted.

In this way, a value of $\bar{M}n$ 53,000 was obtained for sample 11 38/71/3 with dimethylamino terminations.

3.1.6 Synthesis of P.E.S./P.D.M.S. Block Copolymers.

3.1.6.1 Selection of Solvent System.

Shortly after the commencement of the investigation it became apparent that difficulties would arise with the selection of a suitable solvent system in which to carry out the copolymerisation reaction.

Reference to Hildebrand's solubility parameters for the two starting materials, P.E.S. [δ = 25.2 $(J/cm^3)^{0.5}$] and P.D.M.S. [δ = 14.9 $(J/cm^3)^{0.5}$] indicated gross incompatibility between the components. Although this large value of Δ [10.3 $(J/cm^3)^{0.5}$] would be beneficial from the point of view of promoting microphase separation in the resultant copolymer, it also

suggested that the possibility of finding a single solvent which would dissolve both components would be remote.

Initial trials using chlorobenzene [δ = 19.4 $(J/cm^3)^{0.5}$], a solvent employed by Noshay et al in copolymerising polysulphone [δ = 21.7 $(J/cm^3)^{0.5}$] with P.D.M.S., were unsuccessful. Even at temperatures approaching its boiling point (132°C), chlorobenzene was found to dissolve hydroxyl-terminated P.E.S. only sparingly. Other common solvents examined e.g. tetrahydrofuran (T.H.F.), diphenylsulphone (D.P.S.), N-methyl-2-pyrrolidone (N.M.P.), dimethylsulphoxide (D.M.S.O.) and dimethylformamide (D.M.F.) were all found to dissolve one of the oligomers well whilst only partially affecting the other oligomer.

Dichloromethane [δ = 19.8 $J/cm^3)^{0.5}$] was found to be one solvent which did appear to dissolve both P.E.S. and P.D.M.S. However, when this solvent was employed in an attempt to copolymerise hydroxyl-terminated P.E.S. with dimethylamino-terminated P.D.M.S., the resulting product was found to be a physical mixture of the two components. This was verified by selective solubilisation of the P.D.M.S. phase with diethyl ether, and the performing of I.R. and N.M.R. analyses on the solute and residue.

The reason for the lack of success in copolymerisation using dichloromethane is not entirely clear; however, reports that P.E.S. forms a complex compound with dichloromethane (141) lead one to suggest that it is the formation of such a complex compound that inhibits the copolymerisation of P.E.S. with P.D.M.S.

Copolymerisation attempts employing multicomponent solvent systems e.g. toluene/N.M.P., where a completely miscible solution of both components was achieved, resulted, yet again, in the formation of a simple physical mixture of P.E.S. and P.D.M.S.

After some considerable time investigating different solvent systems, a solvent was found which appeared to allow the copolymerisation reaction to proceed. 1,2-Dichlorobenzene [$\delta = 20.5\ (J/cm^3)^{0.5}$] was found to dissolve reasonable quantities of both hydroxyl-terminated P.E.S. and dimethylamino-terminated P.D.M.S. at its boiling point (180°C).

Evidence to suggest that copolymerisation proceeded in this solvent was supplied by the identification of the copolymerisation by-product, dimethylamine, being liberated from the reaction vessel.

Attempts to improve the solubility of the P.E.S. oligomer in 1,2-dichlorobenzene by the inclusion of small quantities of a solvent specific for P.E.S. i.e. D.M.F., resulted in no detectable dimethylamine liberation being observed.

The following mechanism has been proposed to explain the above-mentioned phenomenon.

1,2-dichlorobenzene is a poor hydrogen-bonding solvent, and as such would not lend itself readily to such bonding with any of the reacting oligomers. On the other hand, solvents such as D.M.F. are very strong hydrogen-bonding species and could enter into such bonding with hydroxyl-terminated P.E.S. thus :-

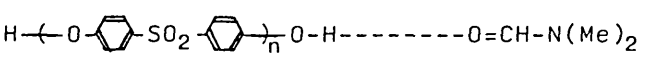

Such hydrogen-bonding can have a fundamental effect on the

rate of a copolymerisation reaction as suggested by Noshay et al (103). These workers found that the reaction between hydroxyl-terminated polysulphone and dimethylamino-terminated P.D.M.S. proceeded at a much slower rate in T.H.F. than in chlorobenzene. They suggested that the effect might be due to hydrogen-bonding between the T.H.F. and the polysulphone oligomer hydroxyl group. This bonding, they claimed, would reduce the availability of the phenolic hydrogen for hydrogen-bonding with the nitrogen of the silylamine end-groups. This -N----H bonding in a solvent such as chlorobenzene would be expected to weaken the Si-N bond and make the Si more susceptible to attack by the O of the polysulphone end-groups, as illustrated by :-

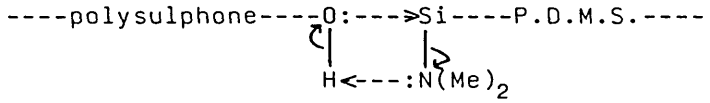

All the evidence collected to date on the P.E.S./P.D.M.S. copolymerisation system corroborates the findings of Noshay et al on the polysulphone/P.D.M.S. system and suggests that any solvent capable of entering into hydrogen-bonding with hydroxyl-terminated P.E.S. should be excluded from use in the copolymerisation reaction between P.E.S. and P.D.M.S.

3.1.6.2 Reaction Procedure.

Presented here are the details relating to the preparation of a block copolymer of hydroxyl-terminated P.E.S. ($\bar{M}n \sim 4,900$), and dimethylamino-terminated P.D.M.S. ($\bar{M}n \sim 5,100$). The reaction proceeds in 1,2-dichlorobenzene solvent as follows :-

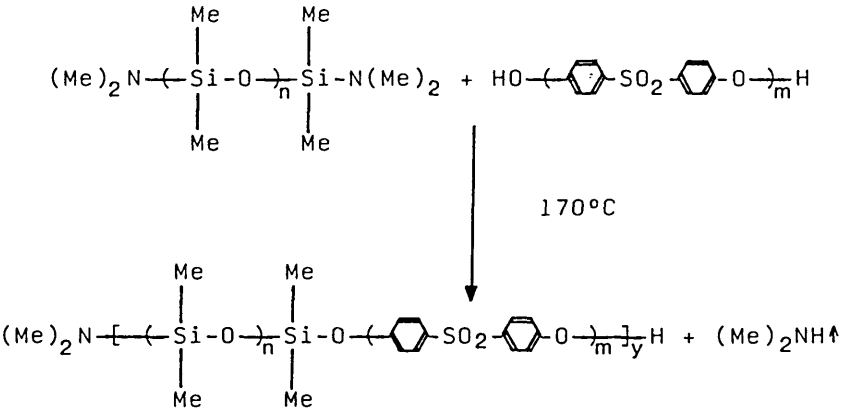

A 1 litre 5-necked flask was fitted with a dry nitrogen inlet, a mechanical stirrer, a thermometer, an addition funnel containing dimethylamino-terminated P.D.M.S. (28.65g/0.0056 mole) and a condenser equipped with a short path distillation take-off. Drying tubes were placed on the condenser and addition funnel (fig 41). Dry hydroxyl-terminated P.E.S. (25.00g/0.0051 mole) was charged to the flask along with 1,2-dichlorobenzene (800ml). The stirrer was switched on and the temperature of the flask raised until a steady reflux was obtained. A stream of dry nitrogen was maintained throughout. 50ml of 1,2-dichlorobenzene were distilled out after which the temperature was adjusted to 170°C and the addition of the P.D.M.S. begun. The additions were incremental with 10ml being added in the first increment. After 30 minutes a further 5ml were added, then at 30 min intervals 5ml, 3ml, 2ml, 2ml, 1ml, and 1ml. By doing this, it was possible to approach the true stoichiometric end-point gradually, thus promoting the formation of high molecular weight product. The evolution of dimethylamine (the reaction by-product) was detected throughout the reaction with moist litmus paper. The mixture was allowed to react for a further 2 hours after the final P.D.M.S. addition, and the bulk of the solvent then removed by heating under vacuo.

The product was taken to complete dryness by heating at 90°C in a vacuum oven.

A similar procedure was adopted for the preparation of all the other copolymers used in this investigation. Details of the copolymers synthesised are contained in TABLE 11.

3.2 CHARACTERISATION OF P.E.S./P.D.M.S. BLOCK COPOLYMERS.

The block copolymers prepared as previously described were characterised using a variety of techniques. The methods employed and the results obtained are discussed here.

3.2.1 Molecular Weight.

Gel Permeation Chromatography and Solution Viscometry were employed in determining the overall molecular weight of the copolymers.

(a) Gel Permeation Chromatography.

The copolymers were dissolved in 1,2-dichlorobenzene and submitted to R.A.P.R.A. for analysis.

Their high temperature G.P.C. system was used to obtain a crude indication of the 'polystyrene equivalent' molecular weights. The results are recorded in TABLE 12.

(b) Viscometric Analysis.

0.1g of each copolymer was dissolved in 50ml dichloromethane. The relative viscosity of each solution was then determined by measuring the time taken for the solution to flow through an Ostwald Viscometer (Type BS/U A) at 25°C and comparing it with the time taken for pure dichloromethane to flow at the same temperature. Values of specific viscosity and reduced

viscosity were then calculated as in section 3.1.3.1 earlier.

The results contained in TABLE 13 support R.A.P.R.A.'s G.P.C. analyses in that the copolymer with the lowest molecular weight as determined by G.P.C. also exhibits the lowest reduced viscosity. By listing the remaining copolymers in order of increasing molecular weight, we can observe that they are also listed in order of increasing reduced viscosity.

3.2.2 Molecular Structure.

Infrared and ^{1}H N.M.R. techniques were employed in the elucidation of the molecular structure of the copolymers.

Examination of the I.R. spectra of the copolymers (figs 42-47) shows them to possess the salient features of the spectra of the P.E.S. (figs 1-3) and P.D.M.S. (figs 34-39) oligomers. However, there is one feature of particular interest which can be observed on the spectra of the copolymers, but which is absent on the spectra of the reacting oligomers. Close examination reveals the presence of a peak at $920cm^{-1}$ on the copolymer spectra. This peak can be attributed to the Si-O str. mode of the Si-O-C_6H_5 linkage (expected range $970-920cm^{-1}$). The presence of this Si-O-C_6H_5 linkage is proof of the formation of a P.E.S./P.D.M.S. block copolymer since it occurs only in this species and in neither of the reacting oligomers. Furthermore, the relative intensity of this peak at $920cm^{-1}$ reflects the number of Si-O-C_6H_5 linkages expected in each polymer; for instance, the peak is at its most intense in the spectrum of copolymer 1 where, because of the small P.E.S. and P.D.M.S. block sizes, a large proportion of Si-O-C_6H_5 linkages can be expected. On the other hand, the peak appears very small on the

spectrum of copolymer 6 where large block sizes and a small proportion of Si-O-C_6H_5 linkages are to be found.

^1H N.M.R. spectra of the copolymers (figs 48-53), obtained using deuterated chloroform/dimethylsulphoxide solvent mixture, display the essential features of both the P.E.S. and P.D.M.S. reacting oligomers (figs 4-6,22-24). Other peaks observed on the spectra at 2.75τ and 7.7τ are due to the presence of residual protons in the deuterated chloroform and dimethylsulphoxide respectively.

3.2.3 Thermal Characteristics.

The thermal stability of the copolymers was assessed using thermogravimetric analysis. The apparatus and instrumental conditions employed were as for the P.E.S. and P.D.M.S. oligomers discussed in sections 3.1.2.3 and 3.1.3.3 earlier.

Reference to TABLE 11 and the resultant sample weight vs temperature curves (figs 54-56) shows there to be no discernable relationship between copolymer block molecular weights and thermal stability. However, there does appear to be a relationship between overall copolymer molecular weight (TABLE 12) and thermal stability, with copolymers possessing higher overall molecular weights also possessing superior high temperature properties.

In general, the thermal stability of the copolymers appears to be marginally inferior to that of P.E.S., but comparable to, or superior to, that of linear P.D.M.S. or physical blends of P.E.S. with P.D.M.S. (fig 56). Copolymer degradation appears to commence at temperatures between 350-400°C.

Further thermogravimetric analysis was performed in an

attempt to assess the effect of subjecting the copolymers to typical P.E.S. injection moulding temperatures.

A Stanton Redcroft TG 762 Thermobalance was employed in this investigation.

The copolymers were heated at a rate of 10°C/min in air to a maximum temperature of 360°C, and held at this temperature for 30 minutes. After this period, the weight loss of each sample was recorded, and the visual appearance noted (TABLE 14).

The results obtained provide further evidence for the existence of a relationship between overall molecular weight and thermal stability as measured in terms of weight loss. Generally, copolymers with high overall molecular weights exhibited low weight losses. Although higher weight losses were observed in low molecular weight copolymers, no copolymer exhibited a weight loss greater than 12.5%.

Visual examination revealed all the copolymers to have been affected after heat-treatment in air at 360°C for 30 minutes. Most copolymers appeared darker in colour, but some of the copolymers with low overall molecular weights displayed evidence of partial dissociation into simple physical blends.

It is obvious from these results that if the copolymers or blends containing the copolymers are to be melt processed at normal P.E.S. processing temperatures (360°C) then the amount of time that the copolymers spend at this temperature should be reduced to a minimum. Failure to do this is likely to result in partial degradation of the copolymers into simple physical blends.

Differential Scanning Calorimetry is often employed as a

means of identifying microphase separation within copolymers - the presence of two transitions on the D.S.C. curve corresponding to the Tgs of the reacting oligomers is indicative of separation, whereas the presence of a single Tg value at some intermediate point between the Tgs of the oligomers denotes the formation of a single phase copolymer.

D.S.C. analysis was performed on the copolymers, the same apparatus and instrumental conditions being employed as for the P.E.S. and P.D.M.S. oligomers (sections 3.1.2.3 and 3.1.3.3).

The curves obtained (figs 57,58) display similar features, all of which correspond to transitions taking place within the P.D.M.S. component of the copolymers. A change in specific heat capacity, corresponding to the Tg of P.D.M.S., is clearly observable in all samples. This occurs at temperatures between -122°C and -124°C as indeed it does in the reacting P.D.M.S. oligomers considered earlier (fig 25). Other peaks corresponding to the cold crystallisation and melting of P.D.M.S. are also visible.

No discernable transitions corresponding either to the Tg of a separate P.E.S. phase within the copolymers or, indeed, to the Tg of a single phase P.E.S/P.D.M.S. copolymer were observed.

This phenomenon is believed to be caused by the migration of the lower surface energy P.D.M.S. segments to the surface of the copolymer. Once at the surface they act as insulators and inhibit the observation of transitions occurring in the P.E.S. segments of the copolymer.

The argument for P.D.M.S. migration is supported by evidence obtained by other workers. For instance, Schmitt et al (142)

identified and quantified surface enrichment with P.D.M.S. in bisphenol A polycarbonate/P.D.M.S. block copolymers. X-ray photoelectron spectroscopy and ion scattering spectroscopy were used in the study.

Clearly the D.S.C. evidence does not provide conclusive proof that microphase separation has occurred in the P.E.S./P.D.M.S. copolymers. However, having identified the P.D.M.S. glass transitions at -123°C and knowing that gross incompatibility exists between P.E.S. and P.D.M.S., it can be tentatively suggested that all the copolymers contain, at least to some extent, P.E.S. and P.D.M.S. phases separated on a micro-scale.

3.2.4 Dynamic Mechanical Analysis.

Dynamic Mechanical Analysis (D.M.A.) was investigated as a means of complementing the D.S.C. analysis performed on the P.E.S./P.D.M.S. block copolymers.

By employing a Toyo Baldwin Rheovibron instrument equipped with specially designed shear grips (fig 59), it was hoped to determine a number of parameters. For instance, by plotting tan δ vs temperature it was expected to detect transitions taking place within the copolymers which were not evident when the samples were subjected to analysis by the less sensitive D.S.C. techniques. In particular, it was hoped to identify transitions corresponding to the Tg of the P.E.S. components within the copolymers. Furthermore, it was hoped that D.M.A. could be used to calculate the dynamic shear modulus (G') and dynamic shear loss modulus (G'') for the samples (143).

However, problems were encountered with the Rheovibron, and despite repeated attempts to calibrate the instrument using polystyrene, polysulphone and P.E.S. as standards, no discernable information was obtained. The investigation was reluctantly terminated.

3.2.5 Chemical Composition.

The relative proportions of P.E.S. and P.D.M.S. in the copolymers were determined using both ^{1}H N.M.R. and elemental micro-analysis techniques.

Integration of the P.E.S. and P.D.M.S. peaks on the ^{1}H N.M.R. spectra for the copolymers (figs 48 - 53) enabled the percentage of each component to be determined. A P.E.S.:P.D.M.S. proton ratio of 8:6 was assumed.

Samples of the copolymers were also submitted to Elemental Micro-Analysis Ltd., Beaworthy, Devon, for silicon and sulphur analysis. Unfortunately it was found that silicon could not be determined on these samples due to volatilisation losses. Instead, the sulphur content of these samples was determined in duplicate and the percentage of P.E.S. and hence P.D.M.S. determined using the mean of these two values.

The results obtained from both ^{1}H N.M.R. and elemental analysis techniques are contained in TABLE 15. Also recorded are the values obtained by averaging the results from both analysis methods along with expected percentages calculated from the weights of the P.E.S. and P.D.M.S. oligomers used in each copolymerisation reaction.

In general, the results obtained by averaging the P.E.S. and

P.D.M.S. percentages from ^1H N.M.R. and sulphur analyses are in good agreement with the expected values.

3.2.6 Film Formation and Clarity.

One characteristic possessed by copolymers which sets them apart from simple physical blends (other than those with components of matching refractive indices) is their ability to form films which, if free from contamination, should appear transparent. This transparency is a result of phase separation occurring on a micro-scale rather than a macro-scale.

A number of solvents were identified from which films of the copolymers produced in this investigation could be cast. These included benzene, dichloromethane, chlorobenzene and 1,2-dichlorobenzene.

The transparency of films cast from such solvents varied from sample to sample, but the general trend was for the copolymers with low P.E.S. and P.D.M.S. block molecular weights to be more transparent than those with higher molecular weight blocks. Any cloudiness observed in the copolymer films was ascribed to homopolymer contamination resulting from incomplete copolymerisation.

Attempts to cast films from solutions containing strong hydrogen-bonding solvents such as D.M.S.O., D.M.F., N.M.P. etc., resulted in the apparent breakdown of the copolymer into a simple physical blend comprising a white/grey solid phase dispersed in a transparent viscous liquid. This phenomenon is believed to be a result of the cleavage of the relatively weak $Si\text{-}O\text{-}C_6H_5$ linkage.

3.2.7 Selective Solvation.

One method of differentiating between a copolymer and a simple physical blend is by the use of selective solvation. This technique may also be used to remove unwanted homopolymer contamination from impure copolymers.

Difficulties were encountered in the application of this technique to the P.E.S./P.D.M.S. copolymers under test, however, owing to the rather suspect solvent resistance of these compounds. Strong hydrogen-bonding solvents had to be avoided, and of the solvents that remained, one had to be found that selectively dissolved P.E.S. and another found that selectively dissolved P.D.M.S. without causing degradation of the copolymer.

Diethyl ether [δ = 15.1 $(J/cm^3)^{0.5}$] was found to selectively dissolve P.D.M.S. without causing copolymer breakdown, but considerable difficulty was encountered in locating a solvent which would selectively solubilise P.E.S.

Only one solvent, nitromethane [δ = 26.0 $(J/cm^3)^{0.5}$] was found to possess the desired qualities. However, the use of this compound was considered too hazardous owing to its toxic, flammable and potentially explosive nature. Selective solvation trials were therefore performed using diethyl ether only.

Procedure.

A preweighed extraction thimble was placed into a Sohxlet extractor containing diethyl ether, and the solvent refluxed for 2 hours. After this time, the thimble was removed, reweighed and the weight loss recorded as 'x' grams.

Another preweighed thimble containing a known amount

(approx. 1g) of one of the P.E.S./P.D.M.S. copolymers was treated in an identical manner, and the weight loss recorded as 'y' grams. The weight loss of the copolymer was then determined as 'y-x' grams. This weight loss was then expressed as a percentage of the total P.D.M.S. content of the copolymer (defined in TABLE 15 as the mean of N.M.R. and Sulphur Analysis). This procedure was repeated for the five remaining copolymers.

As a standard, a simple physical blend of P.E.S. ($\bar{M}n \sim 5,000$) and P.D.M.S. ($\bar{M}n \sim 5,000$) was prepared in and cast from dichloromethane. This blend was then subjected to the same procedure as the copolymers. The weight loss was expressed as a percentage of the P.D.M.S. content of the blend.

The results of this analysis (TABLE 16) indicate almost complete solvation of the P.D.M.S. in the simple P.E.S./P.D.M.S. blend, but only partial solvation of the P.D.M.S. in the remaining samples. Thus, further strong evidence has been obtained to support the argument that the materials synthesised during this investigation are, indeed, block copolymers and not simple physical blends of P.E.S. and P.D.M.S.

3.2.8 Morphology.

A Jeol 100CX Transmission Electron Microscope (T.E.M.) was employed in a study of the morphology of the P.E.S./P.D.M.S. copolymers.

Thin films were prepared by dissolving the copolymers in benzene, pouring the solutions onto water, and allowing the benzene to evaporate naturally.

The films were carefully floated onto copper grids prior to

examination on the T.E.M.

Microphase separation was observed in all the copolymers (figs 60-65), the dark domains corresponding to P.D.M.S. and the lighter domains to P.E.S. No selective staining procedures were required, good contrast between the two phases being obtained because of the difference in electron absorption and scattering of the P.E.S. and P.D.M.S. blocks.

A different morphology was observed for each copolymer, for instance, copolymer 1 (fig 60) appeared as small irregular domains of P.D.M.S. in a matrix of P.E.S.

Copolymers 2 and 3 (figs 61 and 62) comprised spherical domains of P.E.S. in a matrix of P.D.M.S., these domains appearing larger in copolymer 3 than in copolymer 2.

Copolymer 4 (fig 63) displayed two distinct morphological characteristics. The bulk of the material appeared as swirls of P.E.S. in a matrix of P.D.M.S. Interspersed with this were droplets of P.D.M.S. containing occluded P.E.S.

In contrast to this, copolymer 5 (fig 64) appeared as swirls of P.D.M.S. in a P.E.S. matrix.

Copolymer 6 (fig 65) displayed similar morphological characteristics to those seen in copolymer 4.

In the past, workers have sought to correlate the observed morphology of microphase separated copolymers with the block sizes and relative volume fractions of the respective components within the copolymer (84 and 113). However, no attempt has been made to perform such an exercise in this study since there is no reason to believe that the microstructures observed in figs 60 to 65 represent the equilibrium microstructures for the respective

copolymers. Indeed, it would be expected that by casting the copolymer films from a different solvent, or heat-treating the samples prior to examination, different microphase-separated morphologies would be observed (84).

In a further study, thin films of copolymers 1,2 and 5 were prepared at room temperature on a Reichert Om U3 ultramicrotome. These films were floated onto copper grids and examined on the T.E.M.

Copolymer 1 (figs 66 and 67) appeared as very small irregular domains of both P.E.S. and P.D.M.S. with no particular species forming a continuous matrix.

In contrast, copolymer 2 (figs 68 and 69) displayed a peculiar crosshatched lamellar morphology.

Copolymer 5 (figs 70 and 71) comprised large spherical or elliptical domains of P.E.S. in a matrix of P.D.M.S.

This study of ultramicrotomed copolymer films complements the study of benzene-cast films in confirming the presence of microphase separation within the copolymers. Even in copolymer 1 containing low molecular weight P.E.S. and P.D.M.S. blocks, a two-phase morphology was observed.

Furthermore, the different morphologies exhibited by ultramicrotomed films as compared with benzene-cast films, support the argument that equilibrium microstructures are not necessarily being observed in this investigation.

3.3 THE IMPACT MODIFICATION OF 4800P GRADE VICTREX WITH P.E.S./P.D.M.S. BLOCK COPOLYMERS.

The P.E.S./P.D.M.S. copolymers, prepared and characterised as described previously, were blended with 4800P grade Victrex in an attempt to improve the notched impact resistance of the commercial polymer.

The preparation and evaluation of these blends is described here.

3.3.1 Blending Procedure.

*Copolymers 1, 2, 5 and 6 were all added to 4800P grade Victrex powder to yield blends containing 2.5% P.D.M.S. This level of P.D.M.S. was chosen after reference to the work performed by Noshay et al on polysulphone (110). These workers found that optimum impact properties of blends of polysulphone with a 50/50 wt % polysulphone/P.D.M.S. copolymer were obtained when 5% of the copolymer (equivalent to 2.5% P.D.M.S.) was present in the system.

Copolymers 3 and 4 were mixed together to yield one large batch of P.E.S. ($\bar{M}n \sim 4,900$)/P.D.M.S. ($\bar{M}n \sim 5,100$) copolymer. By doing this, enough copolymer was made available for studies to be carried out on the effect of increasing P.D.M.S. content on blend impact strength. Blends containing 0.5%, 1.0% and 2.5% P.D.M.S. were prepared using this mixed copolymer and 4800P grade Victrex powder.

One further blend was prepared using 4800P Victrex and linear, hydroxyl-terminated P.D.M.S. ($\bar{M}n \sim 53,000$). Again the P.D.M.S. level in the final mixture was adjusted to 2.5%. The

* small solid pieces

preparation of this simple blend of Victrex and P.D.M.S. provided the potential for a direct comparison to be made between free and copolymerised P.D.M.S. as impact modifiers for Victrex.

Details of all the blend compositions are outlined in TABLE 17.

All the blends prepared were Henschel mixed for 10 minutes at room temperature. This ensured a fine dispersion of the additive throughout the Victrex matrix. After Henschel mixing, the samples were dried in an oven at 150°C overnight.

The blends of copolymers 1 and 2 with Victrex were extruded using a Betol extruder sited at I.C.I., Wilton. A flat temperature profile of 320°C was used on the four barrel zones and the die zone, and a screw speed of 40 r.p.m. employed during the extrusion process.

Attempts to process the other blends using this extruder and these operating conditions were unsuccessful. The presence of the additive appeared to modify the melt flow characteristics of the Victrex matrix so dramatically that 'feeding' problems were encountered at the entrance to the extruder barrel. Attempts to induce feeding by lowering the barrel temperatures in the feed zones and by lowering the screw speed proved unsuccessful.

Further attempts to extrude these blends using a Betol extruder sited at Sheffield City Polytechnic were more successful. By removing the breaker plate in the die zone and using a temperature profile of zone 1 284°C, zone 2 316°C, zone 3 330°C and die zone 322°C, together with a screw speed of 30 r.p.m., all the remaining blends were extruded successfully. The extrudates were then granulated as a necessary pre-requisite

to injection moulding.

Standard Izod and Tensile test pieces were prepared for pure P.E.S. and all the blends using an Arburg All-rounder injection moulding machine (moulding temperature 360°C).

3.3.2 Visual Examination of Blend Test Pieces.

The effect of adding increased amounts of copolymerised P.D.M.S. to P.E.S. was assessed by visual examination of injection moulded tensile test pieces (fig 72).

The normal transparency of pure P.E.S. is lost on addition of 1% copolymerised P.D.M.S. although no significant delamination appears to occur at this additive level. However, when the copolymerised P.D.M.S. level is raised to 2.5%, extensive delamination becomes apparent.

Examination of a X-section of a tensile test piece containing 2.5% copolymerised P.D.M.S. revealed an apparently inhomogeneous sheath/core type morphology (fig 73).

The observed delamination is an indication that, despite the presence of P.E.S. domains in the copolymer, gross incompatibility exists between the P.E.S. matrix and the P.D.M.S. bearing additive.

3.3.3 Blend Melt Rheology.

Introduction

The production of a satisfactory moulding is dependent upon the ability of the plastic to flow and take up the intimate detail of the mould. The viscosity of the melt and the factors affecting it are therefore extremely important parameters in this process.

The melt temperature is one such factor; for instance, the viscosity of 4800P grade P.E.S. is reduced from 1.4×10^3 $N.s.m^{-2}$ to 2.5×10^2 $N.s.m^{-2}$ upon raising the temperature from 320°C to 380°C (Shear rate = 10^3 s^{-1}). At any given temperature, however, the viscosity is also dependent upon shear rate, and a typical thermoplastic will exhibit a decrease in viscosity with increasing shear rate. The very high injection speeds obtainable with modern injection moulding machines can result in the velocity and hence the shear rate of the melt passing through the gates being very great. The melt viscosity in these areas might as a consequence be substantially reduced. The shear rate may indirectly affect the viscosity further, because of the development of frictional heat. With small gates and rapid mould filling, temperature rises of as much as 20°C may be encountered.

The difficulties encountered by the author during the extrusion blending of the various P.E.S./P.E.S.-co-P.D.M.S. compositions prompted an investigation into the unusual rheological characteristics of these materials. It was expected that the data collected would be useful in two respects. Firstly, it would yield information on the effect on melt viscosity of parameters such as copolymer block molecular

weights, overall copolymer molecular weight, and P.D.M.S. content in the blend. Secondly, it would assist in the selection of injection moulding conditions, thus reducing the amount of precious material lost in 'trial and error' optimisation.

The Determination of Melt Viscosity

Both rotational and capillary methods are commonly employed in the measurement of polymer-melt viscosities, although only one, the capillary method allows the determination of melt viscosity at shear rates relevant to processing operations, i.e. 10^1 - 10^4 s^{-1}. For this reason, the capillary method was chosen as the most suitable method for use in these investigations.

A Davenport constant-rate extrusion capillary rheometer was employed to measure melt viscosity. In this type of rheometer, the sample is charged to a vertical heated barrel, at the bottom of which is a capillary die. The sample is allowed to stabilise at the required processing temperature, after which a rigid piston is driven down the barrel towards the capillary at a constant velocity. The volumetric flow rate may be measured directly as the product of piston velocity and barrel cross-sectional area.

The relationship being sought is that between flow rate and pressure drop through the die. In order to measure the pressure drop directly, a transducer is positioned in the barrel wall just above the entrance to the die. By doing this, it is possible to eliminate any pressure drop associated with the flow in the extruder barrel and also friction losses between the

piston and the barrel wall. A derivation of the Poiseuille law for capillary flow has been presented by Brydson (144). This yields the following relationships:-

$$\text{Wall shear stress } \sigma_s = \frac{PR}{2L} \quad (N.m^{-2}) \qquad - (1)$$

$$\text{Wall shear rate } \dot{\gamma} = \frac{4Q}{\pi R^3} \quad (s^{-1}) \qquad - (2)$$

where P is the pressure drop through the die ($N.m^{-2}$)

R is the capillary radius (m)

L is the capillary length (m)

Q is the volume flow rate ($m^3.s^{-1}$)

Viscosity is then given by:-

$$\text{Apparent viscosity } \eta_v = \sigma_s / \dot{\gamma} \qquad - (3)$$

It should be stressed here that the Poiseuille equation yields an apparent rather than a true measure of viscosity. In order to derive the true viscosity, a number of corrections must be made. These have been summarised by Cogswell (145). In practice, it is recommended that only three of the principle sources of error are corrected for. These are a) barrel-height effects and piston friction, b) the ends pressure drop and c) a correction for non-parabolic velocity profile within the die.

As we have already seen, errors due to barrel-height effects and piston friction may be eliminated by the use of a transducer just above the die entrance. Corrections for the remaining two error sources are outlined below.

The ends pressure drop or Bagley correction

Observations by Bagley (146) revealed that a plot of pressure drop versus die length-to-radius (L/R) at a fixed wall shear rate gives a straight line with an intercept such that the shear stress in capillary flow is more correctly:-

$$\sigma_s = R/2(dP/dL) \qquad -(4)$$

It is possible to determine the pressure gradient by using two dies of different lengths, one a long die (L/R = 20) and one an orifice (L/R = 0) such that

$$\sigma_s = (P_L - P_O)\ R/2L \qquad -(5)$$

where P_L = pressure drop through the long die and

P_O = the orifice pressure drop

The velocity profile in the die - Rabinowitsch correction

The pseudoplastic nature of most melts means that the assumed parabolic velocity profile in the die is actually more plug-like. In order to account for this, the Rabinowitsch correction (147) is often made. This correction defines the true wall shear rate as being:-

$$\dot{\gamma}_{true} = \frac{3n + 1}{4n} \quad \frac{4Q}{\pi R^3} \qquad -(6)$$

where n (the pseudoplasticity index) is the power in the relationship

$$\sigma_s \propto \dot{\gamma}^n \qquad -(7)$$

Experimental

The barrel (radius 1cm) of a Davenport constant-rate extrusion capillary rheometer was heated to 320°C and allowed to stabilise at this temperature. A long capillary die (L = 20mm, R = 1mm) was then inserted into the base of the barrel. Granules of the P.E.S./P.E.S.-co-P.D.M.S. blend under test were dried at 130°C for 3 hours, after which they were charged to the rheometer barrel. The granules were compacted and left to attain the operating temperature (a period of 15 minutes was allowed for equilibration). After this time the piston was switched on, a piston speed of 1 cm/min selected and the pressure drop at this speed recorded. Care was taken to ensure that a stable flow had been established before any pressure reading was taken. In a similar manner, pressure readings were obtained for piston speeds of 2, 3, 4, 5 and 10 cm/min. Upon completion of the test, the rheometer barrel was cleaned and the long capillary die replaced with an orifice (L/R = 0). The entire procedure was then repeated using granules of the same blend and the same piston speeds as before.

Wall shear stresses, corrected shear rates and shear viscosities were calculated using the previously discussed relationships developed by Bagley and Rabinowitsch.

RESULTS AND DISCUSSION

Shear Stress/Shear Rate Relationships.

Figures 74 and 75 depict the relationship between wall shear stress and corrected shear rate for the various blends under investigation.

The variation of shear stress with shear rate for these blends was found to be reasonably linear over the range studied, confirming the validity of the power law relationship for these samples. Values of the exponent, n, of the power law relation, $\sigma_s \propto \dot{\gamma}^n$, determined from this data are presented in TABLE 18.

In all cases, the value of n lay below unity, confirming the pseudoplastic nature of the melt for these samples. The variation in the value of n from sample to sample indicated a change in the extent of pseudoplastic behaviour with changing blend composition. In all but one case, however, the addition of P.E.S./P.D.M.S. copolymers or indeed pure linear P.D.M.S. to P.E.S. resulted in the melts becoming more Newtonian in nature.

Shear Viscosity/Shear Stress Relationships.

The viscosity of a single phase polymer melt is often assessed in terms of its relationship to shear rate. Han (148) has shown, however, that for two-phase systems, a more acceptable parameter for correlating rheological data is shear stress. He argues that in two-phase flow, shear rate may not be continuous at the phase interface, but shear stress may be. With this in mind, shear stress was chosen as the parameter to which blend melt viscosity was correlated. The results are expressed graphically in figures 76 and 77.

Immediately evident from figure 76 is the dramatic effect small additions of copolymerised P.D.M.S. have on the shear viscosity of P.E.S. The trend was observed by adding different amounts of the same copolymer to P.E.S. homopolymer to yield blends containing 0.5%, 1.0% and 2.5% copolymerised P.D.M.S.

A considerable reduction in the shear viscosity of P.E.S. was observed even with blends containing as little as 0.5% P.D.M.S. Further reductions resulted as the percentage of P.D.M.S. in the blend increased. The blends also appeared to become more Newtonian with increasing P.D.M.S. levels.

In a further study of these P.E.S./P.E.S.-co-P.D.M.S. blends, an attempt was made to assess the effect of copolymer molecular structure on blend melt viscosity. Shear stress vs shear viscosity relationships were compared for blends containing different copolymers but fixed (2.5%) P.D.M.S. levels (figure 77). The results obtained, however, proved difficult to interpret for a number of reasons.

Firstly, the differing degrees of pseudoplastic behaviour exhibited by the blends made any relationship between viscosities for the various blends dependent upon the stress level at which they were compared.

Secondly, whilst every endeavour was made to ensure that each blend contained exactly 2.5% P.D.M.S., the extent to which this was achieved depended very much upon the accuracy obtained during chemical analysis of the respective copolymers. As we have already seen, small variations in P.D.M.S. content have dramatic effects upon blend melt viscosity. It follows then that even small departures from a 2.5% P.D.M.S. level can produce significant errors in both the position and slope of blend melt

viscosity vs shear stress curves obtained.

Finally, copolymer viscosity and hence blend viscosity can be affected by a number of copolymer molecular parameters including individual block molecular weights, overall copolymer molecular weight and also overall molecular weight distribution. All of these parameters vary from one blend to another, thus making an assesment of the effect of one particular molecular parameter on melt viscosity rather difficult.

Despite these obvious limitations, one general trend can be observed. At the high shear stresses used, higher melt viscosities are obtained for blends containing copolymers with high overall molecular weights or high molecular weight blocks. This phenomenon may be explained in terms of entanglements between polymer chains. For linear polymers, these entanglements increase as the molecular chains become longer, so giving rise to an increase in polymer melt viscosity. Furthermore, for microphase separated copolymers, where blocks in one molecular chain associate and entangle with like blocks of other chains, we can expect the degree of entanglement to increase with increasing block molecular weight. Once again, an increase in viscosity is the likely result.

Although this investigation does not permit an assessment of the relative contributions of block molecular weights and overall copolymer molecular weight to copolymer melt viscosity and hence blend viscosity, it is nonetheless useful as a guide to the amount of control over blend melt viscosity that could be achieved by judicious control of such copolymer molecular parameters.

CONCLUSION.

The rheological properties of P.E.S. are significantly affected when the homopolymer is blended with small amounts of P.E.S./P.D.M.S. block copolymer.

In a study of the effect of the additive on P.E.S. melt rheology, the following observations have been made:-

a) The melt becomes more Newtonian in nature.

b) Only small amounts of additive (0.5%) are required to dramatically reduce the shear viscosity of the melt. Further viscosity reductions occur with increased additive levels.

c) The molecular parameters of the additive appear to affect melt shear viscosity - at high shear stresses, lower viscosities are obtained for blends containing copolymers with low molecular weight blocks or low overall molecular weight.

The findings which complement the work performed by Collyer et al on P.E.S./P.D.M.S. blends (149), are consistent with the formation of a lamellar structure during extrusion where the P.D.M.S. bearing copolymer behaves in a similar manner to linear P.D.M.S., i.e. migrates to the regions of high shear stress to form a P.D.M.S.-rich sheath around a rubber-depleted core.

This migration phenomenon is common to P.D.M.S.-based additives and has been observed by a number of workers. For instance, Legrand and Gaines (150) have shown that block copolymers of bisphenol-A-carbonate and P.D.M.S. concentrate at the surface when they are incorporated at low concentrations in bisphenol-A-carbonate homopolymer. Other workers (151-153) have shown similar behaviour with P.D.M.S.-polystyrene block

copolymers in polystyrene. P.D.M.S.-polyamide block copolymers of this type have also been reported (154).

The dramatic reduction in apparent shear viscosity that results from blending P.E.S./P.D.M.S. block copolymers with pure P.E.S. has been observed in other multiphase blends. Workers investigating EDPM/Viton blends (155) demonstrated that the reported (156) six-fold reduction of viscosity upon addition of one polymer to another is related to the entrance to the capillary effect and the slippage at the wall.

This viscosity reducing effect can be used to advantage. In the injection moulding of these blends, for instance, it is likely that melt temperatures significantly lower than the recommended minimum for P.E.S. may be used without the melt becoming too viscous to process. The use of a low processing temperature is important if the copolymer which is less thermally stable than pure 4800P grade P.E.S., is not to degrade into a simple physical blend of P.E.S. and P.D.M.S.

In conclusion, it should be noted that, although the melt flow studies described here highlight a number of interesting trends, questions must be asked as to the validity of applying mathematical models developed for single phase polymer systems to systems where two or more phases are present. Indeed, in a recent article, Han (157) has pointed out that the shape of the droplets in a two-phase blend when forced to flow through a plunger-type viscometer will vary continuously from the upstream end of the reservoir section (i.e. barrel) to a distance from the capillary entrance where fully developed flow is established. Therefore, taking pressure measurements in the reservoir section and making

the entrance correction (i.e. Bagley correction), with the data obtained in a capillary viscometer, would not give correct information on the bulk viscosity of incompatible polymer blends.

3.3.4 Impact Testing of Blends.

The three most important factors influencing the behaviour of P.E.S. on impact are the notch root radius in the material, the amount of moisture absorbed and the test temperature.

The effects of two of these parameters on the impact strength of the P.E.S./P.E.S.-co-P.D.M.S. blends under study are described here. Pure 4800P P.E.S. is used as a reference material.

Apparent critical strain energy release rates (G_B) have also been obtained for the blends and pure 4800P P.E.S. by the application of linear elastic fracture mechanics theory to Izod impact data. Further information has been obtained by studying the fracture surfaces of the impact specimen.

Instrumentation and Materials Preparation.

A Davenport Izod Impact Tester was used to determine the impact strength of the materials in accordance with BS2782; Part 3; Method 350; 1984. All measurements of impact energy were performed on injection moulded Izod test pieces of nominal size 76.0mm x 12.7mm x 3.2mm into which notches of the appropriate root radii and depth had been machined.

The specimens were secured in the vice of the instrument at a clamping pressure equal to a torque of 2.26Nm, and struck by a pendulum of known energy at a point 22mm above the top plane of the vice (fig 78).

Because of severe limitations on the amount of material available, each recorded impact energy value represents an average taken from the testing of just two specimens.

Effect of Temperature on Izod Impact Strength.

Ideally the effect of temperature on Izod impact strength is investigated using an impact tester equipped with a heating/cooling chamber within which the sample under test would be positioned and allowed to equilibrate at the required temperature prior to testing (158).

At the time of the investigation, such equipment was not available. Consequently, a need arose for an alternative testing procedure to be developed.

Before any impact tests were performed a standard P.E.S./P.E.S.-co-P.D.M.S. test piece was adapted to accept a thermocouple. The tip of the thermocouple was inserted into a hole in the test piece and positioned at a central point on the plane of fracture (fig 79). The test piece was then placed in an oven and allowed to equilibrate at 225°C for 30 minutes after which it was removed and allowed to cool naturally in an environment of air at 25°C.

By monitoring the temperature of the sample at different time intervals, a cooling curve was obtained (fig 80). This curve was used to determine the instantaneous temperature on the plane of fracture at the moment of impact for a number of 4800P P.E.S. and blend 3 Izod test pieces (nominal notch depth 2.5mm, notch root radius 0.25mm, included angle 45°).

By allowing these test pieces to equilibrate at 225°C for 30 minutes and measuring impact energy after different cooling periods (and hence at different temperatures) a relationship between impact strength and temperature was obtained for the two materials (fig 81).

Figure 81 highlights the improved impact strength obtained when 4800P P.E.S. is combined with a P.E.S.-co-P.D.M.S. copolymer to yield a blend containing 2.5% copolymerised P.D.M.S.

An improvement of 30% on the impact strength of pure 4800P P.E.S. is observed in the temperature range 65-145°C. This improvement increases to 43% at 25°C - a pointer perhaps to the possible attainment of considerably enhanced impact strengths at sub-zero temperatures.

The effect of temperature on the Charpy Impact Strength of 4800P P.E.S. has been demonstrated elsewhere for samples with different root radii (159).

For test pieces with a notch root radius of 0.25mm, the impact strength was shown to increase steadily from a value of $\sim 2KJ/m^2$ at -100°C to a maximum of $\sim 5.6KJ/m^2$ at -20°C. The impact strength then appeared to fall steadily to a value $\sim 3.5KJ/m^2$ at 100°C.

This steady decrease in impact strength with increasing temperature is an unusual phenomenon. Nevertheless, it appears from figure 81 that both the pure 4800P P.E.S. and the P.E.S./P.E.S.-co-P.D.M.S. blend examined by the author exhibits this trend over the temperature range 25-145°C.

Effect of Notch Root Radius on Izod Impact Strength.

The effect of notch root radius on Izod impact strength was studied for 4800P P.E.S. and all the P.E.S./P.E.S.-co-P.D.M.S. blends. Undried injection moulded Izod test pieces were prepared with notches of nominal depth 2.5mm, included angle 45° and root radii of 0.1mm, 0.25mm and 1.0mm. These were impact tested at 25°C as previously described. The results are depicted graphically in figures 82-84.

One striking feature of these curves is the dramatic increase in pure 4800P impact strength with increasing root radius (fig 82). With a root radius of 0.1mm, 4800P P.E.S. impact strength is $\sim 2KJ/m^2$. When the root radius is increased to 1mm, the test specimens fail to break completely indicating an impact strength $\geqslant 125KJ/m^2$. This increase in impact strength can be attributed to an increase in the extent of plastic yielding occurring in the material.

Additions of small amounts of P.E.S.-co-P.D.M.S. improve the impact strength of sharply notched P.E.S. However, these additions have a detrimental effect on the impact performance of bluntly notched P.E.S. by apparently suppressing the extent of plastic yielding occurring during fracture.

The magnitude of this effect is determined by the copolymer concentration in the blend. Thus in figures 82 and 83 the curves for pure P.E.S. and blend 4 (containing 0.5% copolymerised P.D.M.S.) are almost identical. As the copolymerised P.D.M.S. concentration is increased through 1.0% (blend 5) to 2.5% (blend 3) so the sharp notch impact strength increases and the blunt notch impact strength decreases.

Another trend is observable in figures 82 to 84. Blends of constant (2.5%) P.D.M.S. content which contain copolymers with high block molecular weights appear to perform better under impact than those containing low block molecular weight copolymers. This effect is particularly noticeable at large notch root radii.

Although it is generally accepted that compatibilisation is assisted by closely matching the matrix molecular weight with that of the 'like' block in a copolymer and that in this case improved impact resistance is observed where the copolymer P.E.S. block molecular weights are closer to that of the P.E.S. matrix ($\bar{M}n \sim 25,000$), it would be presumptious to attribute the improvement in impact strength to improved adhesion between the rubber phase and the P.E.S. matrix. Indeed it is unlikely that any improvement in impact resistance can be attributed to compatibilisation since from figs 82 to 84 it can be seen that blend 9 (containing only high molecular weight linear P.D.M.S. performs better under impact than some blends containing 'compatibilising' P.E.S. copolymer blocks.

3.3.5 Application of Fracture Mechanics to Izod Impact Data.

When any body is stressed, energy is stored in the material as strain energy. If a crack extends, some of the energy is released. By equating the energy released to that absorbed in plastic deformation and creating new fracture surfaces, it is possible to derive a strain energy release rate, G_{I_c}, which should be constant at failure. The general solution for calculating G_{I_c}, which is applicable to any loading system - geometry is:-

$$G_{I_c} = \frac{P_f}{2B} \frac{dC}{da}$$

where P_f is the applied load at failure, B is the thickness, a is the crack length and dC/da is the change in compliance C (1/stiffness), with respect to crack increase, da.

It is often useful to consider the basic fracture mechanics relationships in terms of energy absorbed at fracture rather than the maximum load, or stress achieved, as is conventional.

If attention is confined to linear elastic fracture mechanics (LEFM) then the specimen is assumed to deform in a totally elastic manner so that the compliance C, is a function only of crack length and geometry.

The following relationships may then be employed:-

$$\text{absorbed energy } U = 1/2\ P.x$$

$$\text{and } C = \frac{x}{P}$$

where x is the sample deflection at load P.

Normalising for sample width W we have:-

$$G_{I_c} = \frac{U}{BW} \cdot \frac{1}{C} \cdot \frac{dC}{d(a/W)} = \frac{U}{BWZ}$$

$$\text{or } U = BWZG_{I_c} \qquad -(8)$$

$$\text{where } Z = \left(\frac{1}{C} \cdot \frac{dC}{da}\right) - 1$$

The parameter Z is a geometrical function which can be evaluated for any geometry - Plati and Williams suggest the following expression for Z in the Izod test (160):-

$$Z = \frac{1}{2}\left(\frac{a}{W}\right) + \frac{1}{36}\left(\frac{S}{W}\right)\left(\frac{W}{a}\right) \qquad -(9)$$

By plotting values of absorbed energy U against BWZ for samples containing different crack depths (this varies Z) a linear plot whose slope is the fracture toughness can be derived.

This analysis applies to brittle fracture initiated from a sharp notch.

Determination of Apparent Critical Strain Energy Release Rate.

A value of apparent critical strain energy release rate (G_B) was determined for pure 4800P P.E.S. and all blends.

For each composition, Izod impact test pieces were prepared with notches of different depths, but identical (0.1mm) root radius. The impact energy of these specimens at 27°C was then found.

By employing equation 9 to calculate values of Z and correlating graphically impact energy with BWZ, the linear plot predicted by equation 8 was obtained for each blend (fig 85).

The plots did not pass through the origin as expected. Instead, positive values of U were obtained for BWZ values of zero. This discrepancy has been attributed by Marshall et al to a kinetic energy term U_{ke} , which must be subtracted from the total impact energy in order to obtain the potential energy stored in the specimen when the crack is initiated (161).

Equation 8 then becomes

$$U - U_{ke} = BWZ\ G_{I_c}$$

Values of G_B, calculated as the slope of these plots are contained in TABLE 18.

It is interesting to note from these values that only two blends, i.e. blend 8 containing high block and high overall molecular weight copolymer and blend 9 containing high molecular weight linear P.D.M.S. only, possess G_B values greater than pure 4800P P.E.S. Other blends, particularly blends 4 and 5 containing low levels of copolymerised P.D.M.S. (0.5% and 1.0% respectively)

appear to offer no benefit in terms of resistance to fracture.

It should be stressed here that the G_B values obtained relate to a specific crack root radius (in this case 0.1mm).

It has been demonstrated that the impact strength of P.E.S. and all the blends is increased with increasing notch root radius. This can be attributed primarily to an increase in the extent of plastic yielding occurring within the specimen.

The presence of plastic yielding devalues any analysis based on LEFM, since rather than being independent of geometry, G_B retains a dependence upon root radius.

Nevertheless, much useful information may be obtained from blunt notch testing, for instance, Plati and Williams derived the following relationships for large root radius values (160):-

$$G_B = G_{I_c}\left[\frac{\rho}{8r_p} + \frac{1}{2}\right]$$

$$G_B = \frac{2}{\pi}.Wp.\rho + \frac{G_{I_c}}{2}$$

where r_p is the plastic zone size, ρ is the notch root radius and Wp is the elastic energy per unit volume at yielding.

From these equations, it can be seen that by determining G_B for a range of ρ values, the slope at large ρ values can be used to determine Wp and with G_{I_c} (i.e. G_B as $\rho \rightarrow 0$) we may find r_p.

This more complete analysis, however desirable, could not be performed on the samples under investigation owing to a shortage of material.

3.3.6 Fracture Surface Morphology.

Philips PSEM-500 and Jeol JSM-T100 Scanning Electron Microscopes were employed in an examination of the fracture surfaces obtained during the impact testing of the various blends.

Figures 86 and 87 depict a typical fracture surface obtained upon impact testing a pure P.E.S. test specimen of notch root radius 0.1 mm at 25°C - note the smooth featureless surface.

In contrast a typical P.E.S./P.E.S.-co-P.D.M.S. blend composition (Blend 1) when impact tested under identical conditions yields a fracture surface that displays clear signs of some plastically deformed material and about which are distributed a number of lipped circular depressions (fig 88).

A silicon map of figure 88 shows these depressions to be sites of high silicon and hence high P.D.M.S. concentration (fig 89).

It is interesting that the rubber particles always appear as depressions for there are no matching protuberances to be found, even on the opposite fracture surface.

This phenomenon was observed by Kinloch et al during their investigations into rubber modified epoxy. These workers proposed two possible mechanisms to explain these observations (22). One is that the material undergoes dilation (volume increase) and the matrix plastically elongates approximately in the direction of the maximum tensile stress ahead of the crack i.e. normal to the fracture surface.

The other possible mechanism arises from the rubber phase having a higher coefficient of thermal expansion than the matrix.

If the material is assumed to be relatively stress free at the moulding temperature, then these physical properties would cause the rubbery particles to be under triaxial tension at temperatures below the Tg of the matrix. Thus when a crack passes through the site of a particle, the rubber can contract to give a depression.

Both of these effects could lead therefore to the stress-free volume of the rubbery particles in the fractured surface being less than the cavity in which they are bonded and so give rise to the rubbery particles appearing as circular depressions.

The fact that the coefficient of thermal expansion for P.D.M.S. (300-800 x 10^{-6}/°C) is considerably greater than that for the P.E.S. matrix (55 x 10^{-6}/°C) (162) suggests that the second of these two mechanisms plays an important role in the occurrence of this phenomenon.

The effect of increasing impact test temperature can be observed in figures 90 to 97.

For pure P.E.S., figures 90 and 91 represent the fracture surface obtained when a standard Izod specimen of notch root radius 0.25mm is impact tested at 25°C. Plastic deformation is observable over a large area of the specimen.

When impact tested at 145°C however, ridges appear on the fracture surface (fig 92) - evidence of unstable crack propagation is provided by the presence of crack arrest lines running normal to these ridges (fig 93) - each line corresponding to a jump/arrest event. The large areas of fracture surface between the arrest lines are relatively smooth and featureless.

In contrast, a blend 3 Izod specimen of notch root radius 0.25mm, impact tested at 25°C displays widespread evidence of plastic deformation (figs 94 and 95). At 145°C this plastic deformation is enhanced (fig 96) and extensive drawing of material is observed (fig 97).

The amount of plastic deformation observed on a blend fracture surface at any particular temperature is dependent upon the concentration of copolymer within the blend. Thus we can see an increase in the extent of plastic deformation on moving from pure P.E.S. (fig 98) through blend 4 containing 0.5% copolymerised P.D.M.S. (fig 99) and blend 5 containing 1.0% copolymerised P.D.M.S. (fig 100) to blend 3 containing copolymerised P.D.M.S. at the 2.5% level (fig 101). These observations were made on test specimens of notch root radius 0.1mm, broken at 25°C.

Figures 102 to 106 depict the fracture surfaces obtained for the five remaining blends (all containing 2.5% P.D.M.S.) when Izod specimens of notch root radius 0.1mm were broken at 25°C.

The particle size distribution of the rubber phase was determined for each blend by consideration of void diameters in figures 99 to 106.

In general, the particle diameters lay in the range 1.0 - 5.0μm although for blend 2 (fig 103) particles with diameters up to 12μm were observed.

There appeared to be no significant difference between the particle size distribution obtained for the majority of the blends containing 2.5% copolymerised P.D.M.S. and that obtained for blend 9 (fig 106) containing 2.5% linear P.D.M.S.

The effect of increasing notch root radius is to increase the amount of plastic deformation which occurs during impact. Thus for P.E.S. if fig 107 depicting the fracture surface of a specimen of notch root radius 1.0mm tested at 25°C is compared with fig 86 depicting a specimen of notch root radius 0.1mm tested at the same temperature, then the extent of this additional deformation becomes apparent.

Similarly, if figs 108 and 109 depicting the fracture surface of blend 3 when a specimen of notch root radius 1.0mm is tested at 25°C are compared with figs 94 and 101 depicting specimens of notch root radius 0.25mm and 0.1mm respectively tested at the same temperature then a considerable increase in the amount of plastic deformation can be observed. This increase in plastic deformation is reflected in the greatly increased impact strengths obtained for bluntly notched specimens.

3.3.7 Tensile Testing of Blends.

Discussed here is the effect of temperature on the tensile strength of test specimens manufactured from P.E.S./P.E.S.-co-P.D.M.S. blends. All specimens were tested at a fixed strain rate, pure P.E.S. being used as a reference material. In addition, blend 3 and pure P.E.S. were examined for the effect of strain rate on tensile strength at constant temperature.

Also presented are values of elongation at break and elastic modulus for all the blends at a fixed temperature and strain rate.

Instrumentation and Materials Preparation.

An Instron Model 3111 Tensile Test machine (fig 110) was used to determine the tensile strength, elongation at break and elastic modulus of the materials in accordance with BS 2782 : Part 3 : Method 320B : 1976.

All measurements were performed on undried, injection moulded, broad-waisted dumbbell test pieces (dimensions as in fig 111). Samples were allowed to equilibrate at the appropriate temperature for 10 minutes prior to testing.

Because of constraints on material availability, each recorded value represents an average taken from the testing of just two specimens.

The Effect of Temperature on Tensile Strength.

Using a fixed strain rate of 50mm/min, the tensile strengths of pure P.E.S. and all the P.E.S./P.E.S.-co-P.D.M.S. blends were determined over the temperature range -50°C to +200°C. The results are presented graphically in figs 112 to 115.

For pure P.E.S. (fig 112) the tensile strength drops steadily from ~119 MN/m^2 at -50°C to ~46MN/m^2 at 200°C. This decrease in tensile strength with increasing temperature is also observed in the P.E.S./P.E.S.-co-P.D.M.S. blends (figs 112-115), all of which possess lower tensile strengths than pure P.E.S. over the entire temperature range studied.

Generally, for a given temperature, the tensile strength of a sample appears to depend upon the amount of P.D.M.S. bearing additive present i.e. higher additive levels will result in lower tensile strengths. Nevertheless, even with samples containing 2.5% copolymerised P.D.M.S., deviations from the tensile strength of pure P.E.S. are usually small.

The only exceptions are blends 1,2 and 9, the tensile strengths of which appear little affected by temperature over the range -50°C to +20°C. This results in significant differences occurring between the tensile strengths of these blends and that of pure P.E.S. at lower temperatures.

The Effect of Strain Rate on Tensile Strength.

Specimens of pure P.E.S. and blend 3 were used in an investigation into the effect of strain rate on tensile strength. Strain rates in the range 1-50mm/min were employed at a fixed temperature of 20°C.

For each material, the tensile strength was seen to increase with increasing strain rate (fig 116). The rate of increase was essentially the same for both materials, with blend 3 exhibiting consistently lower tensile strengths than pure P.E.S.

Elastic Modulus and Elongation at Break.

Values of elastic modulus and elongation at break were determined for all the blends at 20°C using a strain rate of 50mm/min (TABLE 19).

Although the addition of copolymerised or linear P.D.M.S. appeared to have little effect on the elastic modulus of P.E.S. (this varied by less than $\pm$4%), the elongation at break was considerably reduced by the addition of as little as 1% copolymerised P.D.M.S.

Figure 117 depicts typical stress/strain curves for pure P.E.S. and blend 5 when tested at 20°C and a strain rate of 50mm/min. The addition of 1% copolymerised P.D.M.S. suppresses the material's ability to plastically deform, and a reduction in the elongation at break from $\sim$24% to $\sim$5% is observed.

3.3.8 Resistance of Blends to Chemical Reagents.

It is important to be aware of any changes that may occur in a polymer's resistance to chemical reagents when even small quantities of a second material are introduced into the matrix. For this reason, a study was performed on the resistance of two blends, blend 8 (containing 2.5% copolymerised P.D.M.S.) and blend 9 (containing 2.5% linear P.D.M.S.), to selected reagents. Pure P.E.S. was used as a reference material.

The following reagents were employed :-

(a) Tap water at 75°C.

(b) Acetone at 20°C.

(c) Toluene at 20°C.

(d) 10% Hydrochloric acid solution at 20°C.

(e) 10% Sodium Hydroxide solution at 20°C.

(f) Shell Tellus 27 oil at 20°C.

Testing was performed generally in accordance with the requirements of American National Standard ASTM D 543-67 (Reapproved 1978).

Standard injection moulded tensile and Izod test specimens of pure P.E.S. and the two blends were weighed and measured dimensionally prior to total immersion in the appropriate reagent for a period of 7 days. During this immersion period, the solutions were agitated every 24 hours.

Upon removal from the solutions, the specimens were dried, immediately re-weighed and examined visually. Impact and tensile tests were then performed on the appropriate samples in accordance with procedures outlined in sections 3.3.4 and 3.3.7. Pure untreated P.E.S. was used as a reference material.

Calculations of impact and tensile strengths were based on cross-sectional measurements made before immersion, with each recorded value representing an average taken from the testing of just two specimens.

The results of the visual examination of the test specimens after immersion are contained in TABLE 20.

All the samples immersed in toluene, 10% HCl, 10% NaOH and Shell Tellus 27 oil appeared unaffected, and only slight whitening of the surface was observed for blends 8 and 9 after exposure to tap water at 75°C. However, immersion in acetone caused the pure P.E.S. specimens to be rounded and cracked at the edges. The surfaces of blends 8 and 9 displayed signs of softening, swelling and whitening.

All the samples tested displayed evidence of weight gain after immersion (TABLES 21 and 22). In all but one reagent, the weight gain was confined to ~1% or less. Surprisingly, for test pieces immersed in aqueous solutions, the presence of hydrophobic P.D.M.S. in blends 8 and 9 did little to prevent the absorption of water.

The most significant weight gain of all was observed in the specimens immersed in acetone. Weight gains of ~7% for pure P.E.S., ~8.5% for blend 8 and ~8% for blend 9 were recorded.

Examination of the impact test data (TABLE 23) showed most of the samples to possess improved impact resistance after immersion in the various reagents. This improvement was very modest for samples immersed in toluene and Shell Tellus 27 oil, but higher for samples immersed in the three aqueous solutions.

Other workers have observed this phenomenon when

investigating pure 4800P grade P.E.S. (159). They detected slight plasticisation of the material when articles were aged in water either at 23°C or 100°C. At 23°C the impact strength during plasticisation was seen to increase to a high value and remain constant thereafter. Ageing at 100°C caused the impact strength to fall initially and then stabilise.

It is probable, therefore, that the enhanced impact strengths obtained by the author when samples were immersed in aqueous solutions were due more to the plasticising effect of the water than to the presence of either HCl or NaOH.

The extent of this improved impact performance is determined by solution temperature i.e. low solution temperature yields high impact resistance; thus the samples immersed in solutions at 20°C performed better than those immersed in tap water at 75°C.

As expected, poor impact performance was observed for pure P.E.S. and blend 9 after immersion in acetone. Surprisingly though, and despite their appearances, acetone - treated blend 8 test pieces performed well under impact. With this one exception, the underlying trend throughout the investigation was for blend 9 test pieces to perform better under impact than blend 8 specimens. The poorest performance was always observed in pure P.E.S. test pieces.

The results of tensile tests performed on test pieces after immersion are contained in TABLE 24. The tests were performed at 20°C and a strain rate of 50mm/min.

As in the impact tests discussed previously, little difference was observed between the tensile strengths of untreated test specimens and those immersed in toluene or Shell

Tellus 27 oil.

All specimens immersed in aqueous solutions displayed moderately lower tensile strengths than their untreated counterparts, whilst those immersed in acetone exhibited considerably reduced performance.

In all solutions, pure P.E.S. displayed higher tensile strengths than blend 9 which, in turn, performed better than blend 8.

To conclude, the findings of this investigation may be summarised as follows :-

(a) Toluene and Shell Tellus 27 oil have little effect on the appearance and mechanical performance of pure P.E.S. or blends 8 and 9.

(b) Immersion of pure P.E.S. and the blends in aqueous solutions results in plasticisation of the polymers. This, in turn, leads to higher impact strengths and lower tensile strengths being obtained.

The magnitude of this effect is determined by the temperature of the solution in which the specimens are immersed - higher impact strengths and lower tensile strengths being obtained at lower temperatures.

Concentrations of 10% HCl or NaOH in solution appear to have little effect on appearance or performance of test specimens.

(c) Acetone has a pronounced effect on the properties of pure P.E.S. and the blends, its absorption into the materials causing swelling and significant weight increases.

Immersion in acetone dramatically decreases tensile and impact strengths - the only exception being the performance of

blend 8 under impact.

(d) Overall, the addition of 2.5% linear or copolymerised P.D.M.S. appears to have little effect on the resistance of P.E.S. to the selected aqueous and organic reagents studied.

3.3.9 Bulk Morphology of Blends.

Thin films of pure P.E.S. and all the blends were prepared at room temperature on a Reichert Om U3 ultramicrotome. These films were floated onto copper grids and examined on a Jeol 100CX Transmission Electron Microscope.

Fig 118 is an electron micrograph of pure P.E.S. - note the smooth defect-free appearance.

In contrast, figs 119-122 depict films of blends 3, 4, 7 and 9 respectively. These are typified by the presence of voids (believed to have been at one time the sites of rubber particles) and small dark areas, spherical or elliptical in shape (believed to be actual rubber particles).

Fig 123 is a high magnification micrograph of a void in blend 3, and figs 124 and 125 are similar micrographs of rubber particles in blends 2 and 8.

Of particular interest is fig 126 depicting a film of blend 8. Here we can see not only the presence of two rubber particles, but also what appears to be phase separation around the site of a void.

Also of interest is fig 127 where we can observe a rubber particle apparently undergoing fracture and contracting to leave a void.

4. SUMMARY AND CONCLUSIONS

The polycondensation of 4,4'-dichlorodiphenyl sulphone with excess bisphenol 'S' in diphenylsulphone solvent was shown to be a simple and effective route to the preparation of hydroxyl-terminated P.E.S. oligomers.

Although separation of the resultant oligomers from the solvent proved to be somewhat laborious, the end products were shown by ^{1}H N.M.R. to be of reasonable purity.

Numerous analytical techniques were successfully employed in the verification of the molecular structure and molecular weight of the oligomers.

Glass transition temperatures were obtained by D.S.C., and T.G.A. used to identify a relationship between thermal stability and oligomer molecular weight (i.e. higher thermal stability is obtained with higher molecular weight polymer).

The failure of one oligomer [P.E.S. $(\bar{DP})_{max}$ 5] to conform to this trend was attributed to the presence of a certain amount of crosslinking within the polymer.

A series of hydroxyl-terminated P.D.M.S. oligomers was obtained, and the molecular weight and molecular structure of these samples established.

The glass transition temperatures of the P.D.M.S. oligomers were determined by D.S.C., and other transitions associated with cold crystallisation and melting also identified.

As with the P.E.S. oligomers, T.G.A. revealed a relationship between thermal stability and oligomer molecular weight.

The modification of hydroxyl-terminated P.D.M.S. with dichlorodimethylsilane to yield chloro-terminated P.D.M.S.

appeared to proceed readily. Subsequent modification of chloro-terminated P.D.M.S. with dimethylamine to yield dimethylamino-terminated also proved possible. In both cases the elimination of water from the reaction vessel was found to be crucial to the success of the procedure, particularly for high molecular weight oligomers where the number of reactive groups was small.

Despite the obvious problems associated with hydrolysis on exposing both chloro- and dimethylamino-terminated P.D.M.S. oligomers to atmospheric moisture, a limited examination of these oligomers was performed. End group substitution was monitored by Infrared spectrophotometry, and viscometric analysis was used to determine the molecular weight of the dimethylamino-terminated oligomers.

The successful preparation of alternating block copolymers of P.E.S. and P.D.M.S. via the silylamine-hydroxyl condensation reaction was found to be dependent upon the solvent system employed.

The large difference in solubility parameter between P.E.S. and P.D.M.S. [Δ = 10.3 $(J/cm^3)^{0.5}$] inhibited the dissolution of both oligomers in any one particular solvent. Nevertheless, 1,2-dichlorobenzene was found to dissolve both P.E.S. and P.D.M.S. oligomers near its boiling point (180°C). Furthermore, the reaction between hydroxyl-terminated P.E.S. and dimethylamino-terminated P.D.M.S. was observed to proceed in this solvent as evidenced by the liberation of the reaction by-product, dimethylamine, from the reaction vessel. Once again, the elimination of water from the system was found to be crucial

to the success of the operation.

Attempts to copolymerise P.E.S. with P.D.M.S. in solvent systems containing strong hydrogen bonding species e.g. dimethylformamide failed. In these systems, hydrogen bonding between the hydrogen atoms in the P.E.S. hydroxyl terminations and the oxygen atoms in the solvent reduces the availability of the phenolic hydrogen for hydrogen bonding with the nitrogen of the silylamine end-groups, and inhibits the susceptibility of the Si to attack from the oxygen atoms of the P.E.S.

Even dichloromethane is unsuitable as a reaction medium in the copolymerisation procedure as it is believed that this solvent forms a complex compound with P.E.S. (141).

A series of six alternating P.E.S./P.D.M.S. copolymers of varying block and overall molecular weight were synthesised using the silylamine-hydroxyl reaction in hot 1,2-dichlorobenzene. These copolymers were characterised using a variety of analytical techniques.

The molecular weight of each copolymer was determined by G.P.C. The results were complemented by viscometric analysis.

The molecular structure of the copolymers was elucidated using Infrared and ^{1}H N.M.R. techniques. Of particular significance was the identification of peaks on the I.R. spectra of all the copolymers attributable to the Si-O str. mode of the $Si-O-C_6H_5$ linkage. The presence of this linkage is proof of the formation of a P.E.S./P.D.M.S. copolymer since it occurs only in this species and in neither of the reacting oligomers.

Further structural confirmation work is currently being performed at I.C.I. Plastics and Petrochemicals Division, Wilton,

where a reliable solvent system is being developed for the ^{29}Si N.M.R. analysis of the copolymers.

Thermal analysis showed the copolymers to possess a thermal stability marginally inferior to that of P.E.S. but comparable or superior to that of linear P.D.M.S. Copolymers possessing higher overall molecular weights also possessed superior high temperature properties.

Copolymer degradation commences between 350-400°C. At these temperatures the copolymers dissociate initially into simple physical P.E.S./P.D.M.S. blends presumably as a result of the cleavage of the relatively weak $Si-O-C_6H_5$ linkage.

D.S.C. analysis revealed the presence of peaks attributable to transitions occurring within the P.D.M.S. component of the copolymers. No transitions attributable to P.E.S. were observable. This phenomenon is believed to be due to the migration of the lower surface energy P.D.M.S. segments to the surface of the copolymer. Once at the surface they act as insulators and inhibit the observation of transitions occurring in the P.E.S. segments of the copolymer.

Evidence that this migration phenomenon exists has been provided by work carried out at I.C.I., Wilton. Here X-ray photoelectron spectroscopy (XPS or ESCA) was performed on copolymer 1 containing 56.5% P.E.S. and 43.5% P.D.M.S. The results showed there to be a Si/S atomic ratio of 5.05 on the copolymer surface as compared to a Si/S ratio of 2.40 within the bulk of the copolymer.

The chemical composition of the copolymers has been verified by ^{1}H N.M.R. and elemental micro-analysis techniques. Good

agreement has been obtained with the expected values.

The existence of a copolymer (as opposed to a simple physical blend) may be verified by its ability to be cast into transparent films and its resistance to attack during the application of selective solvation techniques.

Transparent films of the copolymers were successfully cast from various weak or non hydrogen bonding solvents. Attempts to cast films from solutions containing strong hydrogen bonding solvents resulted in the apparent breakdown of the copolymer into a simple physical blend. This phenomenon may also be attributed to the cleavage of the relatively weak $Si-O-C_6H_5$ linkage.

The identification of P.D.M.S. in the residue after solvent extraction with diethyl ether confirmed the presence of copolymeric structures.

T.E.M. examination of thin films of the copolymers revealed them all to be microphase separated. These findings are in accordance with the theories of Meier (58) and Krause (68-70), both of which predict extensive phase separation at high differential solubility parameter (Δ).

Each copolymer was shown to display a different morphology. However, it is believed that the observed microstructures were non-equilibrated and quite likely to change when equilibrated, say, by thermal treatment.

The above-mentioned copolymers were blended with 4800P grade P.E.S. in an attempt to improve the notched impact resistance of the commercial polymer. Physical and mechanical testing was performed on Izod and Tensile test pieces injection moulded from these blends.

The rheological properties of 4800P grade P.E.S. were shown to be significantly affected by the addition of small amounts of copolymerised P.D.M.S. The findings, which are summarised in section 3.3.3, are consistent with the formation of a lamellar structure during extrusion where the P.D.M.S. bearing copolymer behaves in a similar manner to linear P.D.M.S. and migrates to the regions of high shear stress to form a P.D.M.S.-rich sheath around a rubber depleted core.

Further work should be performed on melt blended P.E.S./ P.E.S.-co-P.D.M.S. extrudates in order to assess quantitatively any P.D.M.S. migration that may occur in these systems. EDAX, Auger and ESCA analyses may be useful in such an investigation.

Test pieces injection moulded from granulated P.E.S./ P.E.S.-co-P.D.M.S. extrudates displayed evidence of surface delamination (fig 72) particularly at higher (2.5%) P.D.M.S. levels. This, once again, has been attributed to the migration of the P.D.M.S. bearing additive to the surface of the moulding. This migration should also be confirmed by the application of EDAX, Auger and ESCA techniques to blend test pieces.

The impact strength of 4800P P.E.S. was shown to be improved by the addition of 2.5% copolymerised P.D.M.S. For test pieces with a root radius of 0.25mm, nominal notch depth 2.5mm and included angle 45°, a 30% increase in impact strength was observed in the temperature range 65-145°C. This improvement increased to 43% at 25°C, and indications are that greater improvements may be possible at sub-zero temperatures. Further investigations should be carried out on the impact performance of these P.E.S./P.E.S.-co-P.D.M.S. blends at temperatures down to

the Tg of P.D.M.S. (-123°C) and preferably lower.

The effect of notch root radius on the impact strengths of 4800P P.E.S. and the blends is remarkable. Additions of small amounts of P.E.S.-co-P.D.M.S. improve the impact strength of sharply notched P.E.S. at 25°C. However, these additions have a detrimental effect on the impact performance of bluntly notched P.E.S. by apparently suppressing the extent of plastic yielding occurring during fracture. The magnitude of this effect is determined by the level of additive in the blend, i.e. higher P.D.M.S. levels yield higher sharp notch impact strengths but lower blunt notch impact strengths.

Blends containing copolymers with high block molecular weights perform better under impact than those containing low block molecular weight copolymers. Nevertheless, any increase in the impact strength of P.E.S. by the addition of P.E.S./P.E.S.-co-P.D.M.S. copolymers cannot be attributed to the compatibilising effect of the P.E.S. blocks in the copolymers since blends containing only 4800P P.E.S. and linear P.D.M.S. performed better under impact than some blends containing P.E.S. copolymer blocks.

Values of Apparent Critical Strain Energy Release Rate (G_B) obtained for 4800P P.E.S. and all the blends by the application of Linear Elastic Fracture Mechanics to sharp notch Izod impact data (TABLE 19) confirmed the marginally superior impact properties obtainable through the addition of linear P.D.M.S. rather than copolymerised P.D.M.S.

Impact tests performed at I.C.I., Wilton, showed the notched impact strength of 4800P P.E.S. to be dramatically increased by

the presence of the additives.

By carrying out notched Izod impact tests to the ASTM standard, the results contained in TABLE 26 were obtained.

Blends 7 and 8, both containing 2.5% copolymerised P.D.M.S., displayed impact strength increases of 136% and 122% respectively over pure 4800P P.E.S. Blend 9 containing 2.5% linear P.D.M.S. showed a similar increase of 125%. Even blend 4 containing just 0.5% copolymerised P.D.M.S. displayed an impact strength 124% better than that of pure P.E.S.

Although these results do not indicate any significant difference between the impact resistance of blends containing copolymerised or linear P.D.M.S., it is worthwhile noting that, under certain conditions, the impact strength of pure P.E.S. can be more than doubled by the addition of as little as 0.5% copolymerised P.D.M.S.

Examination of the fracture surfaces obtained during the impact testing of the various blends revealed a number of interesting trends.

For a small notch root radius, the presence of linear or copolymerised P.D.M.S. appears to promote plastic deformation within the P.E.S. matrix. The extent of this plastic deformation is increased with increasing temperature and increasing rubber content. Increasing the notch root radius will also increase the extent of plastic deformation observed.

The rubber particles always appear on the blend fracture surfaces as lipped circular depressions of typical diameter 1μm.

By combining the information obtained during the impact testing of the blends with that obtained from fracture surface

studies it is possible to explain the observed phenomena.

A toughening mechanism is proposed whereby the deformation processes are (a) localised cavitation in the rubber or at the particle / matrix interface and (b) plastic shear yielding in the P.E.S. matrix, the latter being the main source of energy dissipation.

Sharply notched pure 4800P P.E.S. requires very little energy for crack initiation and propagation. The resulting fracture surface is smooth and featureless.

The addition of small quantities of copolymerised or linear P.D.M.S. to P.E.S. increases the impact resistance in sharply notched specimens because of the dissipation of energy through localised cavitation accompanied by limited localised matrix yielding - in effect the particles present a barrier to crack propagation.

On the other hand, bluntly notched or unnotched pure P.E.S. requires considerable energy input for crack initiation, and extensive plastic deformation is observed in such specimens when impact tested.

The presence of small quantities of copolymerised or linear P.D.M.S. in such specimens will promote crack initiation but once again retard crack propagation. In this instance the reduction in impact strength resulting from reduced gross plastic deformation is not counterbalanced by the increase in impact strength due to localised cavitation and yielding. Reduced impact performance is the result.

The relative contribution of each of these mechanisms to the overall impact strength is determined by the amount of the

rubber-bearing additive present. For sharply notched specimens, increasing the additive concentration increases the impact strength. For bluntly notched specimens the converse is true.

The results of tensile tests performed on pure 4800P P.E.S. and all the blends support the proposed toughening mechanism. Under uniaxial tension (strain rate 50mm/min, temperature 20°C) unnotched P.E.S. is tough and exhibits considerable elongation prior to failure. The addition of small amounts of P.D.M.S. in both copolymerised and linear forms results in a modest decrease in P.E.S. tensile strength, but a significant decrease in its elongation at break. Clearly the P.D.M.S. bearing additives are promoting crack initiation and inhibiting the extensive plastic deformation observed in pure P.E.S. The effect is comparable to that observed upon impact testing unnotched P.E.S. and blend specimens.

Investigations were performed into the effect of the P.D.M.S. bearing additives on the resistance of P.E.S. to selected organic and inorganic reagents. The findings, which are summarised in section 3.3.8, indicate that the presence of up to 2.5% copolymerised or linear P.D.M.S. has no significant effect on the mechanical performance of P.E.S. after immersion in the reagents for a period of 7 days.

To conclude, it has been shown that it is possible to synthesise P.E.S.-co-P.D.M.S. $(A\text{-}B)_n$ type block copolymers by the silylamine-hydroxyl condensation reaction. Furthermore it has been shown that these copolymers improve the impact strength of sharply notched P.E.S. when added in small quantities.

However, investigations have shown that the magnitude of

this improved impact performance is no greater than that observed when linear P.D.M.S. is added to P.E.S. The reason proposed for this is P.D.M.S. migration.

Analysis has revealed that P.D.M.S. domains migrate to the surface of the P.E.S-co-P.D.M.S. copolymers. Once there they inhibit the formation of the desired adhesive bond between the P.E.S. matrix and the P.E.S. domains in the copolymer. Thus the adhesion obtained between the P.E.S.-co-P.D.M.S. copolymers and the P.E.S. matrix is little better than that obtained between linear P.D.M.S. and the P.E.S. matrix.

A solution to this problem would be to inhibit the migration of P.D.M.S. to the surface during copolymer synthesis. This could perhaps best be achieved by crosslinking the P.D.M.S. component during the copolymerisation reaction itself.

The phenomenon of P.D.M.S. migration is not only confined to P.D.M.S. domains within a copolymer, for it also occurs within the blends themselves. In all the P.E.S.-co-P.D.M.S./P.E.S. blends and the linear P.E.S./P.D.M.S. blend, migration of the P.D.M.S. bearing additive to the surface occurred. This resulted in delamination being observed, particularly in the blends with higher P.D.M.S. contents.

How, then, is this prevented? Would, for instance, the crosslinking of the P.D.M.S. phase during copolymerisation also inhibit the migration of the resultant copolymer to the surface in a P.E.S.-co-P.D.M.S./P.E.S. blend? Would the crosslinking of P.D.M.S. during blending with P.E.S. prevent P.D.M.S. migration in a simple P.E.S./P.D.M.S. blend? These are just two of the questions future workers must answer if optimum impact

REFERENCES

1) R.Y. TING, J. Mater. Sci., 16, 3059 (1981).

2) C.R. HART, I.C.I. communication PL/742/C; J.W. EDWARDS and D. PITMAN, I.C.I. communication PLS/3401/35/B.

3) R. MAY, I.C.I. communication PLS/3401/53/B.

4) E.H. MERZ, G.C. CLAVER and M. BAER, J. Polym. Sci., 22, 325 (1956).

5) S. KUNZ-DOUGLASS, P.W.R. BEAUMONT and M.F.ASHBY, J. Mater. Sci., 15, 1109, (1980).

6) A.F. YEE, J. Mater. Sci., 12, 757 (1977); M.A. MAXWELL and A.F. YEE, Polym. Eng. Sci., 21, 205 (1981).

7) G.C. BRAGAW, Adv. Chem. Ser., 99, 86 (1971).

8) C.B. BUCKNALL, 'TOUGHENED PLASTICS', Applied Science, London, (1977).

9) C.B. BUCKNALL in 'POLYMER BLENDS', Vol 2, Eds. D.R. PAUL and S. NEWMAN, Academic, New York, 91 (1978).

10) J.A. SCHMITT and H. KESKKULA, J. App. Polym. Sci., 3, 132 (1960).

11) C.B. BUCKNALL and R.R. SMITH, Polymer, 6, 437 (1965).

12) C.B. BUCKNALL and D. CLAYTON, J. Mater. Sci., 7, 202 (1972).

13) C.B. BUCKNALL, D. CLAYTON and W.E. KEAST, J. Mater. Sci., 7, 1443 (1972).

14) C.B. BUCKNALL, D. CLAYTON and W.E. KEAST, J. Mater. Sci., 8, 514 (1973).

15) C.B. BUCKNALL and I.C. DRINKWATER, J. Mater. Sci., 8, 1800 (1973).

16) S. NEWMAN in 'POLYMER BLENDS', Vol 2, Eds. D.R. PAUL and S. NEWMAN, Academic, New York, 63 (1978).

17) S. NEWMAN, Polym. Plast. Technol. Eng., 2, 67 (1973).

18) S. NEWMAN and S. STRELLA, J. App. Polym. Sci., 9, 2297 (1965).

19) S. STRELLA, J. Polym. Sci., 4, 528 (1966).

20) J.N. SULTAN, R.C. LIABLE and F.J. McGARRY, App. Polym. Symp., 16, 127 (1971).

21) R.P. PETRICH, Polym. Eng. Sci., 12, 757 (1972).

22) A.J. KINLOCH, S.J. SHAW, D.A. TOD and D.L. HUNSTON, Polymer, 24, 1341 (1983).

23) R.P. PETRICH, Polym. Eng. Sci., 13, 248 (1973).

24) S. WU, J. Polym. Sci., Polym. Phys. Edn., 21, 699 (1983).

25) P.J. HINE, R.A. DUCKETT and I.M. WARD, Polymer, 22, 1745 (1981).

26) C.F. PARSONS and E.L. SUCK, A.C.S. Adv. Chem. Ser., 99, 340 (1971).

27) M. MATSUO, Polym. Eng. Sci., 9, 206 (1970).

28) P. BEAHAN, A. THOMAS and M. BEVIS, J. Mater. Sci., 11, 1207 (1976).

29) E.J. KRAMER in 'POLYMER COMPATIBILITY AND INCOMPATIBILITY : PRINCIPLES AND PRACTICES', Ed. K. SOLC, M.M.I. Press, Midland, M.I., U.S.A., (1982).

30) B.D. LAUTERWASSER and E.J. KRAMER, Phil Mag, 39A, 469 (1979).

31) A.M. DONALD and E.J. KRAMER, J. App. Polym. Sci., 27, 3729 (1982).

32) A.M. DONALD and E.J. KRAMER, J. Mater. Sci., 17, 2351 (1982).

33) R.N. HAWARD and J. MANN, Proc. Roy. Soc. London Ser A282, 120 (1964).

34) S. KOIWA, J. App. Polym. Sci., 19, 1625 (1975).

35) S. WU, Polymer, 26, 1855 (1985).

36) R.L. SCOTT, J. Chem. Phys., 17, 279 (1949).

37) P.J. FLORY, 'PRINCIPLES OF POLYMER CHEMISTRY', CHAP. 12, 495, Cornell, Ithaca, New York, (1953).

38) J.H. HILDEBRAND and R.L. SCOTT, 'THE SOLUBILITY OF NON-ELECTROLYTES', Third Edn., Reinhold, New York, (1950).

39) F.C. STEHLING, T. HUFF, C.S. SPEED and G. WISSLER, J. App. Polym. Sci., 26, 2693 (1981).

40) S. KRAUSE, J. Macromol. Sci., Rev. Macromol. Chem., C7(2), 251 (1972).

41) E. HELFAND and Y. TAGAMI, J. Polym. Sci., 9B, 741 (1971).

42) R. PORTER and J. JOHNSON, Chem. Rev., 66, 1 (1966).

43) C.A. CRUZ, J.W. BARLOW and D.R. PAUL, Macromolecules, 12, 726 (1979).

44) M.T. SHAW, J. App. Polym. Sci., 18, 449 (1974).

45) L.P. McMASTER, Macromolecules, 6, 760 (1973).

46) T.K. KWEI, T. NISHI and R.F. ROBERTS, Macromolecules, 7, 667 (1974).

47) O. OLABISI, Macromolecules, 8, 316 (1975).

48) R.G. KIRSTE and B.R. LEHNEN, Makromol. Chem., 177, 1137 (1976).

49) W.A. KRAUSE, R.G. KIRSTE, J. HAAS, B.J. SCHMITT and D.J. STEIN, Makromol. Chem., 177, 1145 (1976).

50) H. MORAWETZ and F. AMRANI, Macromolecules, 11, 281 (1978).

51) C.W. FRANK and M.A. GASHGARI, Macromolecules, 12, 163 (1979).

52) S. WU in 'POLYMER BLENDS', Vol 1, Eds. D.R. PAUL and S. NEWMAN, Academic Press, New York, (1978).

53) D.R. PAUL in 'POLYMER BLENDS', Vol 2, Eds. D.R. PAUL and S. NEWMAN, Academic Press, New York, (1978).

54) G. REISS and Y. JOLIVET in 'COPOLYMERS, POLYBLENDS AND COMPOSITES', Ed. N.A.J. PLATZER, Adv. Chem. Ser. 142, 243. Amer. Chem. Soc., Washington D.C., (1975).

55) L. DEL GIUDICE, R.E. COHEN, G. ATTALLA and F. BERTINOTTI, J. App. Polym. Sci., 30, 4305 (1985).

56) G. KRAUS in 'POLYMER BLENDS', Vol 2, CHAP 18, Eds. D.R. PAUL and S. NEWMAN, Academic Press, New York, (1978).

57) D.J. MEIER, J. Polym. Sci., Pt C 26, 81 (1969).

58) D.J. MEIER, Polym. Prepr. Amer. Chem. Soc., Div. Polym. Chem., 15, 171 (1974).

59) D.J. MEIER in 'BLOCK AND GRAFT COPOLYMERS', Eds. J.J. BURKE and V. WEISS, 105, Syracuse Univ. Press, Syracuse, New York, (1973).

60) E. HELFAND in 'RECENT ADVANCES IN POLYMER BLENDS, GRAFTS AND BLOCKS', Ed. L.H. SPERLING, Plenum Press, N.Y. and London, (1974).

61) E. HELFAND, Accs. Chem. Res., 8, 295 (1975).

62) E. HELFAND and A.M. SAPSE, J. Chem. Phys., 62(4), 1327 (1975).

63) E. HELFAND, J. Chem. Phys., 62(3), 999 (1975).

64) E. HELFAND, Macromolecules, 8, 552 (1975).

65) E. HELFAND and Z.R. WASSERMAN, Macromolecules, 9, 879 (1976).

66) E. HELFAND and Z.R. WASSERMAN, Macromolecules, 11, 960 (1978).

67) E. HELFAND and Z.R. WASSERMAN, Macromolecules, 13, 994 (1980).

68) S. KRAUSE, J. Polym. Sci. Pt. A-2, 7, 249 (1969).

69) S. KRAUSE, Macromolecules, 3, 84 (1970).

70) S. KRAUSE in 'BLOCK AND GRAFT COPOLYMERS', Eds. J.J. BURKE and V. WEISS, 143, Syracuse Univ. Press, Syracuse, (1973).

71) D.F. LEARY and M.C. WILLIAMS, J. Polym. Sci. Pt. B, 8, 335, (1970).

72) D.F. LEARY and M.C. WILLIAMS, J. Polym. Sci., Polym. Phys. Edn., 11, 345, (1973).

73) D.F. LEARY and M.C. WILLIAMS, J. Polym. Sci., Polym. Phys. Edn., 12, 265, (1974).

74) T. SOEN, T. INOUE, K. MIYOSHI and H. KAWAI, J. Polym. Sci. Pt. A-2, 10, 1757 (1972).

75) D.G. LEGRAND, Polym. Prepr., Amer. Chem. Soc., Div. Polym. Chem., 11, 434 (1970).

76) C.P. HENDERSON and M.C. WILLIAMS, J. Polym. Sci., Polym. Phys. Edn., 23, 1001 (1985).

77) A. DOUY, R. MAYER, R. ROSSI and B. GALLOT, Mol. Cryst. Liq. Cryst., 7, 103 (1971).

78) T. HASHIMOTO, K. NAGATSCHI, A. TODO, H. HASEGAWA and H. KAWAI, Macromolecules, 7, 364 (1974).

79) J.E. McGRATH, M. MATZNER, L.M. ROBESON and R. BARCLAY JR., J. Polym. Sci., Polym. Symp., 60, 29 (1977).

80) D.J. MEIER, Polym. Prepr., 18, 340 (1977).

81) K.M. HONG and J. NOOLANDI, Macromolecules, 14, 727 (1981).

82) J. NOOLANDI and K.M. HONG, Macromolecules, 15, 482 (1982).

83) M.D. WHITMORE and J. NOOLANDI, Macromolecules, 18, 2486 (1985).

84) T. INOUE, T. SOEN, T. HASHIMOTO and H. KAWAI, J. Polym. Sci. Pt. A-2, 17, 1283 (1969).

85) T. INOUE, T. SOEN, T. HASHIMOTO and H. KAWAI, Macromolecules, 3, 87 (1970).

86) A. DOUY and B.R. GALLOT, Mol. Cryst. Liq. Cryst., 14, 191 (1971).

87) G.E. MOLAU and W.M. WITBRODT, Macromolecules, 1, 260 (1968).

88) E.B. BRADFORD in 'COLLOIDAL AND MORPHOLOGICAL BEHAVIOUR OF BLOCK AND GRAFT COPOLYMERS', Ed. G.E. MOLAU, Plenum Press, N.Y., 21 (1971).

89) G.C. EASTMOND and D.G. PHILLIPS in 'POLYMER ALLOYS', Eds. D. KLEMPNER and K.C. FRISCH, Plenum Press, N.Y., 141 (1977).

90) G.C. EASTMOND and D.G. PHILLIPS, Polymer, 20, 1501 (1979).

91) A. NOSHAY and J.E. McGRATH, 'BLOCK COPOLYMERS', Academic Press, N.Y., (1977).

92) J. KOHLER, G. RIESS and A. BANDERET, Eur. Polym. J., 4, 173 (1968).

93) C.W. CHILDERS, G. KRAUS, J.T. GRUVER and E. CLARK in 'COLLOIDAL AND MORPHOLOGICAL BEHAVIOUR IN BLOCK AND GRAFT COPOLYMERS', Ed. G.E. MOLAU, Plenum Press, N.Y., 193 (1971).

94) C.W. CHILDERS, U.S. PATENT Nº 3,429,951, Feb 25 (1969).

95) R.R. DURST, R.M. GRIFFITH, A.J. URBANIC and W.J. VAN ESSEN, Amer. Chem. Soc. Organ. Coatings Plast. Div., Prepr. 34(2), 320 (1974).

96) A.L. BULL and G. HOLDEN, J. Elastomers. Plast., 9, 281 (1977).

97) E. CLARK and C.W. CHILDERS, J. App. Polym. Sci., 22, 1081 (1978).

98) A. NOSHAY, M. MATZNER, B.P. BARTH and R.K. WALTON, U.S. PATENT Nº 3,536,657, Oct 27 (1970).

99) A. NOSHAY, M. MATZNER and C.N. MERRIAM, U.S. PATENT Nº 3,539,656, Nov 10 (1970).

100) A. NOSHAY, M. MATZNER and C.N. MERRIAM, U.S. PATENT Nº 3,539,657, Nov 10 (1970).

101) A. NOSHAY, M. MATZNER and C.N. MERRIAM, Polym. Prepr., Amer. Chem. Soc., Div. Polym. Chem., 12(1), 247 (1971).

102) A. NOSHAY, M. MATZNER and C.N. MERRIAM, J. Polym. Sci., Pt. A-1, 9(11), 3147 (1971).

103) A. NOSHAY, M. MATZNER and T.C. WILLIAMS, Ind. Eng. Chem., Prod. Res. Dev., 12(4), 268 (1973).

104) L.M. ROBESON, A. NOSHAY, M. MATZNER and C.N. MERRIAM, Angew. Makromol. Chem., 29/30, 47 (1973).

105) M. MATZNER, A. NOSHAY and J.E. McGRATH, Polym. Prepr., Amer. Chem. Soc., Div. Polym. Chem., 14(1), 68 (1973).

106) M. MATZNER, A. NOSHAY, L.M. ROBESON, C.N. MERRIAM, R. BARCLAY JR. and J.E. McGRATH, App. Polym. Symp., 22, 143 (1973).

107) M. MATZNER, A. NOSHAY, D.I. SCHOBER and J.E. McGRATH, Ind. Chim. Belge., 38, 1104 (1973).

108) A. NOSHAY and M. MATZNER, Angew. Makromol. Chem., 37, 215 (1974).

109) A. NOSHAY, M. MATZNER, B.P. BARTH and R.K. WALTON, Amer. Chem. Soc., Div. Org. Coat. Plast. Chem. Prepr., 34(2), 217 (1974).

110) A. NOSHAY, M. MATZNER, B.P. BARTH and R.K. WALTON in 'TOUGHNESS AND BRITTLENESS OF PLASTICS', Eds. DEANIN and CRUGNOLA.

111) A. NOSHAY, M. MATZNER and L.M. ROBESON, J. Polym. Sci. Polym. Symp. 60, 87 (1977).

112) H.A. VAUGHN, J. Polym. Sci., Pt. B, 7, 569 (1969).

113) J.C. SAAM and F.W.G. FEARON, Ind. Eng. Chem. Prod. Res. Develop., 10, 10 (1971).

114) J.C. SAAM, A.H. WARD and F.W.G. FEARON in 'POLYMERISATION REACTIONS AND NEW POLYMERS', Ed. N.A.J. PLATZER, Adv. Chem. Ser., 129, Amer. Chem. Soc., Washington D.C., 239 (1973).

115) M. MORTON, Y. KESTEN and L.J. FETTERS, Polym. Prepr., Amer. Chem. Soc., Div. Polym. Chem., 15(2), 175 (1974).

116) R.P. KAMBOUR in 'BLOCK POLYMERS', Ed. S.L. AGGERWAL, Plenum Press, 263 (1970).

117) W.D. MERRITT JR. ET AL, U.S. PATENT N° 3,821,325, June 28 (1974).

118) A. NOSHAY, M. MATZNER, G. KAROLY and G.B. STAMPA, J. App. Polym. Sci., 17, 619 (1973).

119) S.H. TANG, E.A. MEINECKE, J.S. RIFFLE and J.E. McGRATH, Rubber Chem. and Tech., 53, 1160 (1980).

120) C.U. PITTMAN, W.J. PATTERSON and S.P. McMANUS, J. Polym. Sci., Polym. Chem. Edn., 14, 1715 (1976).

121) J.J. O'MALLY, T.J. PACANSKY and W.J. STAUFFER, Macromolecules, 10(6), 1197 (1977).

122) Y. NAGASE, T. MASUBUCHI, K. IKEDA and Y. SEKINE, Polymer, 22, 1607 (1981).

123) T. DUMELOW, S.R. HOLDING, L.J. MAISEY and J.V. DAWKINS, Polymer, 27, 1170 (1986).

124) E. SHCHORI and J.E. McGRATH, J. App. Polym. Sci., App. Polym. Symp., 34, 103 (1978).

125) A.J. WNUK, T.F. DAVIDSON and J.E. McGRATH, J. App. Polym. Sci., App. Polym. Symp., 34, 89 (1978).

126) G.D.B. VAN HOUWELINGEN, Analyst, 106, 1057 (1981).

127) E.A. WILLIAMS, J.D. CARGIOLI and S.Y. HOBBS, Macromolecules, 10(4), 782 (1977).

128) R.W. RICHARDS and J.L. THOMASON, Polymer, 24, 1089 (1983).

129) J.T. KOBERSTEIN and R.S. STEIN, J. Polym. Sci., Polym. Phys. Edn., 21, 1439 (1983).

130) M.E.A. CUDBY, R.G. FEASEY, B.E. JENNINGS, M.E.B. JONES and J.B. ROSE, Polymer, 6, 589 (1965).

131) R.N. JOHNSON, A.G. FARNHAM, R.A. CLENDINNING, W.F. HALE and C.N. MERRIAM, J. Polym. Sci., Pt. A-1, 5, 2375 (1967).

132) T.E. ATTWOOD, D.A. BARR, T. KING, A.B. NEWTON and J.B. ROSE, Polymer, 18, 359 (1977).

133) H.R. KRICHELDORF and G. BIER, J. Polym. Sci., Polym. Chem. Edn., 21, 2283 (1983).

134) R. VISWANATHAN, B.C. JOHNSON and J.E. McGRATH, Polymer, 25, 1827 (1984).

135) M.K. COX, I.C.I. p.l.c., Private communication.

136) V.Z. DEAL and G.E.A. WYLD, Anal. Chem., 27, 47 (1955).

137) M.K. COX, I.C.I. p.l.c., Private communication.

138) B. CROSSLAND, G.J. KNIGHT and W.W. WRIGHT, Brit. Polym. J., 18, 156 (1986).

139) G. MEYERHOFF, Forshr. Hochpolym.-Forsch., 3, 59 (1961).

140) C.L. LEE, O.K. JOHANNSON, O.L. FLANINGAM and P. HAHN, Amer. Chem. Soc., Div. Polym. Chem., Polym. Prepr., 10(2), 1311 (1969).

141) M.K. COX, I.C.I. p.l.c., Private communication.

142) R.L. SCHMITT, J.A. GARDELLA Jr., J.H. MAGILL, L. SALVATI Jr. and R.L. CHIN, Macromolecules, 18, 2675 (1985).

143) T. MURAYAMA in 'DYNAMIC MECHANICAL ANALYSIS OF POLYMERIC MATERIAL', Elsevier Scientific, Amsterdam (1978).

144) J.A. BRYDSON, 'FLOW PROPERTIES OF POLYMER MELTS', 2nd Edn., Godwin (1981).

145) F.N. COGSWELL, 'POLYMER MELT RHEOLOGY', Godwin (1981).

146) E.B. BAGLEY, J. App. Phys., 28, 624 (1957).

147) B. RABINOWITSCH, as described by J.A. BRYDSON in 'FLOW PROPERTIES OF POLYMER MELTS', 2nd Edn., Chapter 2, Godwin (1981).

148) C.D. HAN and Y.W. KIM, J. App. Polym. Sci., 19, 2831 (1975).

149) A.A. COLLYER, D.W. CLEGG, G.H. FRANCE, M. MORRIS, K. BLAKE, D.J. GROVES and M.K. COX., Proc. IX Intl. Congress on Rheology, Mexico, 543 (1984).

150) D.G. LEGRAND and G.L. GAINES Jr., Amer. Chem. Soc., Polym. Prepr., 11, 442 (1970).

151) G.L. GAINES Jr. and G.W. BENDER, Macromolecules, 5, 82 (1972).

152) M.J. OWEN and T.C. KENDRICK, Macromolecules, 3, 458 (1970).

153) M.P.L. HILL, P.L. MILLARD and M.J. OWEN, Amer. Chem. Soc., Org. Coating and Plas. Prepr., 34, 334 (1974).

154) M.J. OWEN and J.THOMPSON, Br. Polym. J., 4, 297 (1972).

155) R. KANN and M.T. SHAW, Amer. Chem. Soc., Div. Polym. Chem., 22, 365 (1981).

156) C.K. SHIH, Polym. Eng. Sci., 16, 742 (1976).

157) C.D. HAN, Polym. Eng. Rev., 1, 363 (1981).

158) E. PLATI and J.G. WILLIAMS, Polymer, 16, 915 (1975).

159) 'VICTREX' POLYETHERSULPHONE TECHNICAL NOTE VX101, 3rd Edn., I.C.I. Ltd. (1978).

160) E. PLATI and J.G. WILLIAMS, Polym. Eng. Sci., 15(6), 470 (1975).

161) G.P. MARSHALL, J.G. WILLIAMS and C.E. TURNER, J. Mater. Sci., 8, 949 (1973).

162) MODERN PLASTICS ENCYCLOPAEDIA, 62(10A), Mc.Graw - Hill (1985-86).

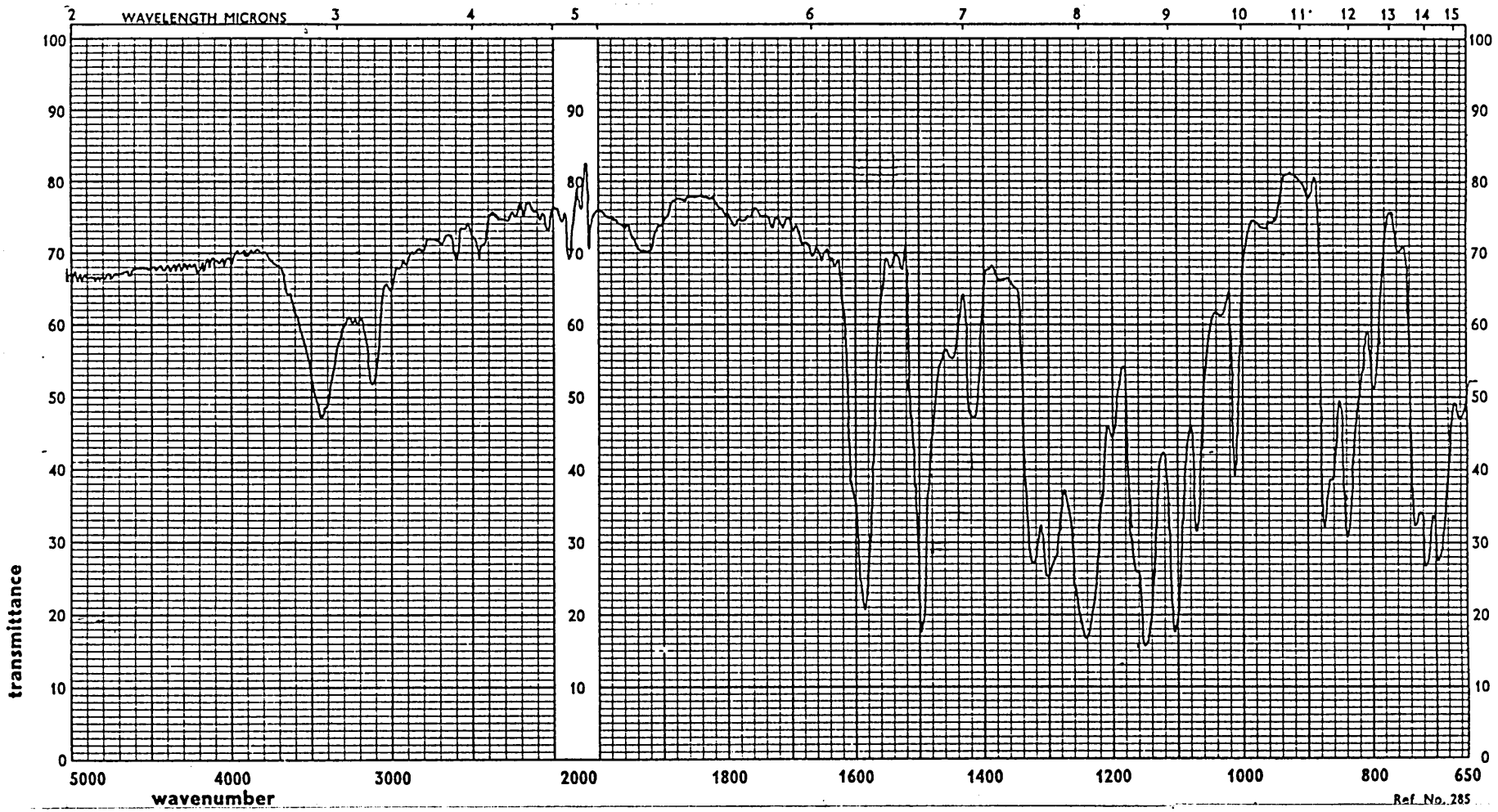
WAVELENGTH MICRONS
2
3
4
5
6
7
8
9
10
11
12
13
14
15
100
90
80
70
60
50
40
30
20
10
0
transmittance
5000
4000
3000
2000
1800
1600
1400
1200
1000
800
650
wavenumber
Ref. No. 285

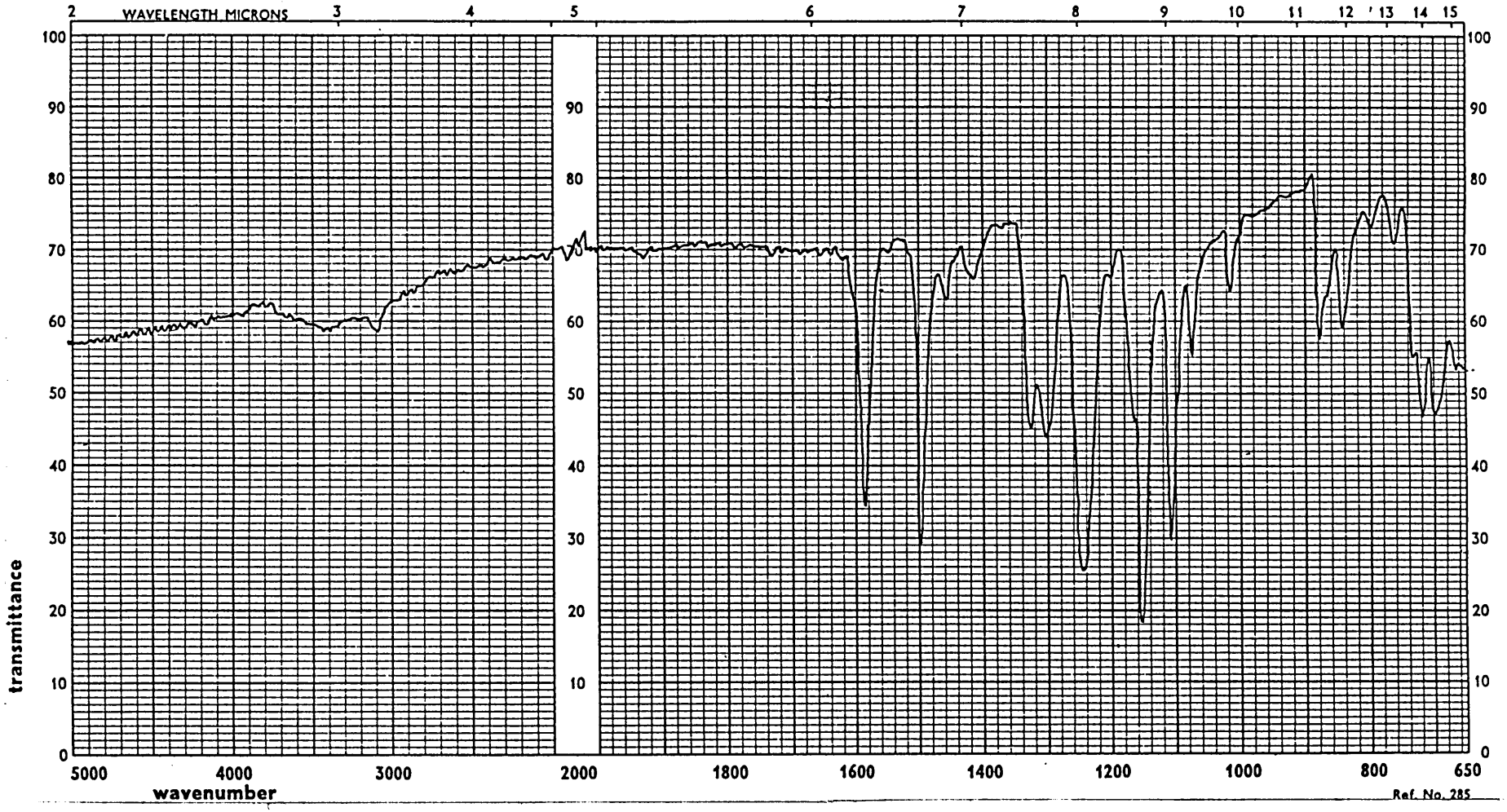
WAVELENGTH MICRONS
2
3
4
5
6
7
8
9
10
11
12
13
14
15
100
90
80
70
60
50
40
30
20
10
0
transmittance
5000
4000
3000
2000
1800
1600
1400
1200
1000
800
650
wavenumber
Ref. No. 285

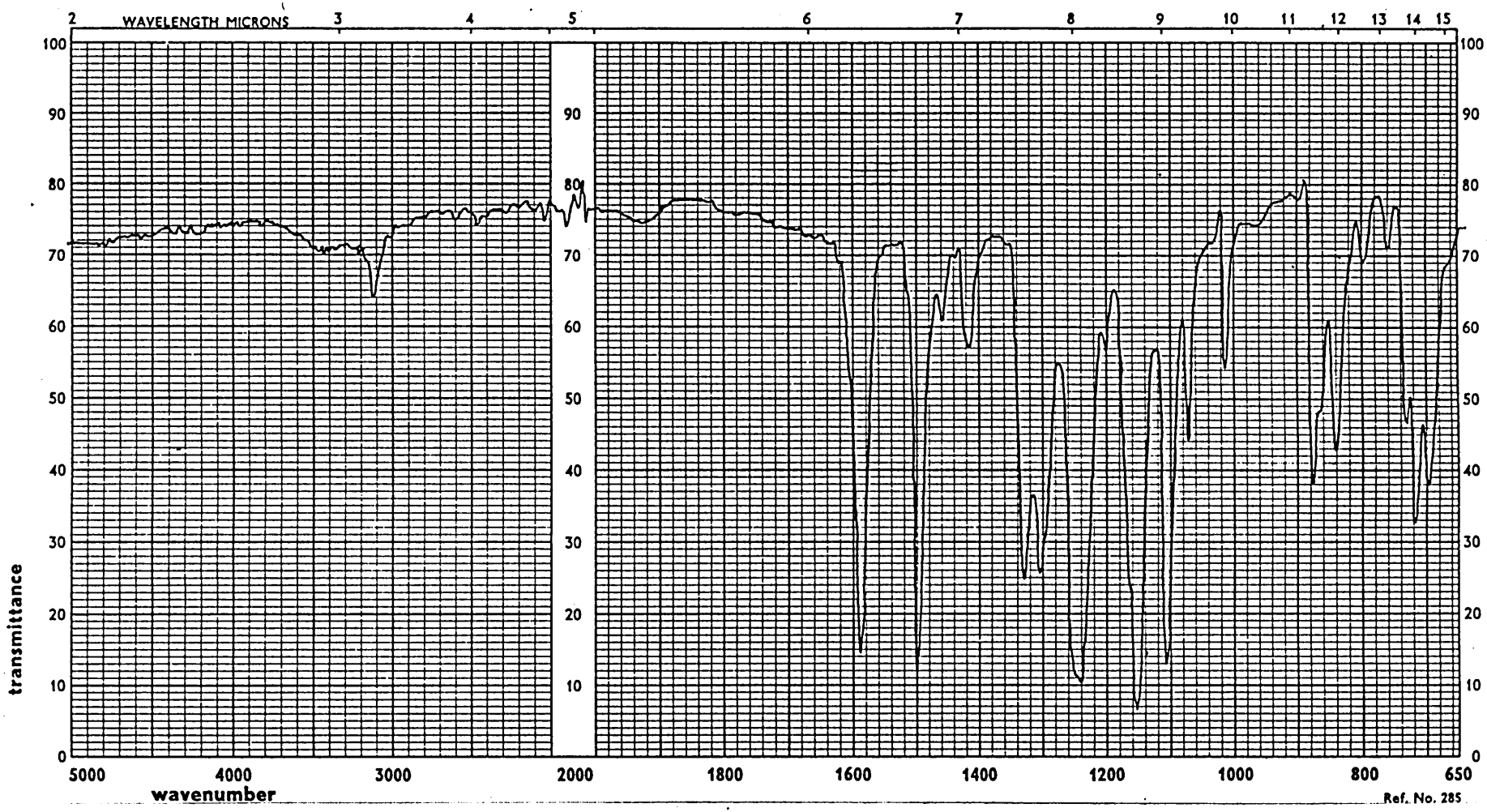
WAVELENGTH MICRONS
2
3
4
5
6
7
8
9
10
11
12
13
14
15
100
90
80
70
60
50
40
30
20
10
0
transmittance
5000
4000
3000
2000
1800
1600
1400
1200
1000
800
650
wavenumber
Ref. No. 285

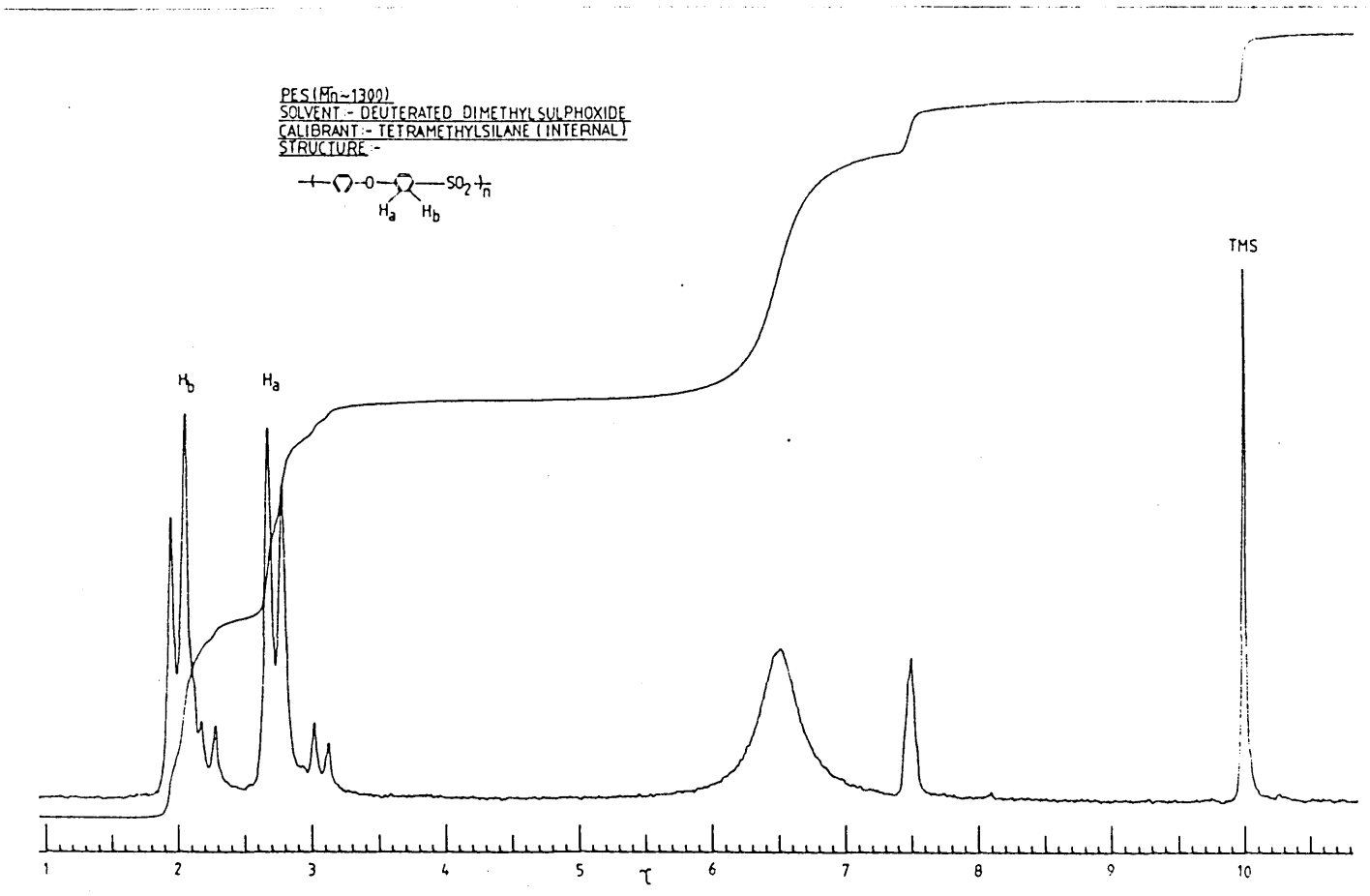
PES ($\bar{M}_n$ ~1300)
SOLVENT :- DEUTERATED DIMETHYLSULPHOXIDE
CALIBRANT :- TETRAMETHYLSILANE (INTERNAL)
STRUCTURE :-
H_a
H_b
H_b
H_a
TMS
1
2
3
4
5
τ
6
7
8
9
10

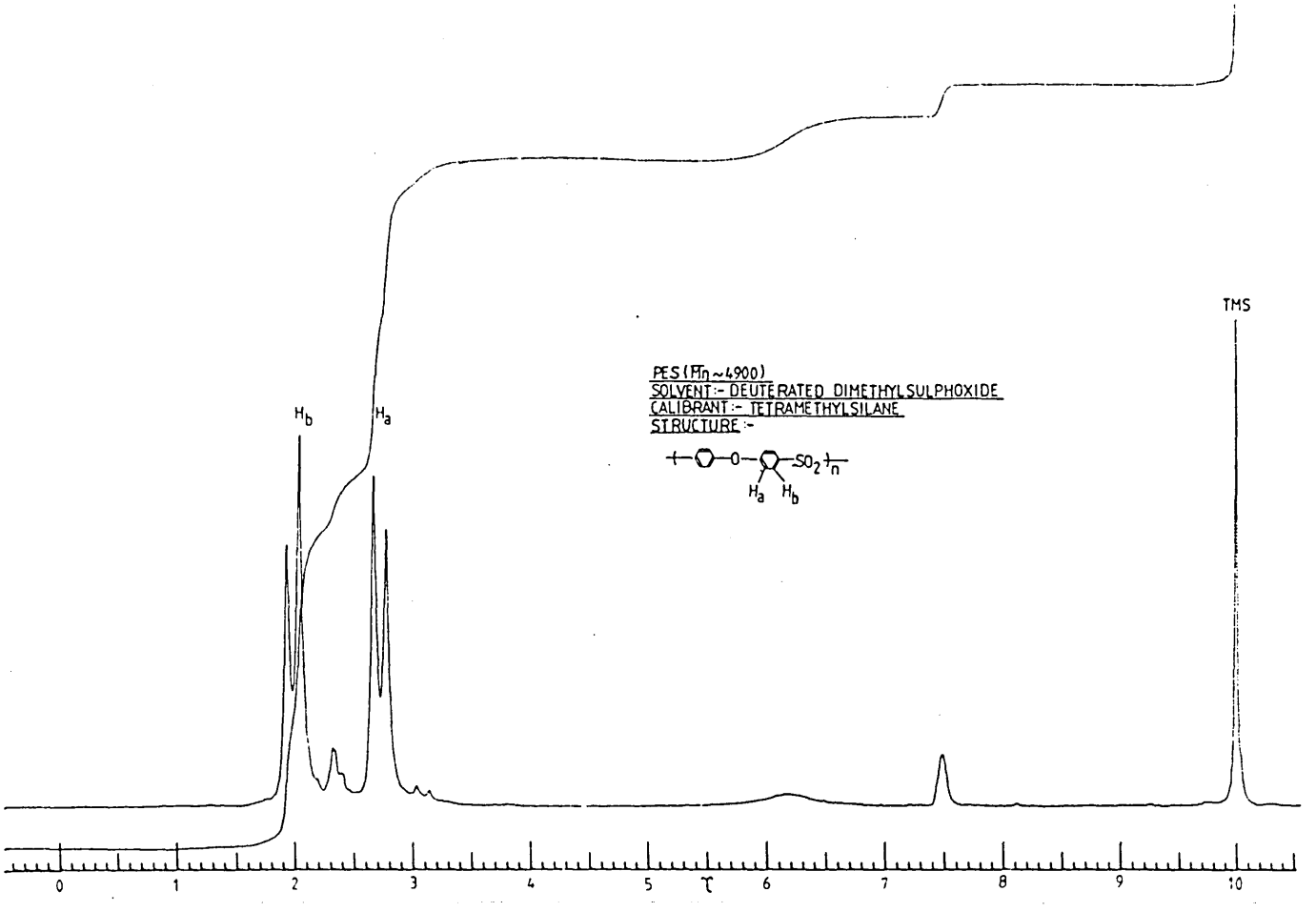
PES (Mn ~ 4900)
SOLVENT :- DEUTERATED DIMETHYL SULPHOXIDE
CALIBRANT :- TETRAMETHYLSILANE
STRUCTURE :-
Hb
Ha
TMS
0
1
2
3
4
5
τ
6
7
8
9
10

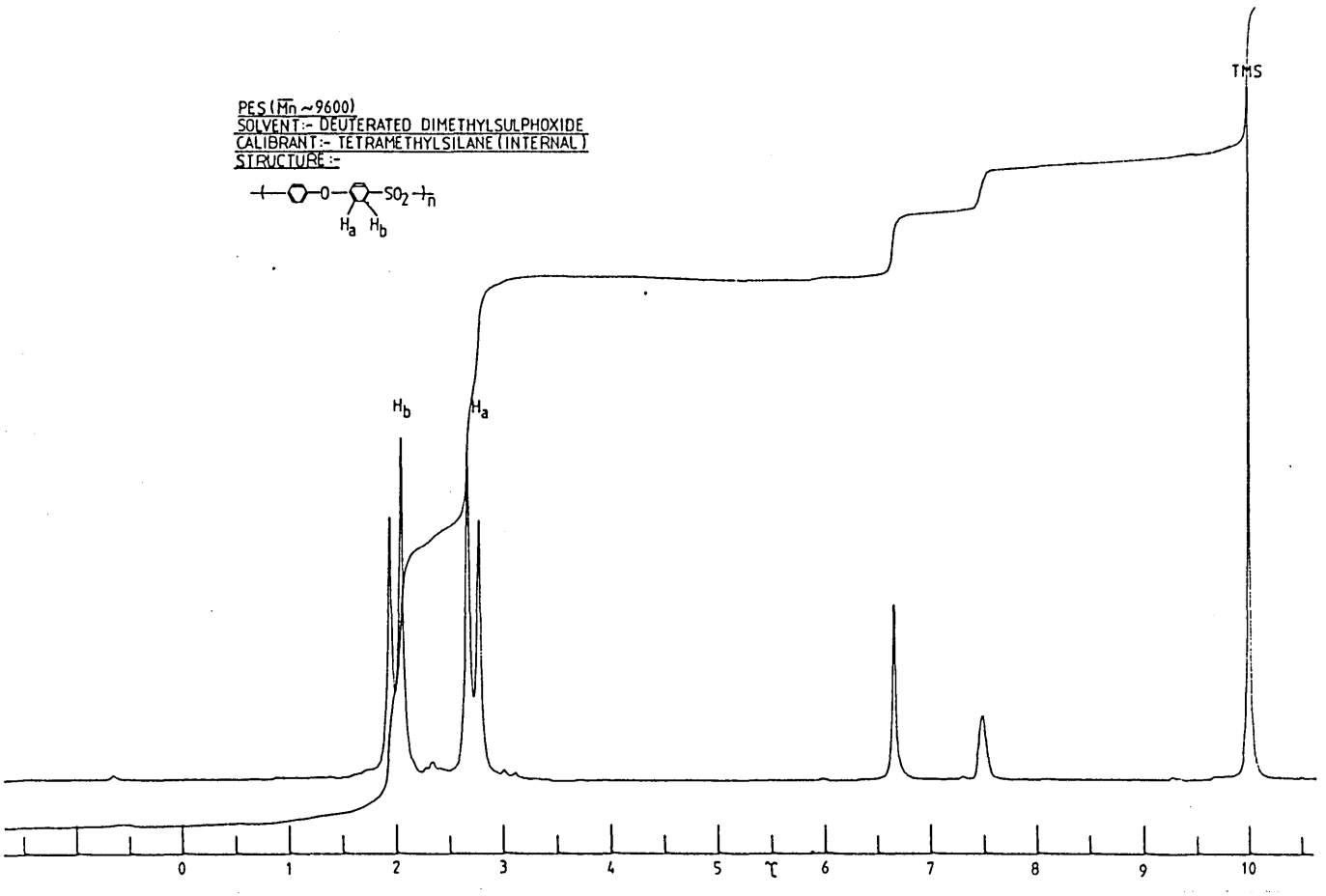
PES ($\overline{Mn}$ ~9600)
SOLVENT:- DEUTERATED DIMETHYLSULPHOXIDE
CALIBRANT:- TETRAMETHYLSILANE (INTERNAL)
STRUCTURE:-
H_a H_b
H_b
H_a
TMS
0 1 2 3 4 5 τ 6 7 8 9 10

BISPHENOL 'S' (HO—Φ—SO_2—Φ—OH)
SOLVENT:- DEUTERATED DIMETHYLSULPHOXIDE

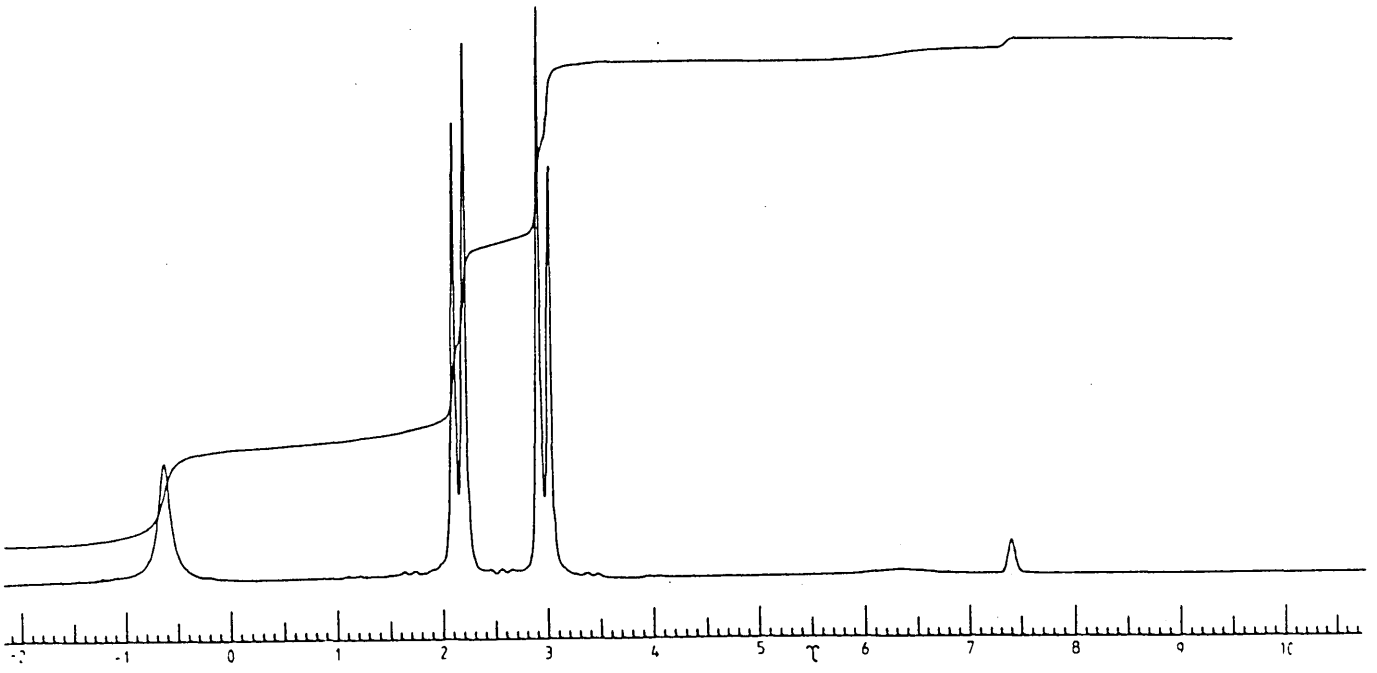

DICHLORODIPHENYLSULPHONE (Cl—Φ—SO_2—Φ—Cl)
SOLVENT - DEUTERATED DIMETHYLSULPHOXIDE

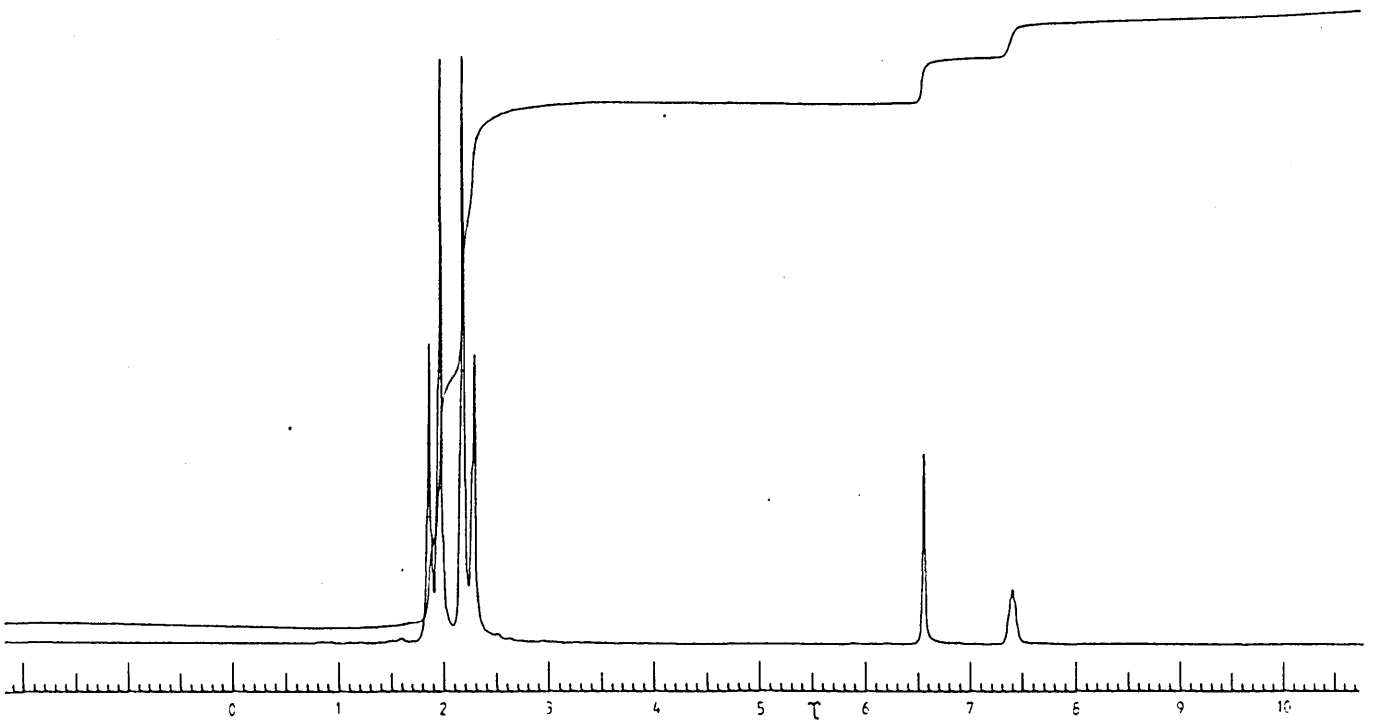

DIPHENYLSULPHONE ($\Phi-SO_2-\Phi$)
SOLVENT - DEUTERATED DIMETHYLSULPHOXIDE

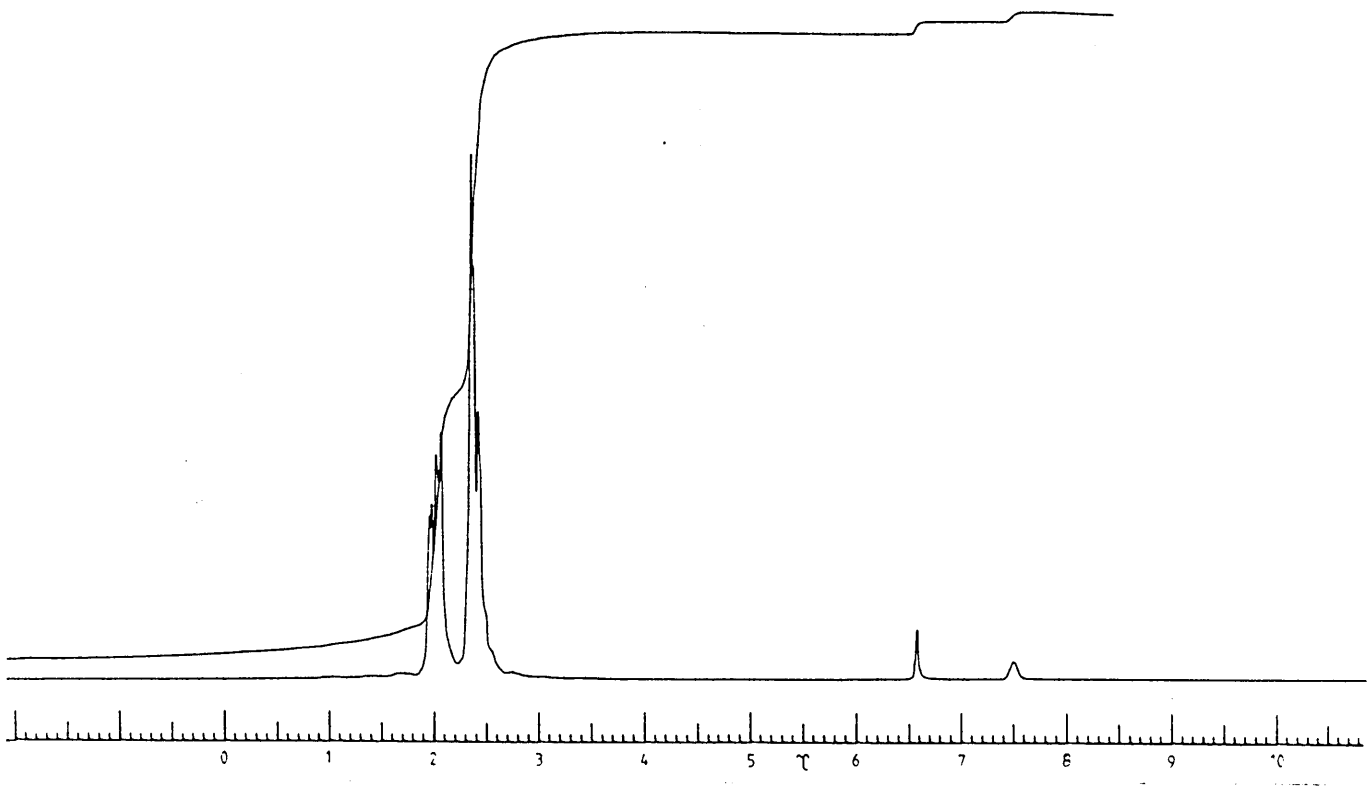

Figure 10. Apparatus for Potentiometric Titration of P.E.S. Oligomers

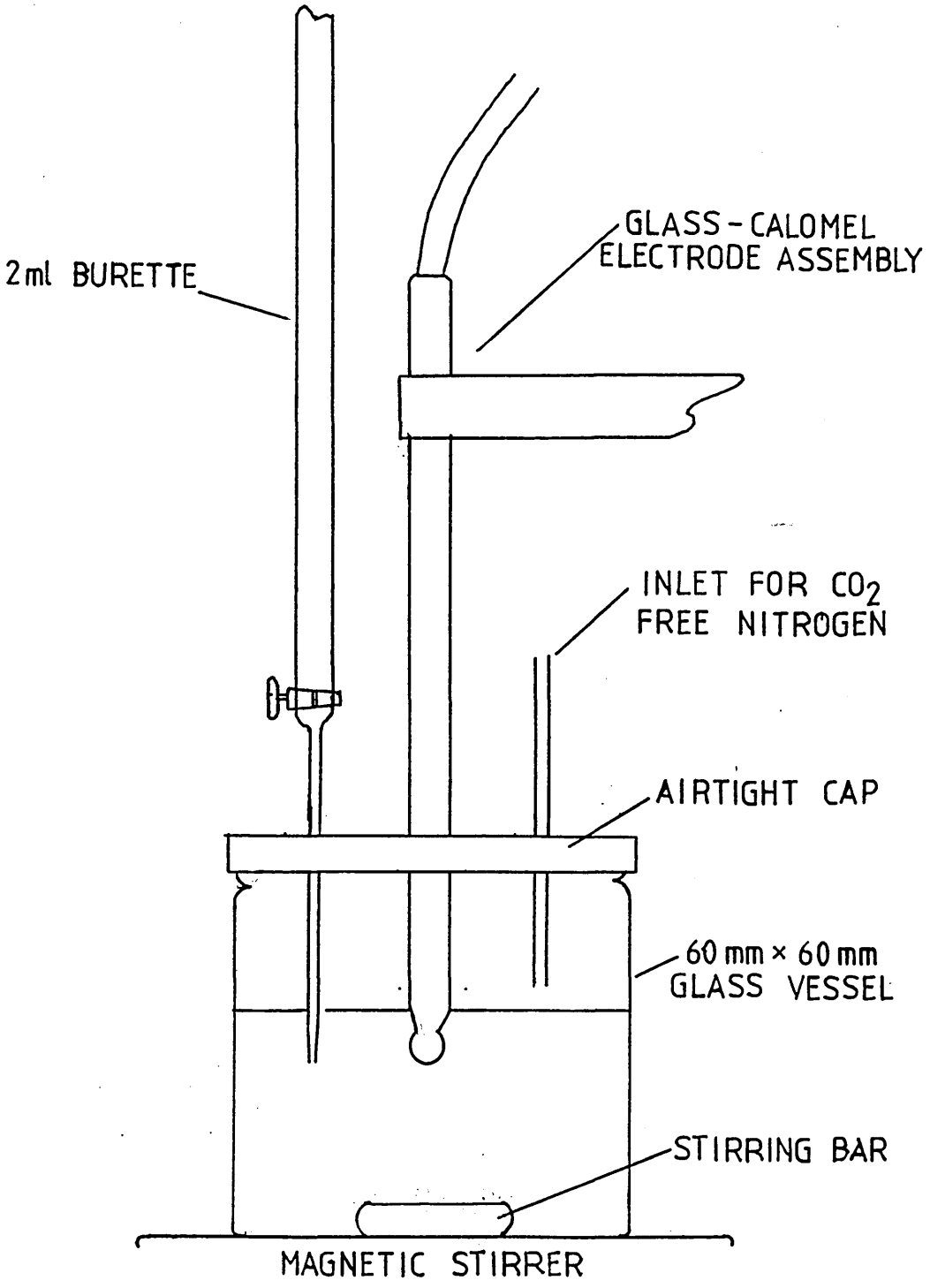
2ml BURETTE
GLASS - CALOMEL ELECTRODE ASSEMBLY
INLET FOR CO_2 FREE NITROGEN
AIRTIGHT CAP
60 mm × 60 mm GLASS VESSEL
STIRRING BAR
MAGNETIC STIRRER

Figure 11. Potentiometric Titration Curves for P.E.S. Oligomers

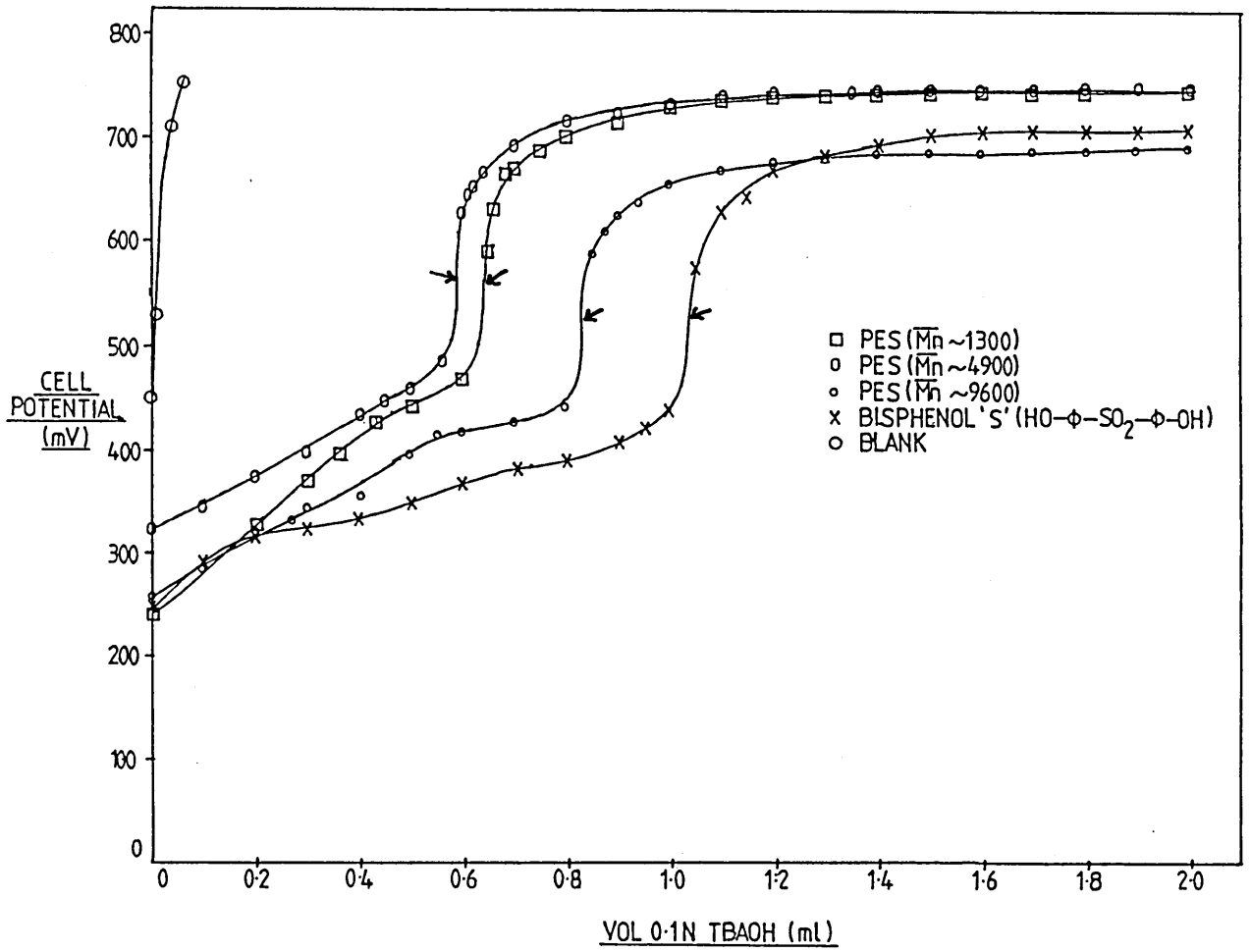
800
700
600
500
400
300
200
100
0
CELL POTENTIAL (mV)
0
0·2
0·4
0·6
0·8
1·0
1·2
1·4
1·6
1·8
2·0
VOL 0·1N TBAOH (ml)
PES ($\overline{Mn}$ ~1300)
PES ($\overline{Mn}$ ~4900)
PES ($\overline{Mn}$ ~9600)
BISPHENOL 'S' (HO–Φ–SO_2–Φ–OH)
BLANK

Figure 12. D.S.C. Curves for P.E.S. Oligomers. (a) 4800P Victrex, (b) P.E.S. [$\overline{Mn} \sim 1300$], (c) P.E.S. [$\overline{Mn} \sim 4900$], and P.E.S. [$\overline{Mn} \sim 9600$]

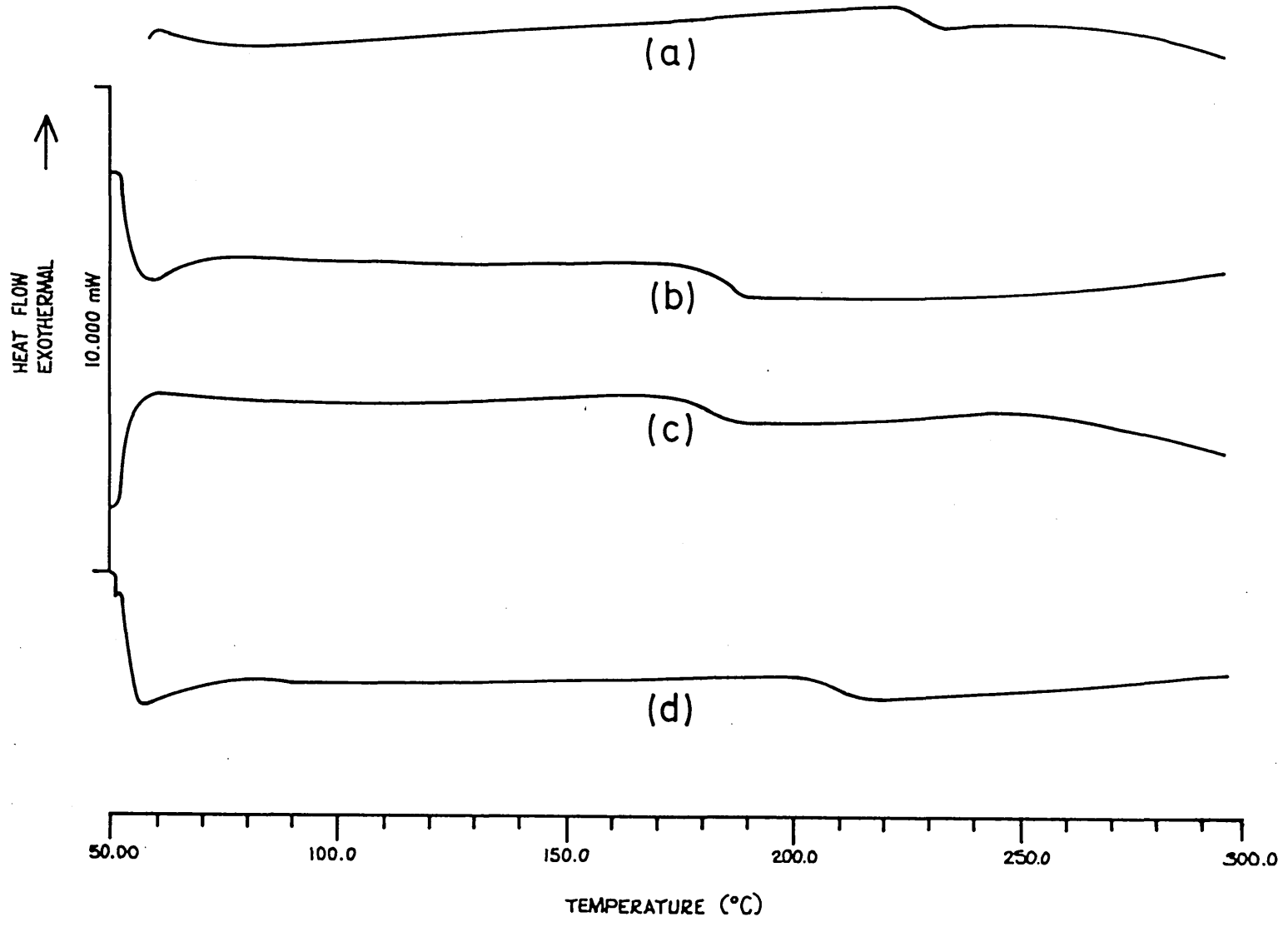
(a)
(b)
(c)
(d)
HEAT FLOW
EXOTHERMAL
10.000 mW
50.00
100.0
150.0
200.0
250.0
300.0
TEMPERATURE (°C)

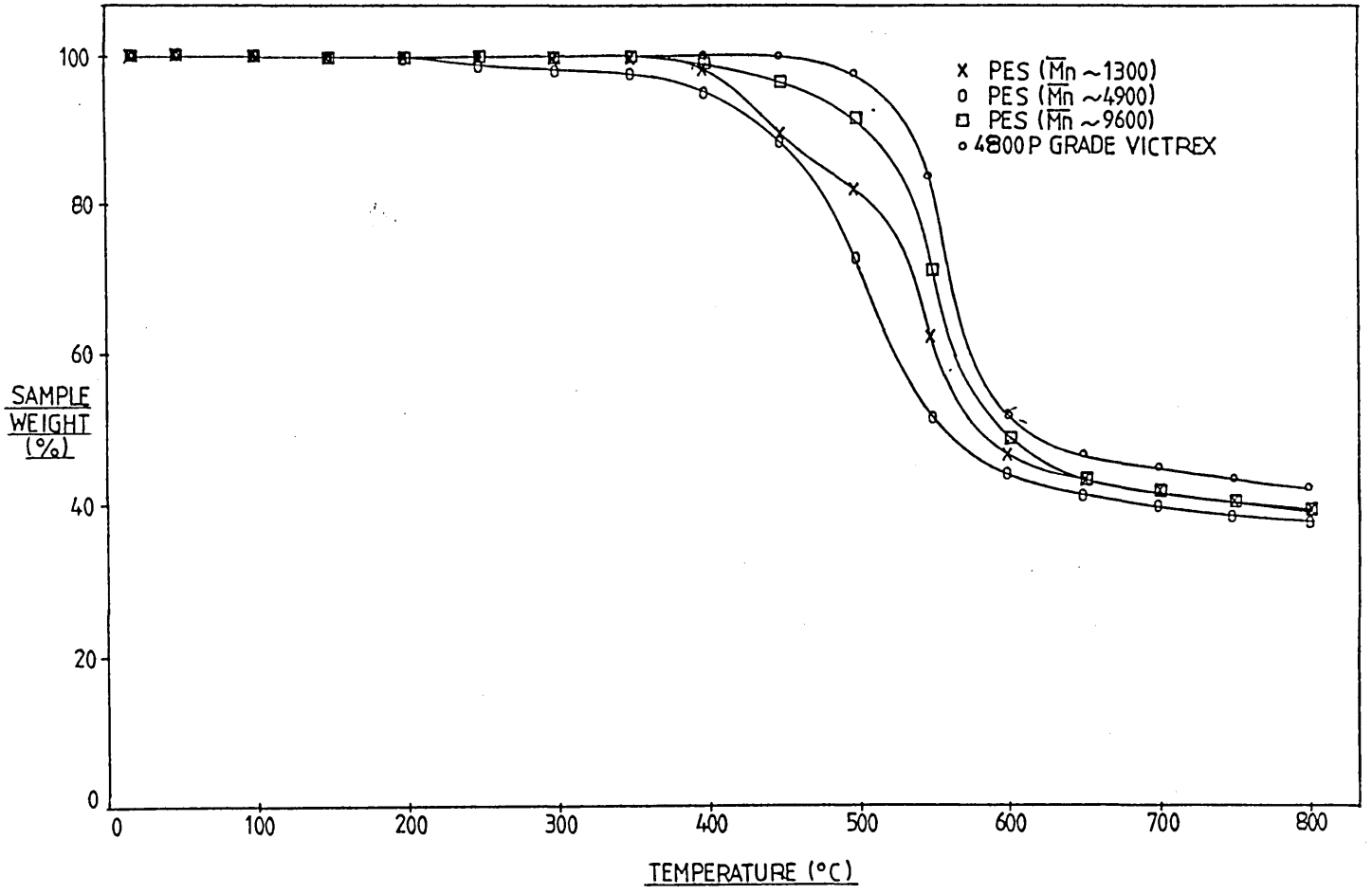
100
80
60
40
20
0
SAMPLE WEIGHT (%)
0
100
200
300
400
500
600
700
800
TEMPERATURE (°C)
x PES ($\bar{M}n$ ~1300)
o PES ($\bar{M}n$ ~4900)
□ PES ($\bar{M}n$ ~9600)
∘ 4800P GRADE VICTREX

Figure 14. Reduced Viscosity vs Concentration Curves for three P.D.M.S. Oligomers in Toluene at 25°C

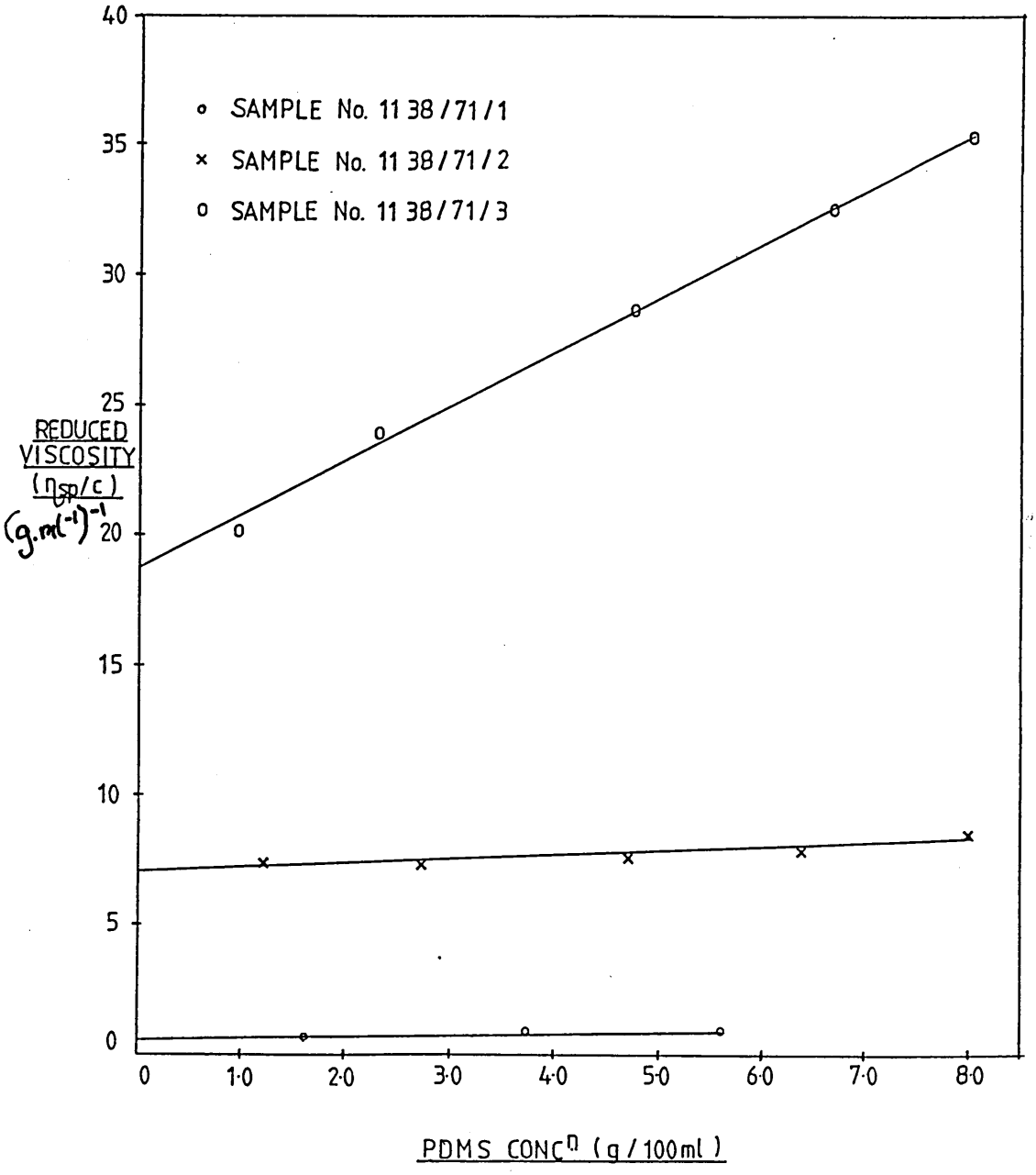
SAMPLE No. 1138/71/1
SAMPLE No. 1138/71/2
SAMPLE No. 1138/71/3
REDUCED VISCOSITY (ηsp/c) (g.ml(-1))-1
PDMS CONC^n (g/100ml)
0
5
10
15
20
25
30
35
40
0
1·0
2·0
3·0
4·0
5·0
6·0
7·0
8·0

Figure 15. Reduced Viscosity vs Concentration Curves for two P.D.M.S. Oligomers in Toluene at 25°C

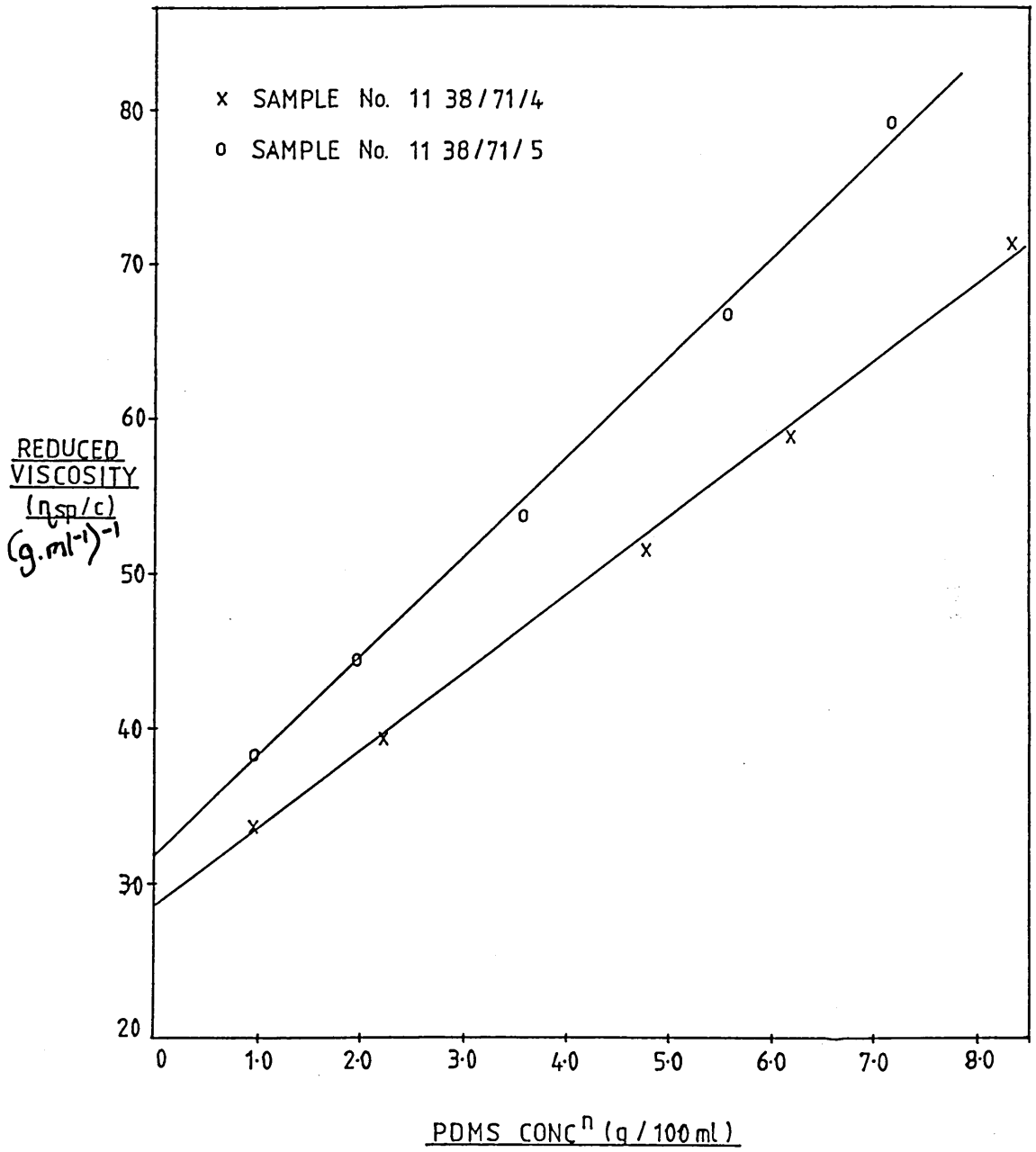
x SAMPLE No. 11 38/71/4
o SAMPLE No. 11 38/71/5
REDUCED VISCOSITY (ηsp/c) (g.ml⁻¹)⁻¹
80
70
60
50
40
30
20
0
1·0
2·0
3·0
4·0
5·0
6·0
7·0
8·0
PDMS CONCⁿ (g / 100 ml)

Figure 16. Infrared Spectrum of Hydroxyl-terminated P.D.M.S. ($\overline{Mn}$ ~600) - Range 4000-1200cm^{-1}

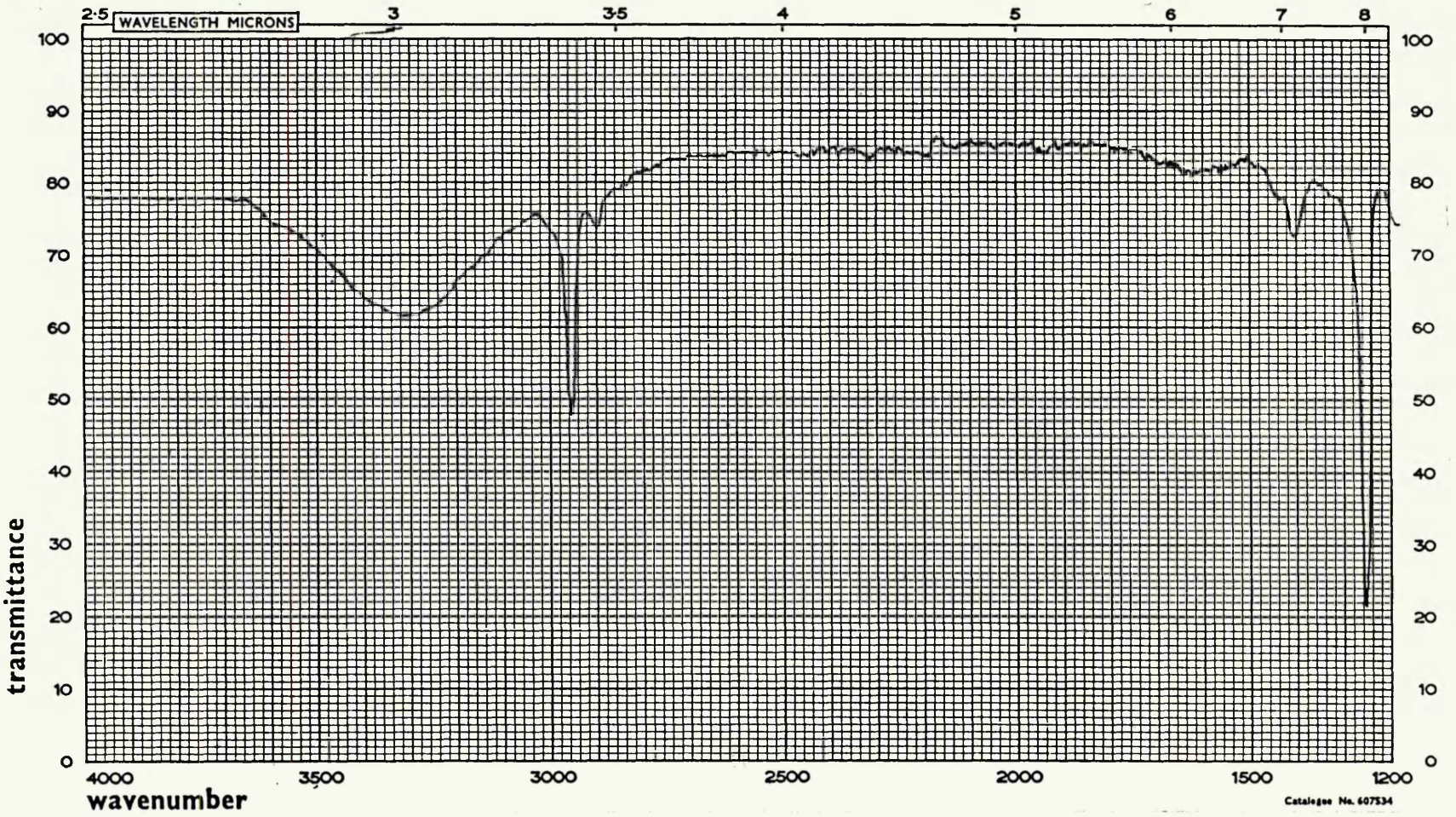
WAVELENGTH MICRONS
2·5
3
3·5
4
5
6
7
8
100
90
80
70
60
50
40
30
20
10
0
transmittance
4000
3500
3000
2500
2000
1500
1200
wavenumber
Catalogue No. 607534

Figure 17. Infrared Spectrum of Hydroxyl-terminated P.D.M.S. ($\bar{M}n \sim 600$) - Range 1300-400cm^{-1}

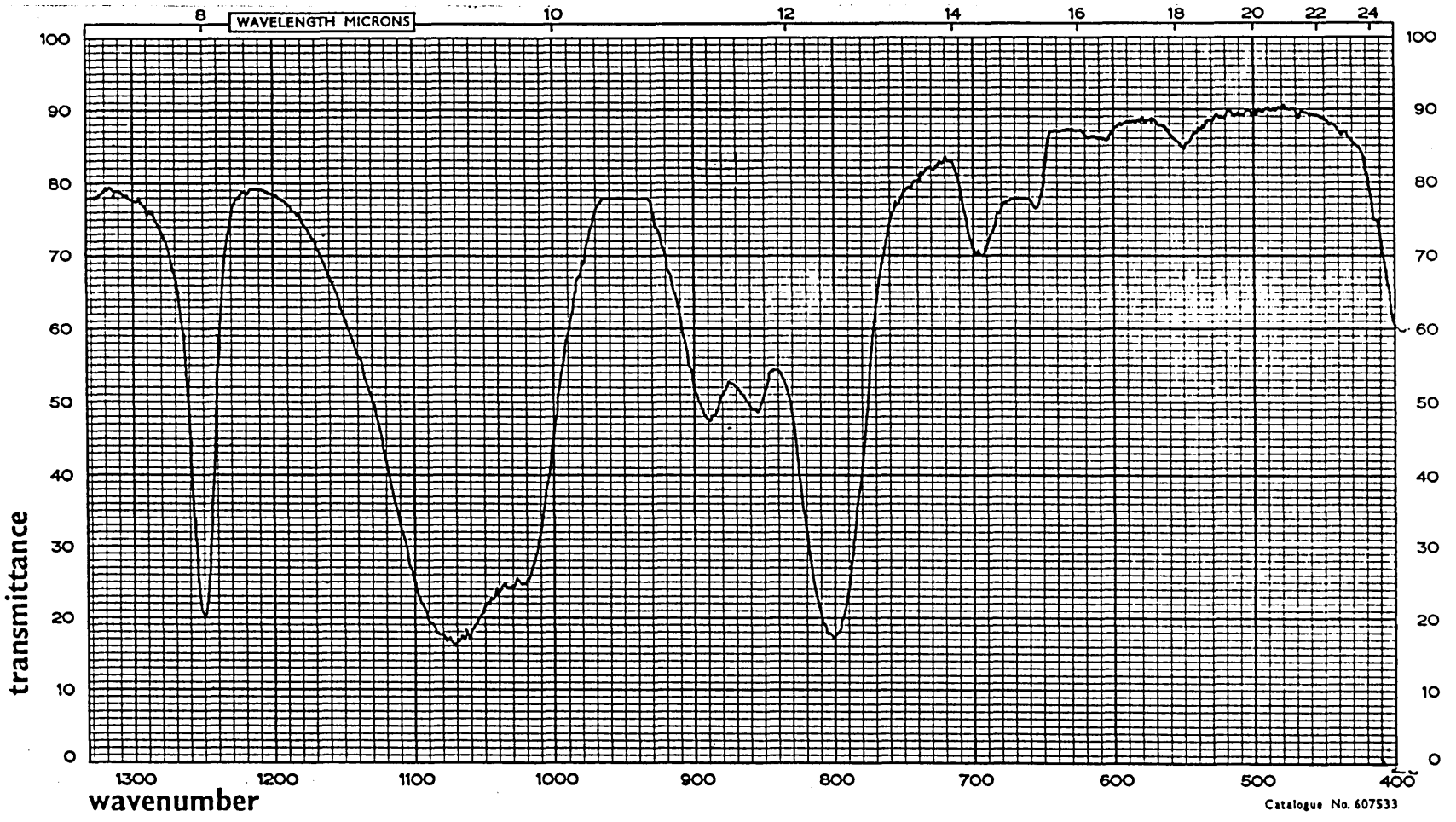
WAVELENGTH MICRONS
8
10
12
14
16
18
20
22
24
100
90
80
70
60
50
40
30
20
10
0
transmittance
1300
1200
1100
1000
900
800
700
600
500
400
wavenumber
Catalogue No. 607533

Figure 18. Infrared Spectrum of Hydroxyl-terminated P.D.M.S. ($\bar{M}n \sim 4900$) - Range 4000-1200cm^{-1}

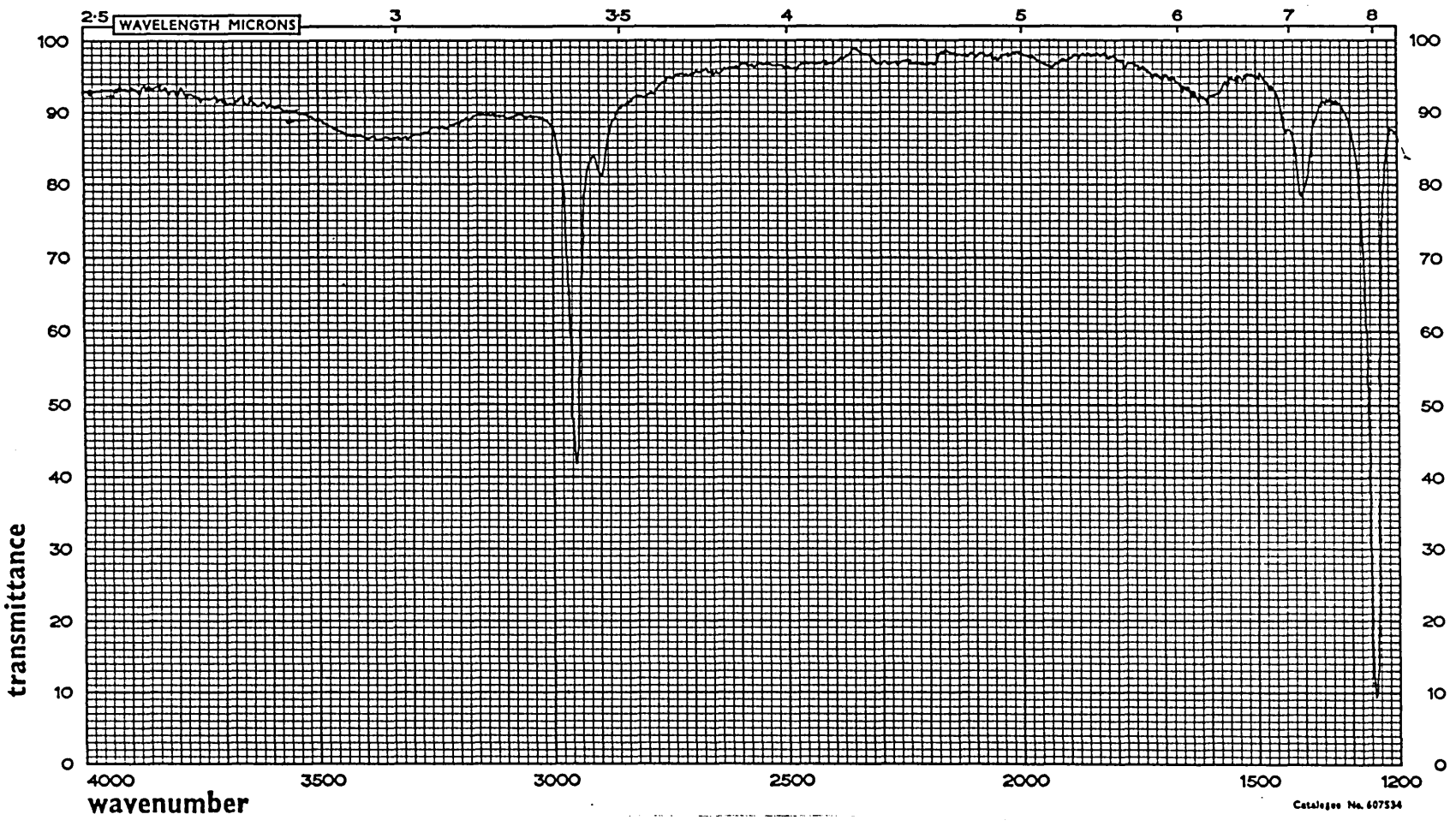
2·5
WAVELENGTH MICRONS
3
3·5
4
5
6
7
8
100
90
80
70
60
50
40
30
20
10
0
transmittance
4000
3500
3000
2500
2000
1500
1200
wavenumber
Catalogue No. 607534

Figure 19. Infrared Spectrum of Hydroxyl-terminated P.D.M.S. ($\bar{M}n \sim 4900$) - Range 1300-400cm^{-1}

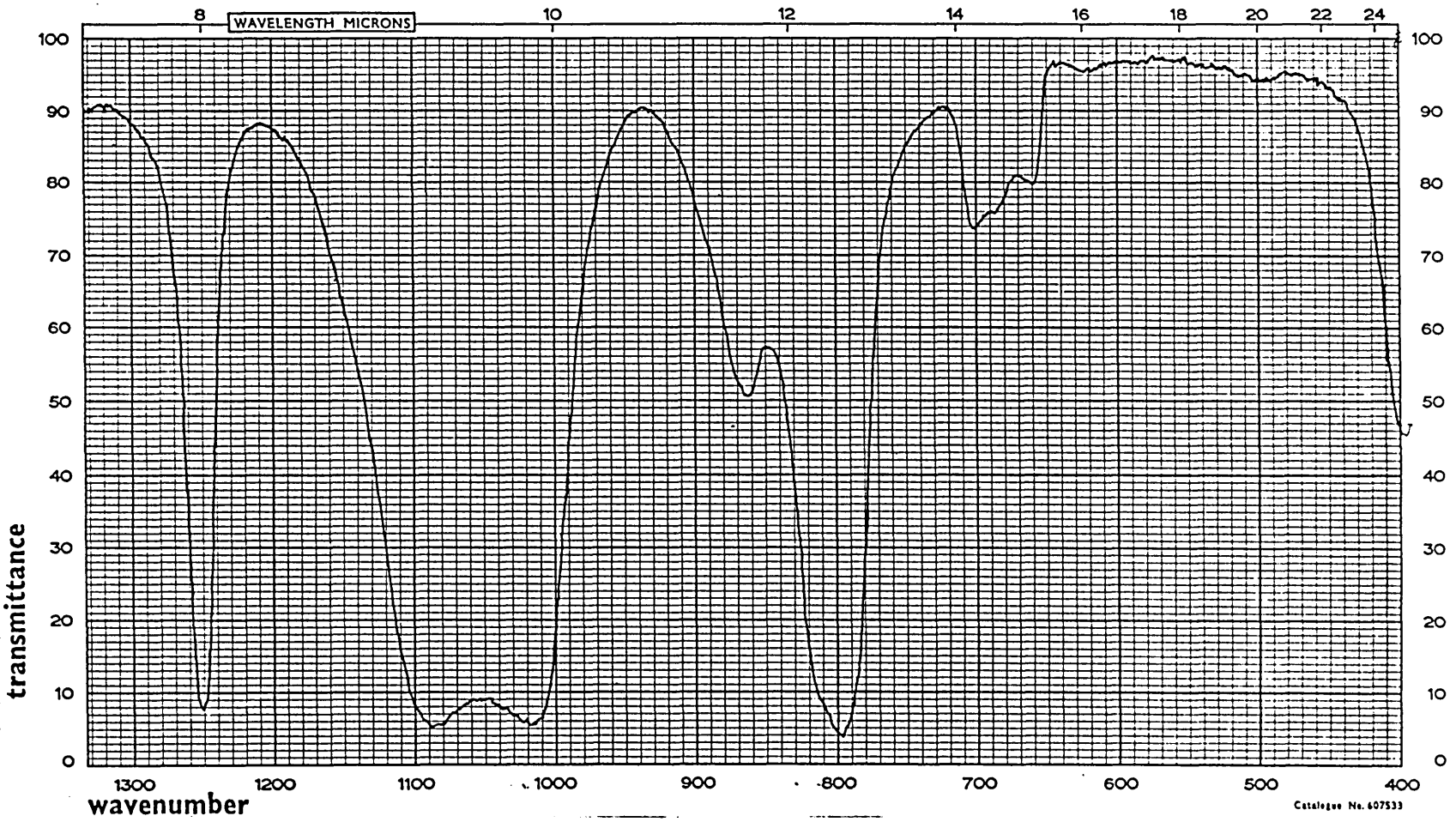
WAVELENGTH MICRONS
8
10
12
14
16
18
20
22
24
100
90
80
70
60
50
40
30
20
10
0
transmittance
1300
1200
1100
1000
900
800
700
600
500
400
wavenumber
Catalogue No. 607533

Figure 20. Infrared Spectrum of Hydroxyl-terminated P.D.M.S. ($\overline{Mn} \sim 29000$) - Range 4000-1200cm^{-1}

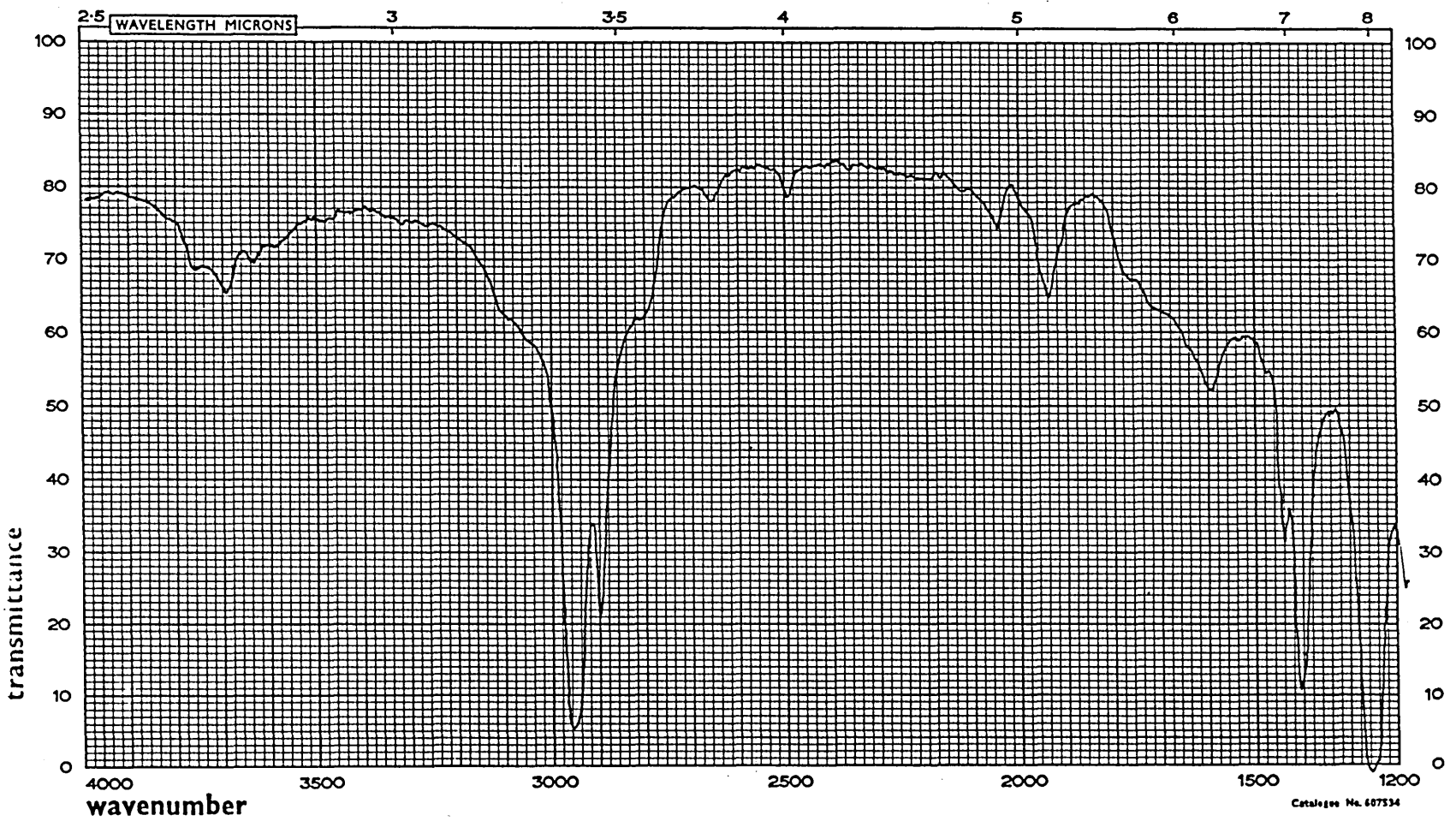
2·5
WAVELENGTH MICRONS
3
3·5
4
5
6
7
8
100
90
80
70
60
50
40
30
20
10
0
transmittance
4000
3500
3000
2500
2000
1500
1200
wavenumber
Catalogue No. 607534

Figure 21. Infrared Spectrum of Hydroxyl-terminated P.D.M.S. ($\bar{M}n \sim 29000$) - Range 1300-400cm^{-1}

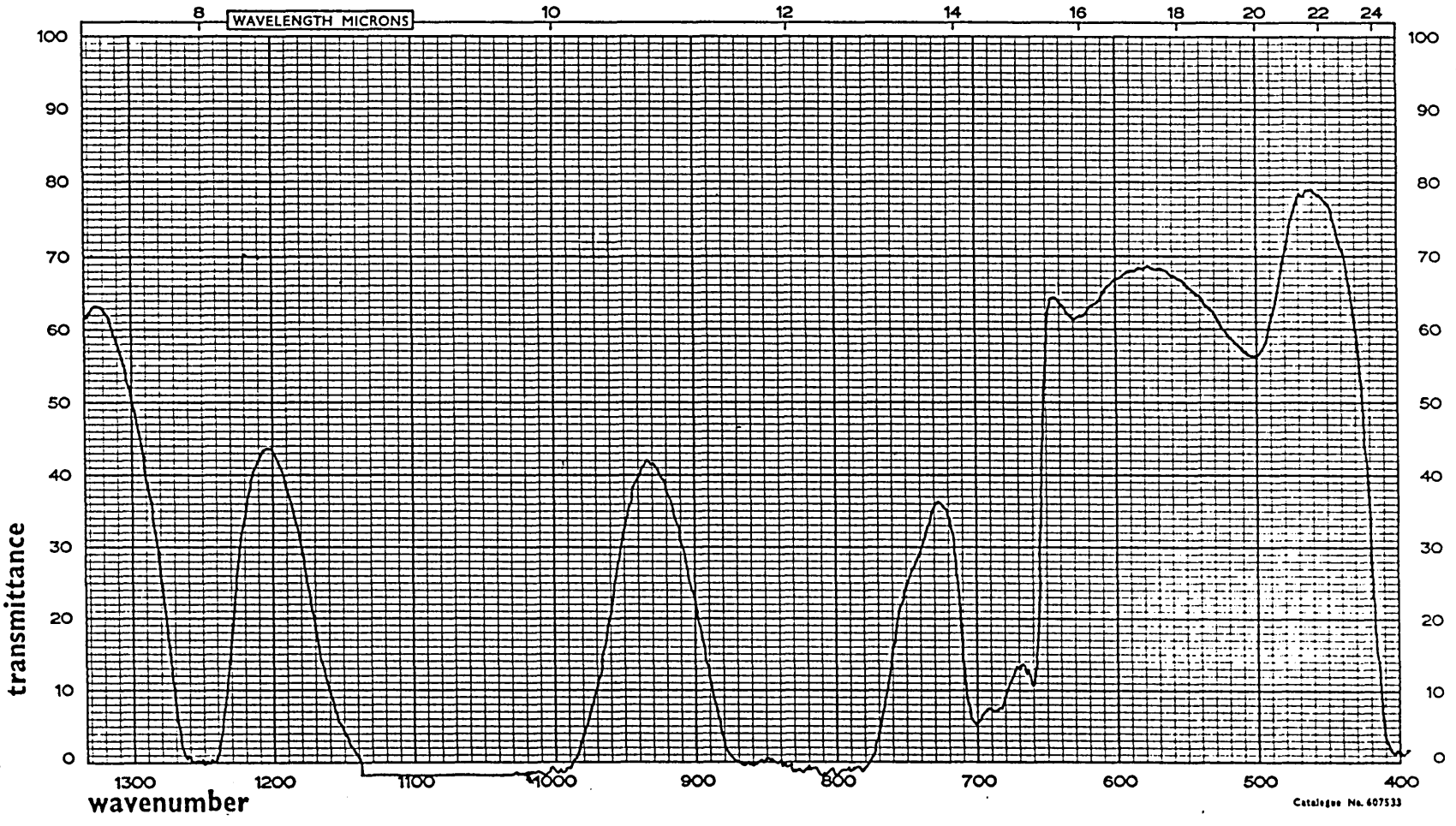
WAVELENGTH MICRONS
8
10
12
14
16
18
20
22
24
100
90
80
70
60
50
40
30
20
10
0
transmittance
1300
1200
1100
1000
900
800
700
600
500
400
wavenumber
Catalogue No. 607533

Figure 22. ^{1}H N.M.R. Spectrum of Hydroxyl-terminated P.D.M.S. ($\bar{M}n \sim 600$)

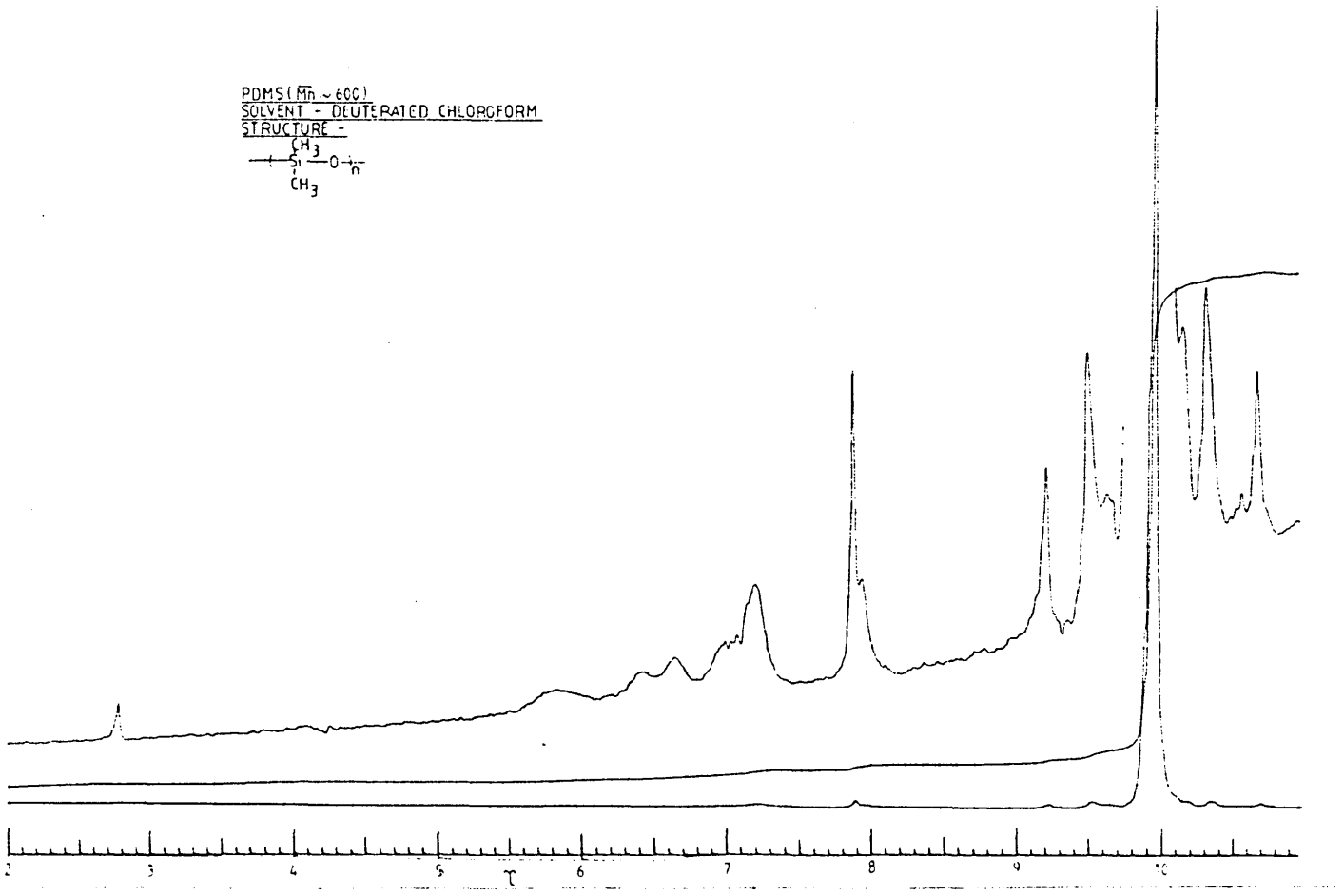
PDMS ($\overline{Mn}$ ~ 600)
SOLVENT - DEUTERATED CHLOROFORM
STRUCTURE -
CH3
Si
O
n
CH3
2
3
4
5
τ
6
7
8
9
10

Figure 23. ^{1}H N.M.R. Spectrum of Hydroxyl-terminated P.D.M.S. ($\bar{M}n$ ~4900)

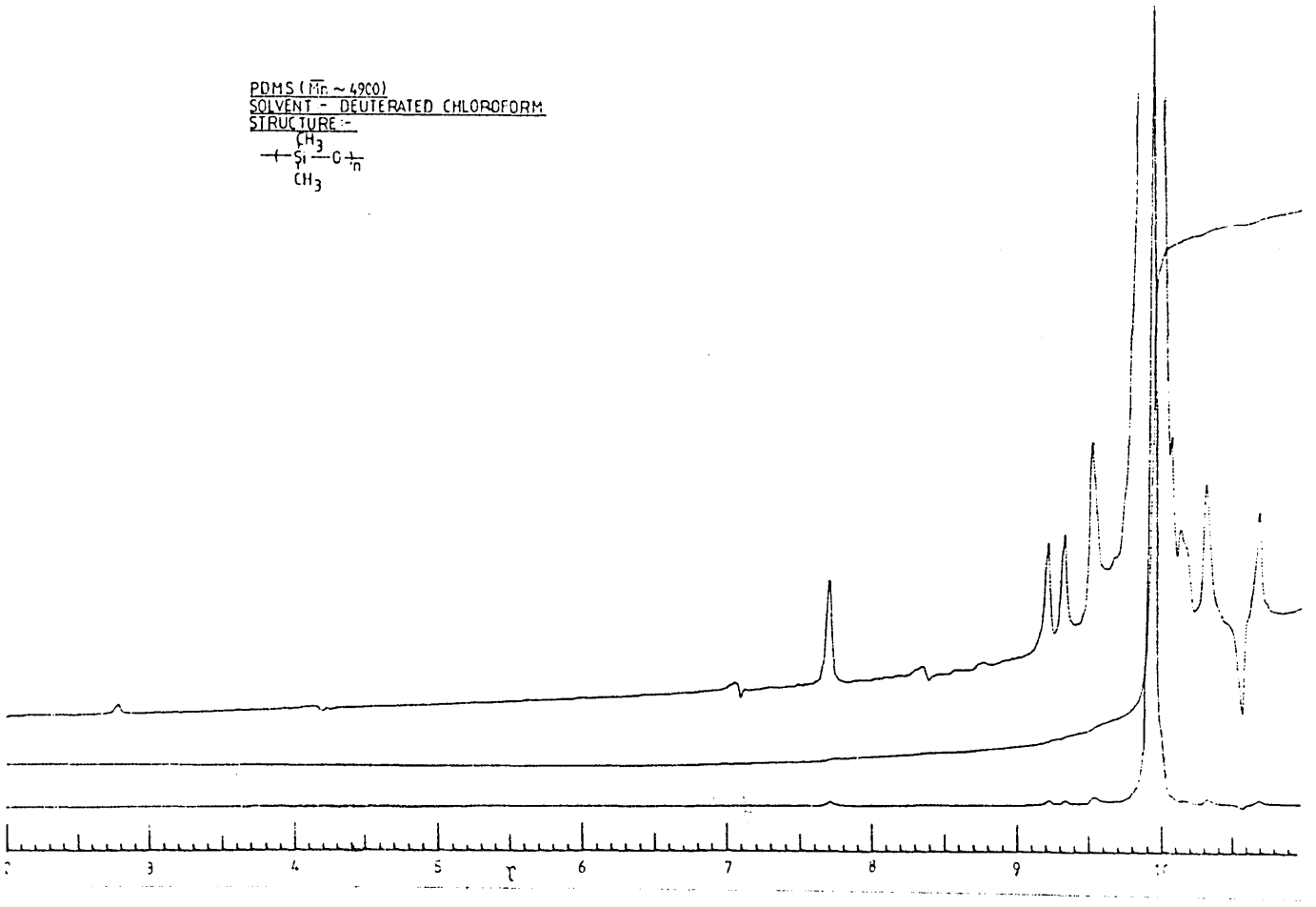
PDMS ($\overline{M}_n$ ~ 4900)
SOLVENT - DEUTERATED CHLOROFORM
STRUCTURE :-
CH_3
$-Si-O-$
CH_3
3
4
5
τ
6
7
8
9

Figure 24. ^{1}H N.M.R. Spectrum of Hydroxyl-terminated P.D.M.S. ($\bar{M}n \sim 29000$)

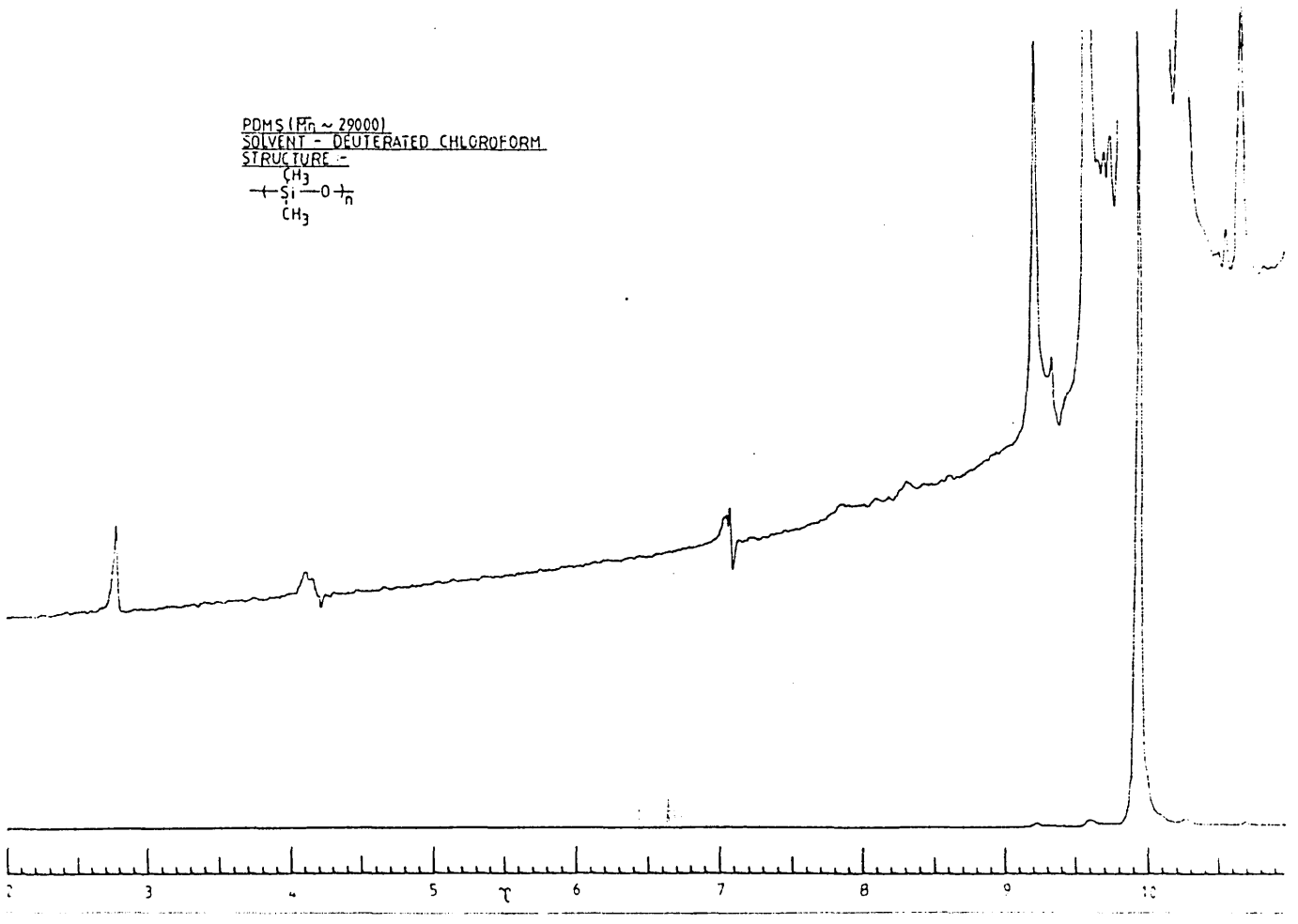
PDMS ($\overline{M}_n$ ~ 29000)
SOLVENT - DEUTERATED CHLOROFORM
STRUCTURE :-
$-\left[-\underset{CH_3}{\overset{CH_3}{\underset{|}{\overset{|}{Si}}}}-O-\right]_n-$
3
4
5
τ
6
7
8
9
10

Figure 25. D.S.C. Curves for Hydroxyl-terminated P.D.M.S. Oligomers, (a) P.D.M.S. ($\overline{Mn}$ ~ 600), (b) P.D.M.S. ($\overline{Mn}$ ~ 4900) and (c) P.D.M.S. ($\overline{Mn}$ ~ 29000).

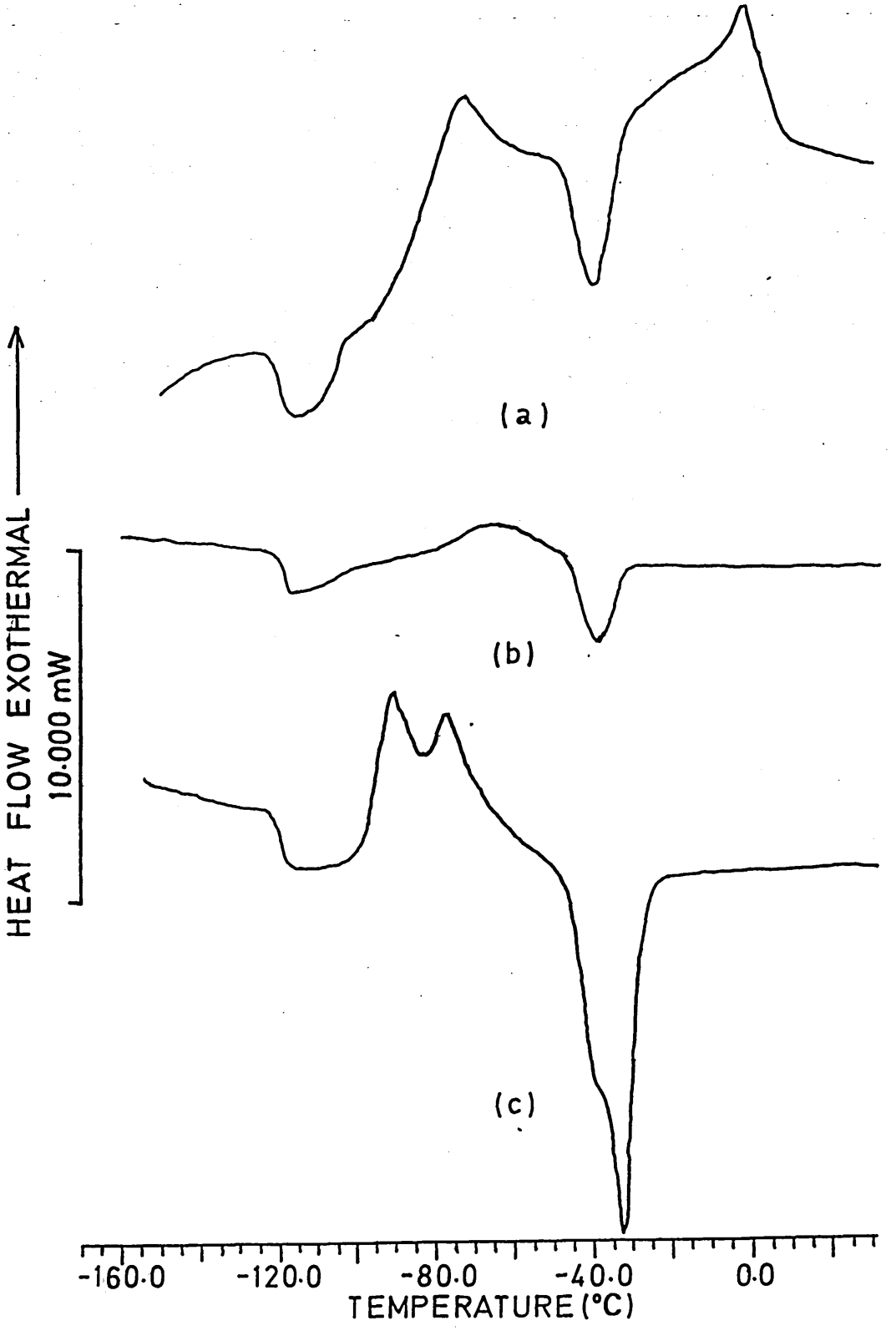
HEAT FLOW EXOTHERMAL
10.000 mW
(a)
(b)
(c)
-160.0
-120.0
-80.0
-40.0
0.0
TEMPERATURE (°C)

Figure 26. T.G.A. Curves for Hydroxyl-terminated P.D.M.S. Oligomers

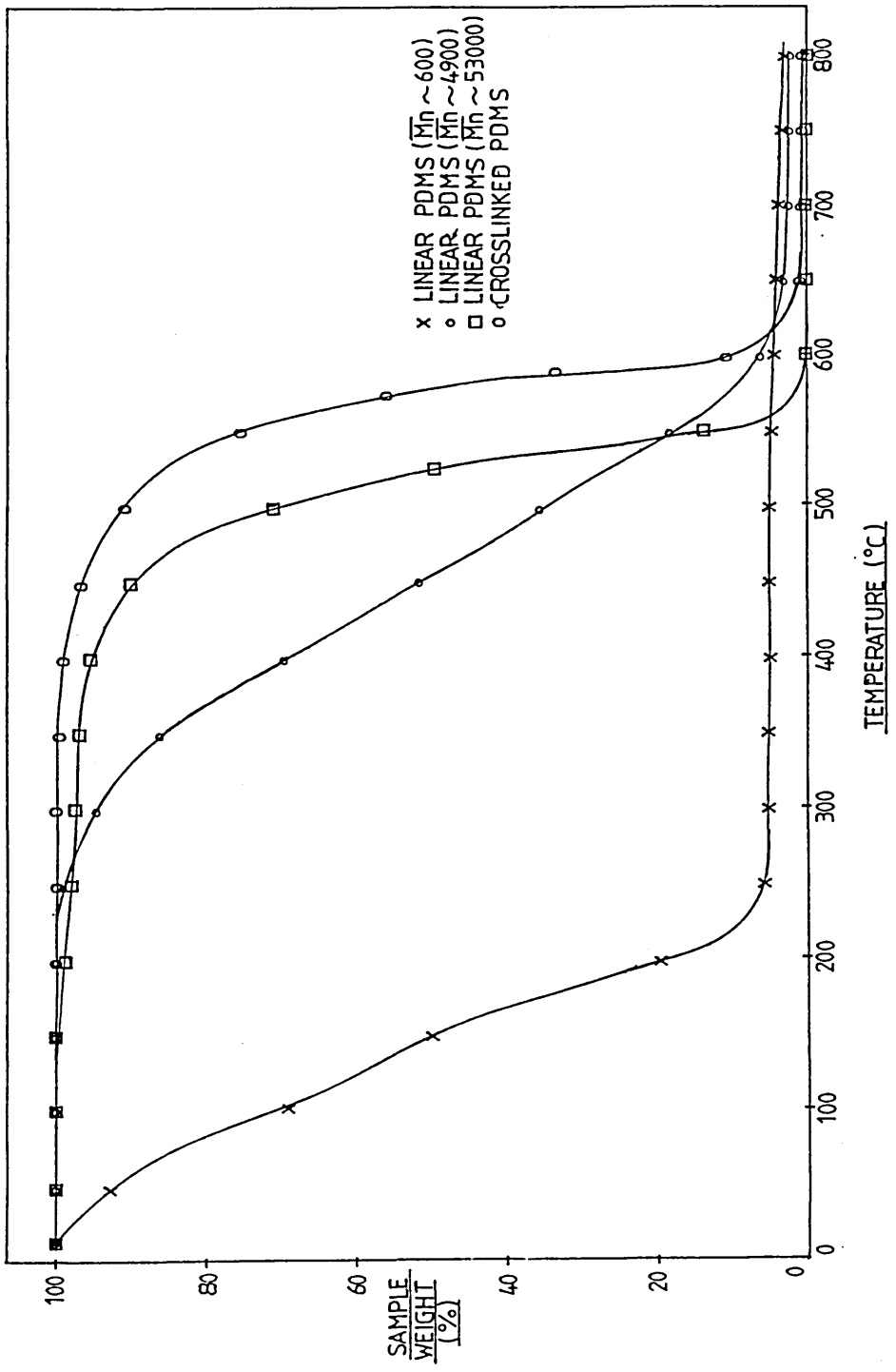
× LINEAR PDMS ($\overline{Mn}$ ~ 600)
∘ LINEAR PDMS ($\overline{Mn}$ ~ 4900)
□ LINEAR PDMS ($\overline{Mn}$ ~ 53000)
o CROSSLINKED PDMS
SAMPLE WEIGHT (%)
100
80
60
40
20
0
0
100
200
300
400
500
600
700
800
TEMPERATURE (°C)

Figure 27. Apparatus for the Chlorination of Hydroxyl-terminated P.D.M.S.

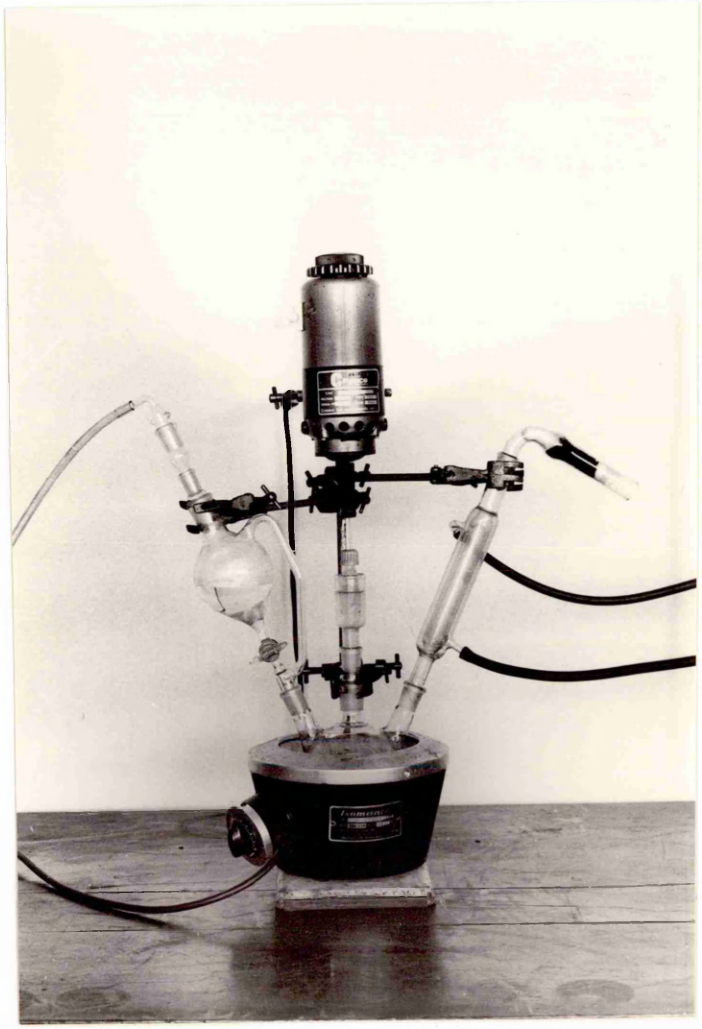

Figure 28. Infrared Spectrum of Chloro-terminated P.D.M.S. ($\overline{Mn}$ ~800) - Range 4000-1200cm^{-1}

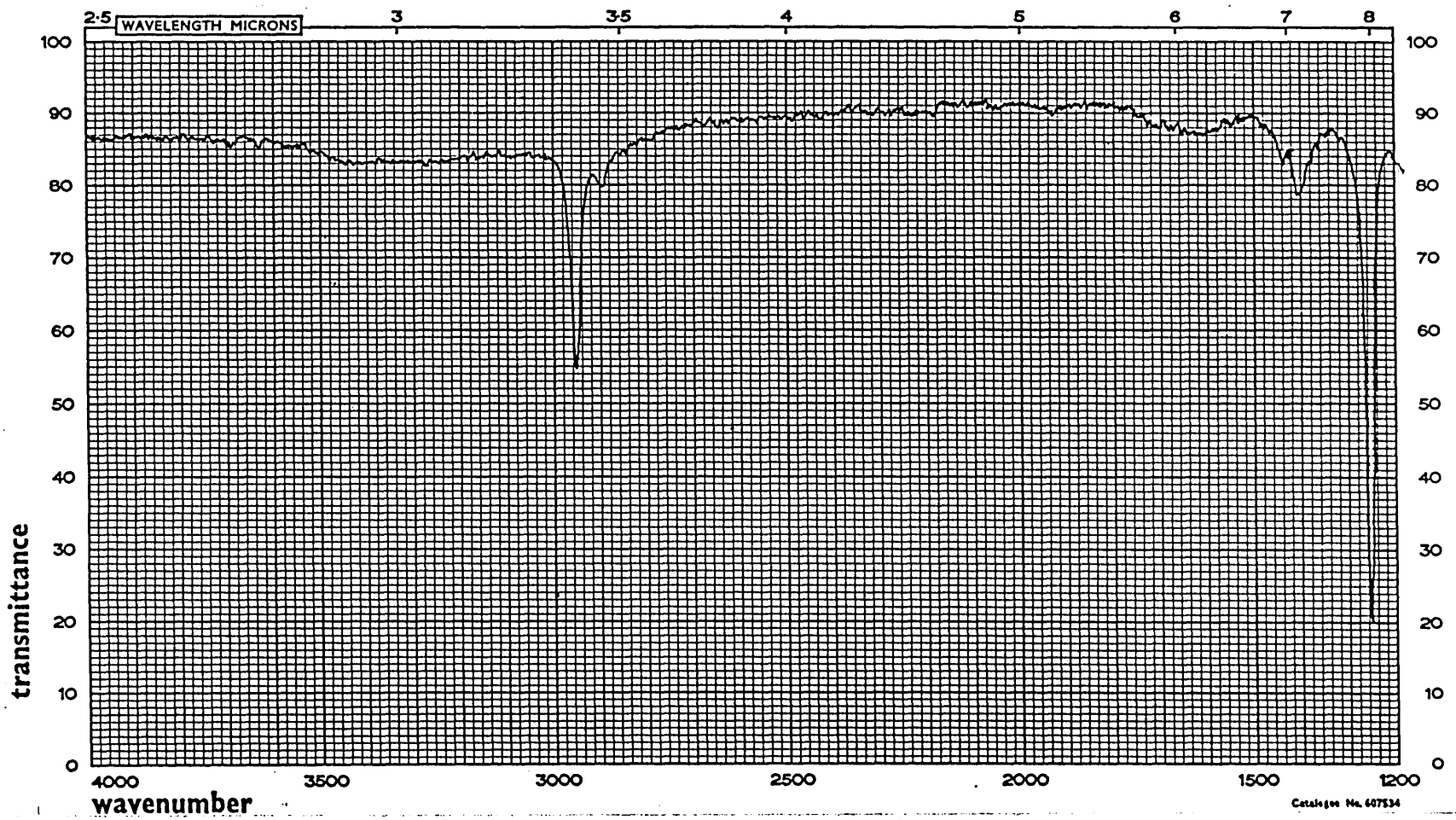
2·5
WAVELENGTH MICRONS
3
3·5
4
5
6
7
8
100
90
80
70
60
50
40
30
20
10
0
transmittance
4000
3500
3000
2500
2000
1500
1200
wavenumber
Catalogue No. 607534

Figure 29. Infrared Spectrum of Chloro-terminated P.D.M.S. ($\overline{Mn} \sim 800$) - Range 1300-400cm^{-1}

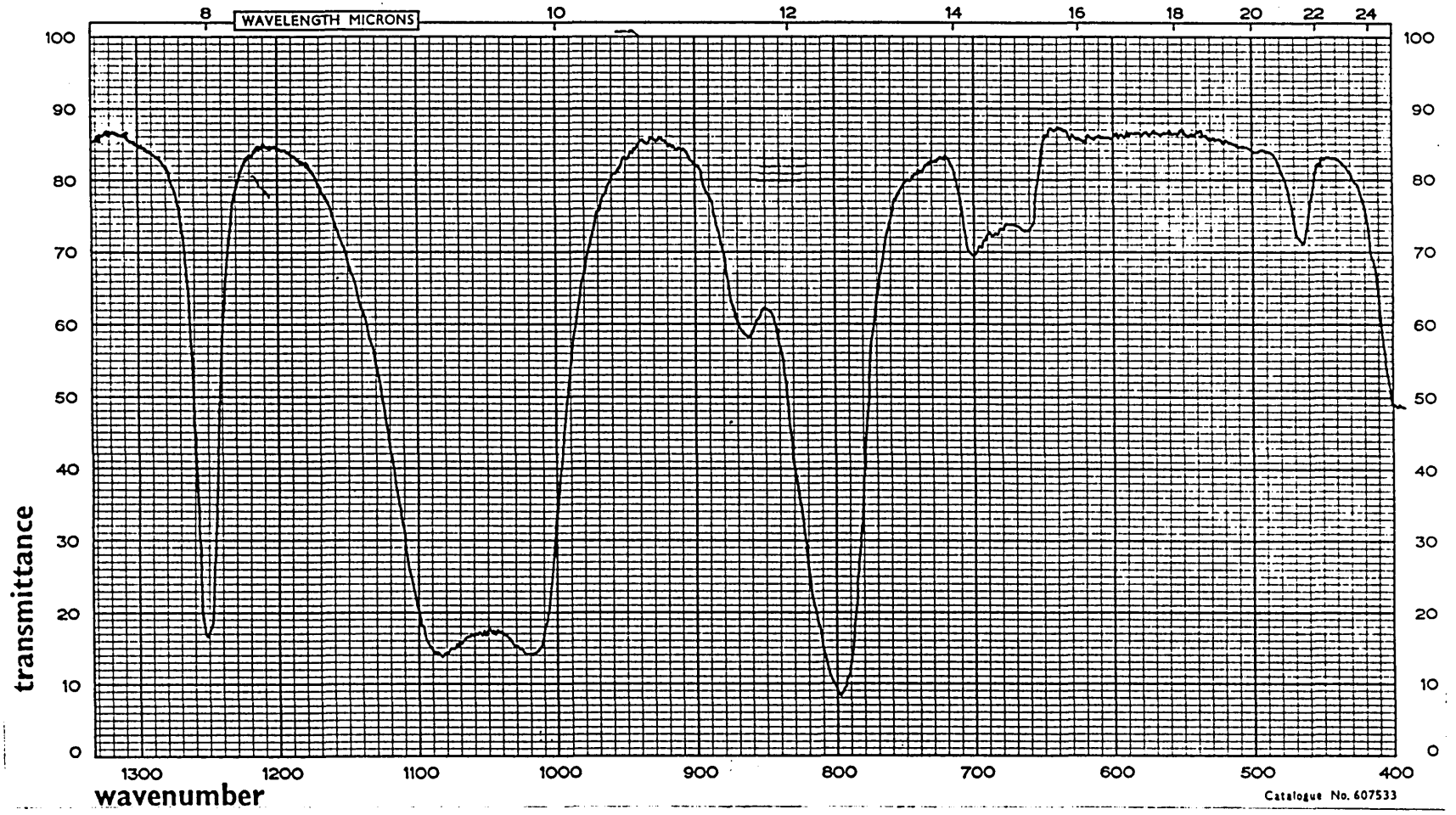
WAVELENGTH MICRONS
8
10
12
14
16
18
20
22
24
100
90
80
70
60
50
40
30
20
10
0
transmittance
1300
1200
1100
1000
900
800
700
600
500
400
wavenumber
Catalogue No. 607533

Figure 30. Infrared Spectrum of Chloro-terminated P.D.M.S. ($\bar{M}n \sim 5100$) - Range 4000-1200cm^{-1}

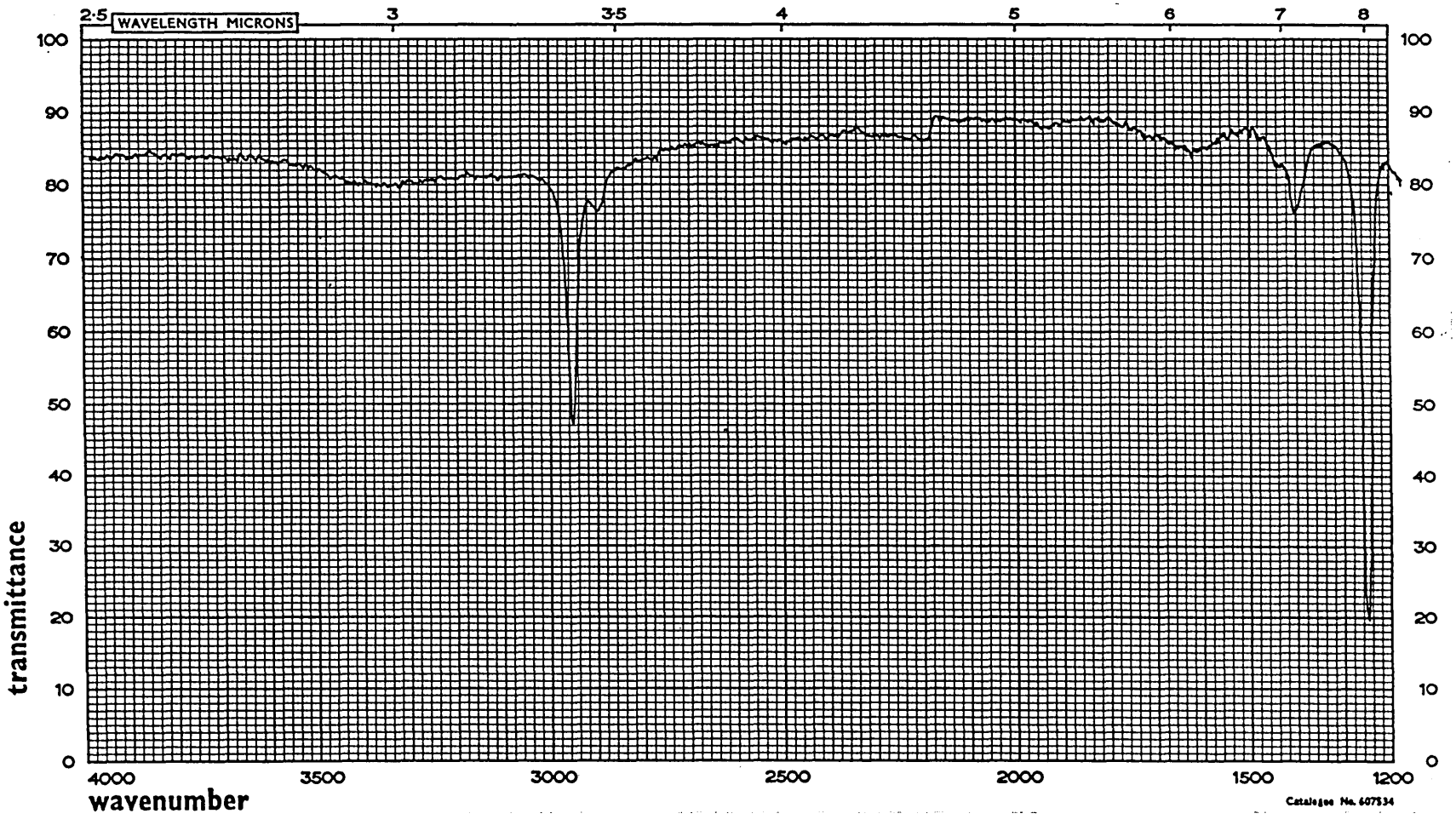
2·5
WAVELENGTH MICRONS
3
3·5
4
5
6
7
8
100
90
80
70
60
50
40
30
20
10
0
transmittance
4000
3500
3000
2500
2000
1500
1200
wavenumber
Catalogue No. 607534

Figure 31. Infrared Spectrum of Chloro-terminated P.D.M.S. ($\overline{Mn}$ ~5100) - Range 1300-400cm^{-1}

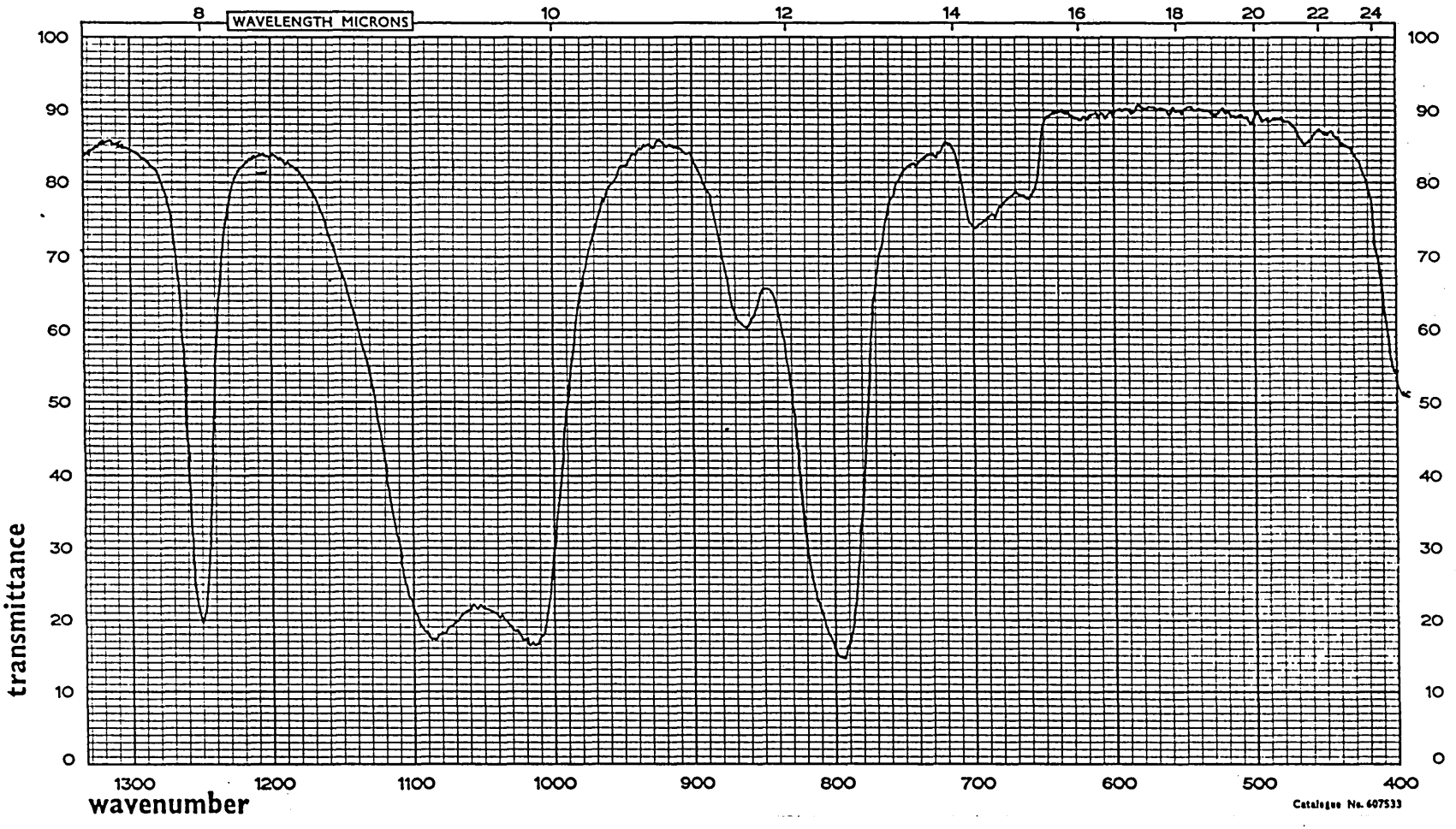
WAVELENGTH MICRONS
8
10
12
14
16
18
20
22
24
100
90
80
70
60
50
40
30
20
10
0
transmittance
1300
1200
1100
1000
900
800
700
600
500
400
wavenumber
Catalogue No. 607533

Figure 32. Infrared Spectrum of Chloro-terminated P.D.M.S. ($\bar{M}n \sim 29000$) - Range 4000-1200cm^{-1}

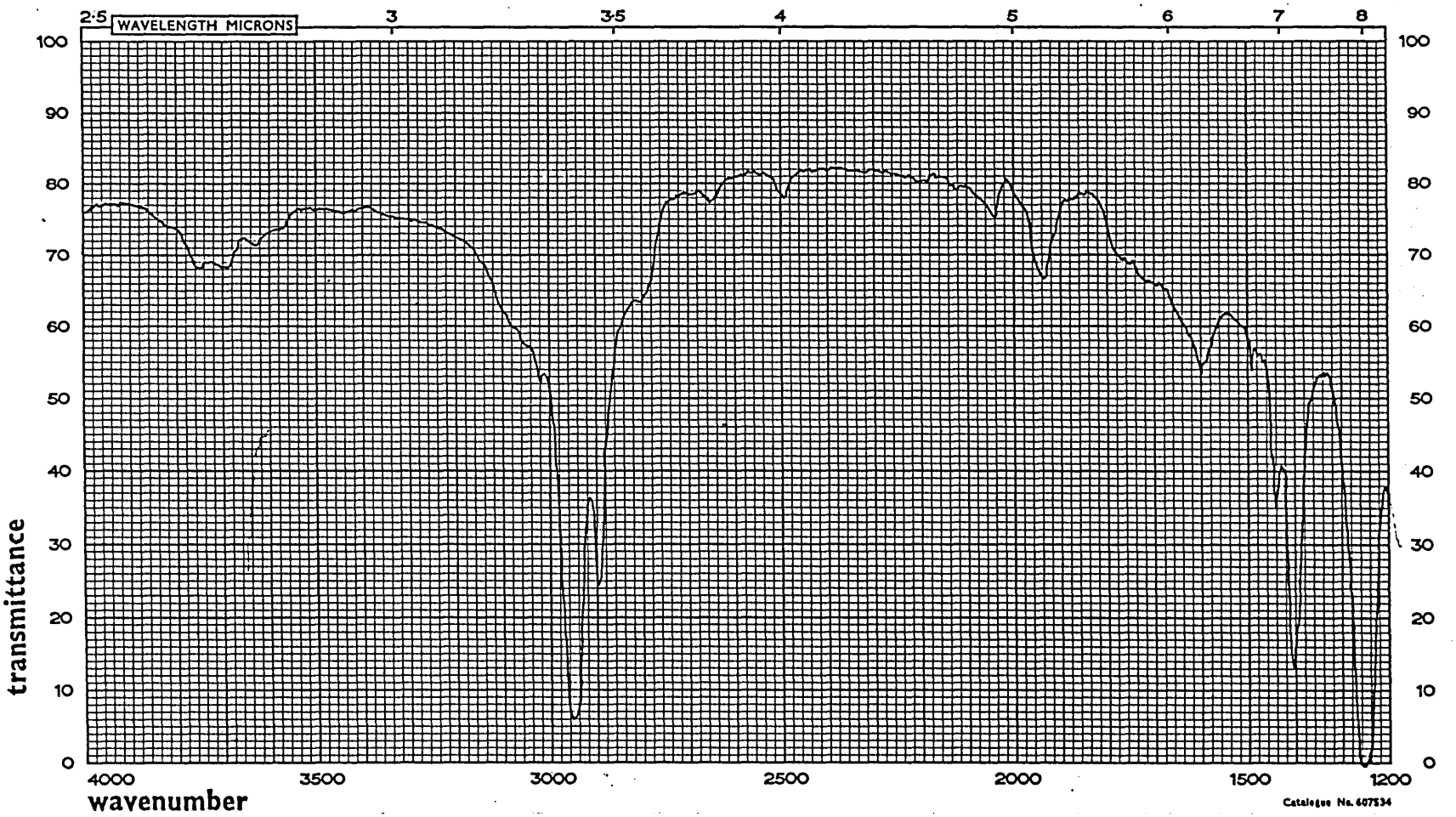
WAVELENGTH MICRONS
2·5
3
3·5
4
5
6
7
8
100
90
80
70
60
50
40
30
20
10
0
transmittance
4000
3500
3000
2500
2000
1500
1200
wavenumber
Catalogue No. 607534

Figure 33. Infrared Spectrum of Chloro-terminated P.D.M.S. ($\overline{Mn}$ ~29000) - Range 1300-400cm^{-1}

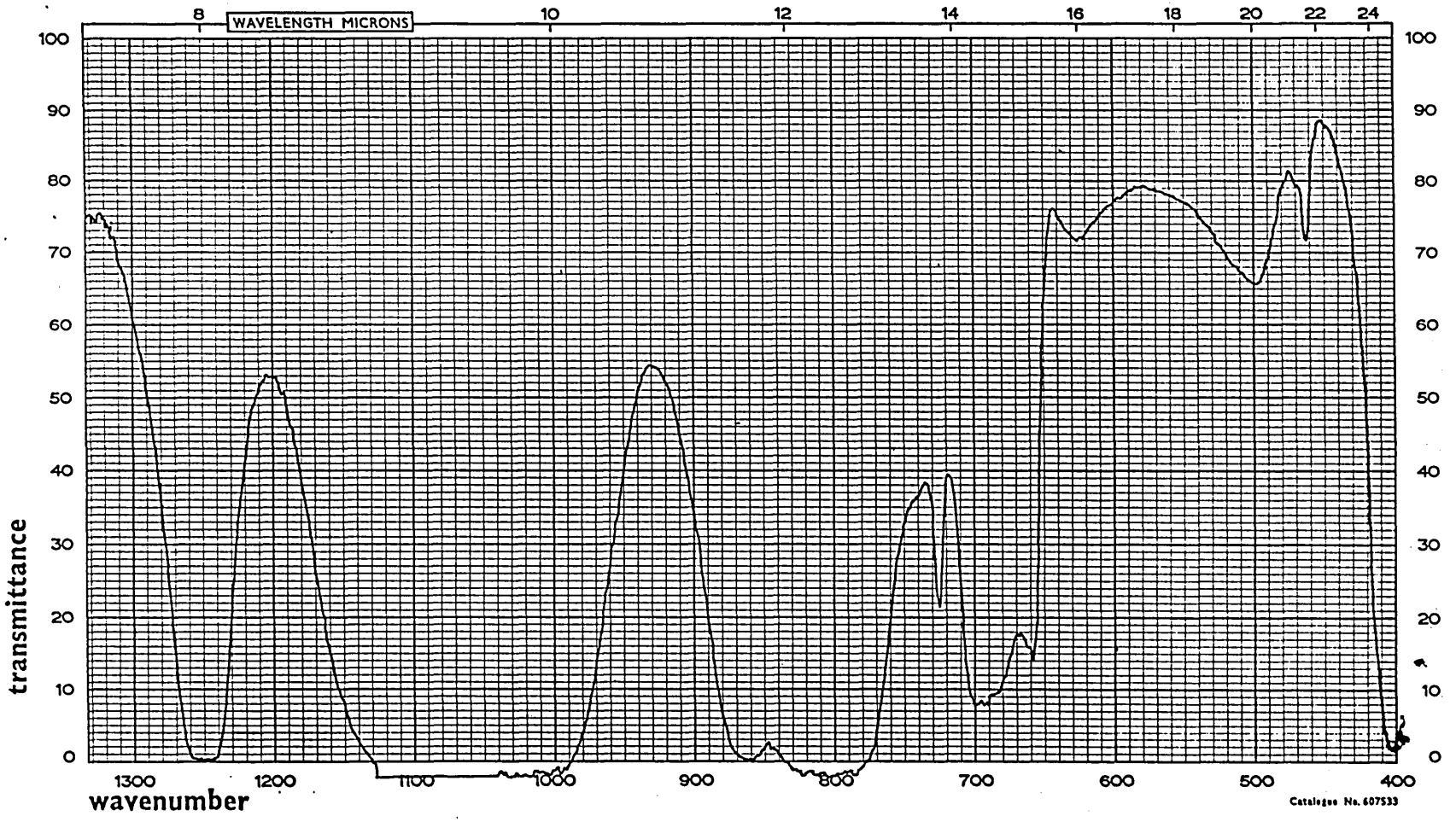
WAVELENGTH MICRONS
8
10
12
14
16
18
20
22
24
100
90
80
70
60
50
40
30
20
10
0
transmittance
1300
1200
1100
1000
900
800
700
600
500
400
wavenumber
Catalogue No. 607533

Figure 34. Infrared Spectrum of Amine-terminated P.D.M.S. ($\bar{M}n$ ~800) - Range 4000-1200cm^{-1}

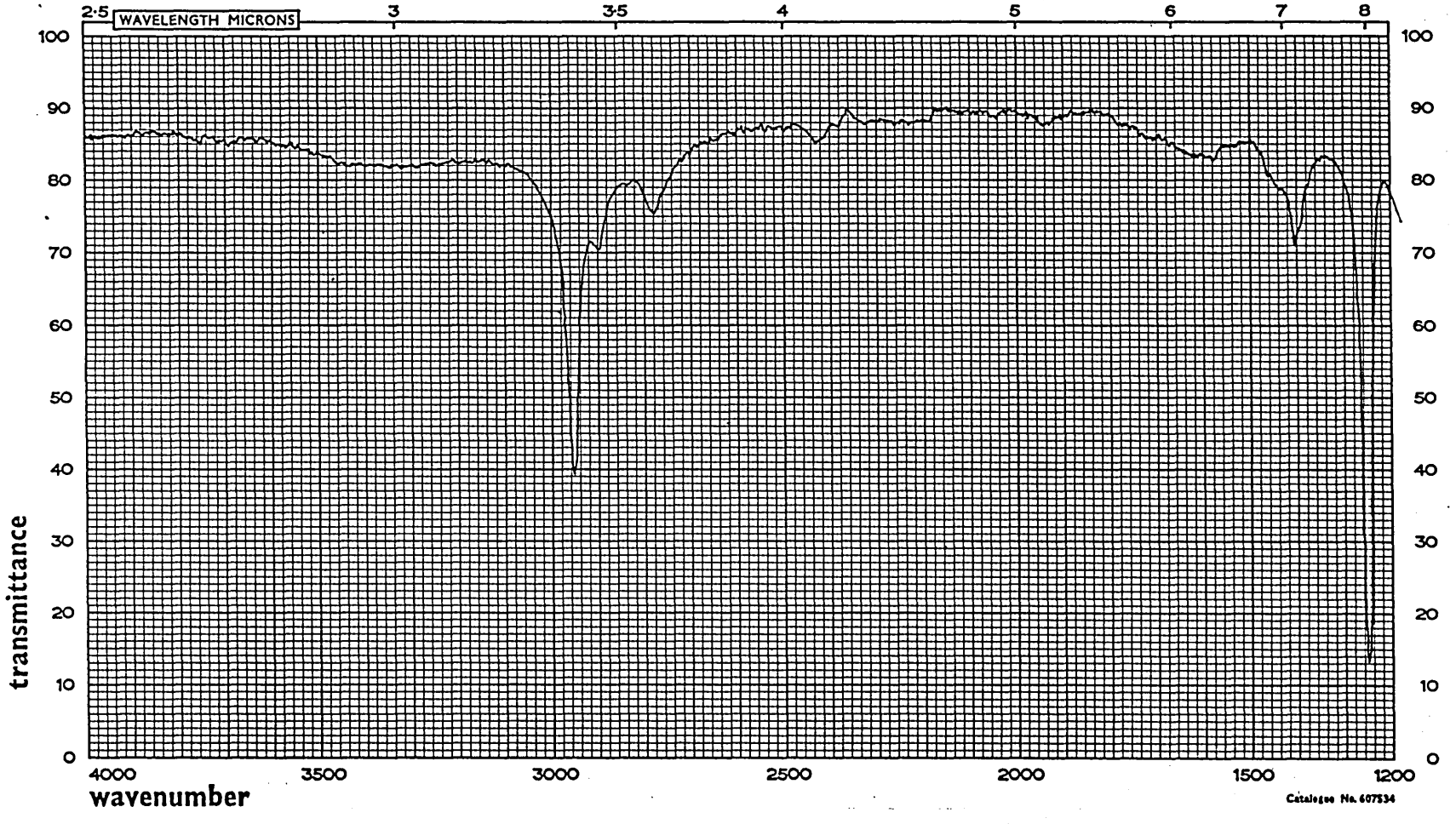
WAVELENGTH MICRONS
2·5
3
3·5
4
5
6
7
8
100
90
80
70
60
50
40
30
20
10
0
transmittance
4000
3500
3000
2500
2000
1500
1200
wavenumber
Catalogue No. 607534

Figure 35. Infrared Spectrum of Amine-terminated P.D.M.S. ($\overline{Mn}$ ~800) - Range 1300-400cm^{-1}

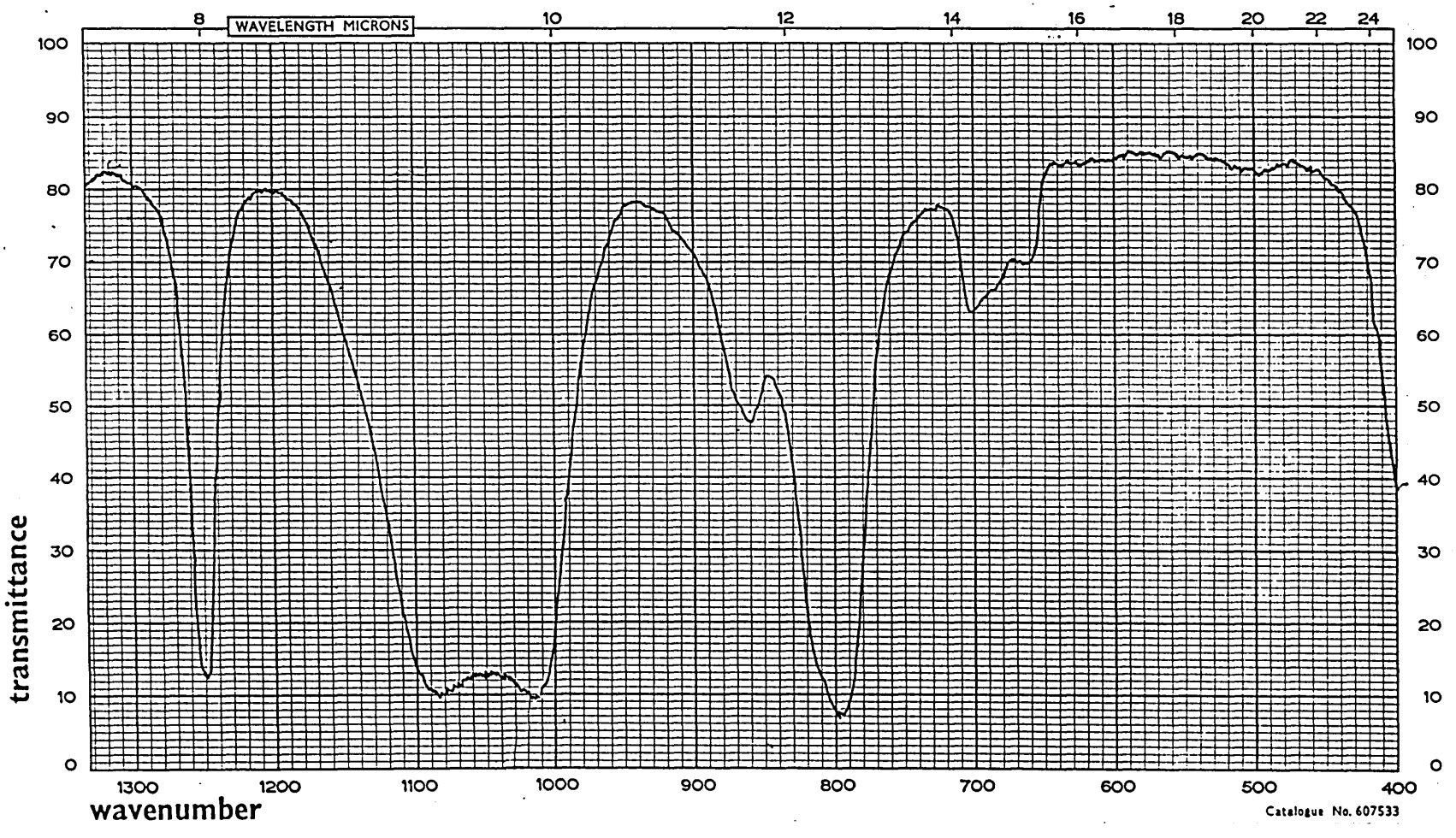
WAVELENGTH MICRONS
8
10
12
14
16
18
20
22
24
100
90
80
70
60
50
40
30
20
10
0
transmittance
1300
1200
1100
1000
900
800
700
600
500
400
wavenumber
Catalogue No. 607533

Figure 36. Infrared Spectrum of Amine-terminated P.D.M.S. ($\bar{M}n \sim 5100$) - Range 4000-1200cm^{-1}

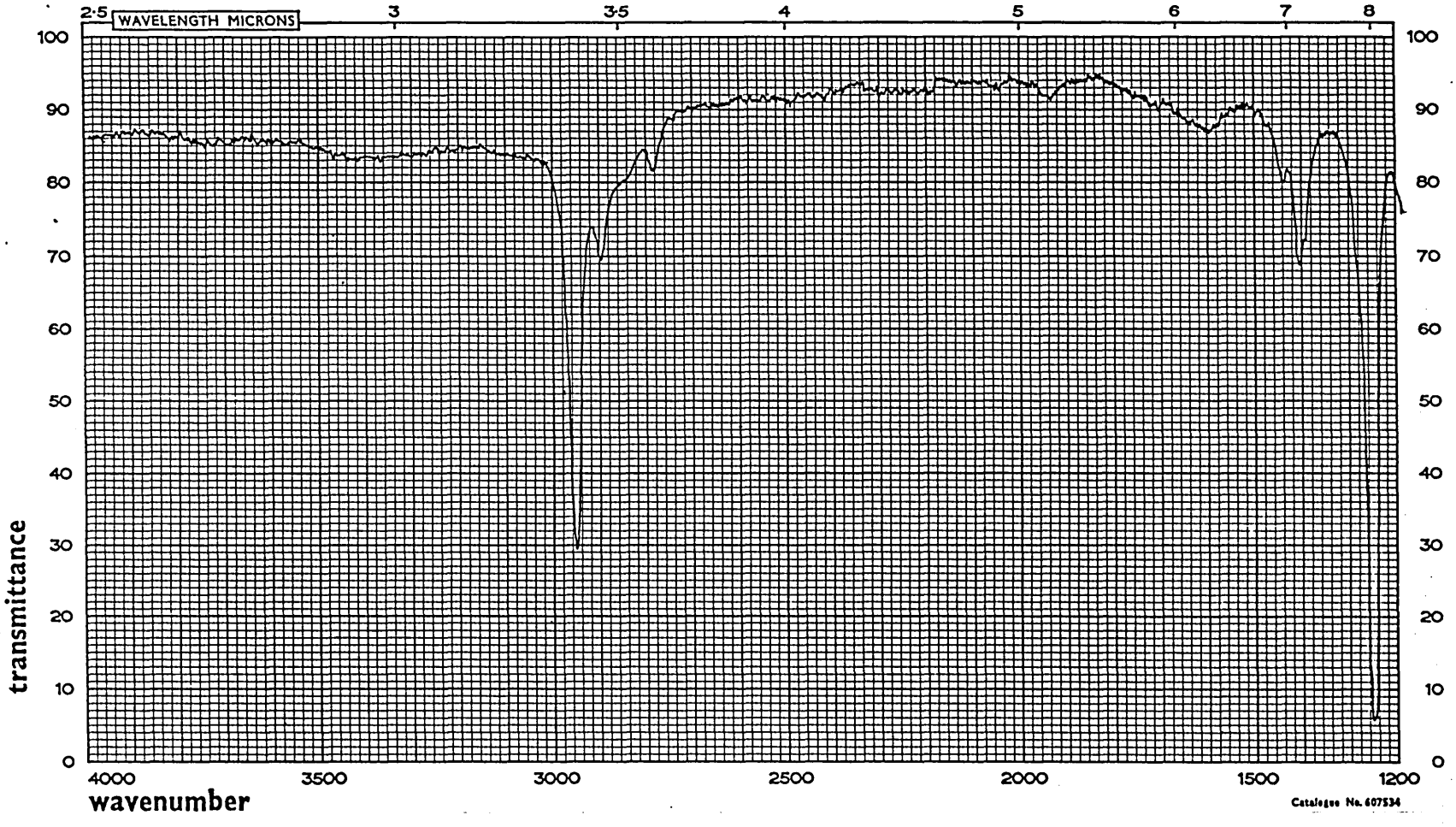
2·5
WAVELENGTH MICRONS
3
3·5
4
5
6
7
8
100
90
80
70
60
50
40
30
20
10
0
transmittance
4000
3500
3000
2500
2000
1500
1200
wavenumber
Catalogue No. 607534

Figure 37. Infrared Spectrum of Amine-terminated P.D.M.S. ($\overline{Mn} \sim 5100$) - Range 1300-400cm^{-1}

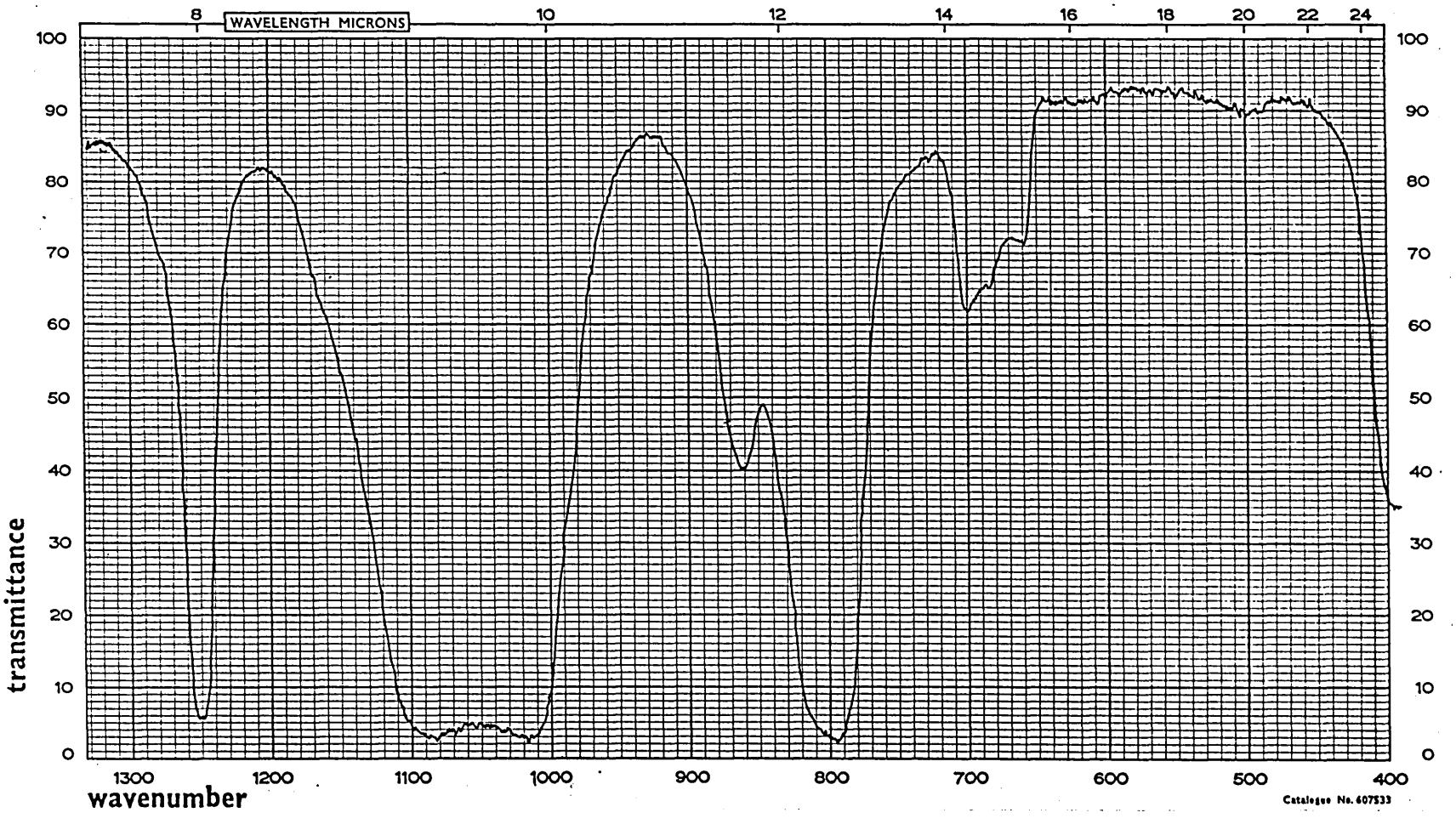
WAVELENGTH MICRONS
8
10
12
14
16
18
20
22
24
100
90
80
70
60
50
40
30
20
10
0
transmittance
1300
1200
1100
1000
900
800
700
600
500
400
wavenumber
Catalogue No. 607533

Figure 38. Infrared Spectrum of Amine-terminated P.D.M.S. ($\bar{M}n$ ~53000) - Range 4000-1200cm^{-1}

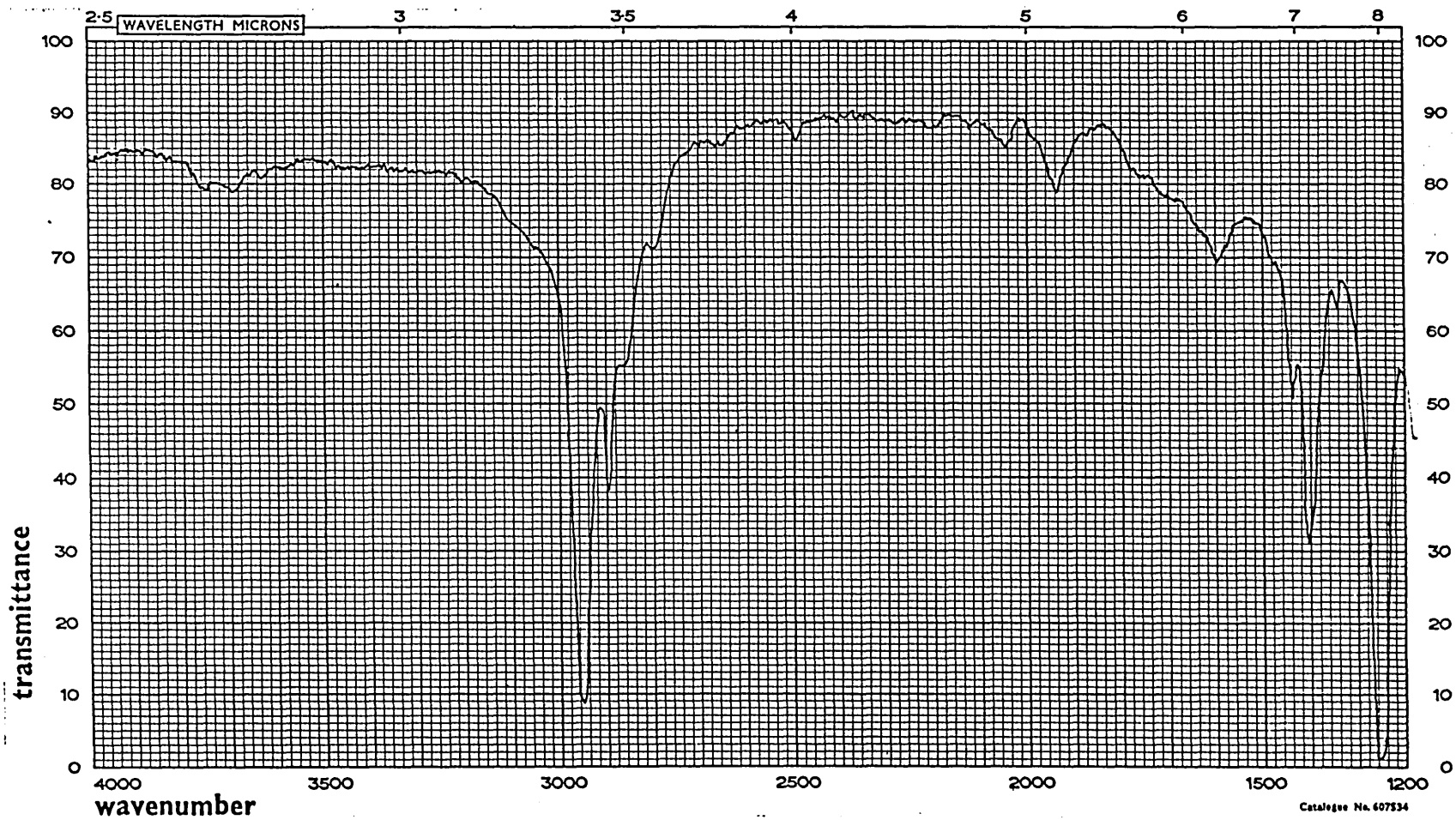
2·5
WAVELENGTH MICRONS
3
3·5
4
5
6
7
8
100
90
80
70
60
50
40
30
20
10
0
transmittance
4000
3500
3000
2500
2000
1500
1200
wavenumber
Catalogue No. 607534

Figure 39. Infrared Spectrum of Amine-terminated P.D.M.S. ($\bar{M}n$ ~53000) - Range 1300-400cm^{-1}

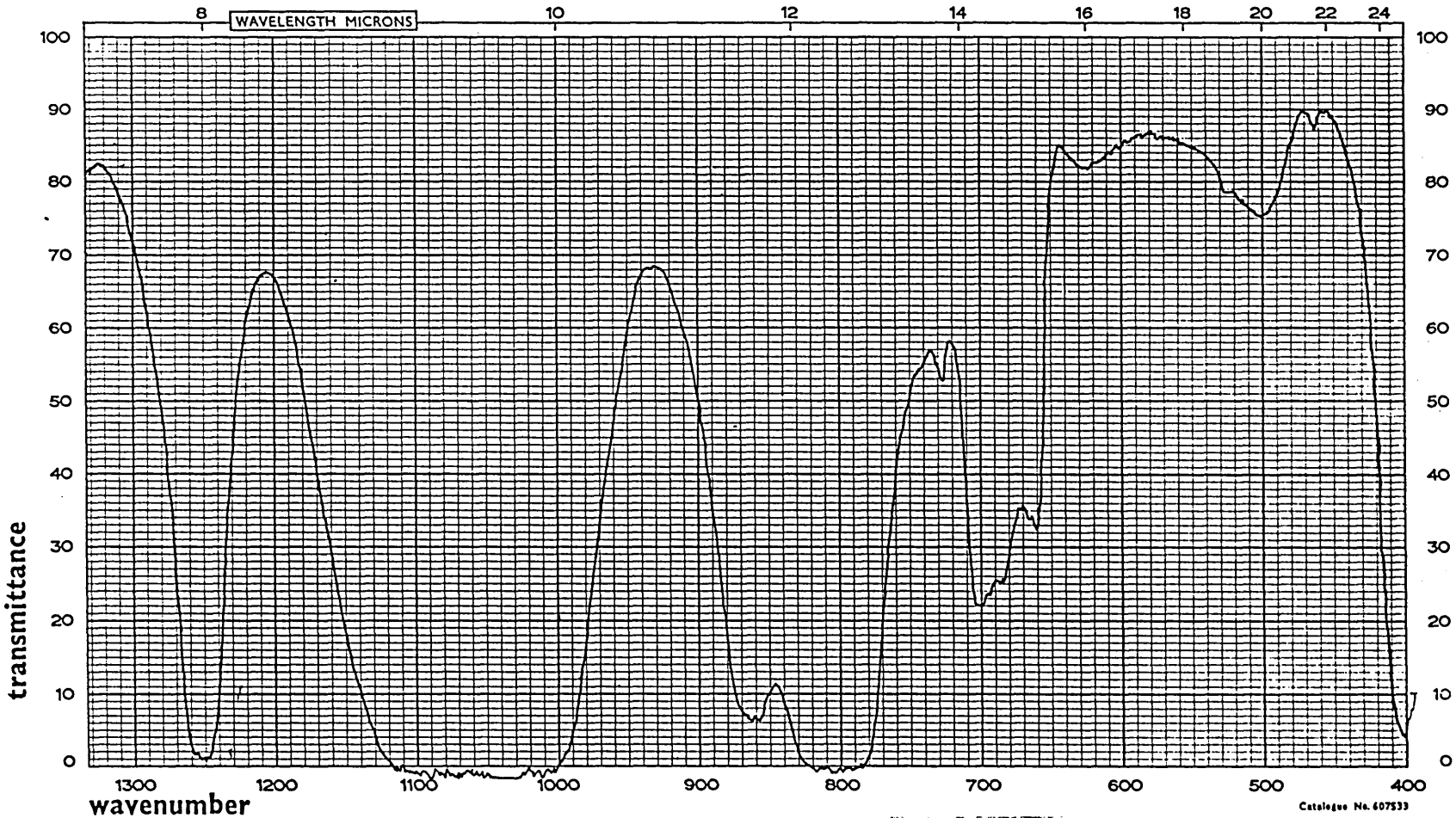
WAVELENGTH MICRONS
8
10
12
14
16
18
20
22
24
100
90
80
70
60
50
40
30
20
10
0
transmittance
1300
1200
1100
1000
900
800
700
600
500
400
wavenumber
Catalogue No. 607533

Figure 40. $\overline{Mv}$ (Determined Viscometrically) vs $\overline{Mn}$ (Determined by G.P.C.) for Hydroxyl-terminated P.D.M.S. Oligomers

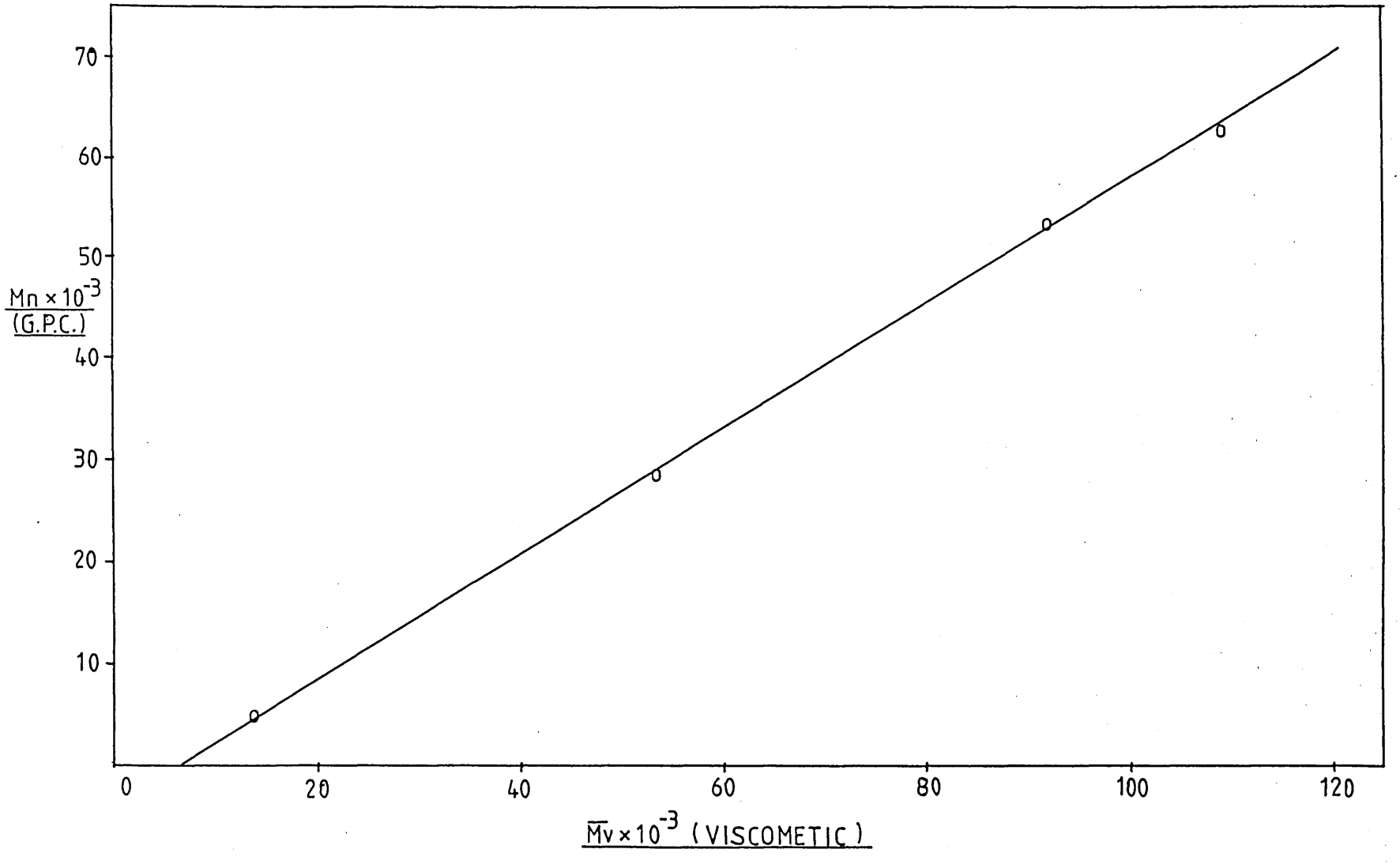
70
60
50
40
30
20
10
Mn × 10^-3
(G.P.C.)
0
20
40
60
80
100
120
M̄v × 10^-3 (VISCOMETIC)

Figure 41. Apparatus for the Preparation of P.E.S./P.D.M.S. Block Copolymers

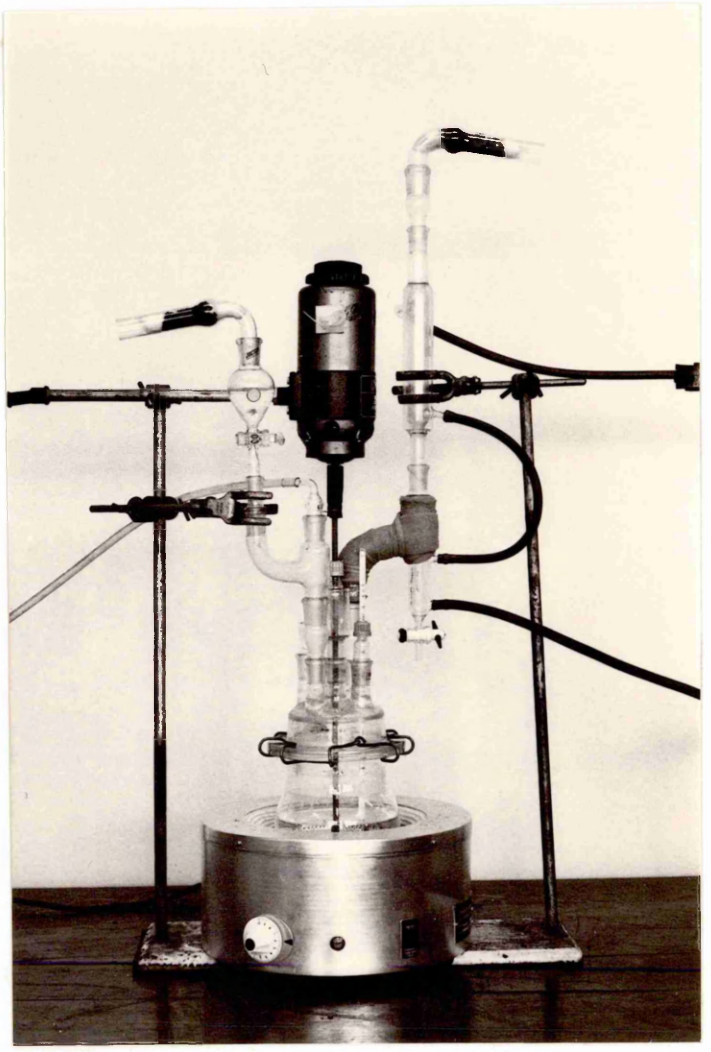

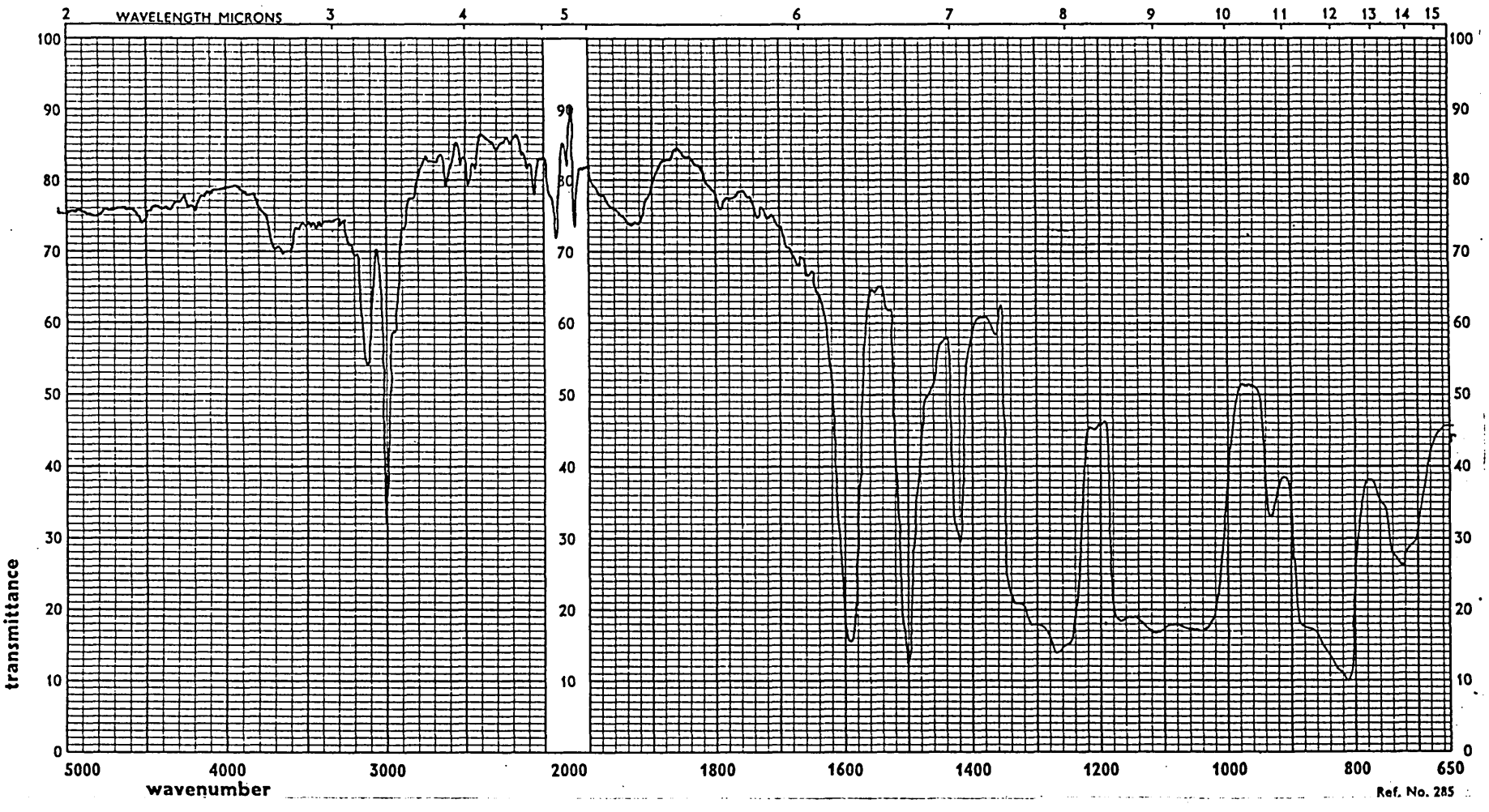
WAVELENGTH MICRONS
2
3
4
5
6
7
8
9
10
11
12
13
14
15
100
90
80
70
60
50
40
30
20
10
0
transmittance
5000
4000
3000
2000
1800
1600
1400
1200
1000
800
650
wavenumber
Ref. No. 285

Figure 43. I.R. Spectrum of P.E.S./P.D.M.S. Block Copolymer No 2

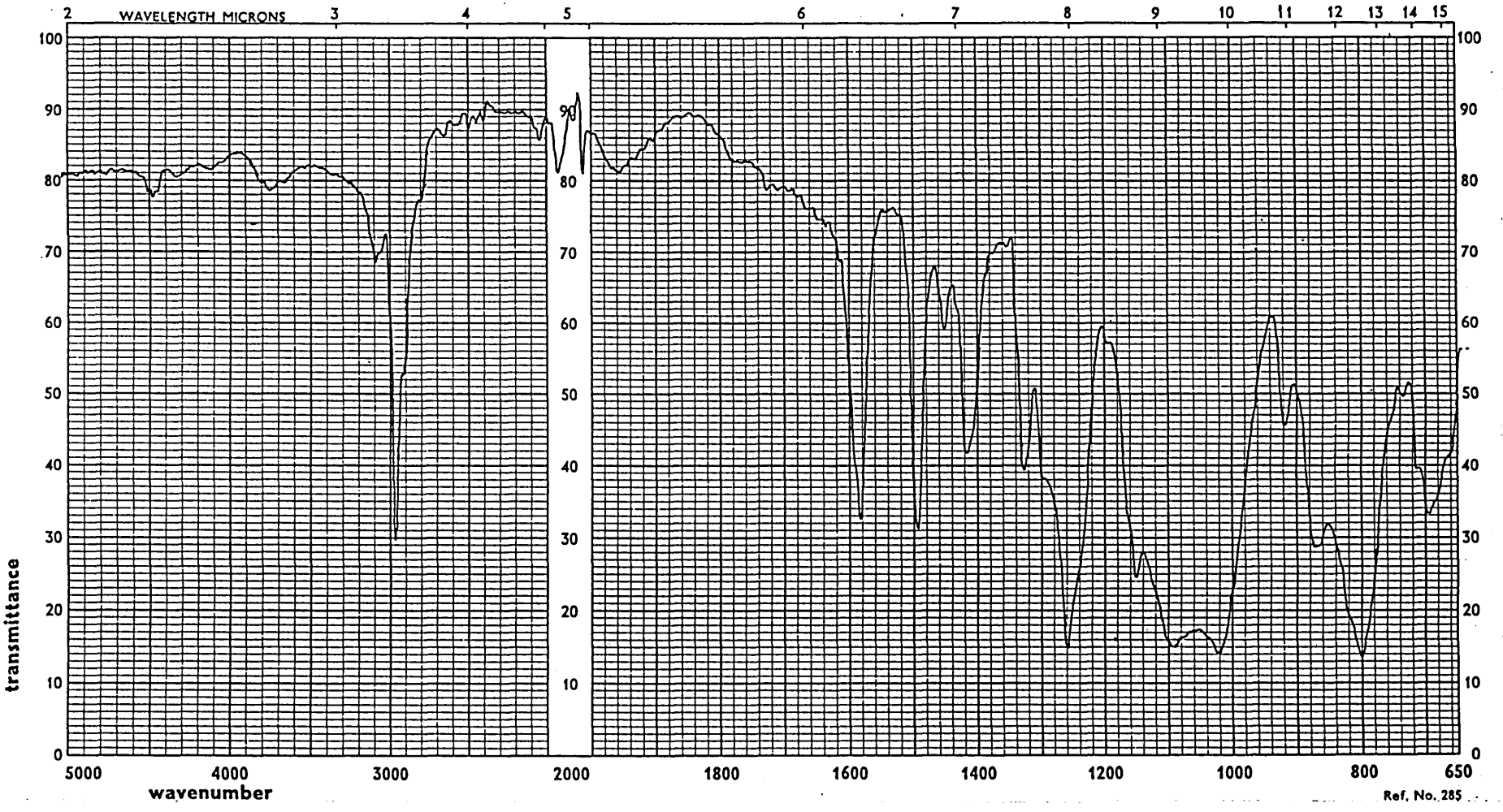
WAVELENGTH MICRONS
2
3
4
5
6
7
8
9
10
11
12
13
14
15
100
90
80
70
60
50
40
30
20
10
0
transmittance
5000
4000
3000
2000
1800
1600
1400
1200
1000
800
650
wavenumber
Ref. No. 285

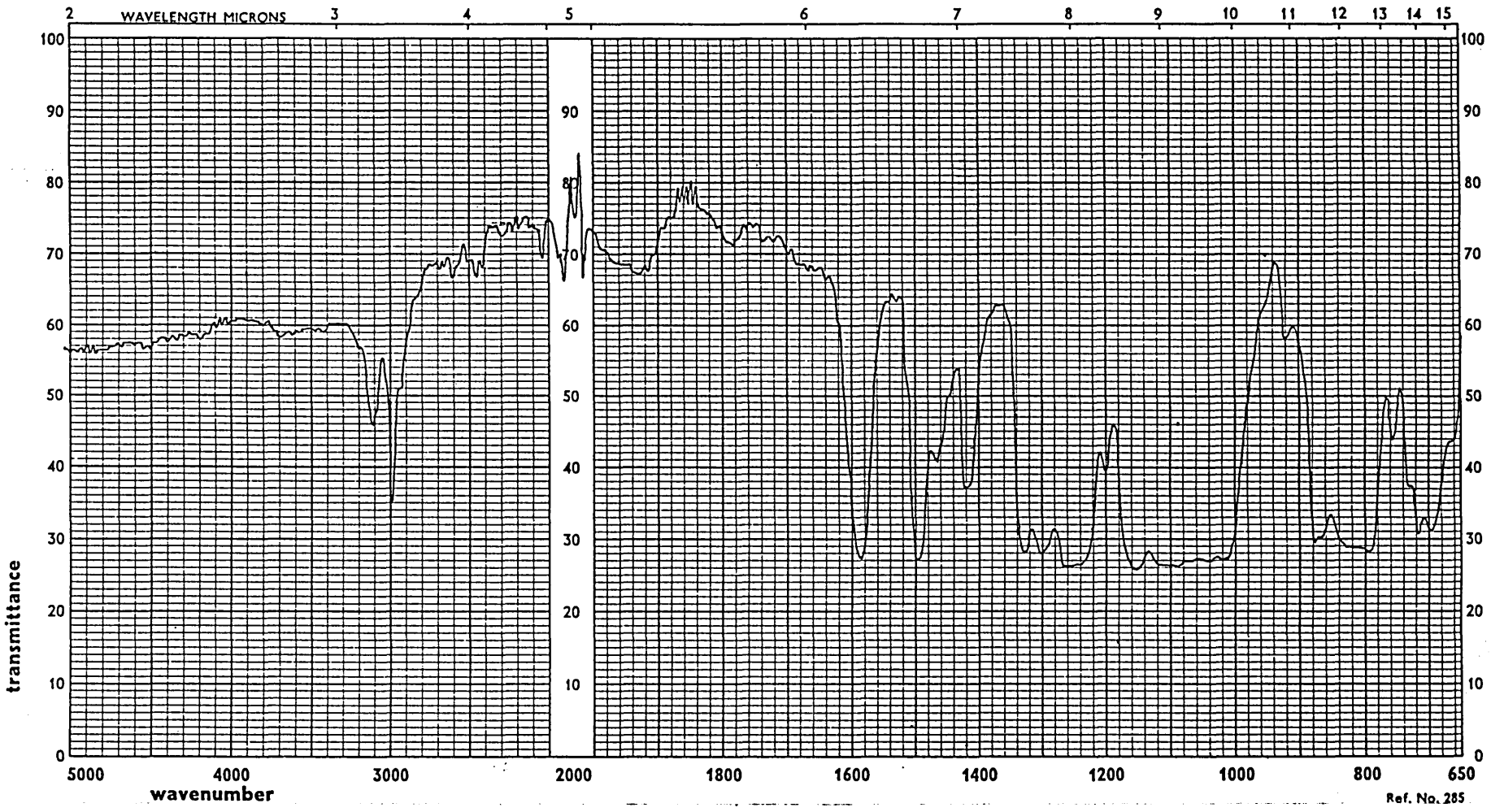
WAVELENGTH MICRONS
2
3
4
5
6
7
8
9
10
11
12
13
14
15
100
90
80
70
60
50
40
30
20
10
0
transmittance
5000
4000
3000
2000
1800
1600
1400
1200
1000
800
650
wavenumber
Ref. No. 285

Figure 45. I.R. Spectrum of P.E.S./P.D.M.S. Block Copolymer No 4

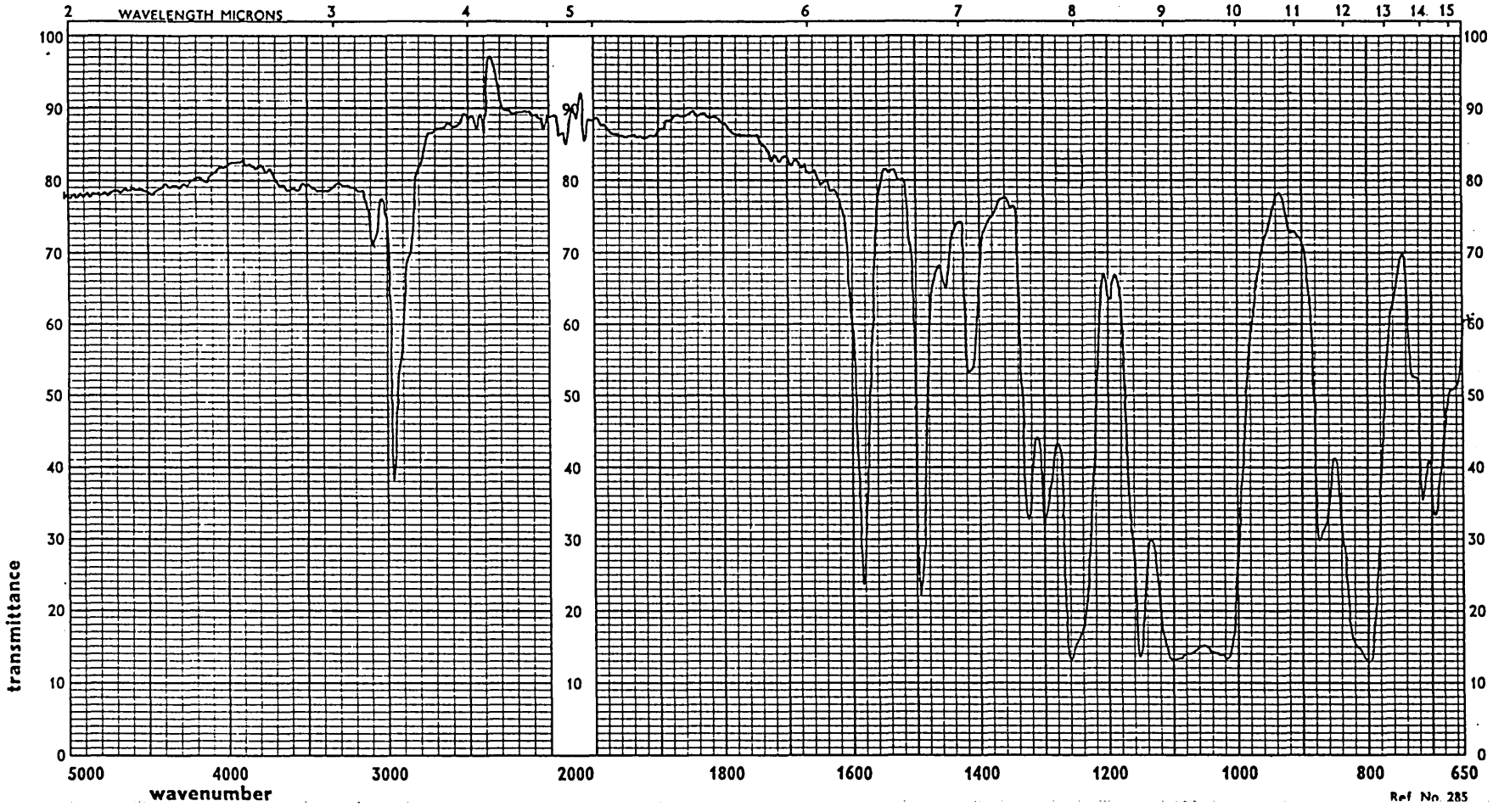
WAVELENGTH MICRONS
2
3
4
5
6
7
8
9
10
11
12
13
14
15
100
90
80
70
60
50
40
30
20
10
0
transmittance
5000
4000
3000
2000
1800
1600
1400
1200
1000
800
650
wavenumber
Ref. No. 285

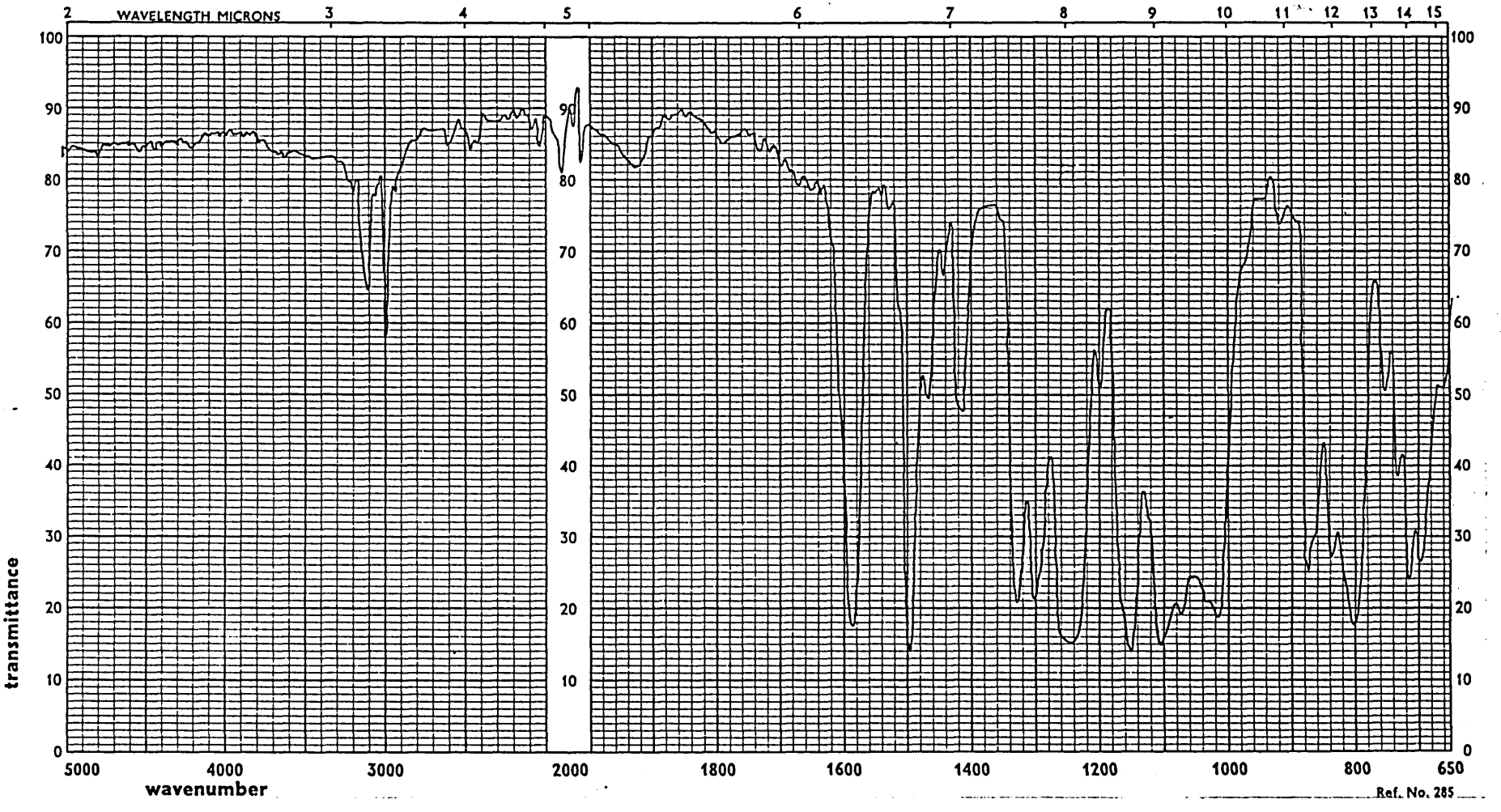
WAVELENGTH MICRONS
2
3
4
5
6
7
8
9
10
11
12
13
14
15
transmittance
100
90
80
70
60
50
40
30
20
10
0
5000
4000
3000
2000
1800
1600
1400
1200
1000
800
650
wavenumber
Ref. No. 285

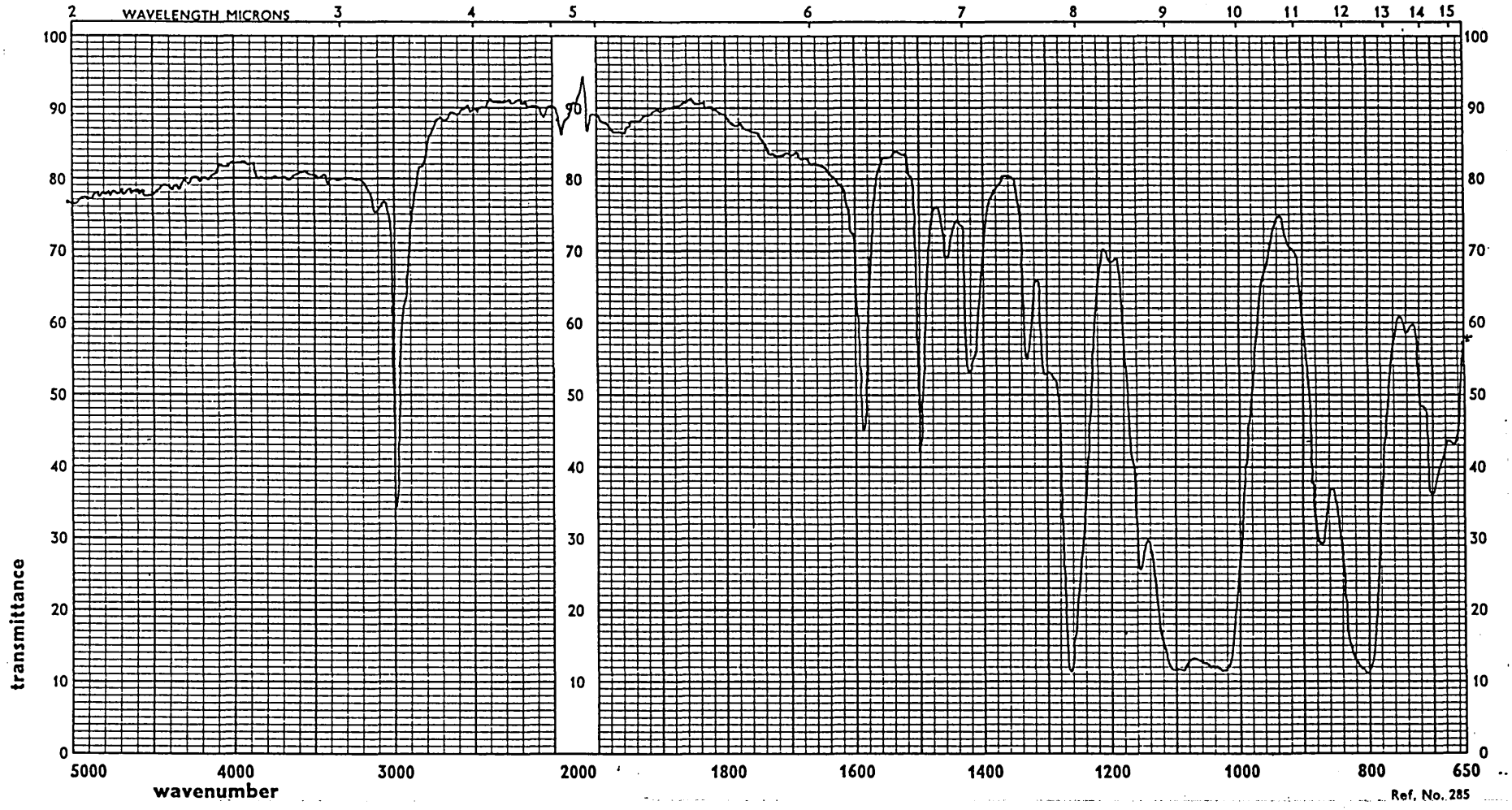
WAVELENGTH MICRONS
2
3
4
5
6
7
8
9
10
11
12
13
14
15
100
90
80
70
60
50
40
30
20
10
0
transmittance
5000
4000
3000
2000
1800
1600
1400
1200
1000
800
650
wavenumber
Ref. No. 285

PES ($\bar{M}_n$ ~ 1300) / PDMS ($\bar{M}n$ ~ 800) COPOLYMER
SOLVENT - DEUTERATED CHLOROFORM / DIMETHYLSULPHOXIDE MIXTURE
STRUCTURE -

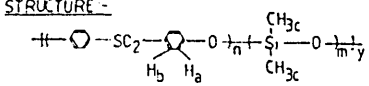

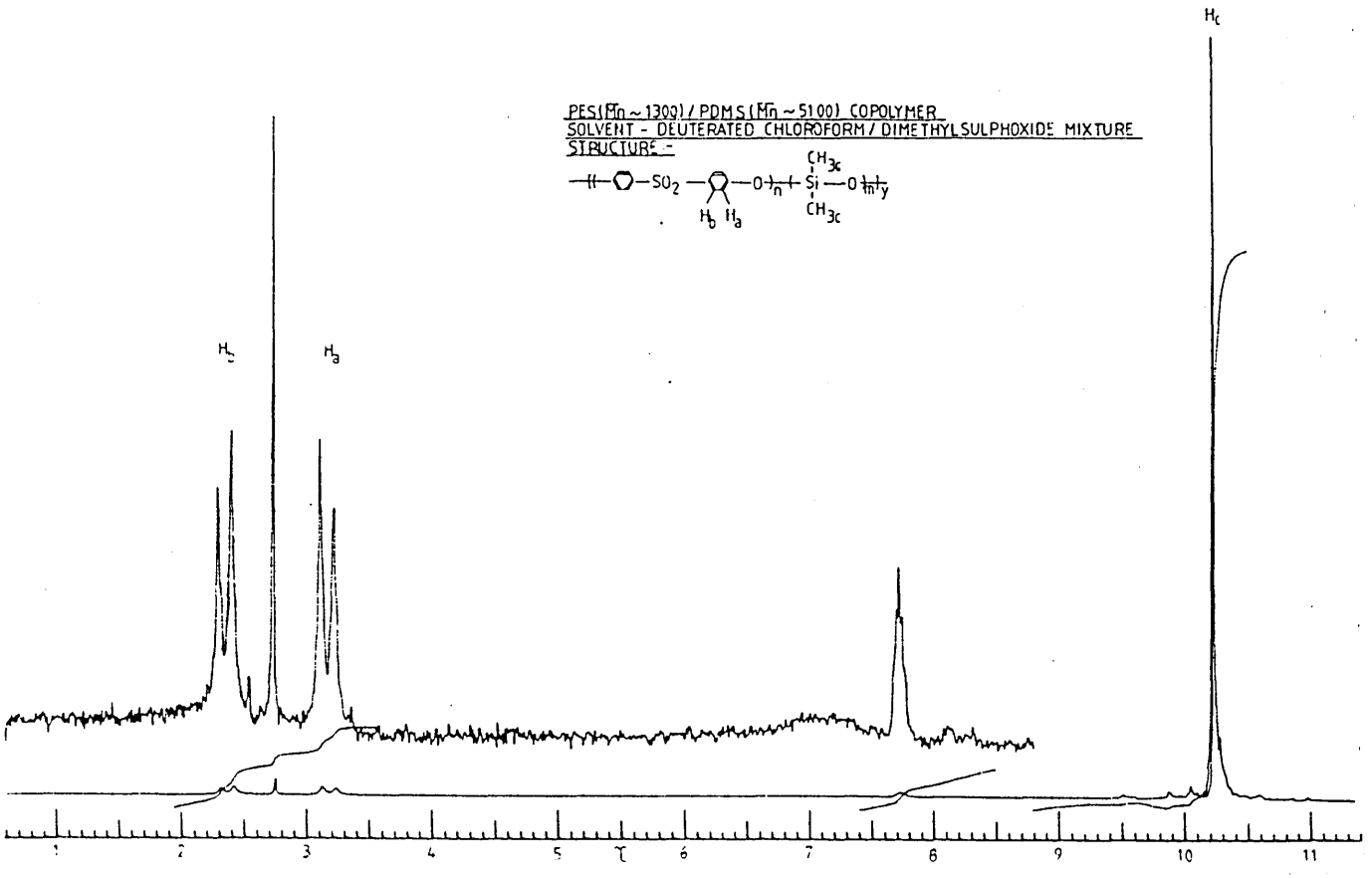
PES(Mn ~ 1300) / PDMS(Mn ~ 5100) COPOLYMER
SOLVENT - DEUTERATED CHLOROFORM / DIMETHYLSULPHOXIDE MIXTURE
STRUCTURE :-
H_c
H_b
H_a
1
2
3
4
5
τ
6
7
8
9
10
11

PES($\overline{Mn}$~4900) / PDMS($\overline{Mn}$~5100) COPOLYMER I
SOLVENT - DEUTERATED CHLOROFORM / DIMETHYLSULPHOXIDE MIXTURE
STRUCTURE -

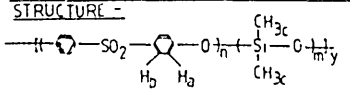

PES($\bar{M}_n$ ~ 4900) / PDMS($\bar{M}_n$ ~ 5100) COPOLYMER II
SOLVENT - DEUTERATED CHLOROFORM / DIMETHYLSULPHOXIDE MIXTURE
STRUCTURE -

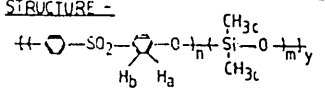

PES($\overline{Mn}$~9600)/PDMS($\overline{Mn}$~5100) COPOLYMER
SOLVENT - DEUTERATED CHLOROFORM/DIMETHYLSULPHOXIDE MIXTURE
STRUCTURE :-

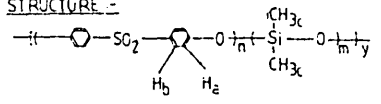

PES($\overline{Mn}$ ~9600) / PDMS($\overline{Mn}$ ~53000) COPOLYMER
SOLVENT :- DEUTERATED CHLOROFORM / DIMETHYLSULPHOXIDE
STRUCTURE :-

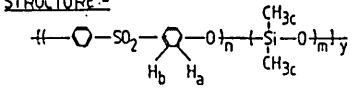

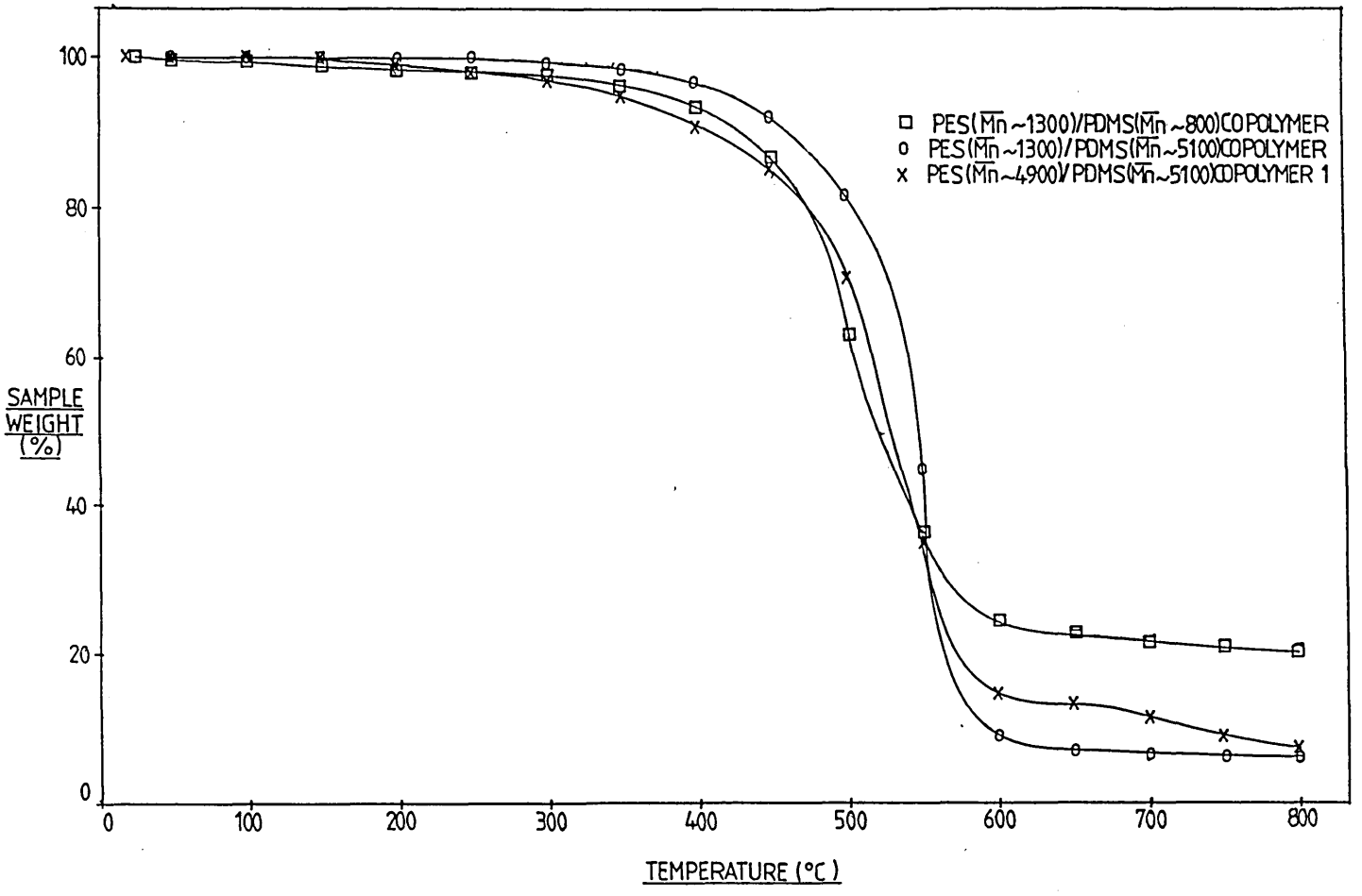
□ PES(Mn ~1300)/PDMS(Mn ~800)COPOLYMER
o PES(Mn ~1300)/PDMS(Mn ~5100)COPOLYMER
x PES(Mn ~4900)/PDMS(Mn ~5100)COPOLYMER 1
SAMPLE WEIGHT (%)
100
80
60
40
20
0
0
100
200
300
400
500
600
700
800
TEMPERATURE (°C)

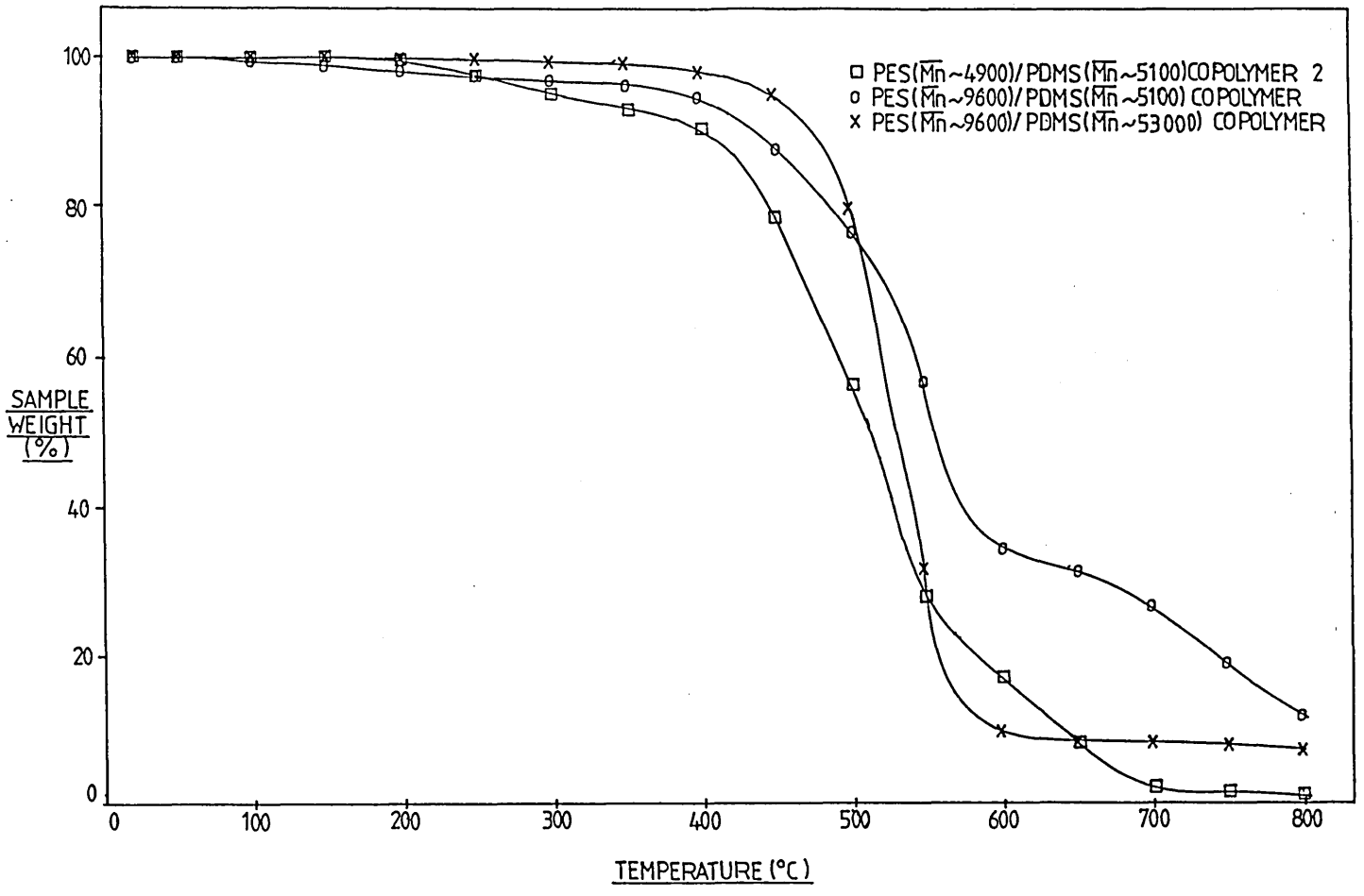
□ PES($\overline{Mn}$~4900)/PDMS($\overline{Mn}$~5100)COPOLYMER 2
o PES($\overline{Mn}$~9600)/PDMS($\overline{Mn}$~5100) COPOLYMER
x PES($\overline{Mn}$~9600)/PDMS($\overline{Mn}$~53000) COPOLYMER
SAMPLE WEIGHT (%)
100
80
60
40
20
0
0
100
200
300
400
500
600
700
800
TEMPERATURE (°C)

Figure 56. Comparison between the Thermal Stabilities of (O) a P.E.S. oligomer, (x) a P.D.M.S. oligomer, (o) a simple physical blend of these oligomers and (□) a block copolymer derived from these oligomers.

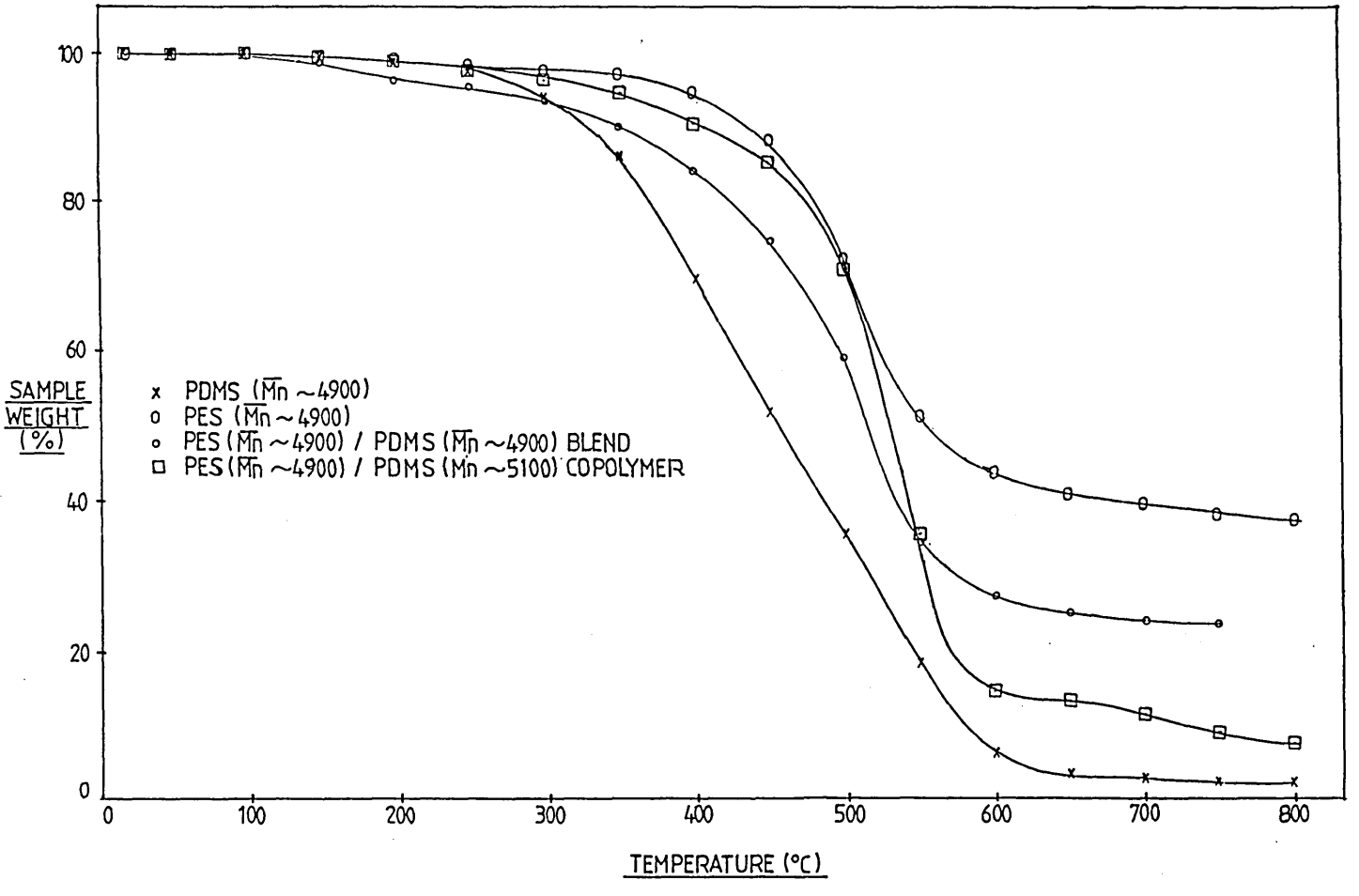
100
80
60
40
20
0
SAMPLE WEIGHT (%)
x PDMS ($\overline{Mn}$ ~4900)
o PES ($\overline{Mn}$ ~4900)
∘ PES ($\overline{Mn}$ ~4900) / PDMS ($\overline{Mn}$ ~4900) BLEND
□ PES ($\overline{Mn}$ ~4900) / PDMS (Mn ~5100) COPOLYMER
0
100
200
300
400
500
600
700
800
TEMPERATURE (°C)

Figure 57. D.S.C. curves for three P.E.S./P.D.M.S. block copolymers, (a) Copolymer 1, (b) Copolymer 2, and (c) Copolymer 3.

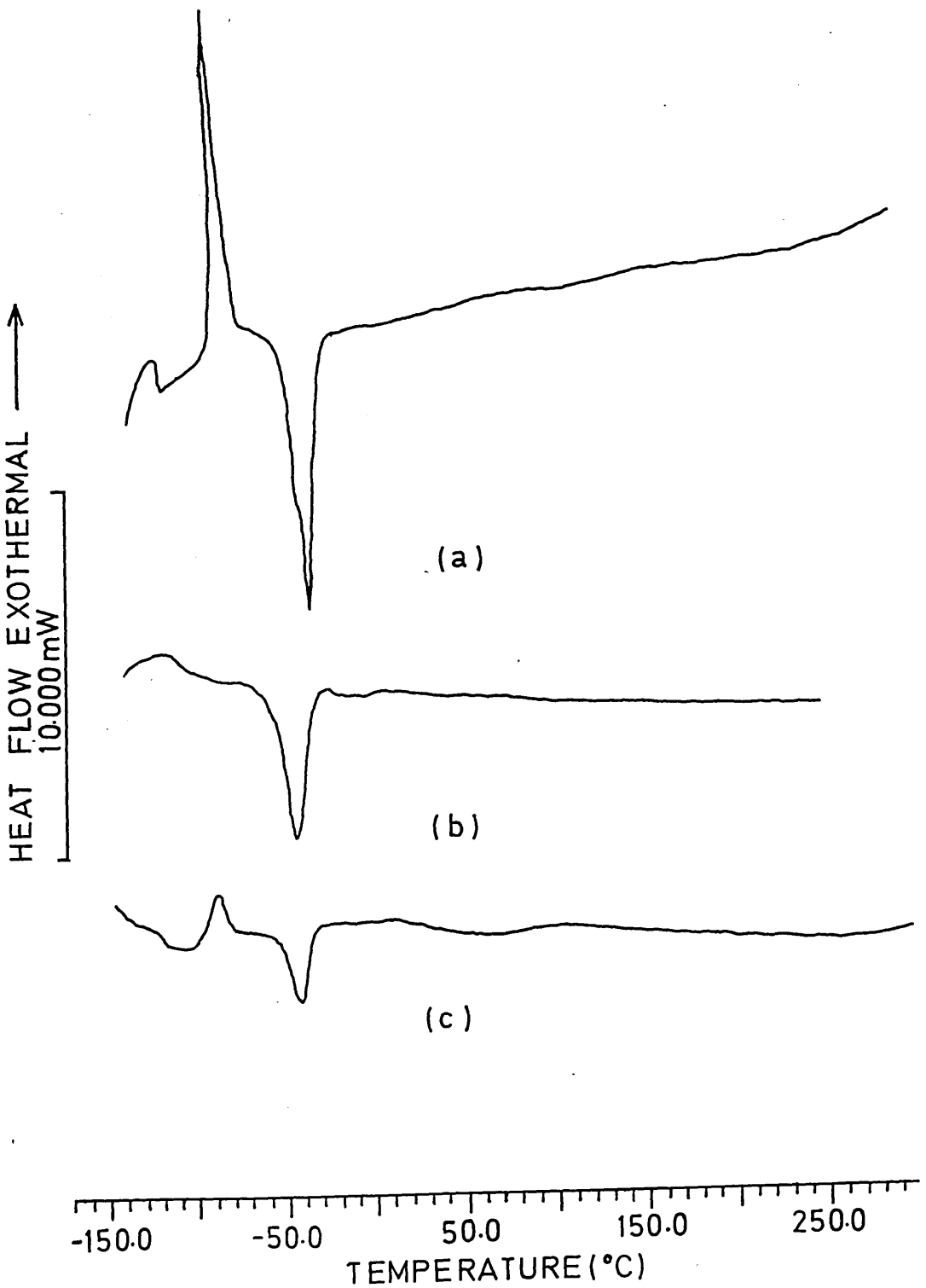
HEAT FLOW EXOTHERMAL
10.000mW
(a)
(b)
(c)
-150.0
-50.0
50.0
150.0
250.0
TEMPERATURE (°C)

Figure 58. D.S.C. curves for three P.E.S./P.D.M.S. block copolymers, (d) Copolymer 4, (e) Copolymer 5, and (f) Copolymer 6.

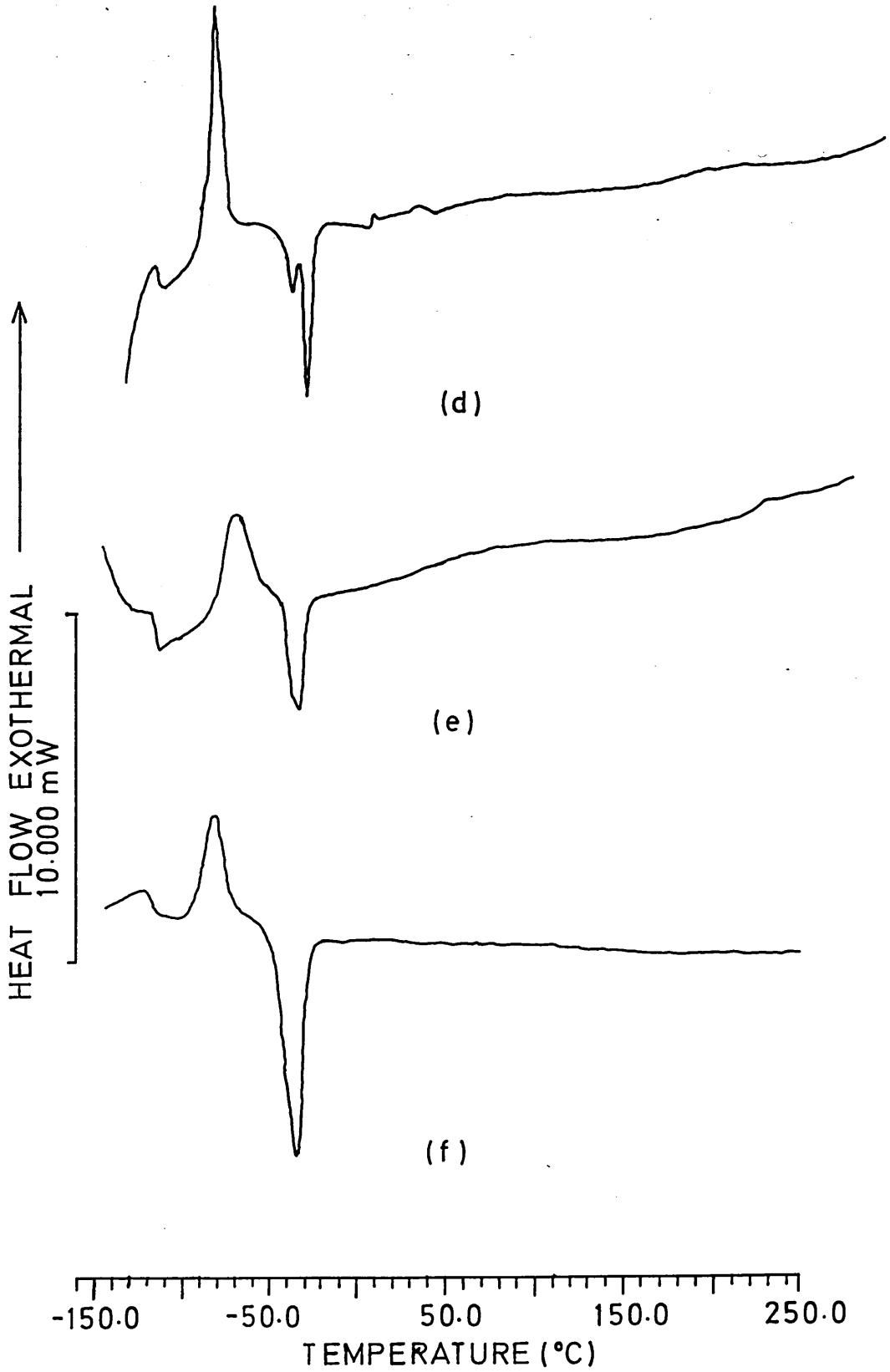
(d)
(e)
(f)
HEAT FLOW EXOTHERMAL
10.000 mW
-150.0
-50.0
50.0
150.0
250.0
TEMPERATURE (°C)

Figure 59. Schematics of Shear Grips specially designed for use on Toyo Baldwin Rheovibron.

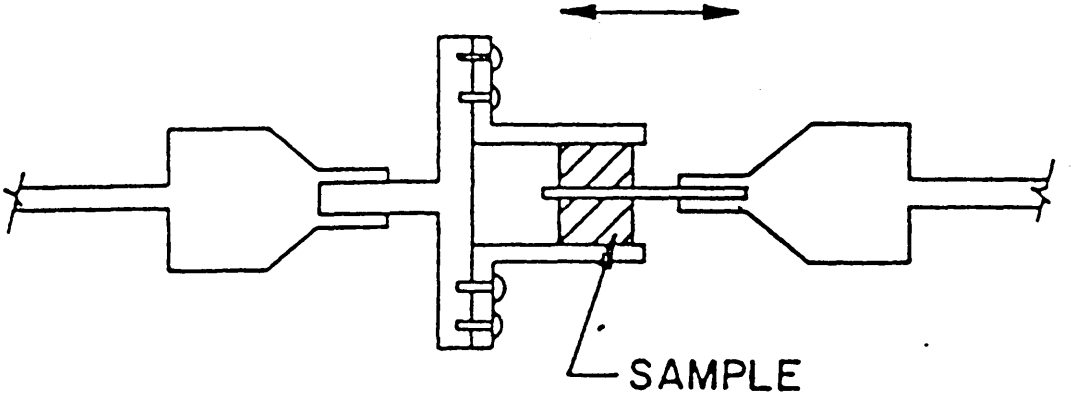

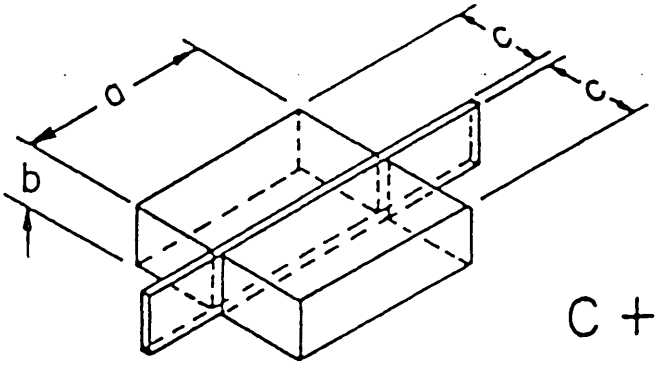

$$C + C = h$$

Figure 60. Transmission Electron Micrograph of Copolymer 1 (cast from benzene solution).

Figure 61. Transmission Electron Micrograph of Copolymer 2 (cast from benzene solution).

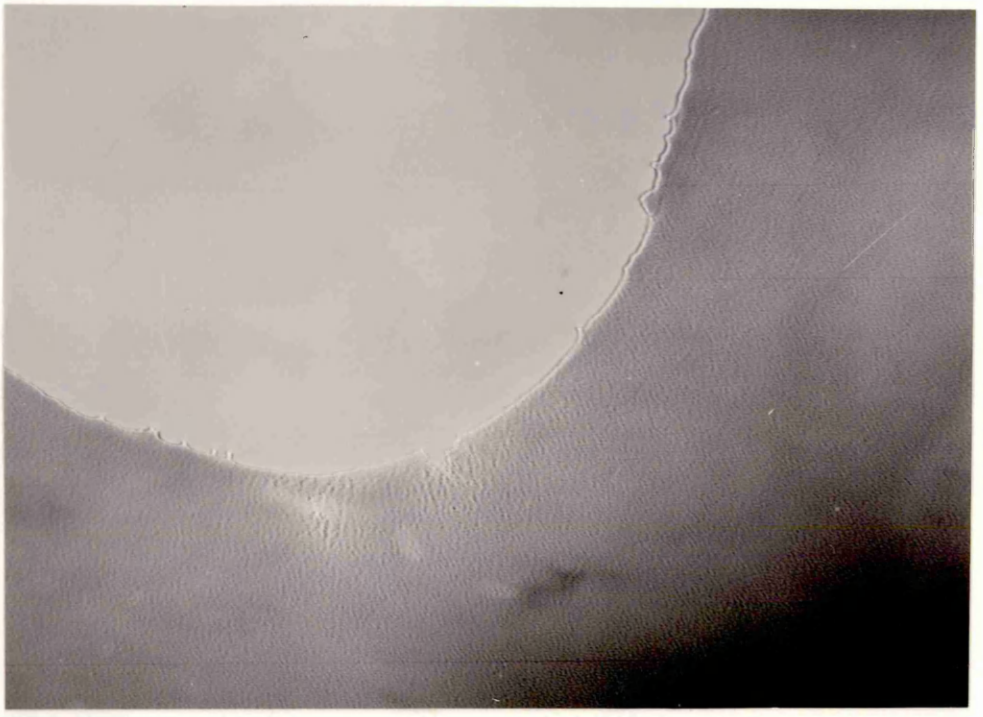

1 μm

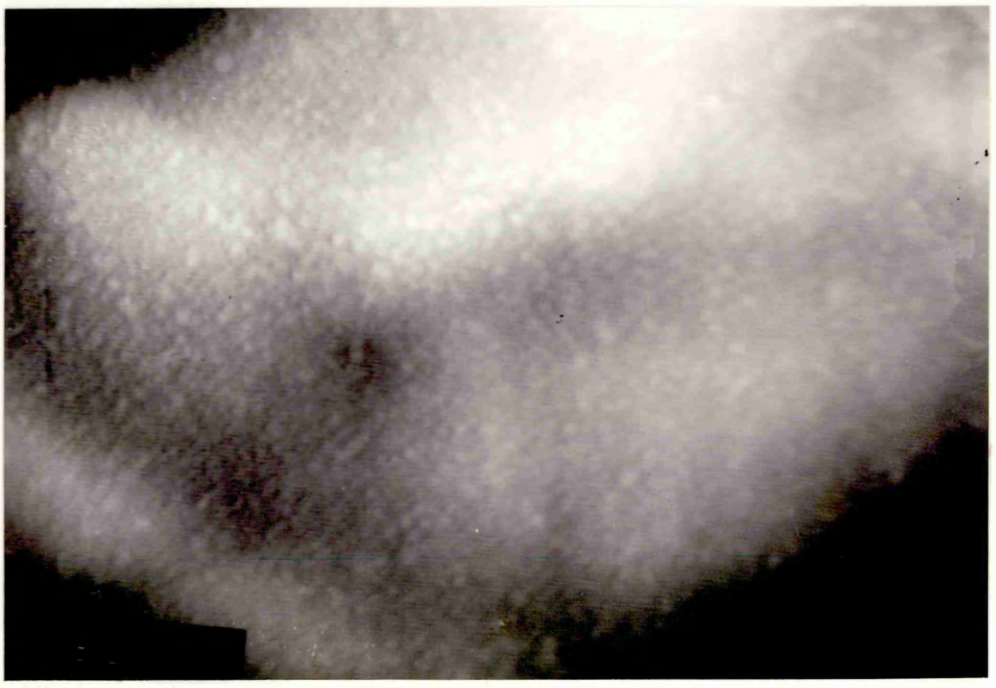

1 μm

Figure 62. Transmission Electron Micrograph of Copolymer 3 (cast from benzene solution).

Figure 63. Transmission Electron Micrograph of Copolymer 4 (cast from benzene solution).

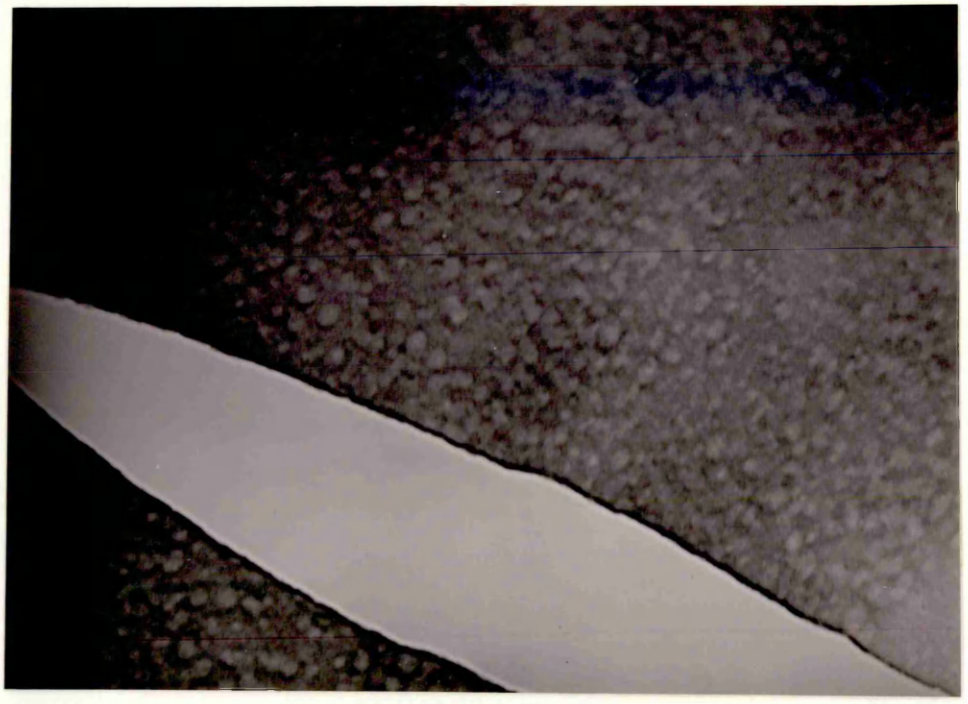

1μm

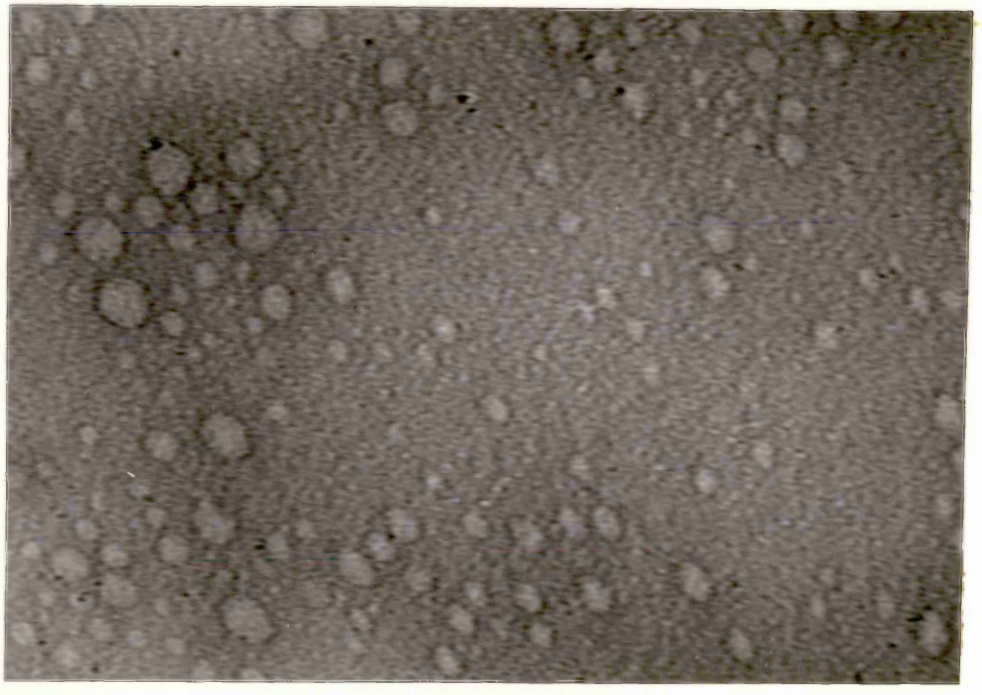

0.5μm

Figure 64. Transmission Electron Micrograph of Copolymer 5 (cast from benzene solution).

Figure 65. Transmission Electron Micrograph of Copolymer 6 (cast from benzene solution).

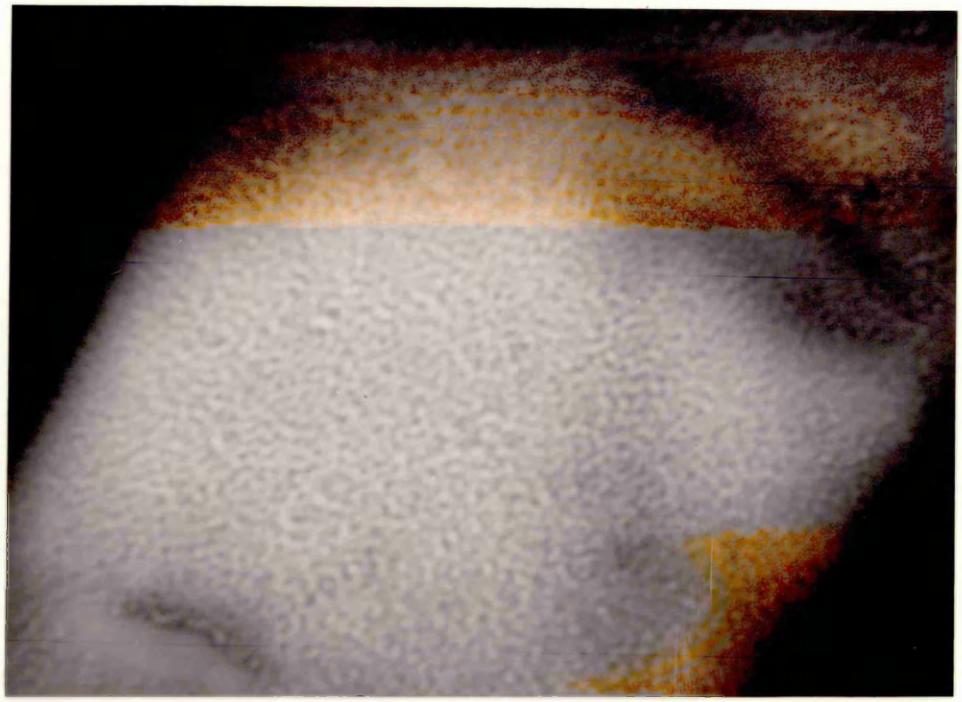

1μm

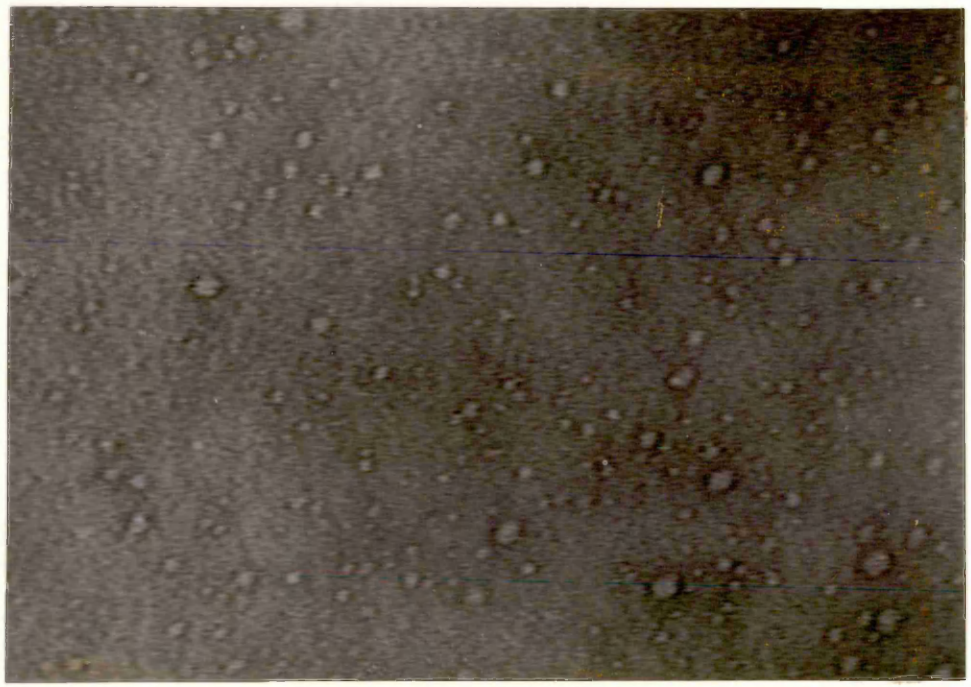

0.5μm

Figure 66. Transmission Electron Micrograph of Copolymer 1 (ultramicrotomed).

Figure 67. High Magnification Transmission Electron Micrograph of Copolymer 1 (ultramicrotomed).

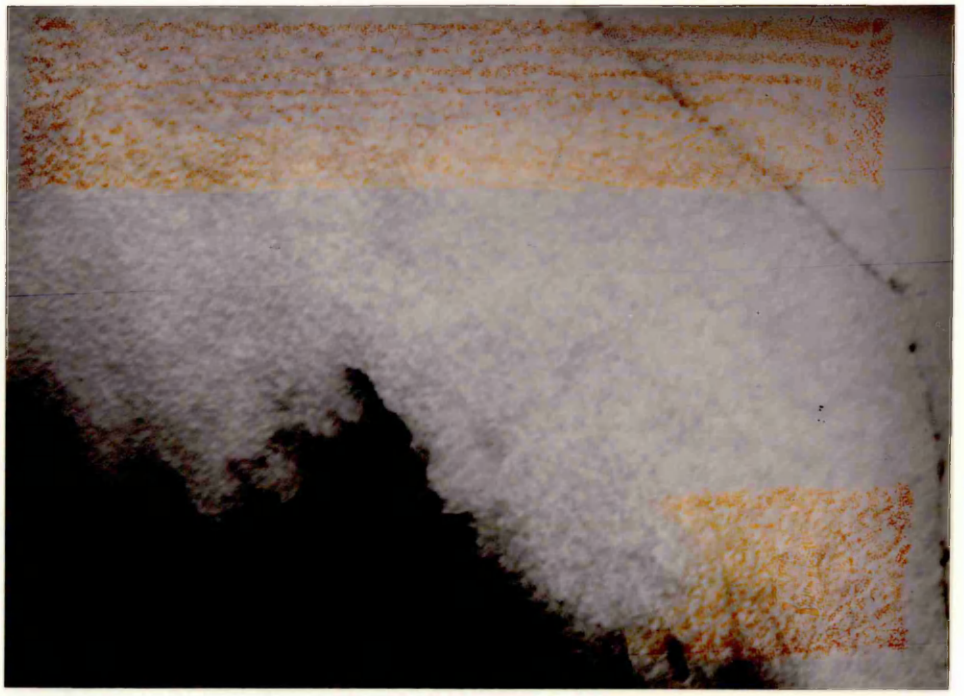

0.5μm

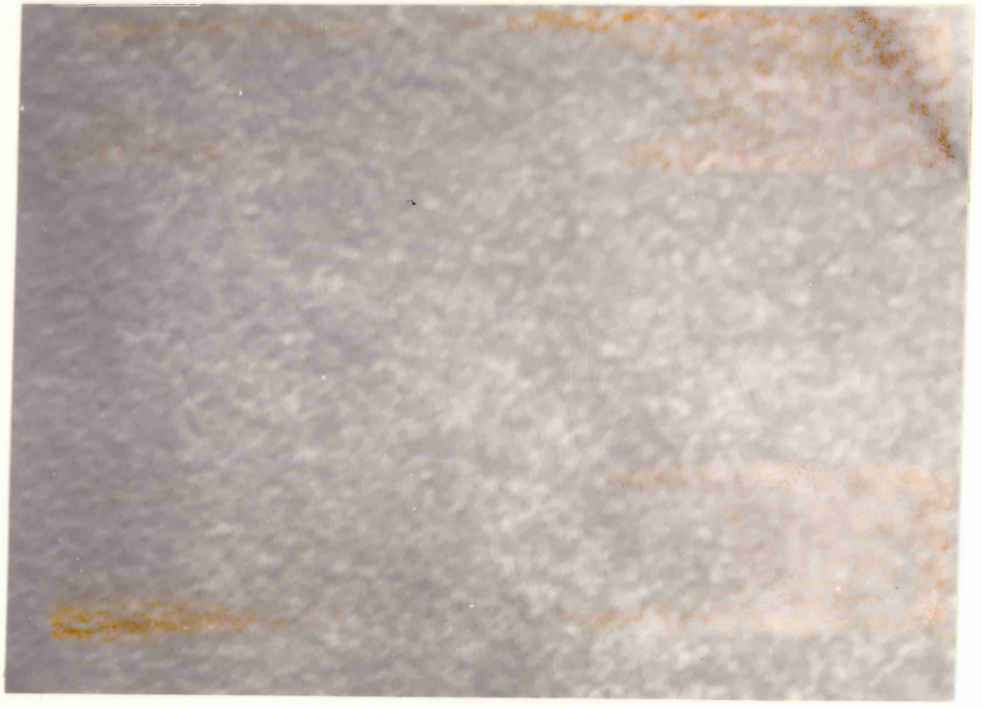

0.1μm

Figure 68. Transmission Electron Micrograph of Copolymer 2 (ultramicrotomed).

Figure 69. High Magnification Transmission Electron Micrograph of Copolymer 2 (ultramicrotomed).

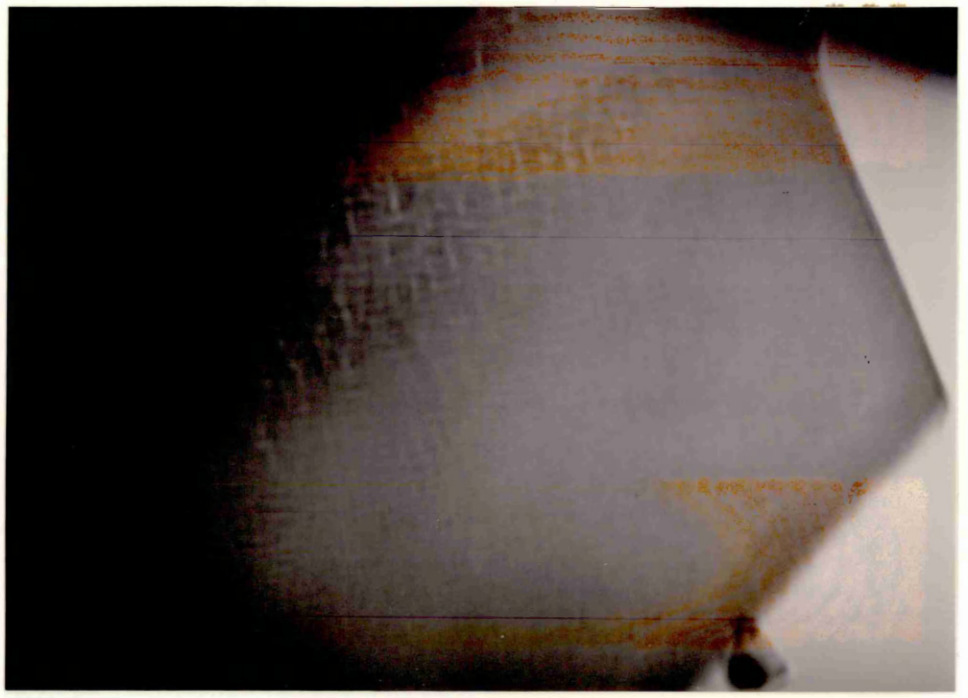

0.1μm

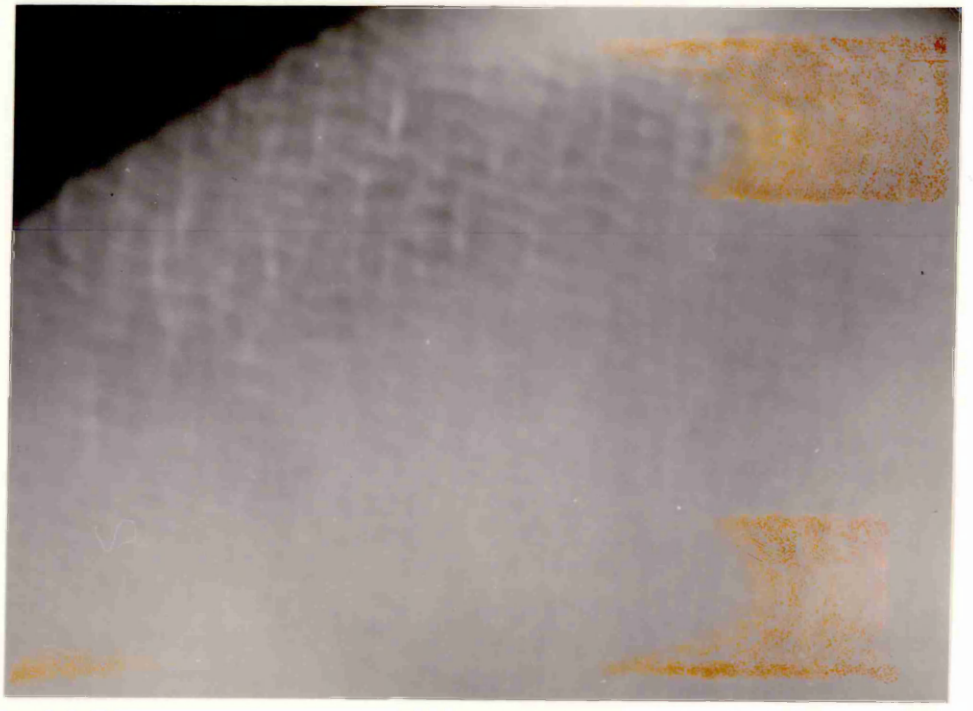

0.1μm

Figure 70. Transmission Electron Micrograph of Copolymer 5 (ultramicrotomed).

Figure 71. High Magnification Transmission Electron Micrograph of Copolymer 5 (ultramicrotomed).

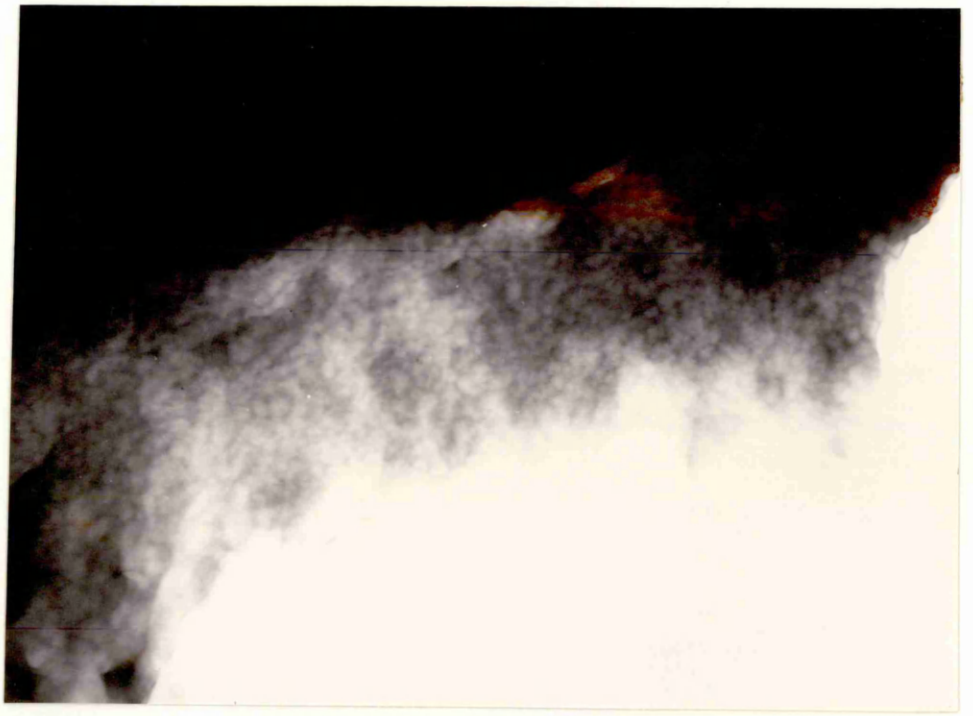

1μm

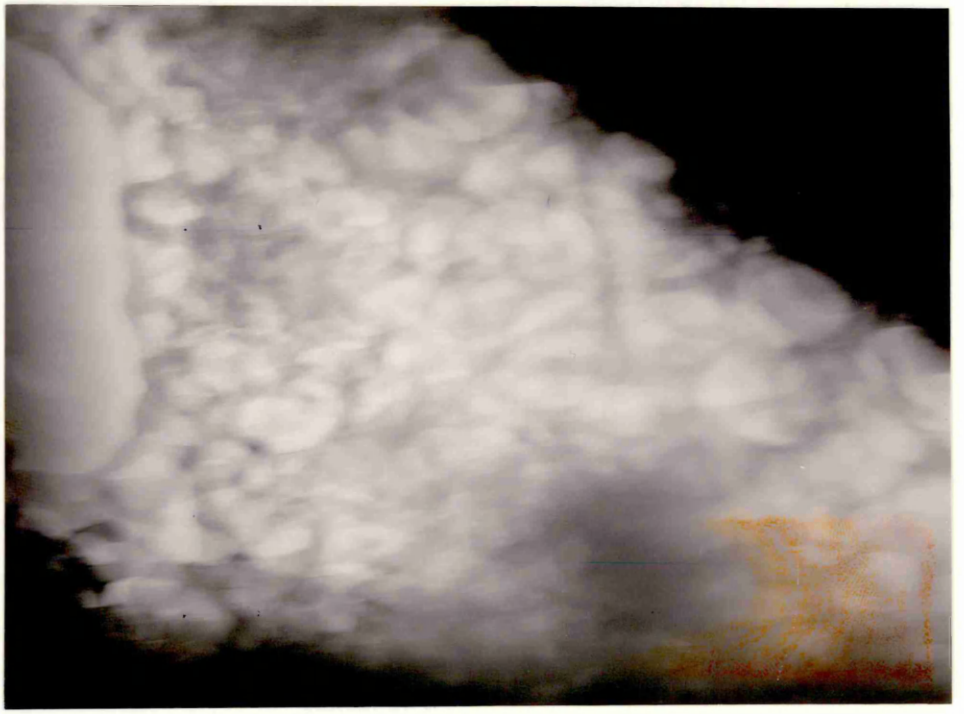

0.1μm

Figure 72. Injection moulded tensile test pieces, (a) Pure P.E.S. (b) Blend 5 (1% copolymerised P.D.M.S.) and (c) Blend 3 (2.5% copolymerised P.D.M.S.).

Figure 73. X-section of Blend 3 tensile test piece.

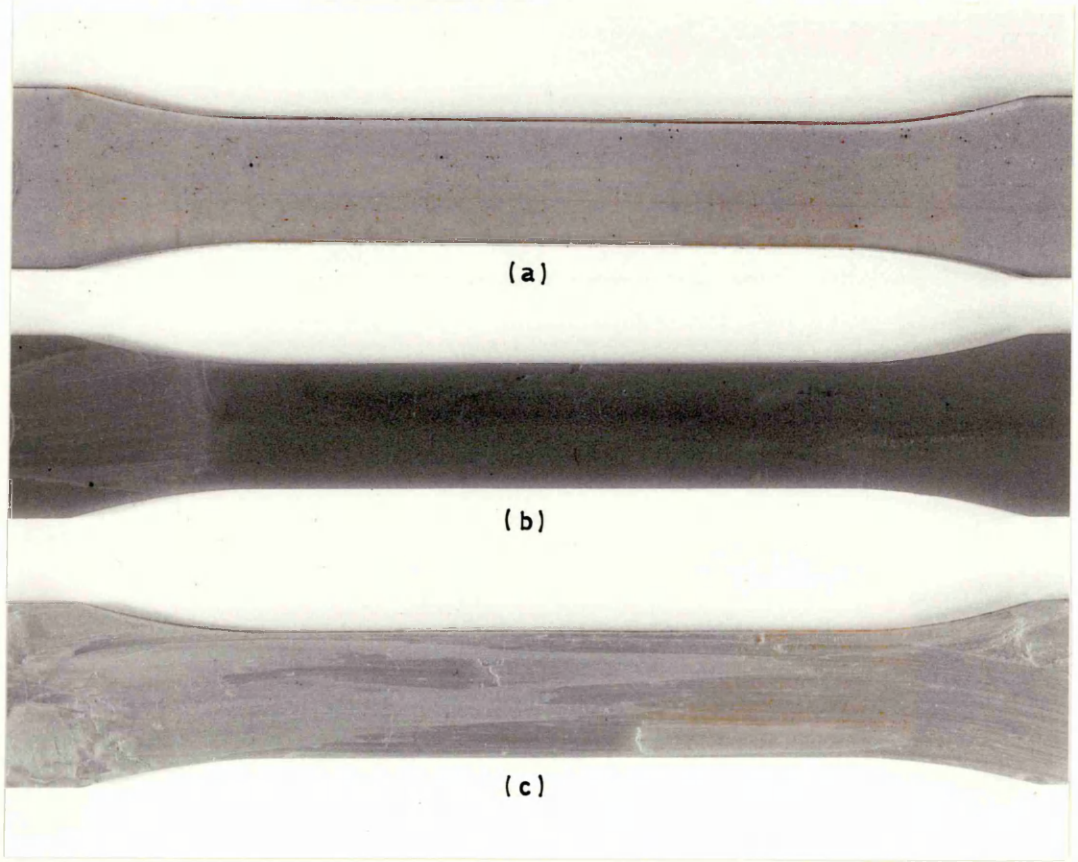
(a)
(b)
(c)

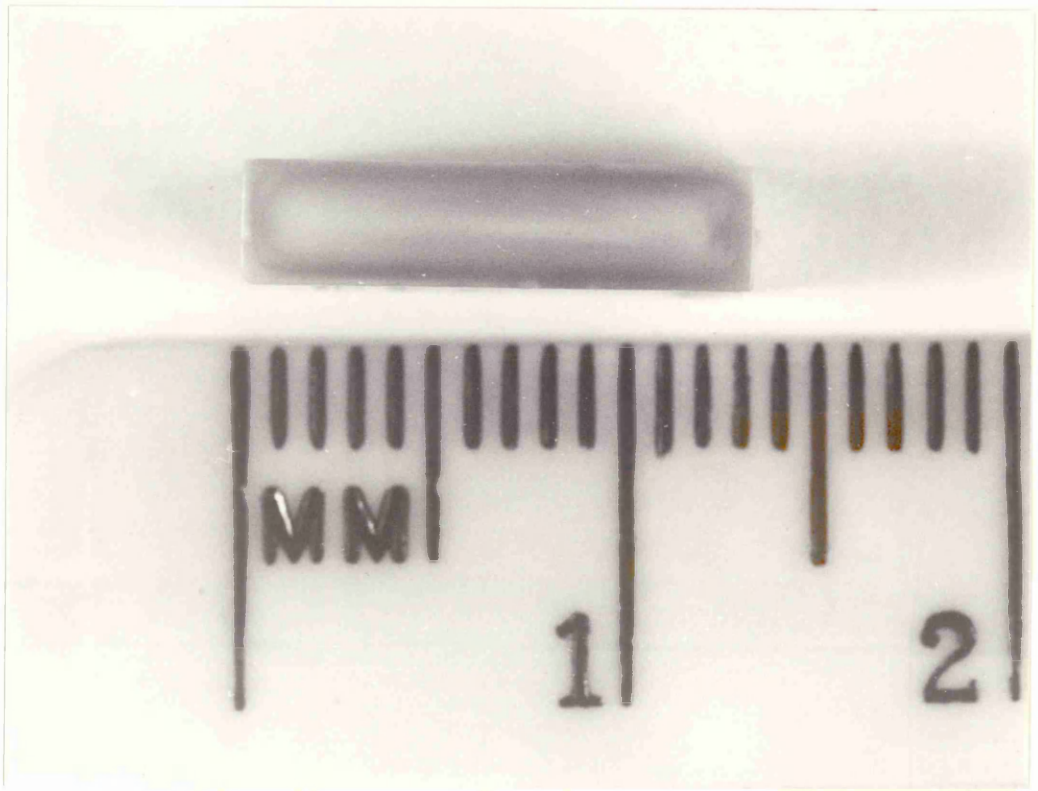
MM
1
2

Figure 74. Wall Shear Stress vs Corrected Shear Rate, (x) Pure 4800P P.E.S., (o) Blend 4, (■) Blend 5 and (●) Blend 3.

Figure 75. Wall Shear Stress vs Corrected Shear Rate, (■) Blend 9 (●) Blend 8, (x) Blend 7, (o) Blend 1 and (▼) Blend 2.

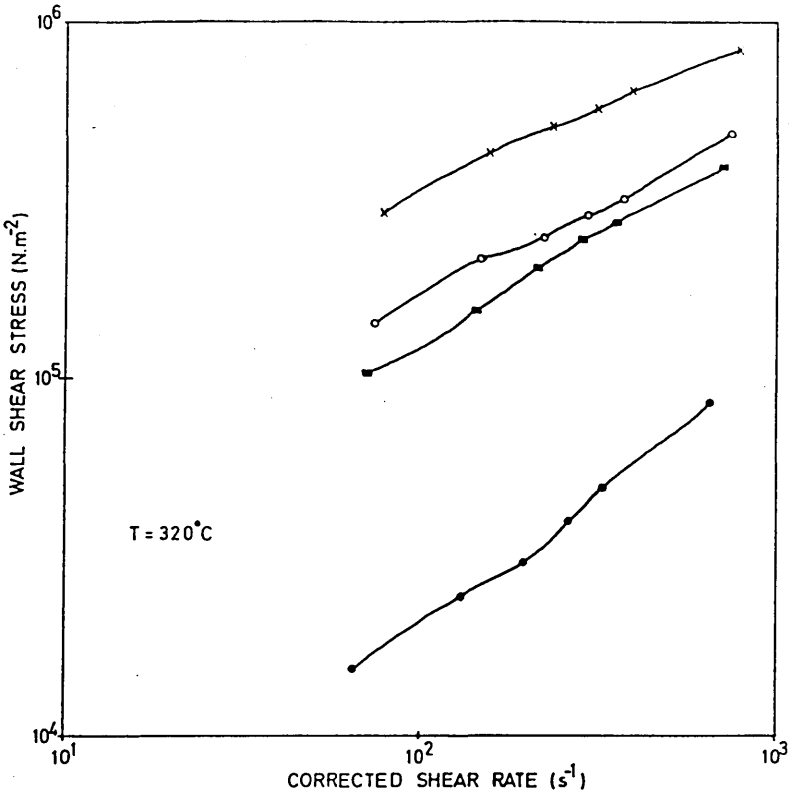
WALL SHEAR STRESS (N.m^{-2})
10^6
10^5
10^4
T = 320°C
10^1
10^2
10^3
CORRECTED SHEAR RATE (s^{-1})

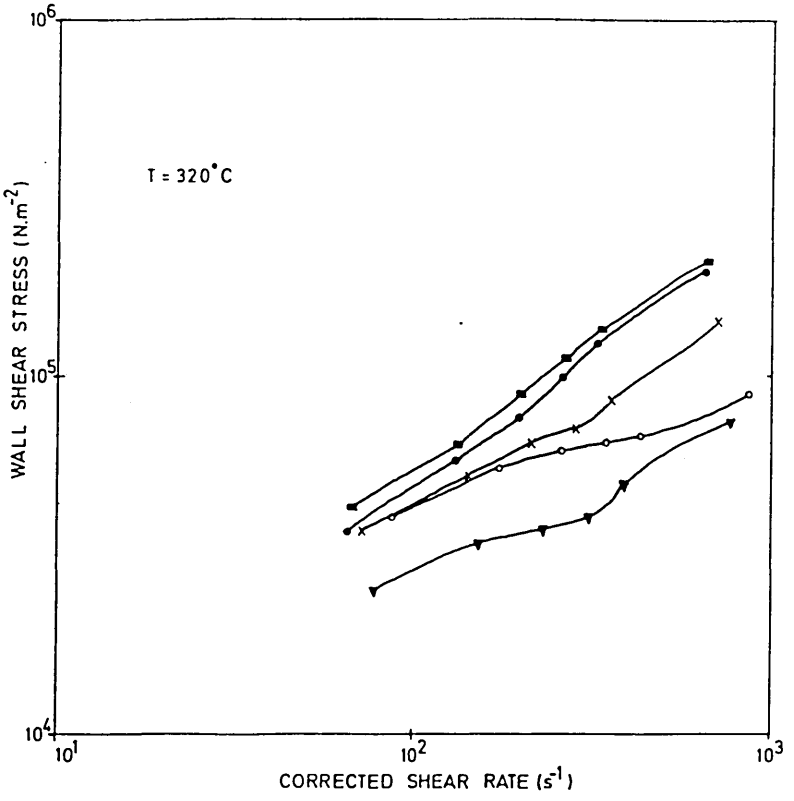
WALL SHEAR STRESS (N.m^{-2})
10^6
10^5
10^4
T = 320°C
10^1
10^2
10^3
CORRECTED SHEAR RATE (s^{-1})

Figure 76. Shear Viscosity vs Wall Shear Stress, (x) Pure 4800P P.E.S., (●) Blend 4, (■) Blend 5 and (o) Blend 3.

Figure 77. Shear Viscosity vs Wall Shear Stress, (x) Blend 9, (●) Blend 8, (■) Blend 7, (o) Blend 1 and (▲) Blend 2.

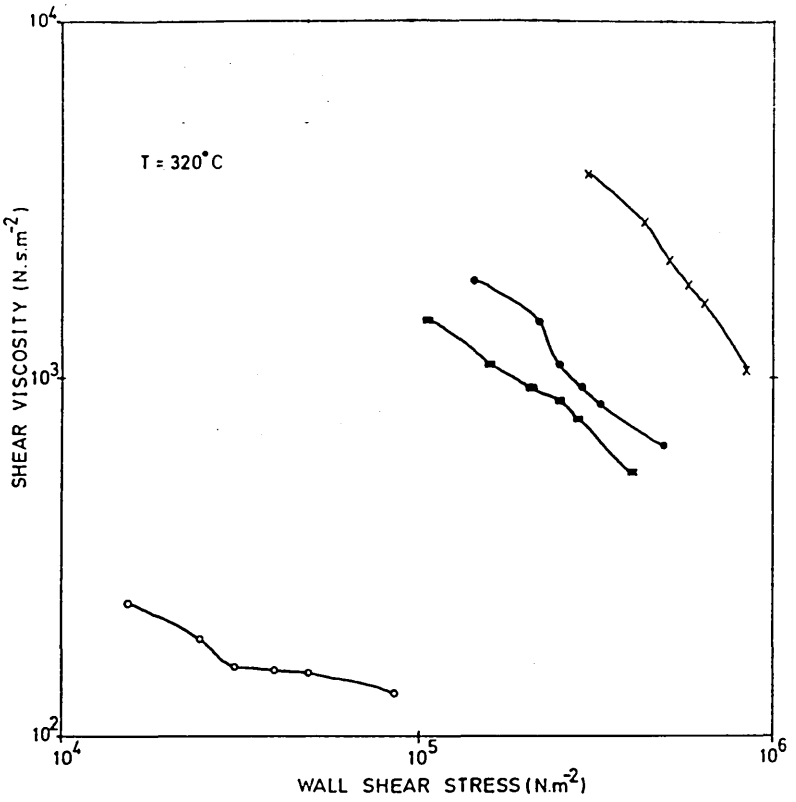
T = 320°C
SHEAR VISCOSITY (N.s.m^{-2})
10^4
10^3
10^2
10^4
10^5
10^6
WALL SHEAR STRESS (N.m^{-2})

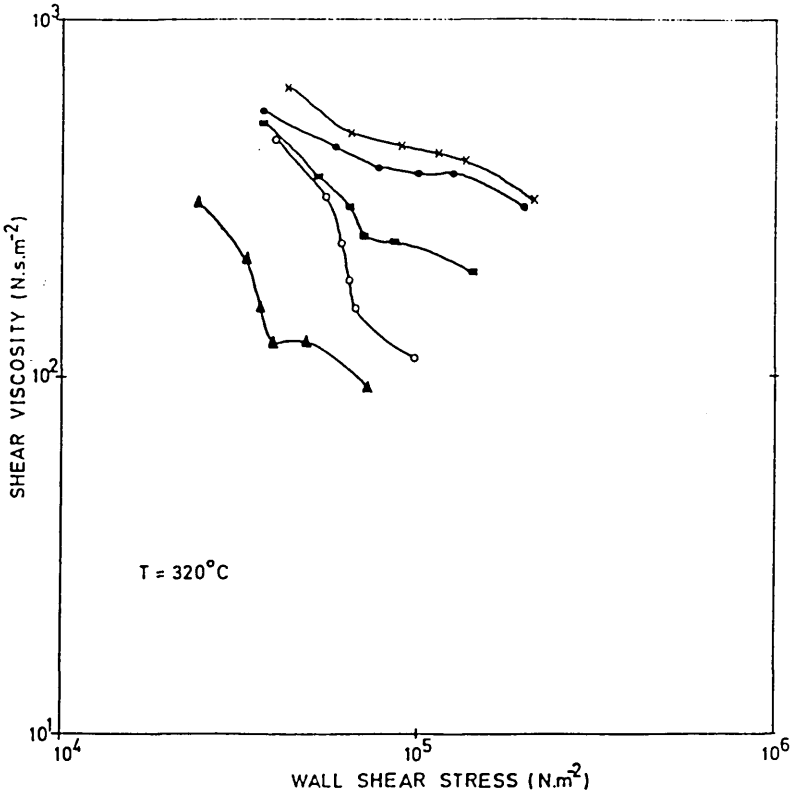
T = 320°C
SHEAR VISCOSITY (N.s.m^{-2})
10^3
10^2
10^1
10^4
10^5
10^6
WALL SHEAR STRESS (N.m^{-2})

Figure 78. Arrangement for the impact testing of blend specimens in the Davenport Izod Impact Tester.

Figure 79. Location of Thermocouple within Izod test specimen.

Dimensions in millimetres

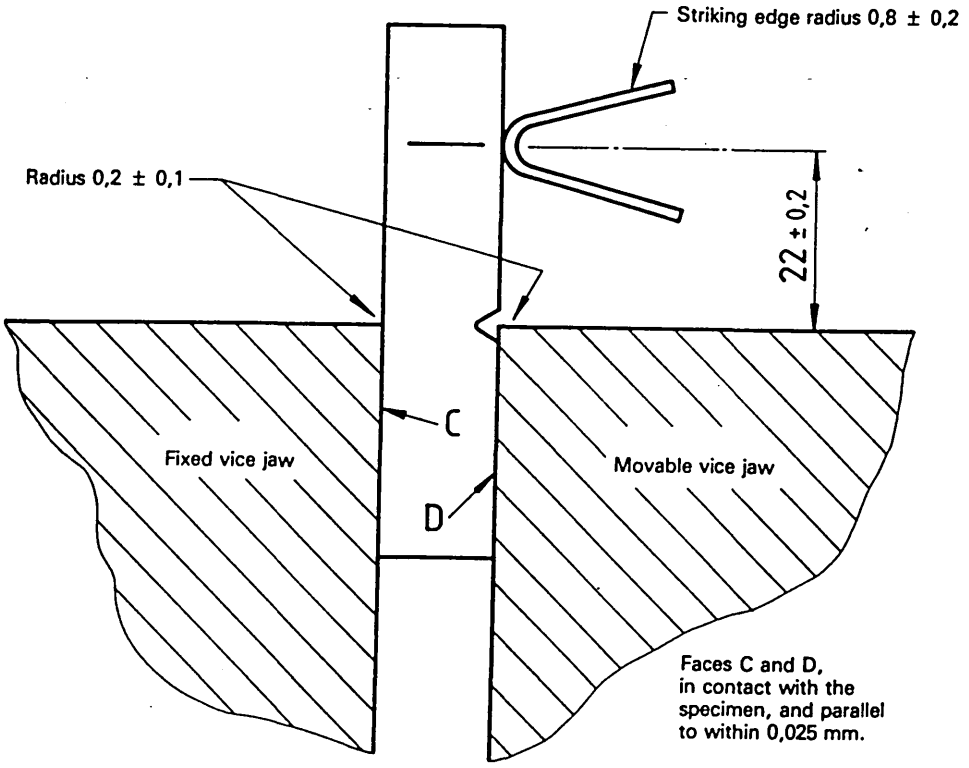

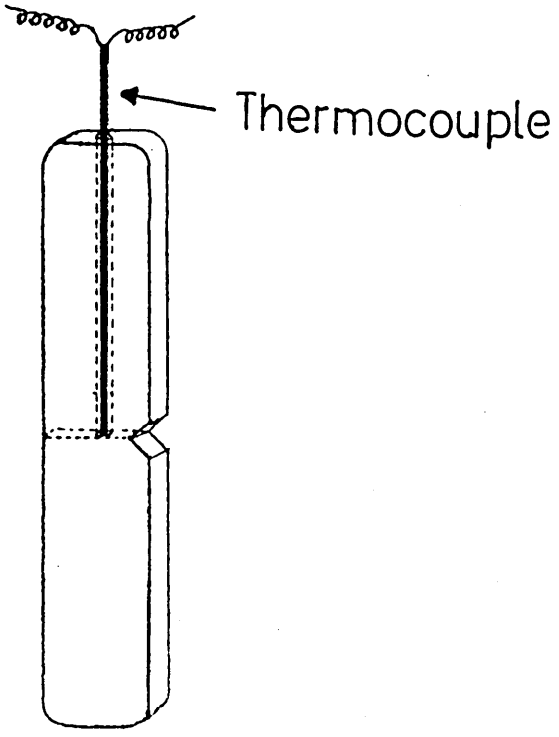

Figure 80. Cooling curve for Izod test specimen (sample allowed to cool naturally in an environment of air at 25°C).

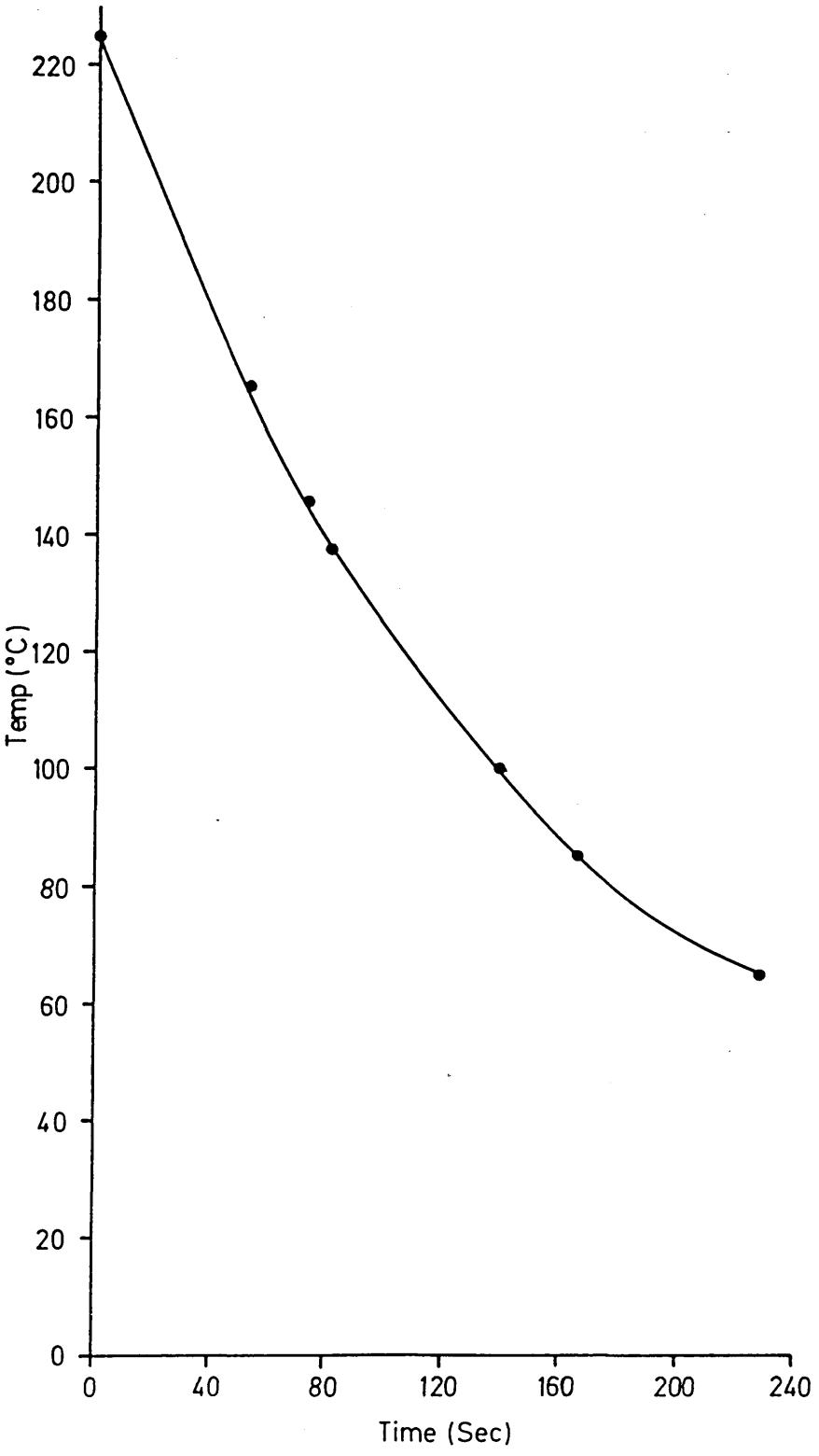
220
200
180
160
140
120
100
80
60
40
20
0
Temp (°C)
0
40
80
120
160
200
240
Time (Sec)

Figure 81. Izod Impact Strength vs Temperature curves - nominal notch depth 2.5mm, root radius 0.25mm and included angle 45°. (□) Blend 3 and (o) pure 4800P P.E.S.

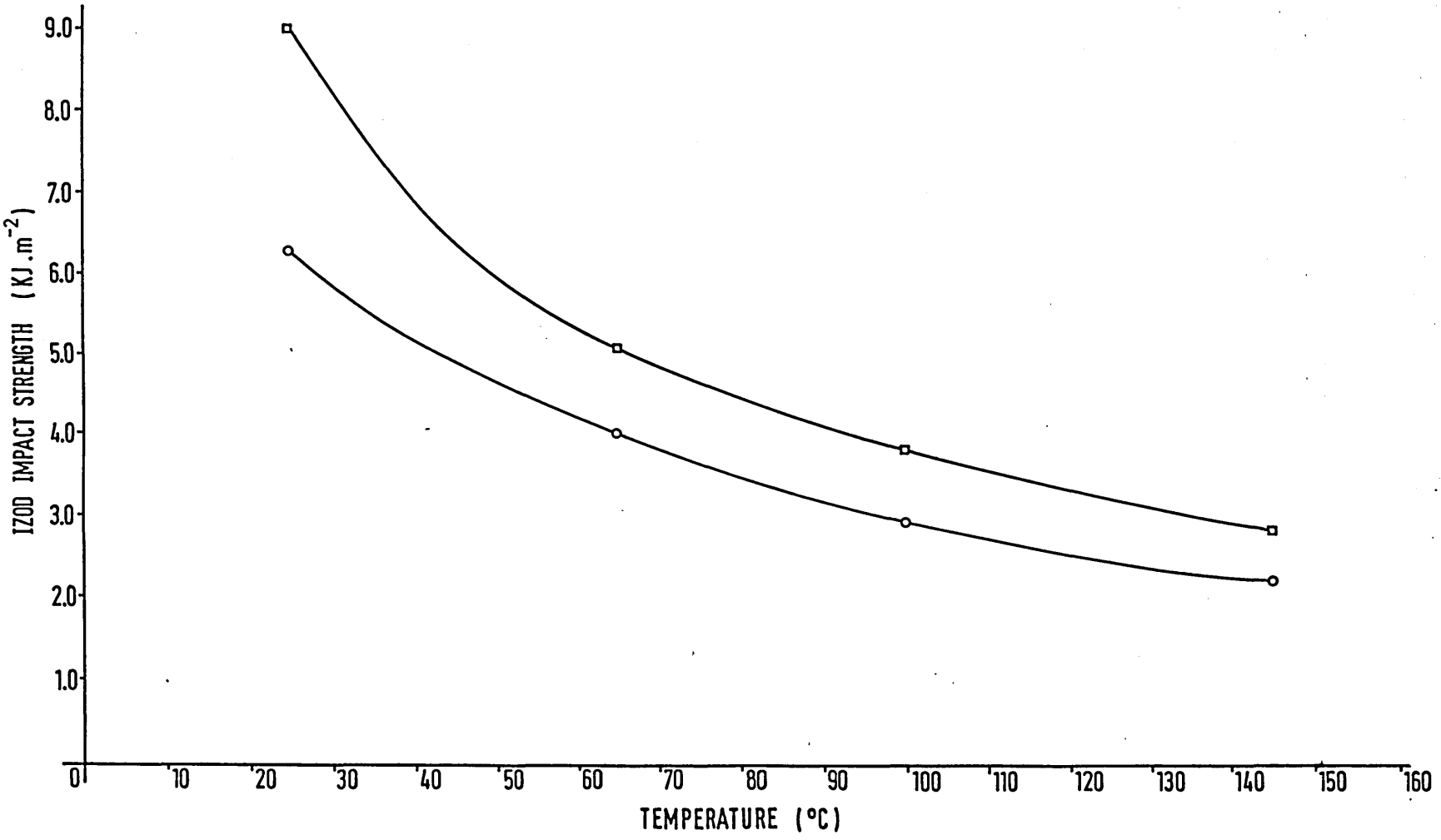
IZOD IMPACT STRENGTH (KJ.m^{-2})
9.0
8.0
7.0
6.0
5.0
4.0
3.0
2.0
1.0
0
10
20
30
40
50
60
70
80
90
100
110
120
130
140
150
160
TEMPERATURE (°C)

Figure 82. Izod Impact Strength vs Notch Root Radius curves (notch depth 2.5mm, included angle 45° and test temperature 25°C).

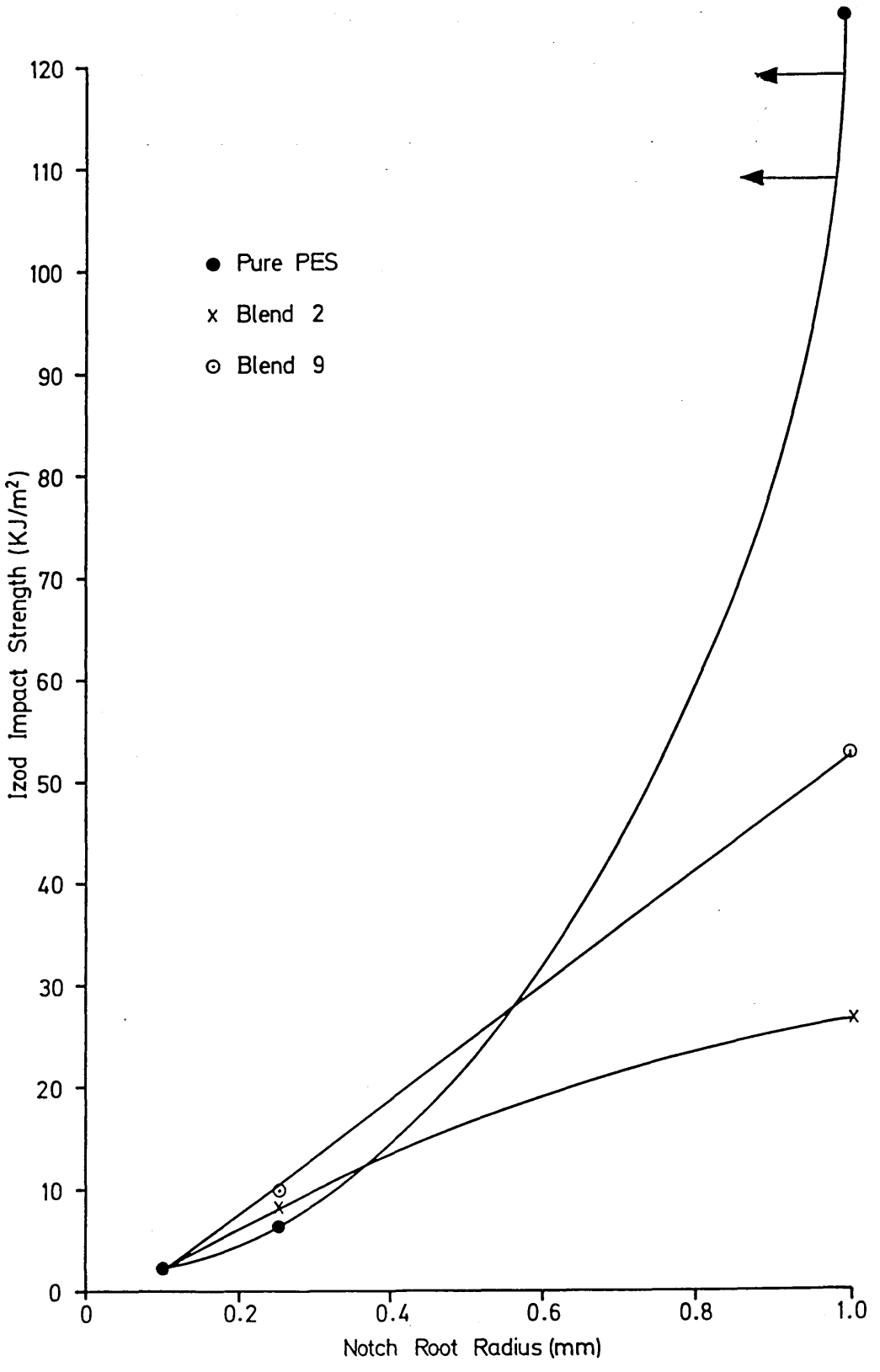
120
110
100
90
80
70
60
50
40
30
20
10
0
Izod Impact Strength (KJ/m²)
Pure PES
Blend 2
Blend 9
0
0.2
0.4
0.6
0.8
1.0
Notch Root Radius (mm)

Figure 83. Izod Impact Strength vs Notch Root Radius curves (notch depth 2.5mm, included angle 45° and test temperature 25°C).

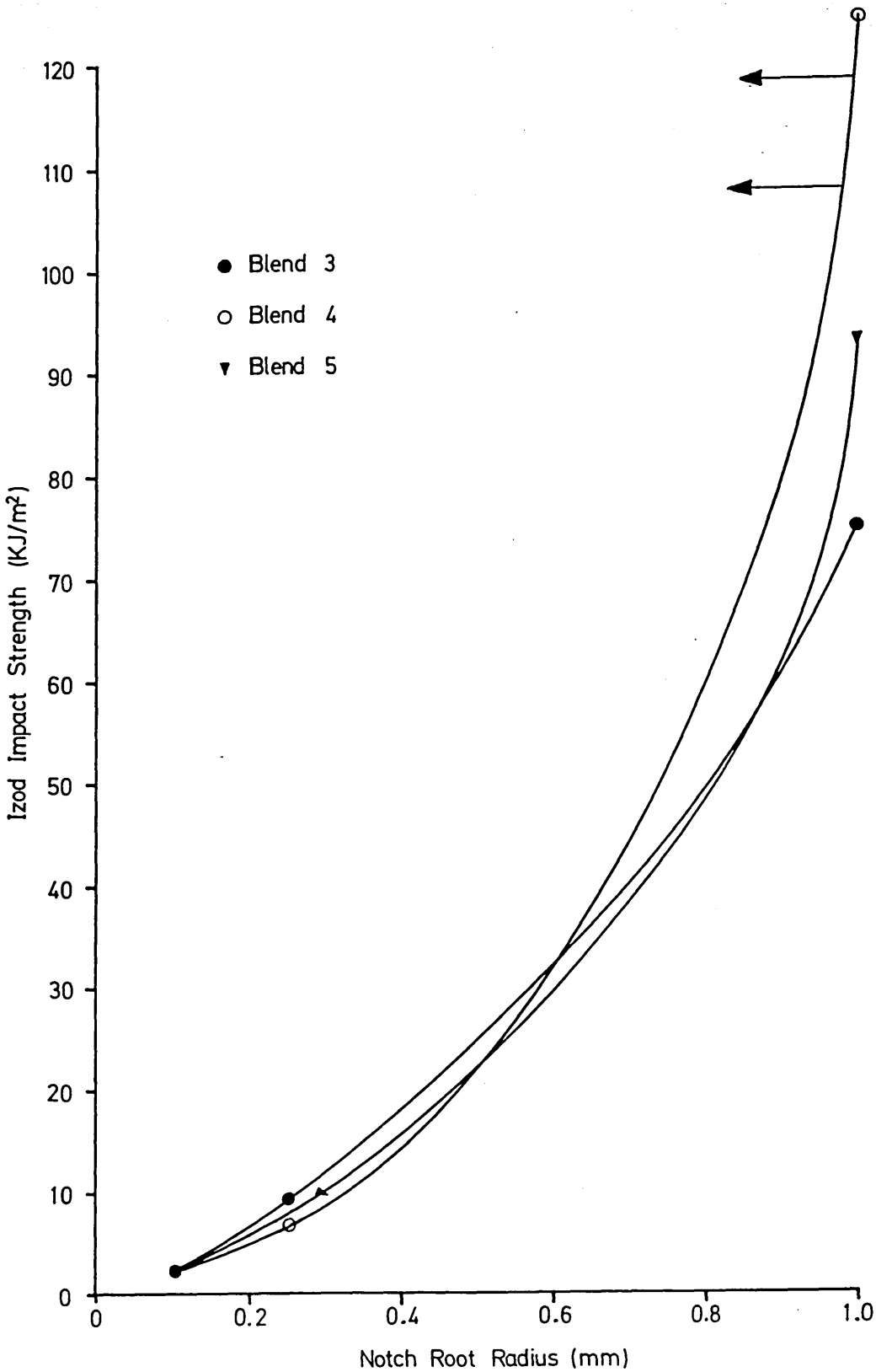
120
110
100
90
80
70
60
50
40
30
20
10
0
Izod Impact Strength (KJ/m²)
Blend 3
Blend 4
Blend 5
0
0.2
0.4
0.6
0.8
1.0
Notch Root Radius (mm)

Figure 84. Izod Impact Strength vs Notch Root Radius curves (notch depth 2.5mm, included angle 45° and test temperature 25°C).

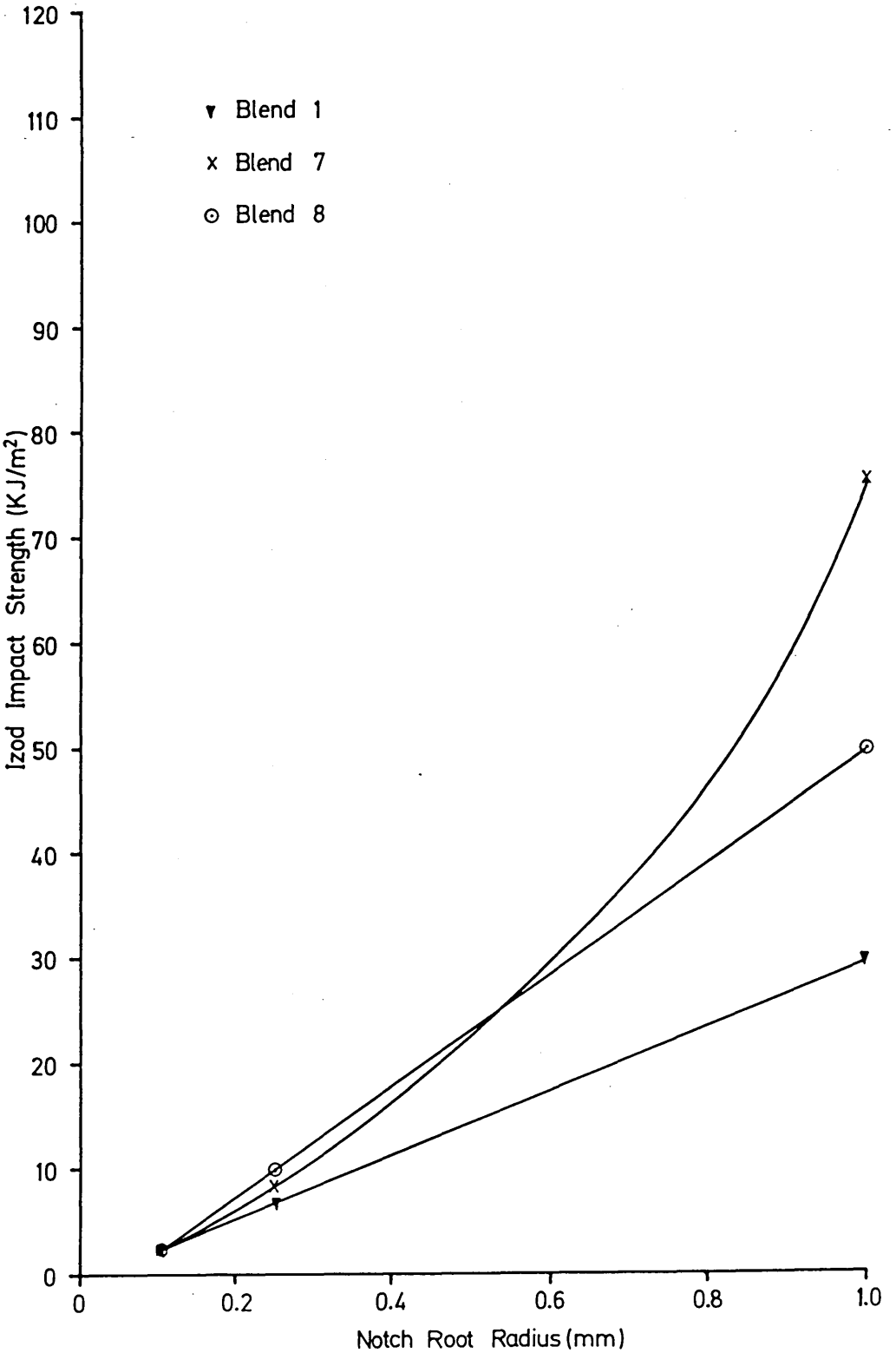
Blend 1
Blend 7
Blend 8
Izod Impact Strength (KJ/m²)
120
110
100
90
80
70
60
50
40
30
20
10
0
0
0.2
0.4
0.6
0.8
1.0
Notch Root Radius (mm)

Figure 85. Impact Energy vs BWZ curves - notch root radius 0.1mm, test temperature 27°C. (a) [x] Blend 1 and [o] Blend 2 (b) [o] Blend 3 and [x] Blend 4, (c) [o] Blend 5, [•] Blend 7 and [x] Blend 8, (d) [o] Blend 9 and [x] Pure 4800P P.E.S.

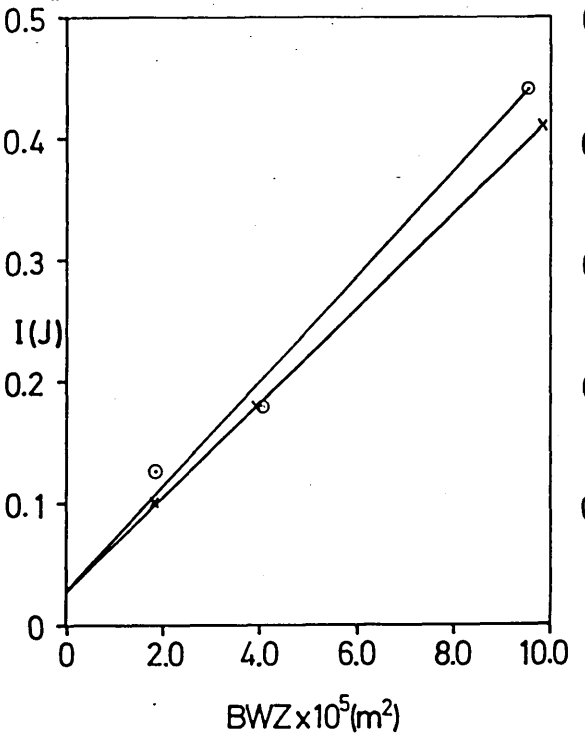
0.5
0.4
0.3
I(J)
0.2
0.1
0
0
2.0
4.0
6.0
8.0
10.0
BWZ x 10^5(m^2)

(a)

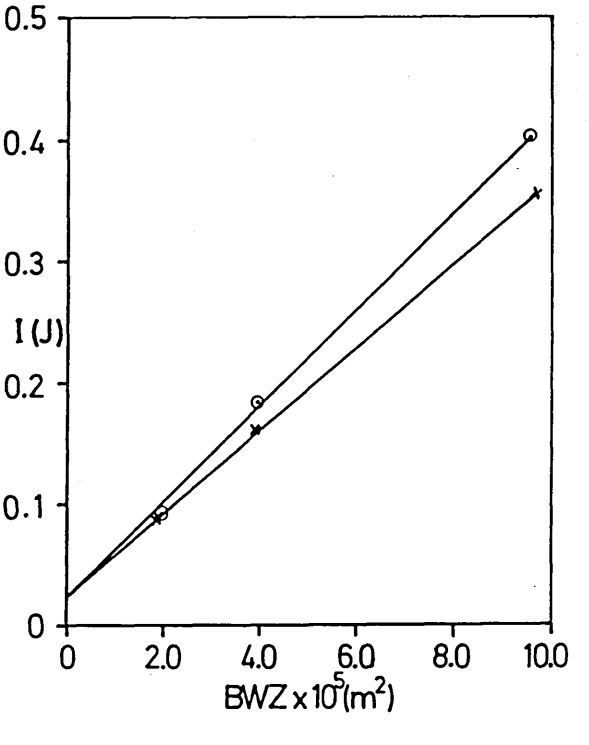
0.5
0.4
0.3
I(J)
0.2
0.1
0
0
2.0
4.0
6.0
8.0
10.0
BWZ x 10^5(m^2)

(b)

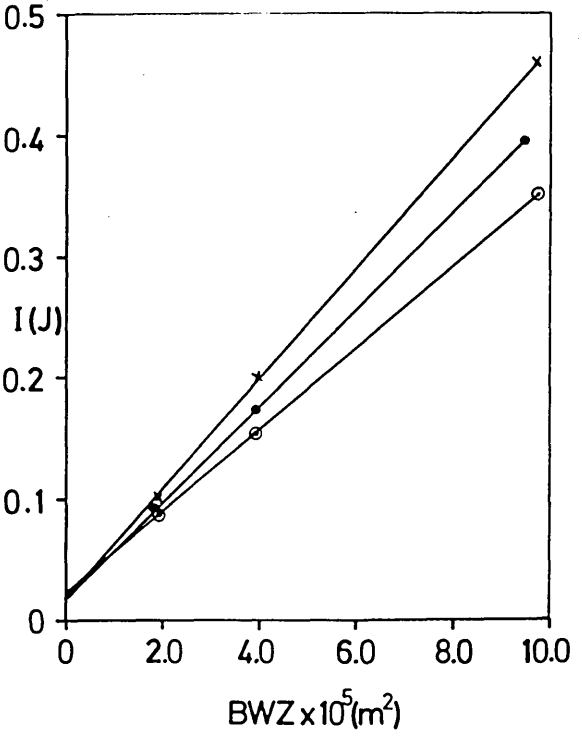
0.5
0.4
0.3
I(J)
0.2
0.1
0
0
2.0
4.0
6.0
8.0
10.0
BWZ x 10^5(m^2)

(c)

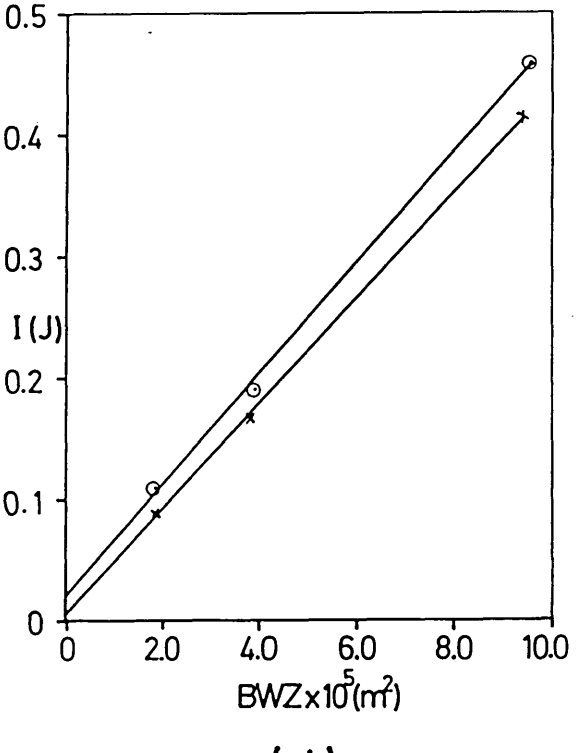
0.5
0.4
0.3
I(J)
0.2
0.1
0
0
2.0
4.0
6.0
8.0
10.0
BWZ x 10^5(m^2)

(d)

Figure 86. Scanning Electron Micrograph of pure 4800P P.E.S. impact fracture surface (notch root radius 0.1mm temperature 25°C).

Figure 87. High Magnification Scanning Electron Micrograph of pure 4800P P.E.S. impact fracture surface (notch root radius 0.1mm, temperature 25°C).

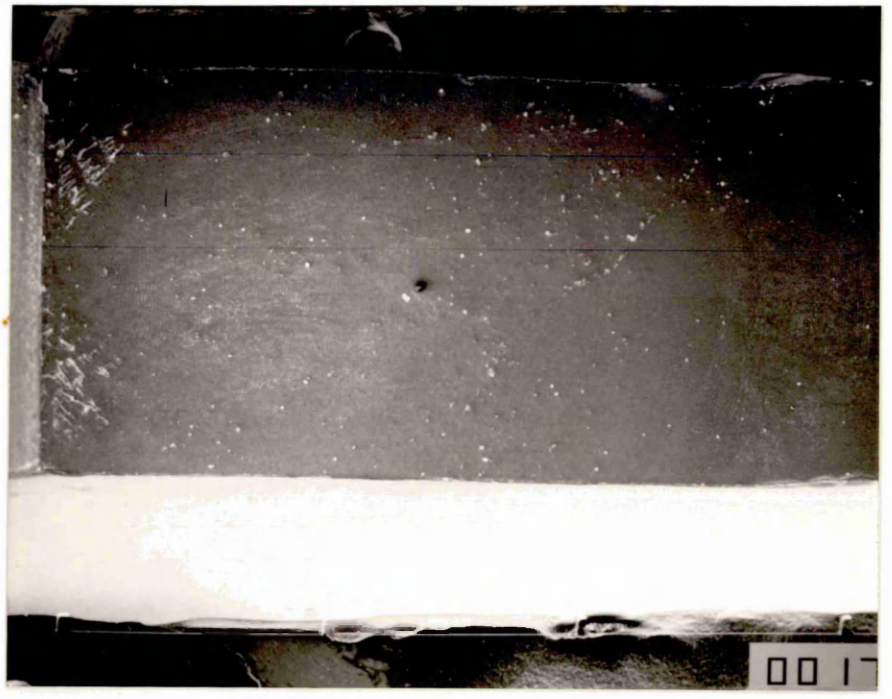

1mm

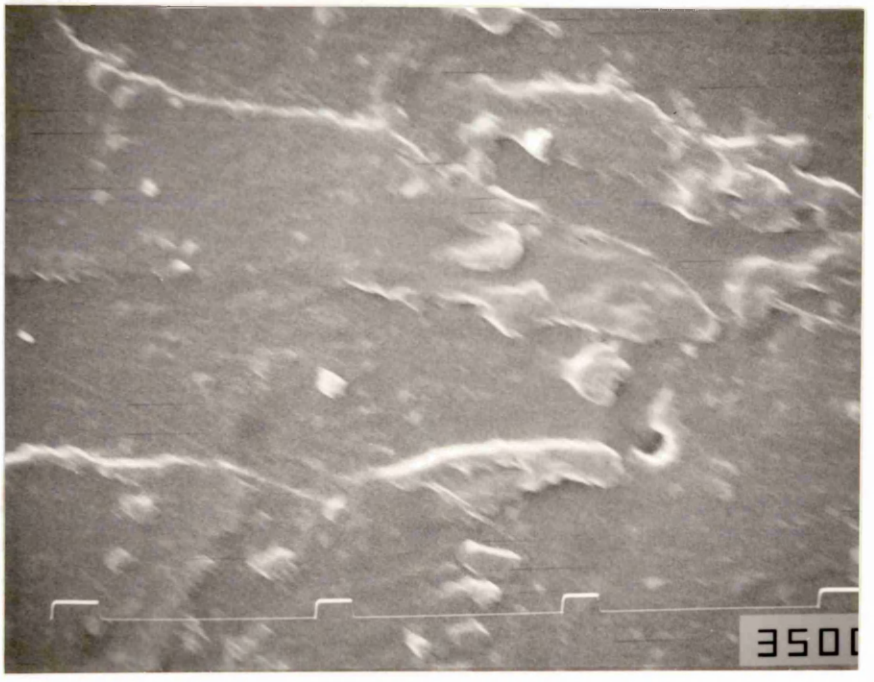

10μm

Figure 88. High Magnification Scanning Electron Micrograph of Blend 1 impact fracture surface (notch root radius 0.1mm, temperature 25°C).

Figure 89. Silicon Map of above fracture surface area.

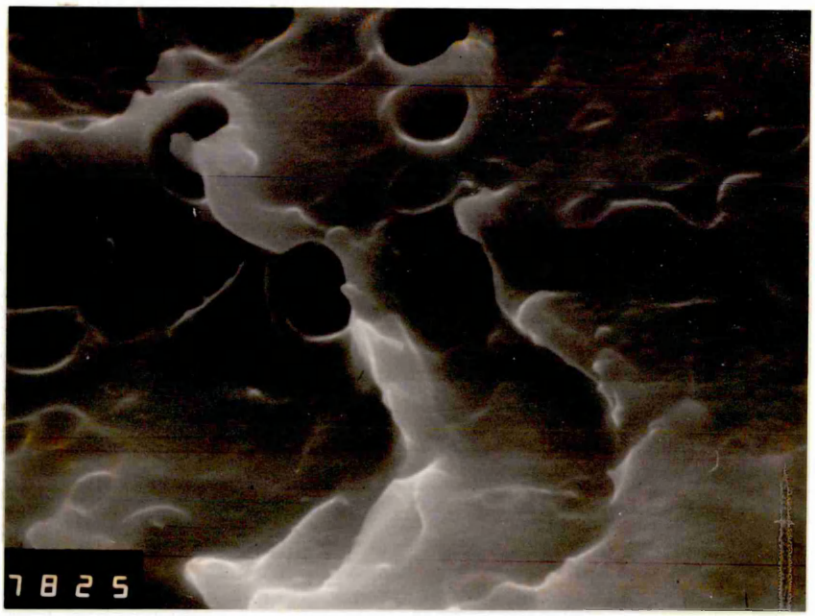

10μm

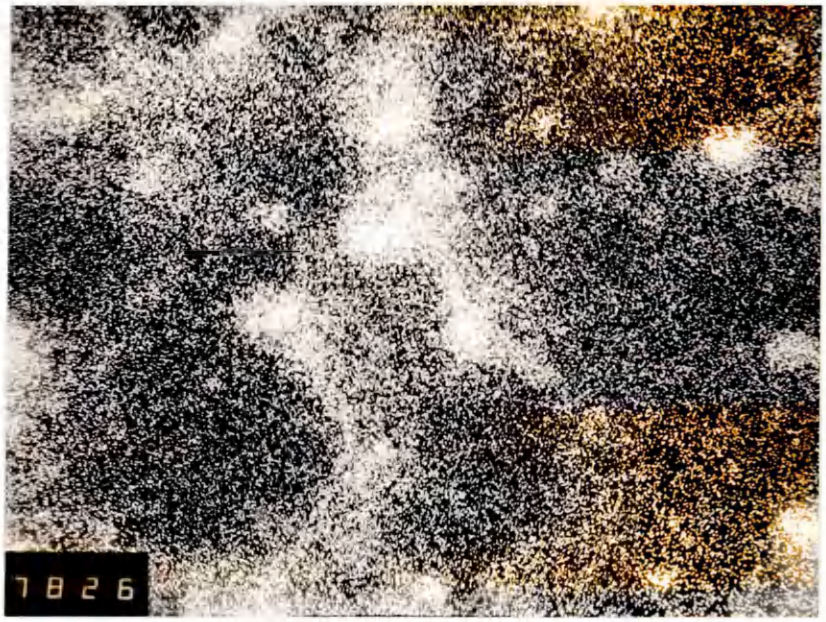

10μm

Figure 90. Scanning Electron Micrograph of pure 4800P P.E.S. impact fracture surface (notch root radius 0.25mm temperature 25°C).

Figure 91. High Magnification Scanning Electron Micrograph of pure 4800P P.E.S. impact fracture surface (notch root radius 0.25mm, temperature 25°C).

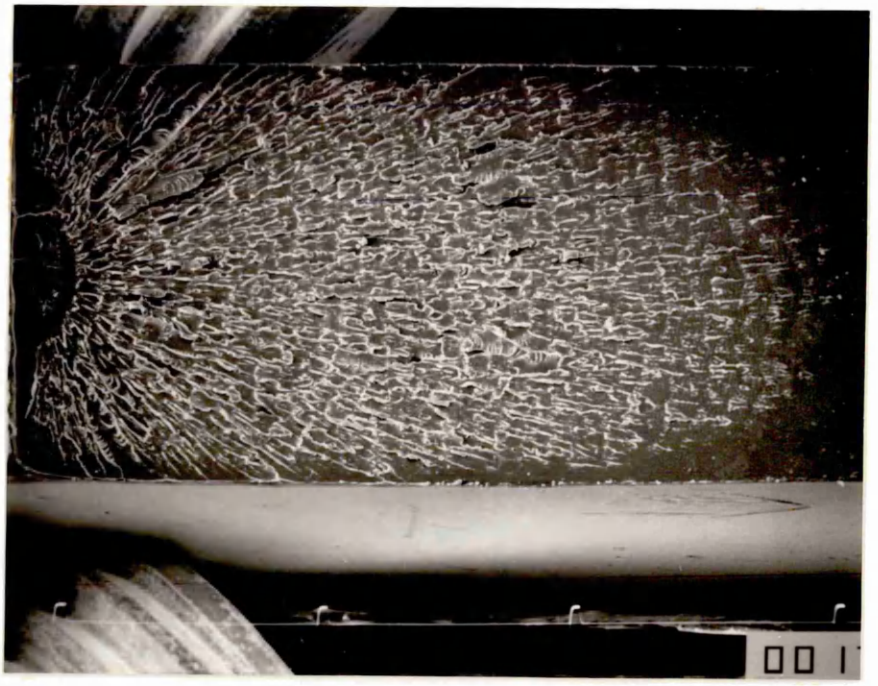

1mm

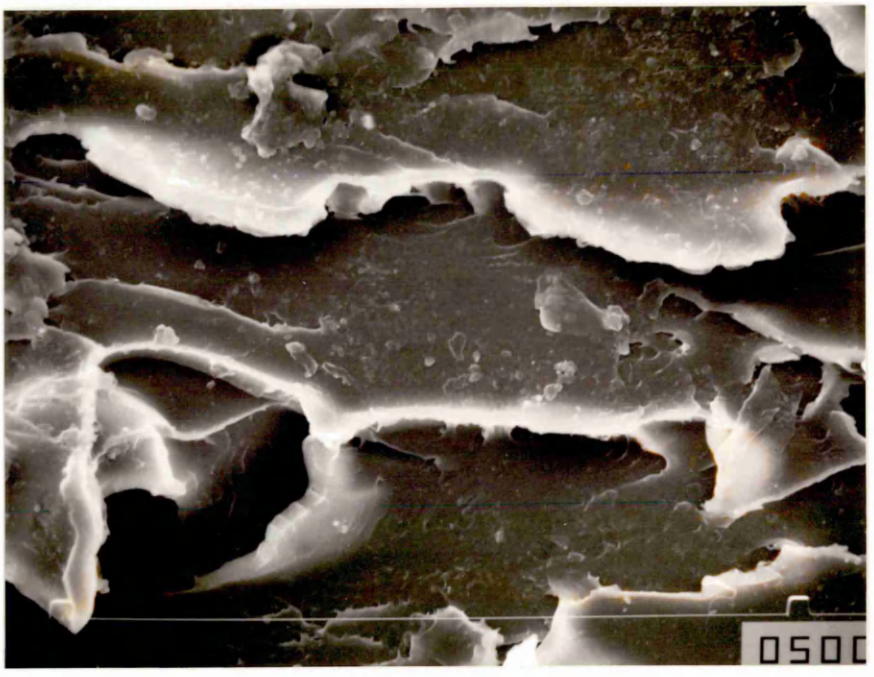

100μm

Figure 92. Scanning Electron Micrograph of pure 4800P P.E.S. impact fracture surface (notch root radius 0.25mm temperature 145°C).

Figure 93. High Magnification Scanning Electron Micrograph of pure 4800P P.E.S. impact fracture surface (notch root radius 0.25mm, temperature 145°C).

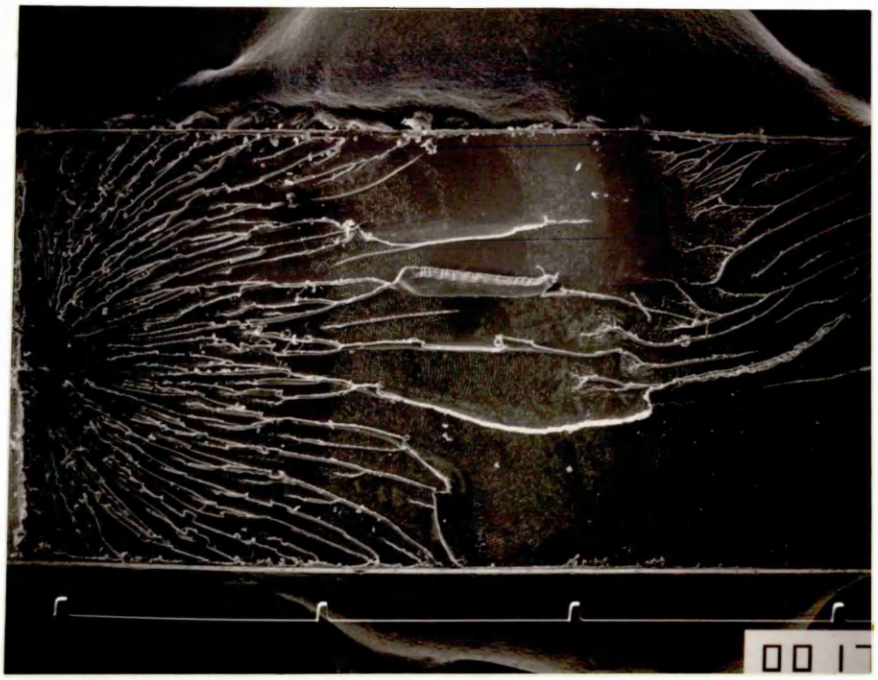

1mm

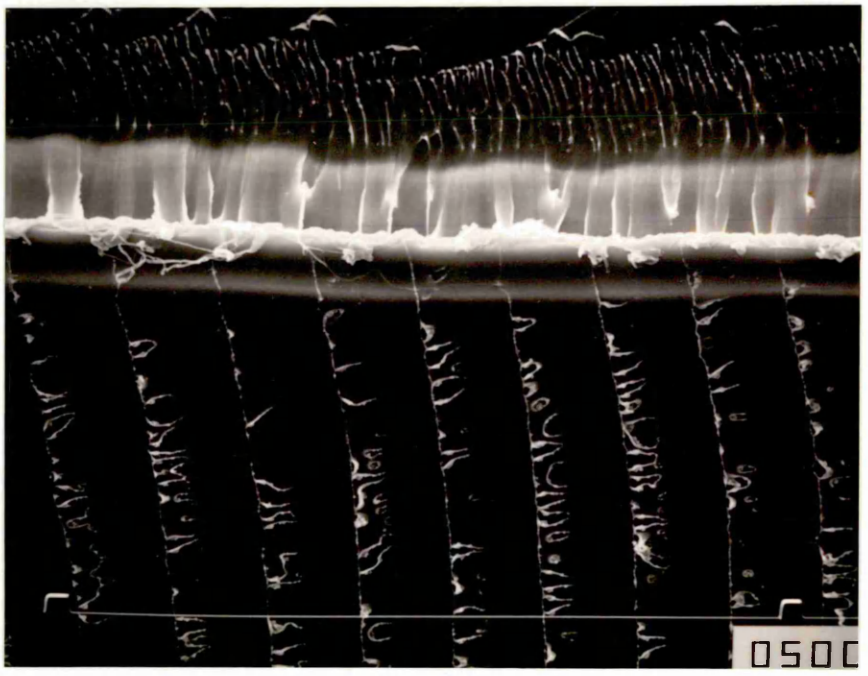

100μm

Figure 94. Scanning Electron Micrograph of Blend 3 impact fracture surface (notch root radius 0.25mm, temperature 25°C).

Figure 95. High Magnification Scanning Electron Micrograph of Blend 3 impact fracture surface (notch root radius 0.25mm, temperature 25°C).

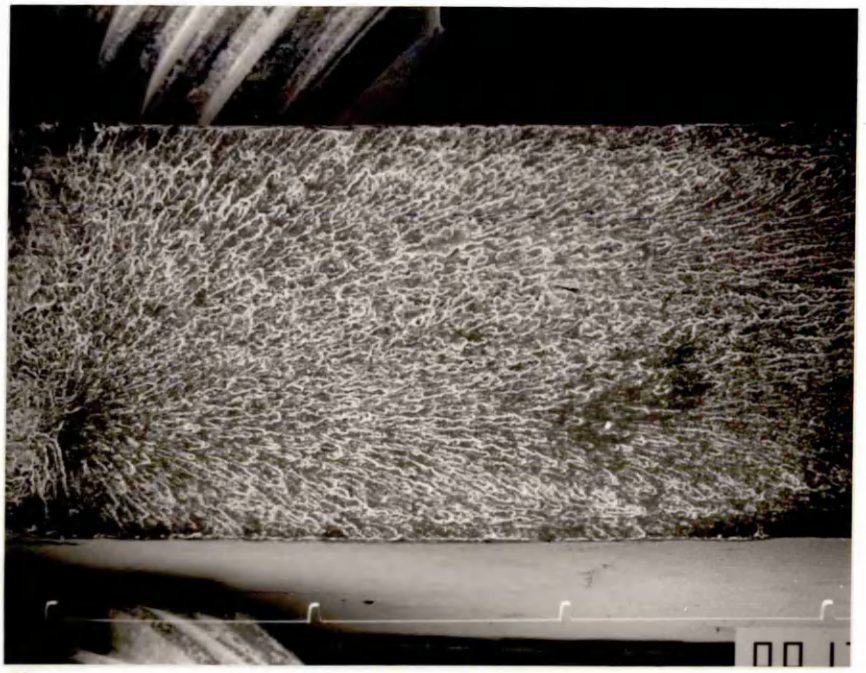

1mm

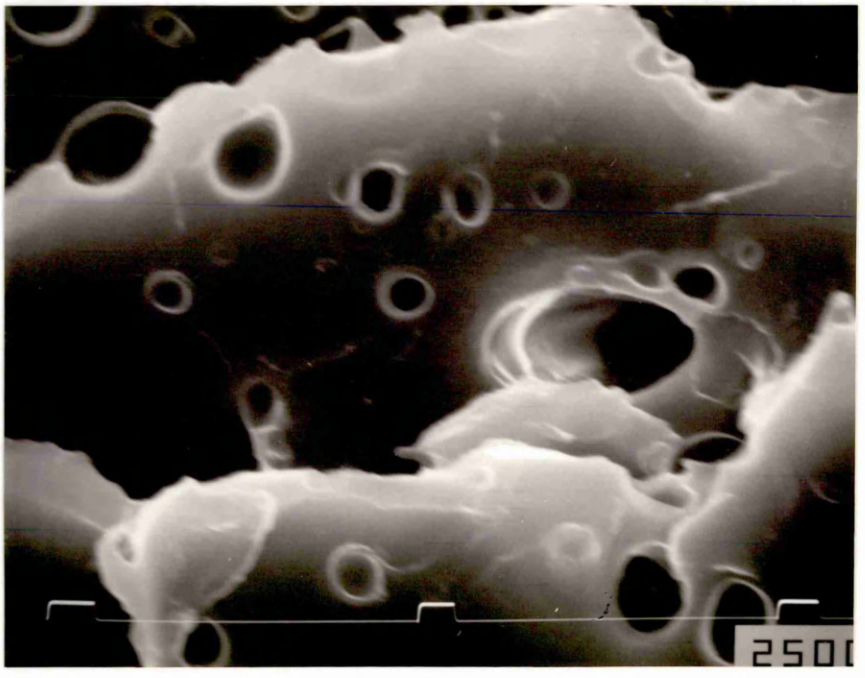

10μm

Figure 96. Scanning Electron Micrograph of Blend 3 impact fracture surface (notch root radius 0.25mm, temperature 145°C).

Figure 97. High Magnification Scanning Electron Micrograph of Blend 3 impact fracture surface (notch root radius 0.25mm, temperature 145°C).

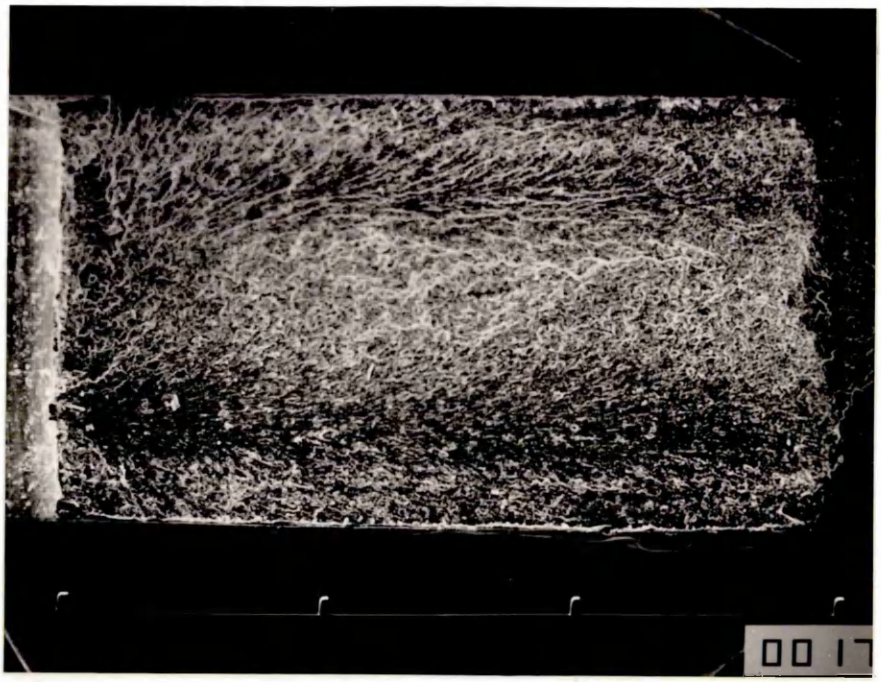

1mm

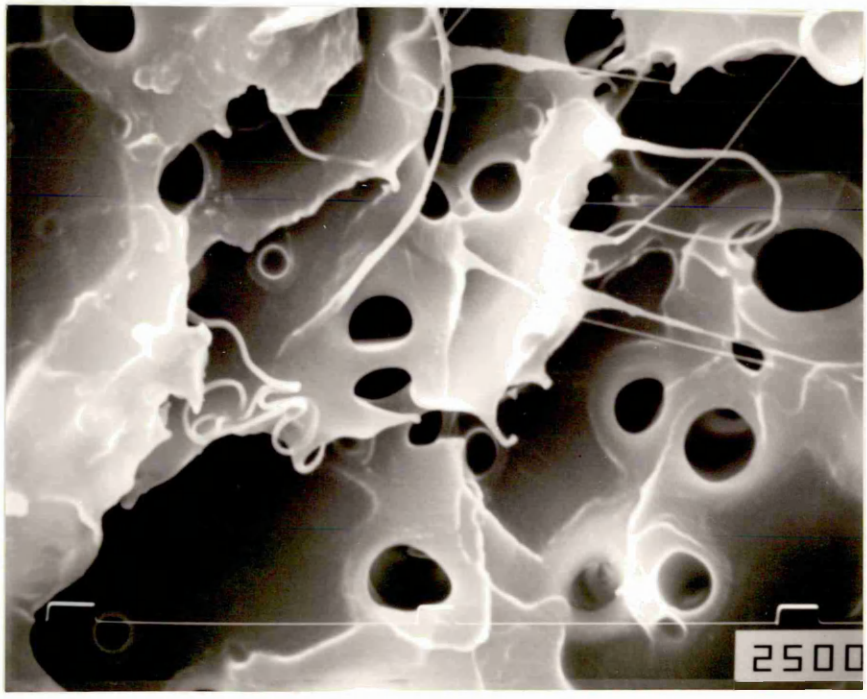

10μm

Figure 98. Scanning Electron Micrograph of pure 4800P P.E.S. impact fracture surface (notch root radius 0.1mm, temperature 25°C).

Figure 99. Scanning Electron Micrograph of Blend 4 impact fracture surface (notch root radius 0.1mm, temperature 25°C).

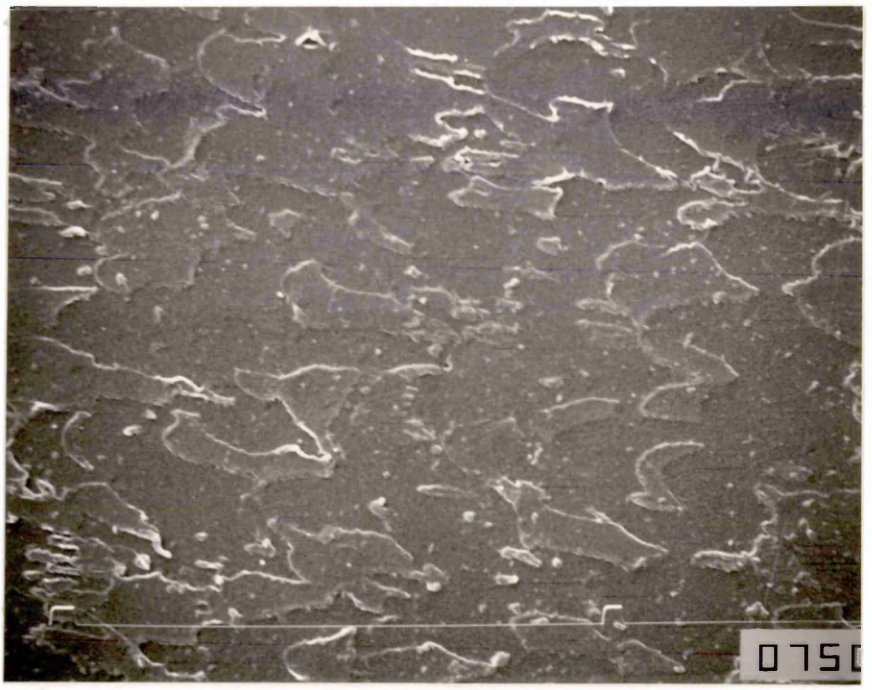

100μm

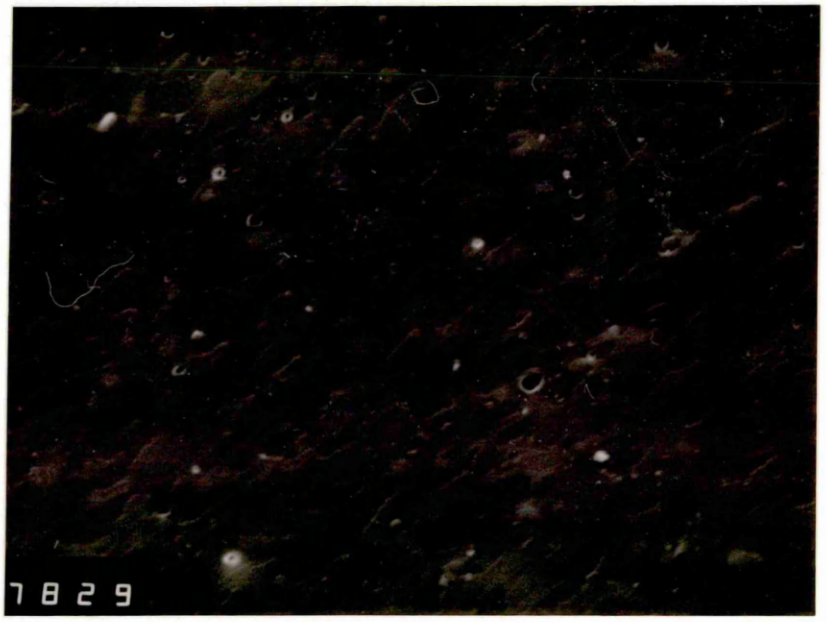

100μm

Figure 100. Scanning Electron Micrograph of Blend 5 impact fracture surface (notch root radius 0.1mm, temperature 25°C).

Figure 101. Scanning Electron Micrograph of Blend 3 impact fracture surface (notch root radius 0.1mm, temperature 25°C).

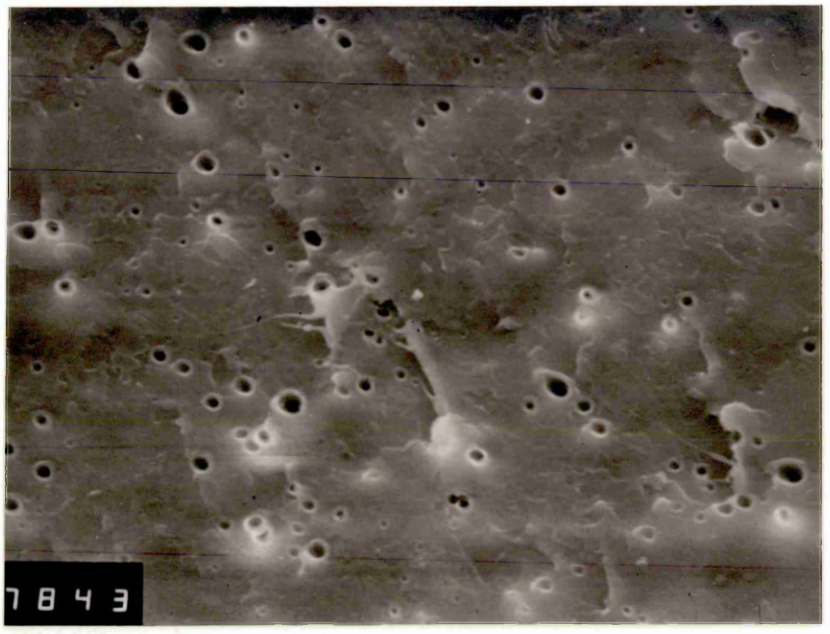

100μm

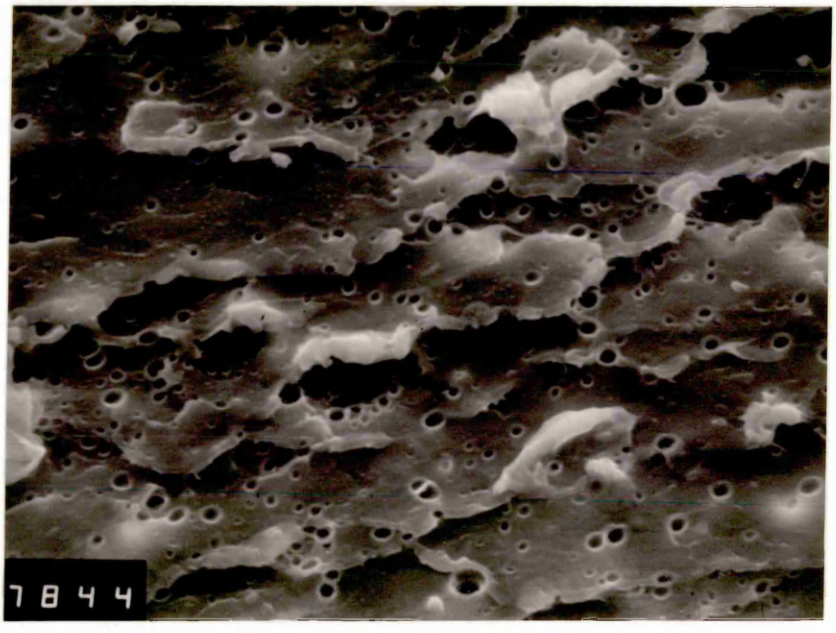

100μm

Figure 102. Scanning Electron Micrograph of Blend 1 impact fracture surface (notch root radius 0.1mm, temperature 25°C).

Figure 103. Scanning Electron Micrograph of Blend 2 impact fracture surface (notch root radius 0.1mm, temperature 25°C).

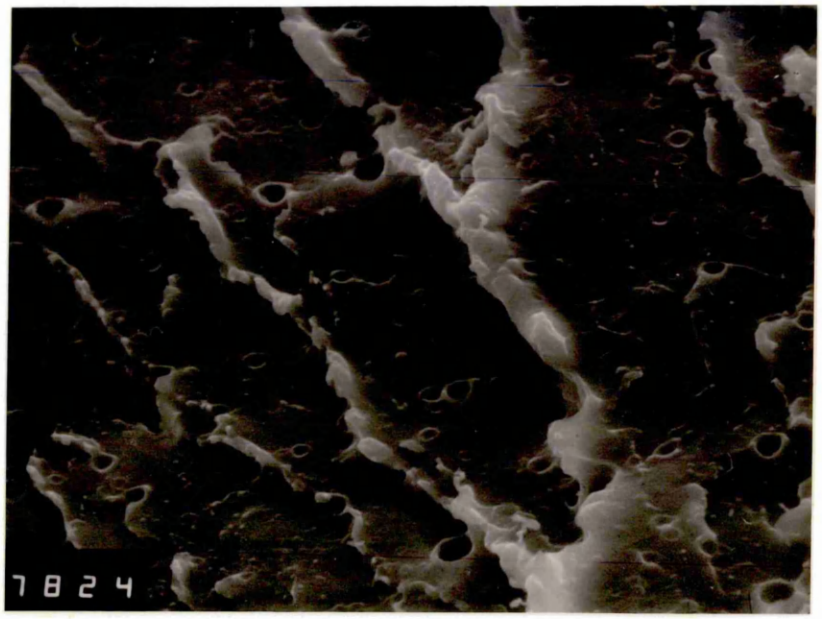

100μm

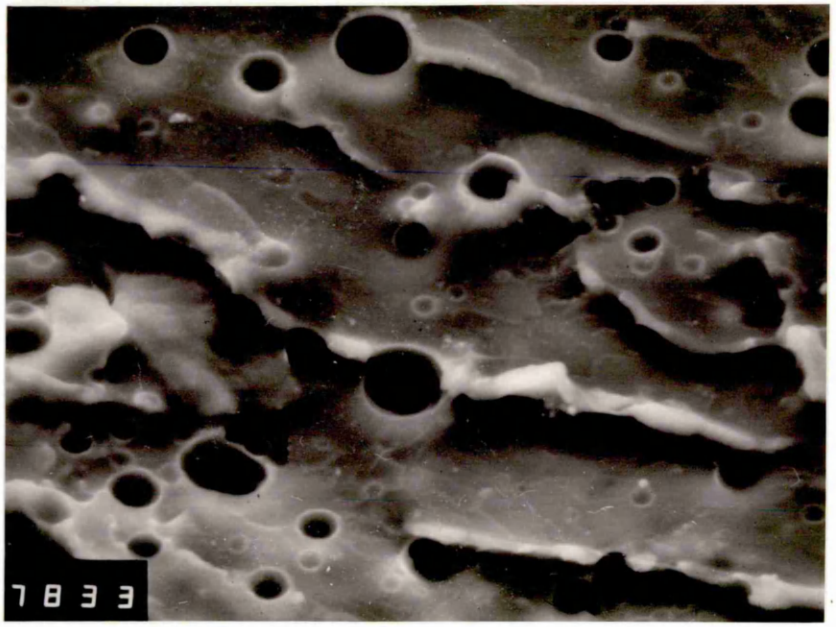

100μm

Figure 104. Scanning Electron Micrograph of Blend 7 impact fracture surface (notch root radius 0.1mm, temperature 25°C).

Figure 105. Scanning Electron Micrograph of Blend 8 impact fracture surface (notch root radius 0.1mm, temperature 25°C).

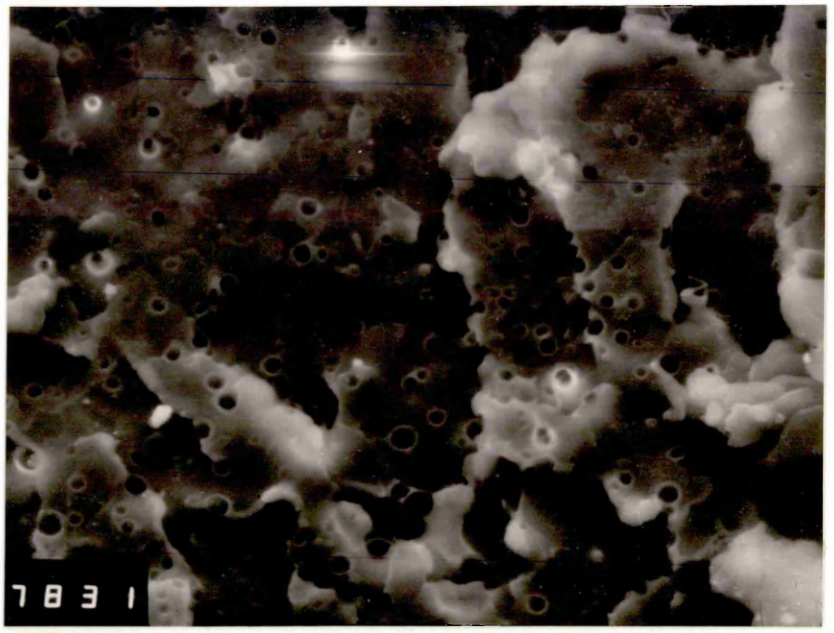

100μm

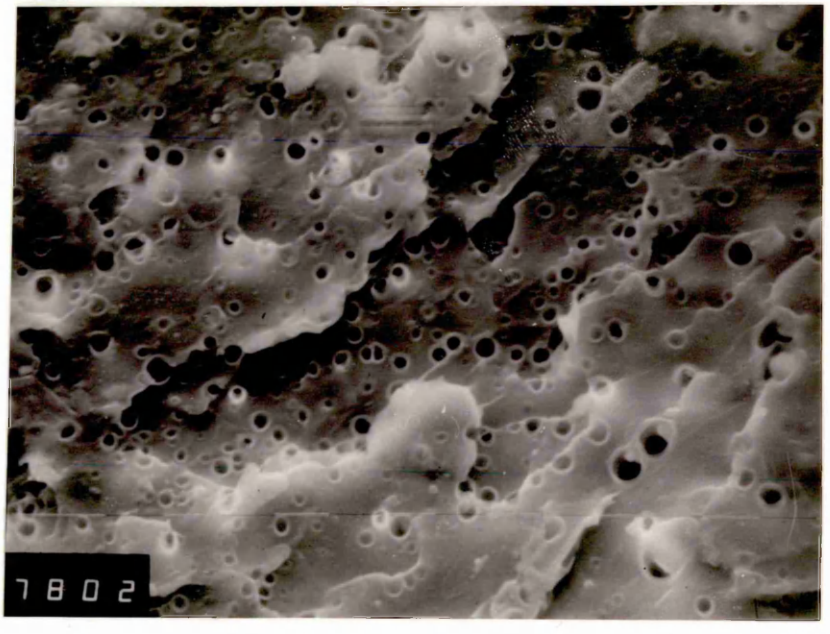

100μm

Figure 106. Scanning Electron Micrograph of Blend 9 impact fracture surface (notch root radius 0.1mm, temperature 25°C).

Figure 107. Scanning Electron Micrograph of pure 4800P P.E.S. impact fracture surface (notch root radius 1.0mm temperature 25°C).

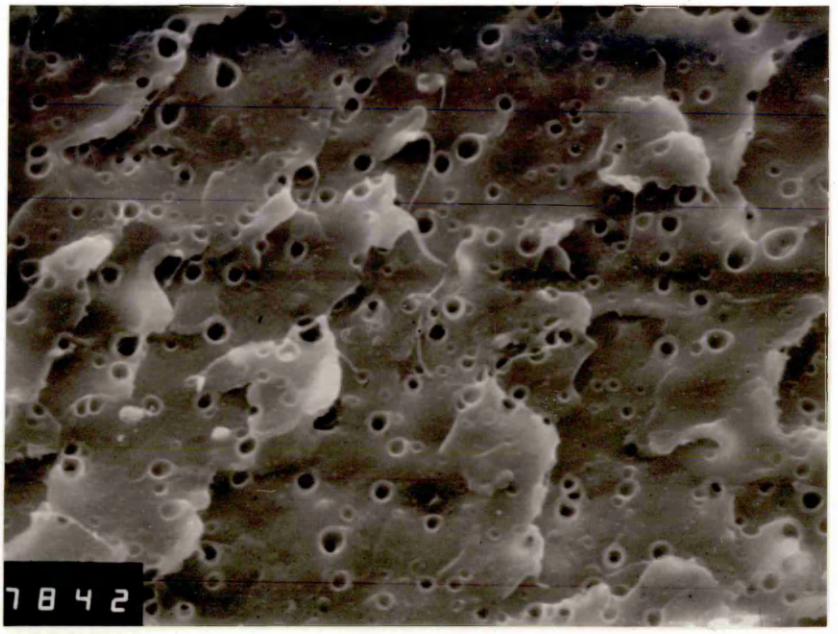

100μm

1mm

Figure 108. Scanning Electron Micrograph of Blend 3 impact fracture surface (notch root radius 1.0mm, temperature 25°C).

Figure 109. High Magnification Scanning Electron Micrograph of Blend 3 impact fracture surface (notch root radius 1.0mm, temperature 25°C).

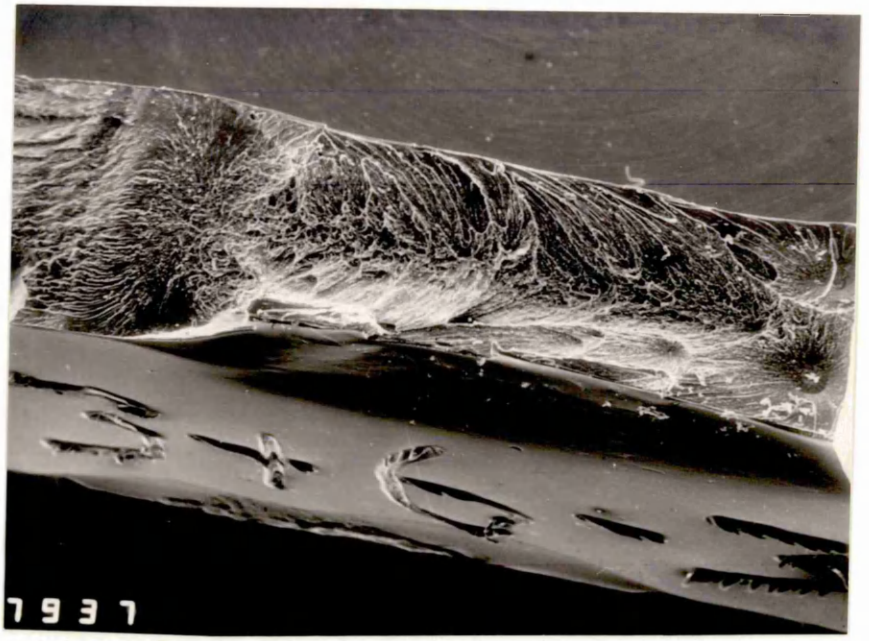

1mm

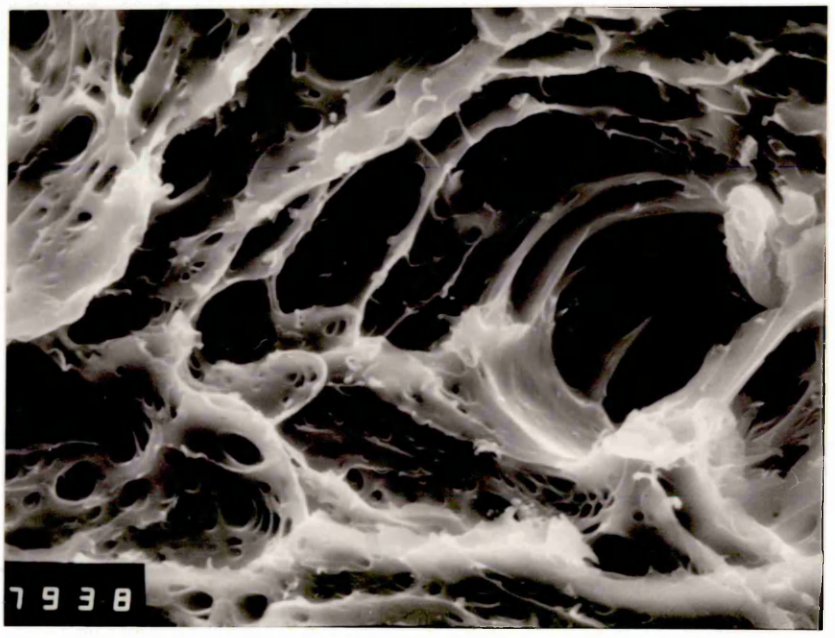

100μm

Figure 110. Instron Model 3111 Tensile Test machine.

Figure 111. Tensile test piece geometry.

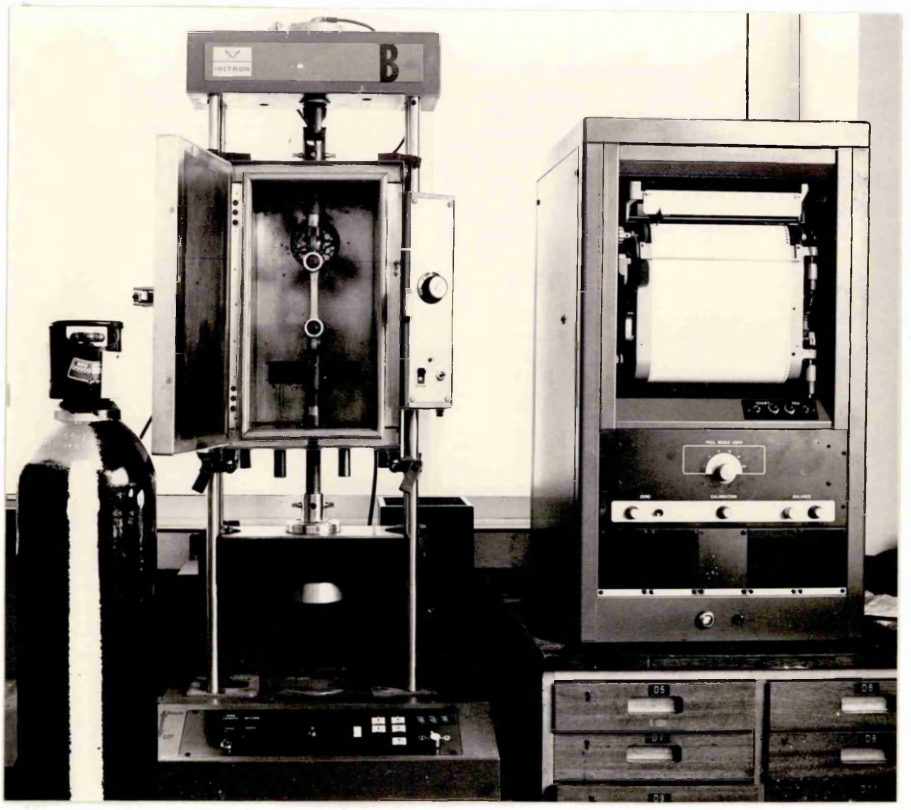

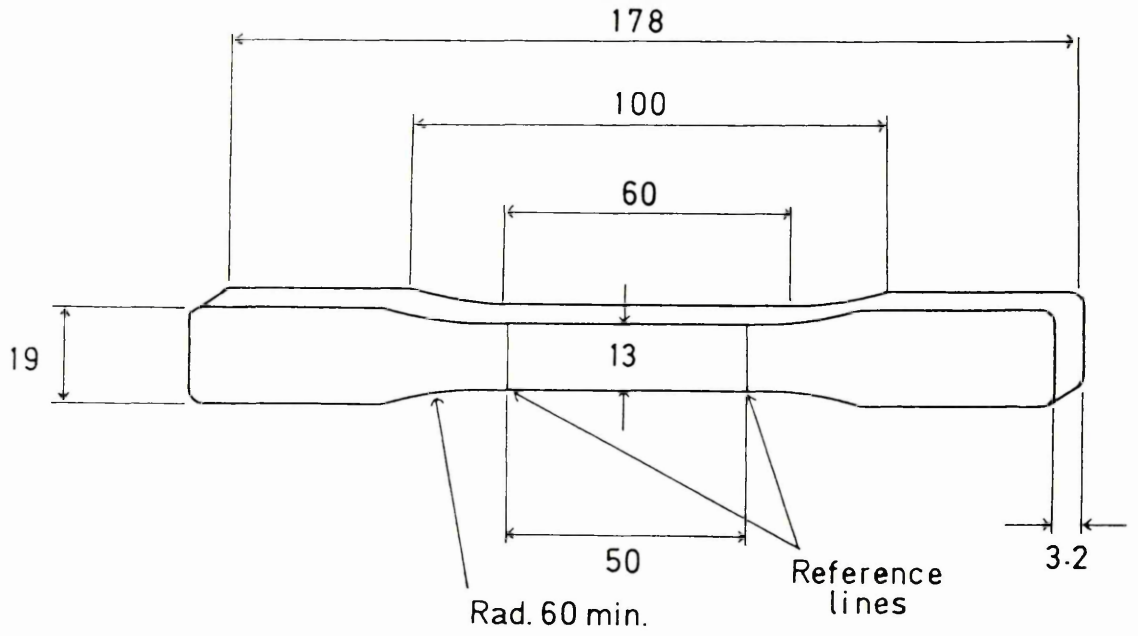

Dimensions in mm.
Tolerances ±0·5

Figure 112. Tensile Strength vs Temperature. (——x——) Pure 4800P P.E.S., (- - o - -) Blend 1. (Strain rate 50mm/min.)

Figure 113. Tensile Strength vs Temperature. (——x——) Blend 2, (- - o - -) Blend 3. (Strain rate 50mm/min.)

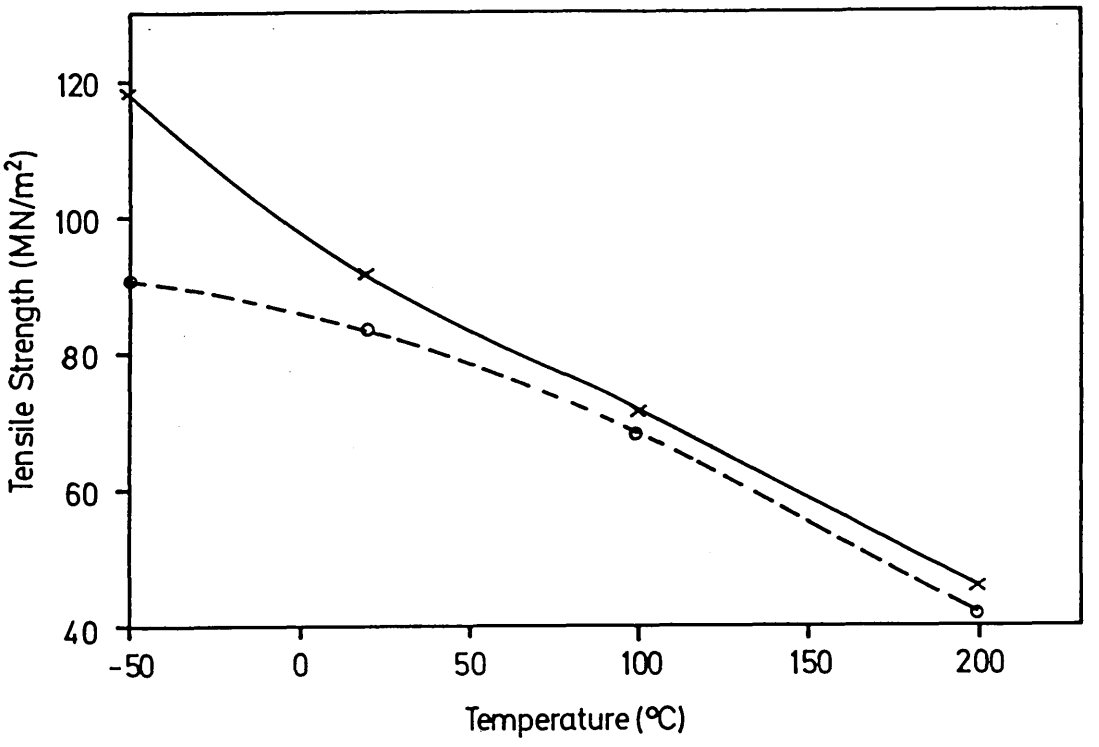
Tensile Strength (MN/m²)
120
100
80
60
40
-50
0
50
100
150
200
Temperature (°C)

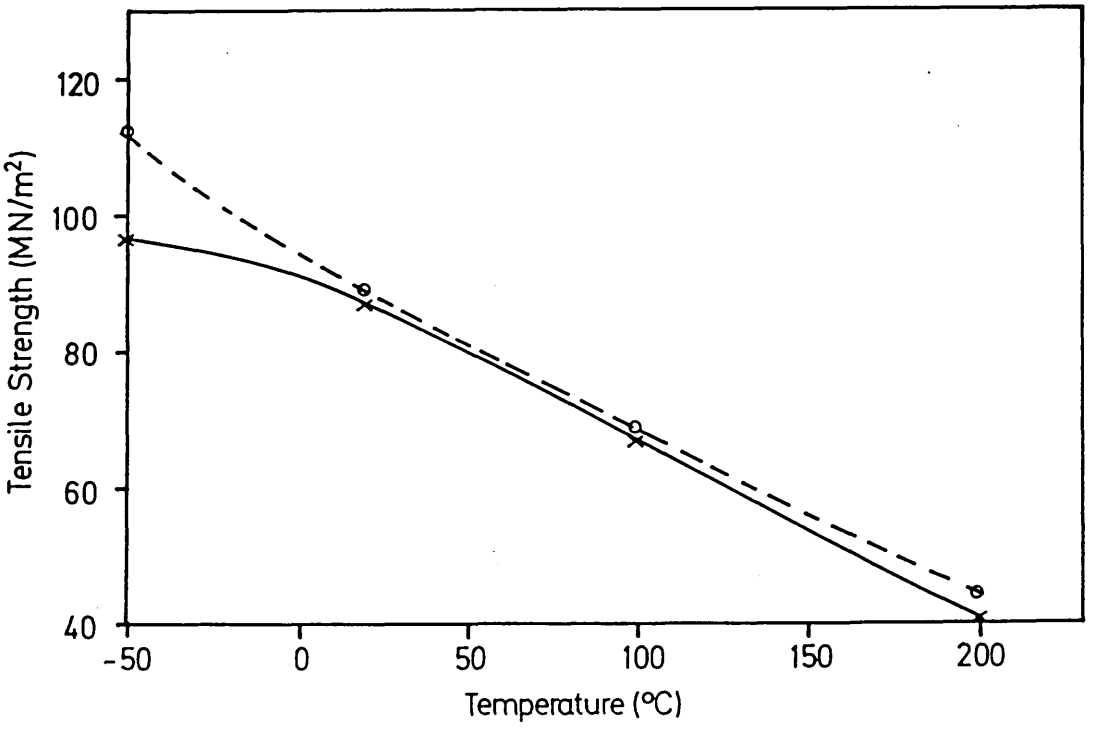
Tensile Strength (MN/m²)
120
100
80
60
40
-50
0
50
100
150
200
Temperature (°C)

Figure 114. Tensile Strength vs Temperature. (——x——) Blend 4, (- - o - -) Blend 5. (Strain rate 50mm/min.)

Figure 115. Tensile Strength vs Temperature. (——x——) Blend 7, (- - o - -) Blend 8, (— - —■— - —) Blend 9. (Strain rate 50mm/min.)

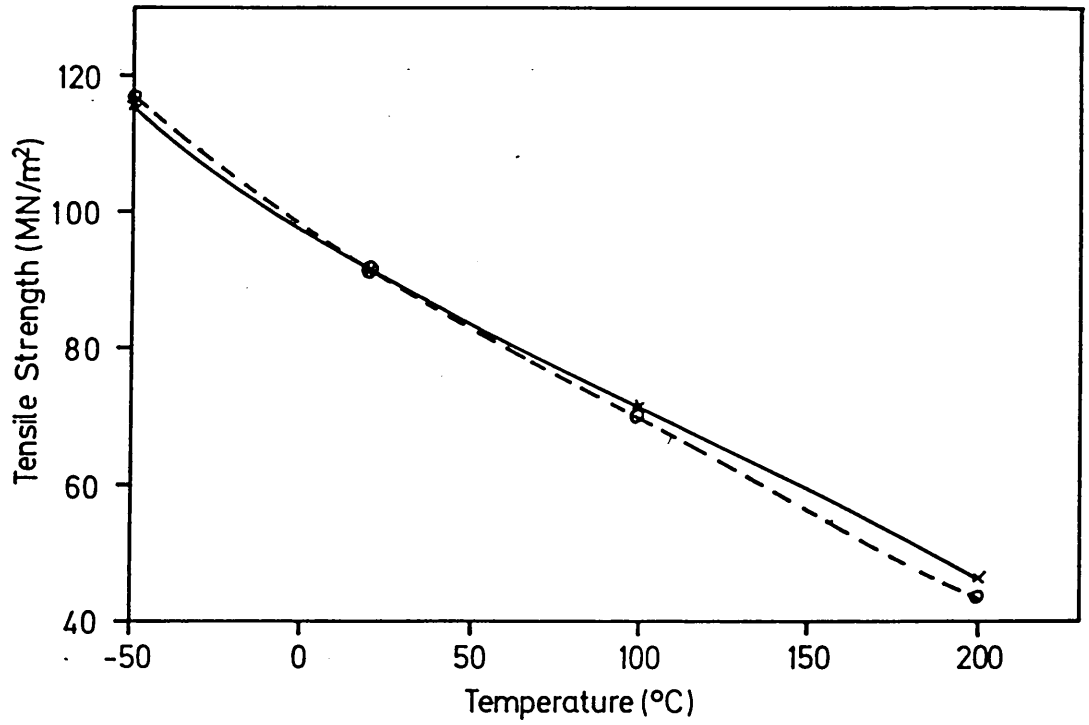
120
100
80
60
40
Tensile Strength (MN/m²)
-50
0
50
100
150
200
Temperature (°C)

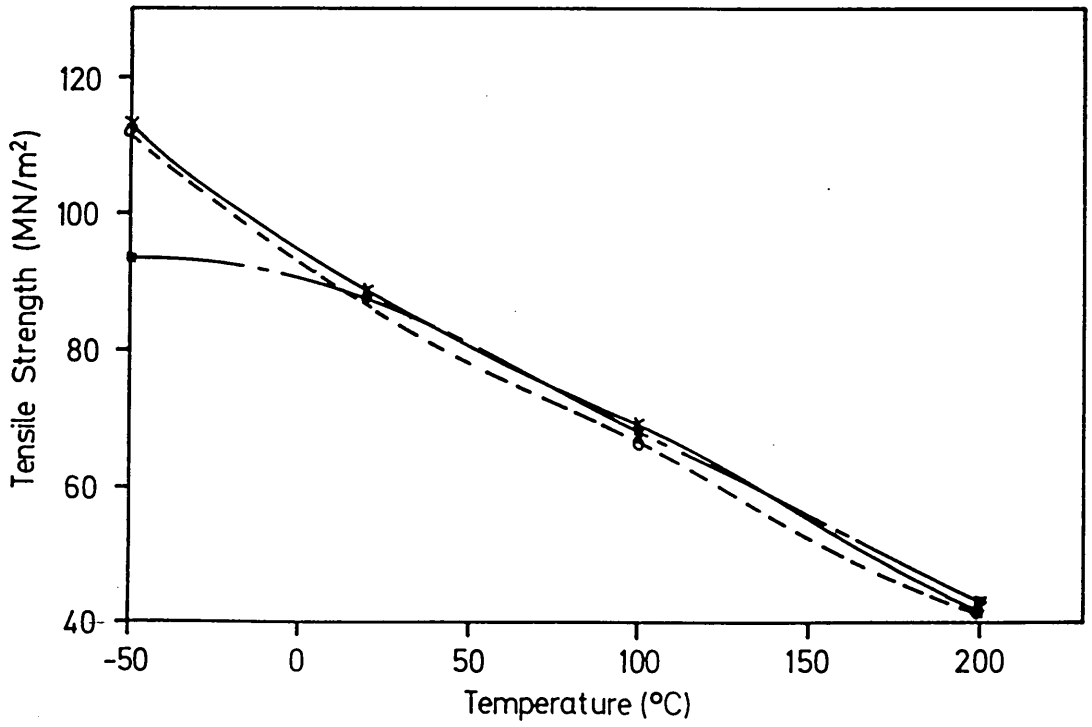
120
100
80
60
40
Tensile Strength (MN/m²)
-50
0
50
100
150
200
Temperature (°C)

Figure 116. Tensile Strength vs Strain Rate. (□) Pure 4800P P.E.S., (o) Blend 3. (Temperature 20°C.)

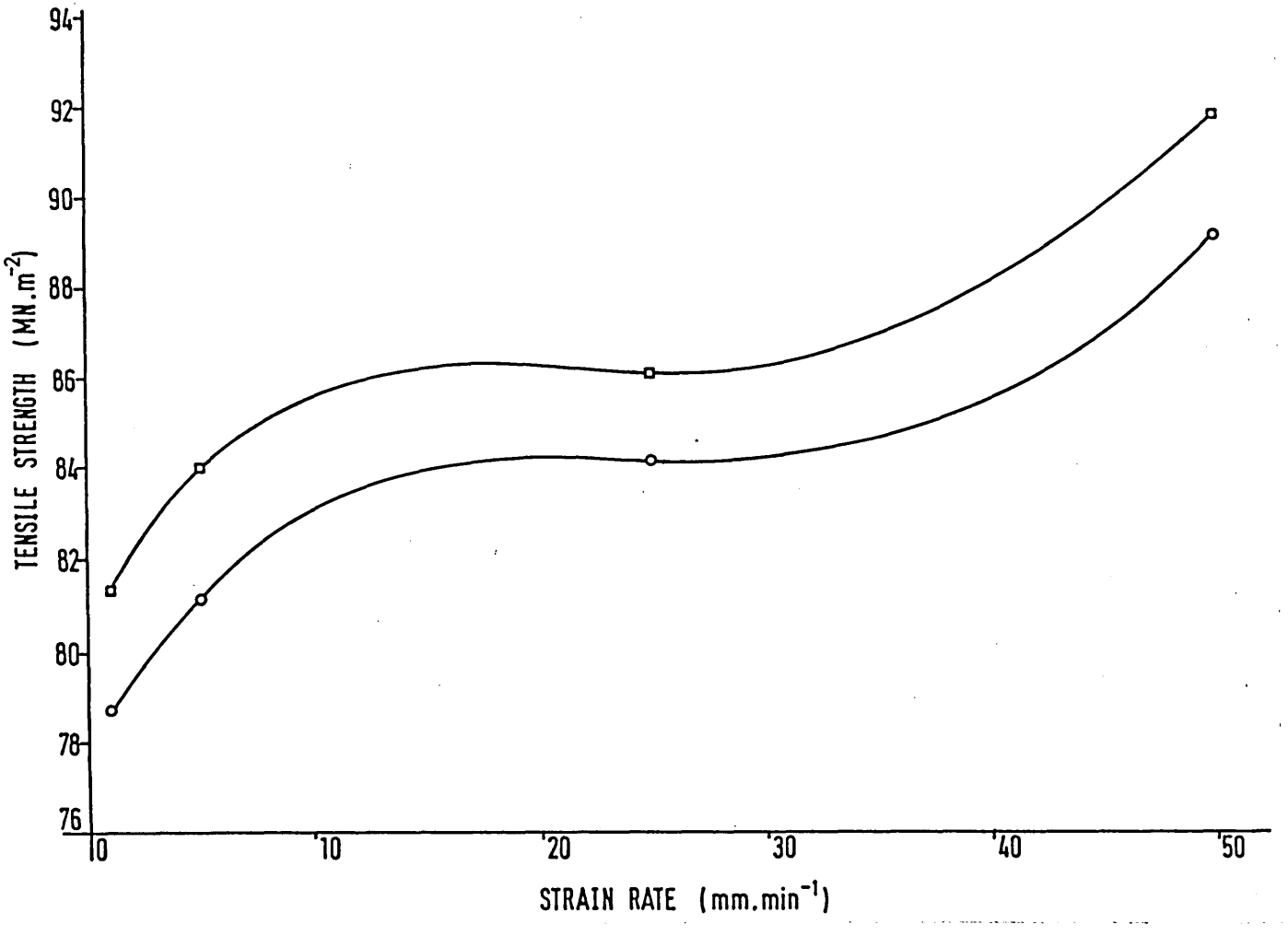
94
92
90
88
86
84
82
80
78
76
TENSILE STRENGTH (MN.m^{-2})
0
10
20
30
40
50
STRAIN RATE (mm.min^{-1})

Figure 117. Stress vs Strain curves. (a) Pure 4800P P.E.S., (b) Blend 5. (Temperature 20°C, strain rate 50mm/min.)

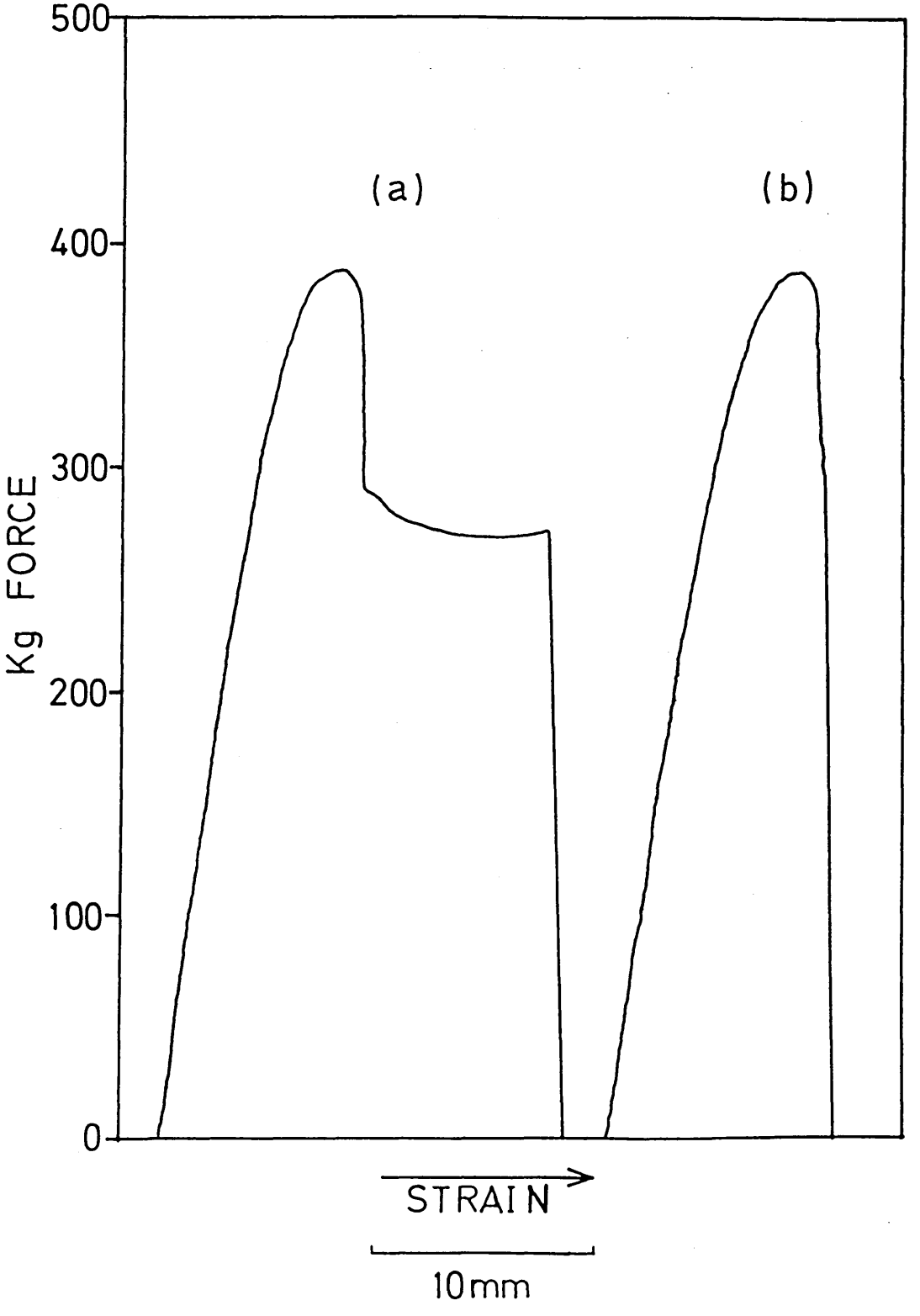
500
400
300
200
100
0
Kg FORCE
(a)
(b)
STRAIN
10mm

Figure 118. Transmission Electron Micrograph of pure 4800P P.E.S. (ultramicrotomed at room temperature).

Figure 119. Transmission Electron Micrograph of Blend 3 (ultramicrotomed at room temperature).

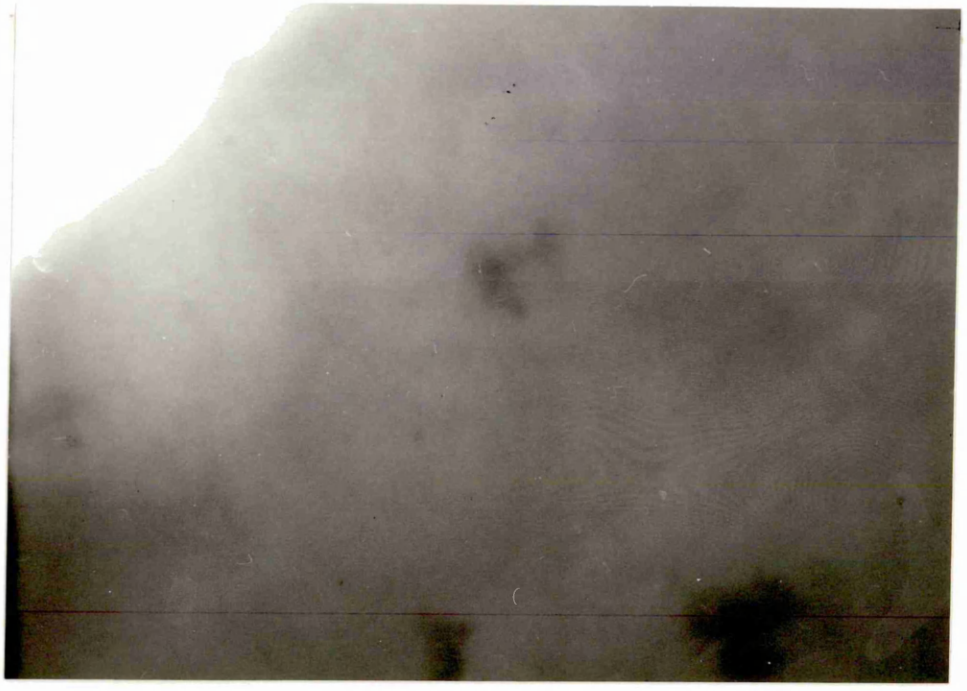

1μm

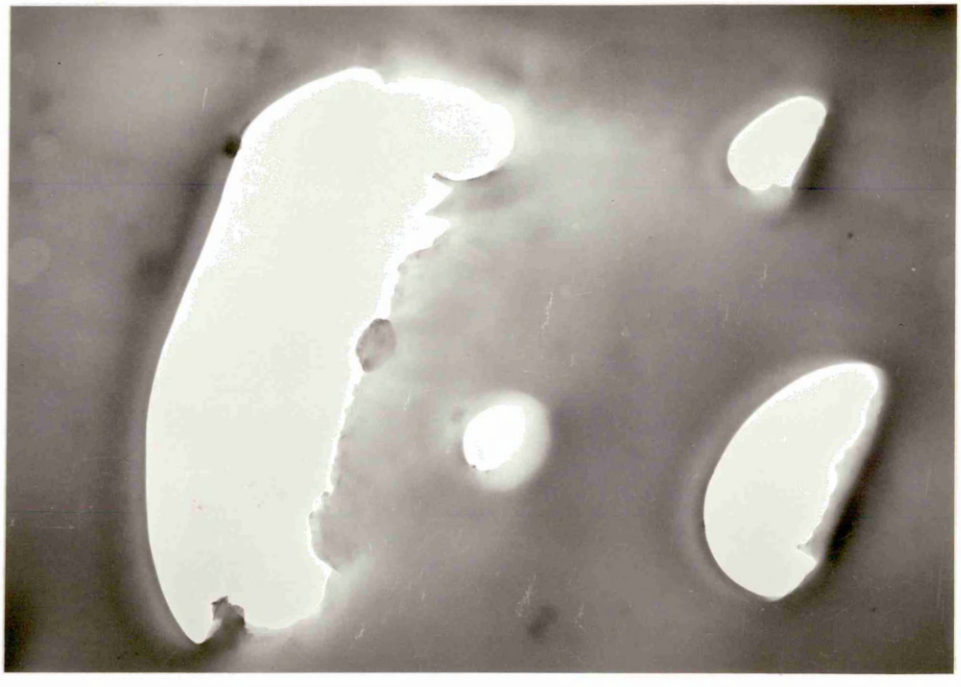

1μm

Figure 120. Transmission Electron Micrograph of Blend 4 (ultramicrotomed at room temperature).

Figure 121. Transmission Electron Micrograph of Blend 7 (ultramicrotomed at room temperature).

1μm

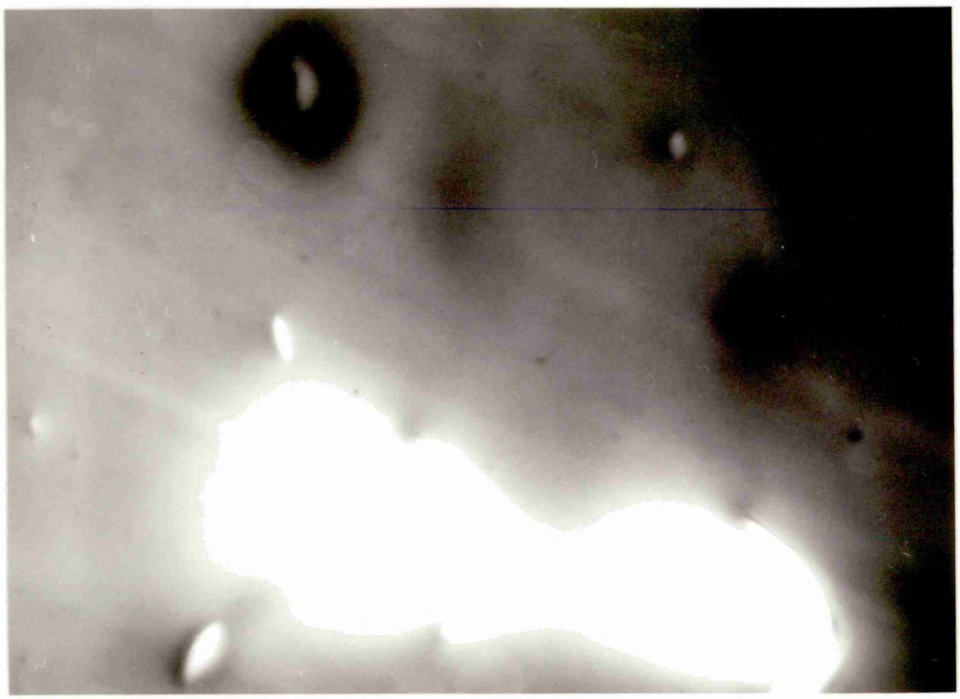

1μm

Figure 122. Transmission Electron Micrograph of Blend 9 (ultramicrotomed at room temperature).

Figure 123. High Magnification Transmission Electron Micrograph of a void in Blend 3.

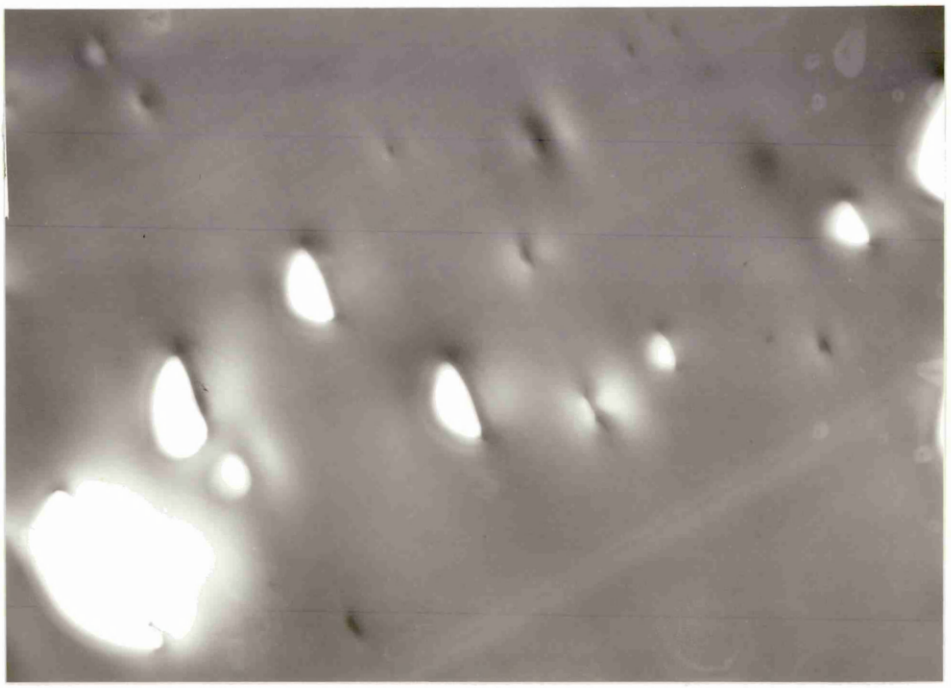

1μm

0.5μm

Figure 124. High Magnification Transmission Electron Micrograph of a rubber particle in Blend 2.

Figure 125. High Magnification Transmission Electron Micrograph of rubber particles in Blend 8.

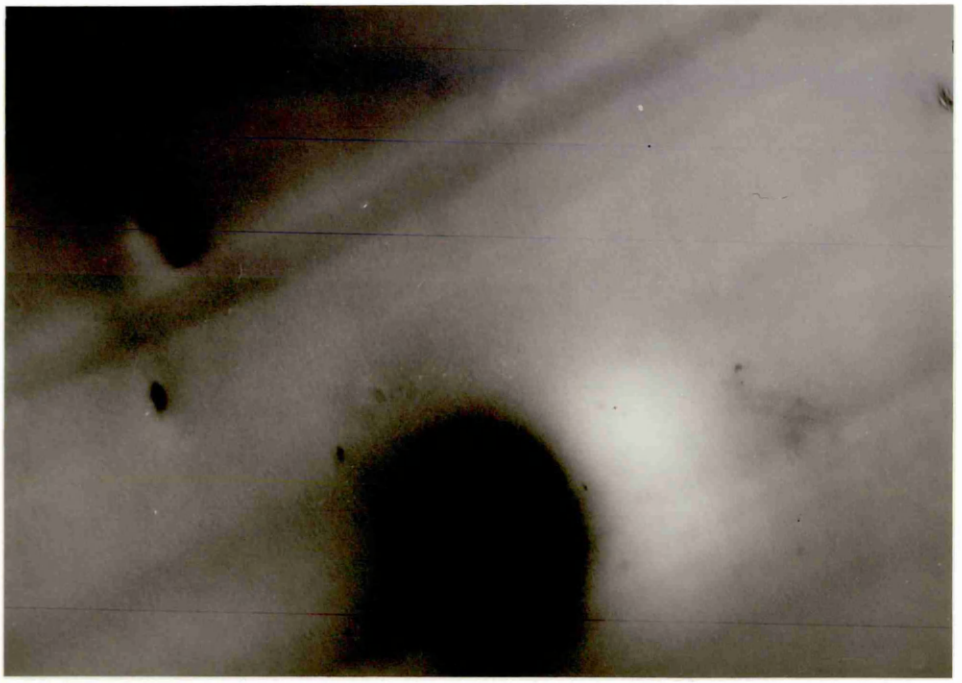

1μm

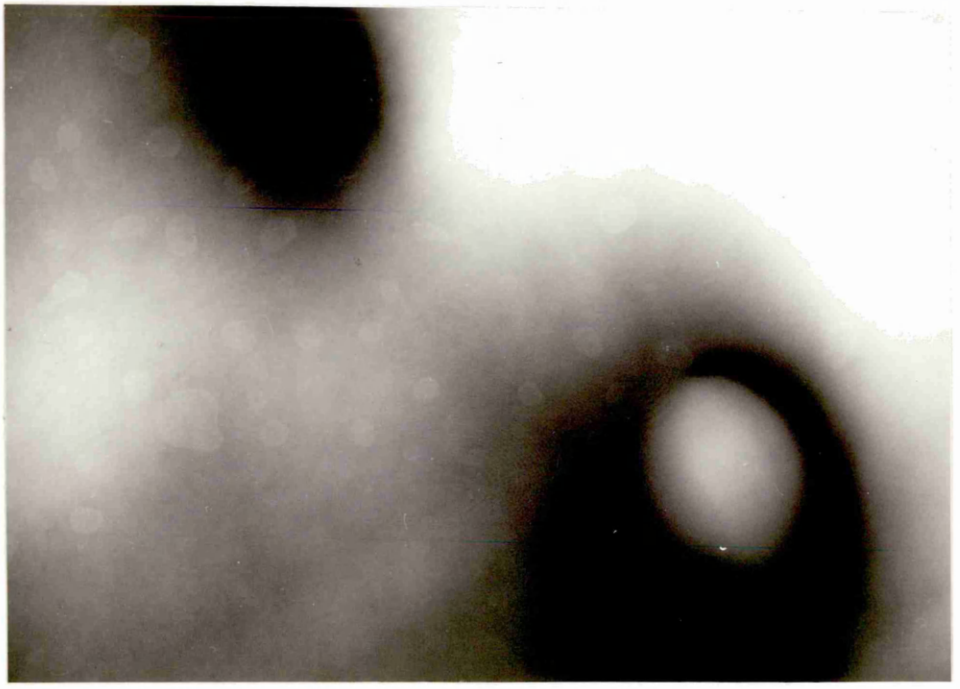

1μm

Figure 126. High Magnification Transmission Electron Micrograph of rubber particles and phase separation around the site of a void in Blend 8.

Figure 127. High Magnification Transmission Electron Micrograph of a rubber particle apparently undergoing fracture and contractiong to leave a void.

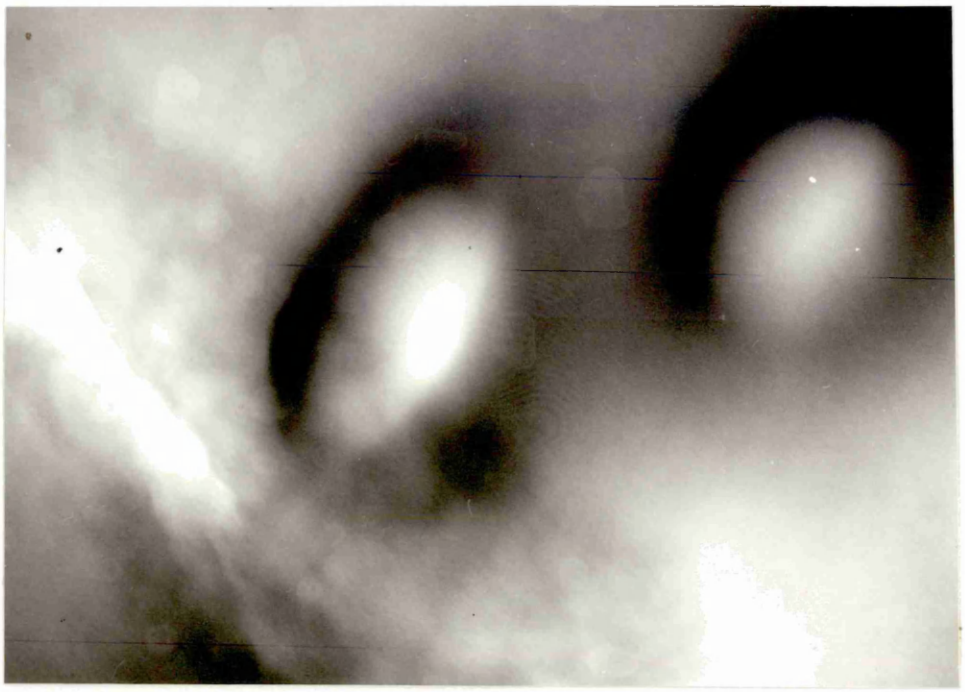

0.5μm

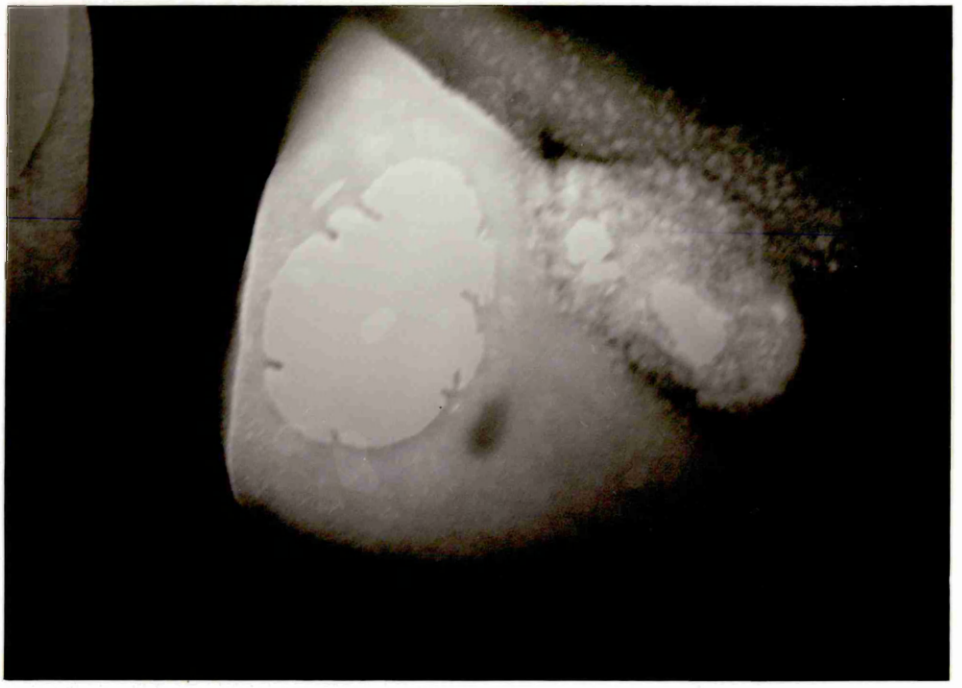

0.5μm

OBSERVED PEAK (cm^{-1})	INTERPRETATION	EXPECTED RANGE (cm^{-1})
3400	O-H str.	3645-3200
3100	C-H str. aromatic	3100-3000
1585	C-H str. arom.	1600-1585
1500	C-H str. arom.	1500-1430
1325 & 1300	SO_2 asymm. str. (doublet)	1340-1290
1240	C-O-C asymm. str.	1310-1210
1150	SO_2 symm. str.	1165-1120
695	out of plane ring bending	710-675

TABLE 1. Infrared Correlation for P.E.S. Oligomers.

SAMPLE	$\bar{M}n$	$\bar{M}w$	$\bar{M}z$	$\bar{M}w/\bar{M}n$	$\bar{M}z/\bar{M}n$
1. $(\bar{DP})_{max}$ 5	1959	11460	181646	5.85	92.72
2. $(\bar{DP})_{max}$ 27	6660	406984	15004568	61.11	2253
3. $(\bar{DP})_{max}$ 108	11075	1478645	183501871	*133.5	16569

* SEE TEXT

TABLE 2. P.E.S. Oligomer Molecular Weights obtained by G.P.C.

SAMPLE	REDUCED VISCOSITY	$\bar{M}n$
1. $(\bar{DP})_{max}$ 5	0.0724	1294
2. $(\bar{DP})_{max}$ 27	0.1759	4932
3. $(\bar{DP})_{max}$ 108	0.2726	9552

TABLE 3. P.E.S. Oligomer Molecular Weights by Viscometry.

SAMPLE	WEIGHT(g)	CORRECTED END POINT VOL. (cm^3)	$\bar{M}n$
BISPHENOL 'S'	0.0125	1.025	244
1. $(\bar{DP})_{max}$ 5	0.0652	0.625	2086
2. $(\bar{DP})_{max}$ 27	0.2468	0.580	8510
3. $(\bar{DP})_{max}$ 108	0.4970	0.825	12048

TABLE 4. P.E.S. Oligomer Molecular Wts. by Potentiometric Titrn.

SAMPLE	$\bar{M}n$		
	G.P.C.	VISCOMETRY	TITRATION
BISPHENOL 'S'	-	-	244*
1. $(\bar{DP})_{max}$ 5	1959	1294	2086
2. $(\bar{DP})_{max}$ 27	6660	4932	8510
3. $(\bar{DP})_{max}$ 108	11075	9552	12048

* BISPHENOL 'S' Molecular Weight is 250

TABLE 5. P.E.S. Oligomer Molecular Weights: results from three different evaluation procedures.

SAMPLE	Tg(°C)
4800P VICTREX	224
1. $(\bar{DP})_{max}$ 5	179
2. $(\bar{DP})_{max}$ 27	174
3. $(\bar{DP})_{max}$ 108	202

TABLE 6. P.E.S. Oligomer Glass Transition Temperatures by Differential Scanning Calorimetry.

SAMPLE	$\bar{M}n$	$\bar{M}w$	$\bar{M}z$	$\bar{M}v$	$\bar{M}w/\bar{M}n$	$\bar{M}z/\bar{M}n$
11 38/71/1	APPROX. MOL. WT. QUOTED AT 600				-	-
11 38/71/2	4945	11970	32440	10420	2.42	6.56
11 38/71/3	28510	58310	91020	53930	2.05	3.19
11 38/71/4	53370	119900	207900	109300	2.25	3.90
11 38/71/5	62580	145100	247700	132600	2.32	3.96

TABLE 7. G.P.C. Analysis of Hydroxyl-Terminated P.D.M.S. Oligomers.

SAMPLE	$[\eta]$ $(g.ml^{-1})^{-1}$	$\bar{M}v$
11 38/71/1	0.60	450
11 38/71/2	7.06	13802
11 38/71/3	18.70	53392
11 38/71/4	27.60	91684
11 38/71/5	31.28	109092

TABLE 8. Viscometric Analysis of Hydroxyl-Terminated P.D.M.S. Oligomers.

OBSERVED PEAK (cm^{-1})	INTERPRETATION	EXPECTED RANGE (cm^{-1})
3700-3100	Si-OH assym. str.	3700-3200
2960	C-H str. aliphatic	just below 3000
1250	$Si-CH_3$ str.	1250
1100-1000	Si-O-Si str.	1100-1000
800	Si-C str.	800
700	$Si-CH_3$ vib.	700

TABLE 9. Infrared Correlation for Hydroxyl-Terminated P.D.M.S. Oligomers.

SAMPLE	$[\eta]$	$\bar{M}v$
11 38/71/1	0.62	450
11 38/71/2	7.06	13802
11 38/71/3	27.6	91684

TABLE 10. Viscometric Analysis of Dimethylamino-Terminated P.D.M.S. Oligomers.

SAMPLE No.	BLOCK $\bar{M}n$	
	P.E.S.	P.D.M.S.
1	1300	800
2	1300	5100
3	4900	5100 BATCH 1
4	4900	5100 BATCH 2
5	9600	5100
6	9600	53000

TABLE 11. Copolymer Block Molecular Weights.

SAMPLE	$\bar{M}n$	$\bar{M}w$	$\bar{M}z$	$\bar{M}v$	$\bar{M}w/\bar{M}n$	$\bar{M}z/\bar{M}n$
1	10800	14700	18900	21500	1.36	1.99
2	34300	80300	144000	74600	2.34	4.20
3	24600	37100	50500	32400	1.51	2.05
4	15700	28100	39300	25300	1.79	2.50
5	26600	34100	42100	49200	1.28	1.58
6	70500	139000	310000	74600	1.97	4.40

TABLE 12. G.P.C. Analysis of Copolymers.

SAMPLE	RELATIVE VISCOSITY (η_r)	SPECIFIC VISCOSITY (η_{sp})	REDUCED VISCOSITY (η_{sp}/c)
1	1.05	0.05	24.0
2	1.10	0.10	50.5
3	1.07	0.07	33.8
4	1.06	0.06	28.3
5	1.08	0.08	38.5
6	1.11	0.11	55.0

TABLE 13. Viscometric Analysis of Copolymers.

COPOLYMER	WEIGHT LOSS (%)	APPEARANCE
1	12.5	DARKENING OF COLOUR
2	7.0	SLIGHT DARKENING
3	8.0	SLIGHT DISSOCIATION
4	12.5	SOME DISSOCIATION
5	5.6	SOME DISSOCIATION
6	6.0	SLIGHT DARKENING

TABLE 14. Weight Loss and Appearance of Copolymers after heat-treatment in air at 360°C for 30 minutes.

SAMPLE No.	EXPECTED VALUES		^{1}H.N.M.R. ANALYSIS		SULPHUR ANALYSIS		MEAN OF N.M.R. & SULPHUR ANALYSIS	
	P.E.S. (%)	P.D.M.S. (%)	P.E.S. (%)	P.D.M.S. (%)	P.E.S. (%)	P.D.M.S. (%)	P.E.S. (%)	P.D.M.S. (%)
1	55.13	44.87	59.76	40.24	53.29	46.71	56.52	43.48
2	19.62	80.38	21.50	78.50	17.69	82.31	19.59	80.41
3	46.60	53.40	50.60	49.40	43.79	56.21	47.19	52.81
4	48.37	51.63	44.36	55.74	35.89	64.11	40.12	59.88
5	64.49	35.51	63.90	36.90	59.31	40.69	61 20	38.80
6	15.16	84.84	19.80	80.20	13.41	86.59	16.60	83.40

TABLE 15. Copolymer Compositions

SAMPLE	PDMS CONTENT OF SAMPLE (%)	WEIGHT LOSS (% OF PDMS CONTENT)
COPOLYMER 1	43.5	33.0
COPOLYMER 2	80.4	24.4
COPOLYMER 3	52.8	59.0
COPOLYMER 4	59.9	42.7
COPOLYMER 5	38.8	15.8
COPOLYMER 6	83.4	24.0
PES/PDMS BLEND	58.3	99.1

TABLE 16. Selective Solvation Analysis (Solvent - Diethyl Ether).

BLEND No.	ADDITIVE	ADDITIVE CONTENT IN BLEND (%)	P.D.M.S. CONTENT IN BLEND (%)
1	COPOLYMER 1	5.75	2.50
2	COPOLYMER 2	3.11	2.50
3	COPOLYMERS 3&4	4.33	2.50
4	COPOLYMERS 3&4	0.87	0.50
5	COPOLYMERS 3&4	1.73	1.00
7	COPOLYMER 5	6.44	2.50
8	COPOLYMER 6	3.00	2.50
9	LINEAR P.D.M.S.	2.50	2.50

TABLE 17. Blend Compositions (Matrix 4800P Grade P.E.S.)

BLEND No	SHEAR THINNING INDEX (n)
PURE PES	0.45
1	0.36
2	0.46
3	0.75
4	0.52
5	0.58
7	0.57
8	0.74
9	0.70

TABLE 18. Values of Shear Thinning Index for the various Blends

BLEND No	G_B (KJ/m^2)
PURE P.E.S.	4.33
1	3.87
2	4.32
3	4.00
4	3.46
5	3.33
7	3.93
8	4.50
9	4.60

TABLE 19. Values of Apparent Critical Strain Energy Release Rate (G_B) for the various Blends. (Test temperature 27°C, notch root radius 0.1mm.)

BLEND No.	TENSILE STRENGTH (MN/m^2)	ELONGATION AT BREAK (%)	ELASTIC MODULUS (MN/m^2)
PURE PES	91.9	24.4	1013
1	83.8	2.86	990
2	87.0	3.75	1005
3	89.2	5.00	1011
4	91.3	17.0	1052
5	91.3	4.91	995
7	88.9	5.53	1016
8	87.4	5.00	1021
9	87.7	4.91	1004

TABLE 20. Tensile Data for the Blends. (Strain Rate 50mm/min, temperature 20°C.

SAMPLE	TAP WATER AT 75°C	ACETONE	TOLUENE	HCl (10%)	NaOH (10%)	TELLUS 27 OIL
PURE PES	U	BAD ATTACK, CRACKS AT EDGES	U	U	U	U
BLEND 8	SLIGHT SURFACE WHITENING	SOFTENING, SWELLING & WHITENING	U	U	U	U
BLEND 9	SLIGHT SURFACE WHITENING	SOFTENING, SWELLING & WHITENING	U	U	U	U

U = Unaffected

TABLE 21. Visual Appearance of Blends after immersion in selected chemical reagents for a period of 7 days.

SAMPLE	TAP WATER AT 75°C	ACETONE	TOLUENE	HCl (10%)	NaOH (10%)	TELLUS 27 OIL
PURE PES	1.21	6.60	0.36	0.66	0.75	0.09
BLEND 8	1.21	8.13	0.35	0.61	0.67	0.06
BLEND 9	1.20	7.49	0.29	0.62	0.69	0.06

TABLE 22. Percentage Weight Gain in Izod test specimens after immersion in selected chemical reagents for 7 days.

SAMPLE	TAP WATER AT 75°C	ACETONE	TOLUENE	HCl (10%)	NaOH (10%)	TELLUS 27 OIL
PURE PES	1.68	7.41	0.61	1.11	1.06	0.35
BLEND 8	1.24	8.77	0.41	0.58	0.69	0.10
BLEND 9	1.22	8.30	0.44	0.63	0.71	0.17

TABLE 23. Percentage Weight Gain in Tensile test specimens after immersion in selected chemical reagents for 7 days.

SAMPLE	UNTREATED	TAP WATER AT 75°C	ACETONE	TOLUENE	HCl (10%)	NaOH (10%)	TELLUS 27 OIL
PURE PES	6.29	7.70	3.79	6.92	8.64	9.38	6.99
BLEND 8	7.77	9.69	11.6	9.62	11.1	11.2	9.51
BLEND 9	9.51	11.7	6.70	10.6	11.3	12.9	10.6

TABLE 24. Impact Strength (KJ/m^2) of Izod test specimen after immersion in selected chemical reagents for 7 days. (Test temperature 20°C, notch root radius 0.25mm, notch depth 2.5mm).

SAMPLE	UNTREATED	TAP WATER AT 75°C	ACETONE	TOLUENE	HCl (10%)	NaOH (10%)	TELLUS 27 OIL
PURE PES	85.5	82.2	68.1	86.2	81.1	81.6	86.3
BLEND 8	81.3	77.1	59.0	79.6	76.9	76.3	80.9
BLEND 9	82.6	77.5	60.0	80.2	77.9	76.6	81.4

TABLE 25. Tensile Strength (MN/m^2) of test specimens after immersion in selected chemical reagents for 7 days. (Strain rate 50mm/min, test temperature 20°C.)

BLEND No.	P.D.M.S. CONTENT (%)	IMPACT STRENGTH (KJ/m^2)
4800P PES	0.0	7.80
4	0.5 COPOLYMERISED	17.44
7	2.5 COPOLYMERISED	18.38
8	2.5 COPOLYMERISED	17.35
9	2.5 LINEAR	17.56

TABLE 26. Notched Izod Impact Data for Blends using ASTM Standard (Information supplied by I.C.I., Wilton)

APPENDIX 1

MODULE 4 - 30 HOUR CASE STUDY

INVESTMENT IN MACHINERY FOR THE RECYCLING OF I.C.I. APC-2 COMPOSITE MATERIAL - AN ECONOMIC ASSESSMENT.

INTRODUCTION

The market for high temperature engineering thermoplastics continues to grow, with these materials constantly finding applications in areas where traditionally metals and ceramics have enjoyed unquestionable usage. This may be attributable not only to the development of new high performance homopolymers, but also to the advancements made in the technology of polymer blending.

Over recent years considerable work has been performed on the enhancement of specific polymer properties by blending with soft rubbery additives e.g. copolymers or hard, rigid components e.g. glass or carbon fibres. This has enabled the manufacturers to supply each polymer in a number of grades formulated to suit a range of applications.

'Victrex' PEEK (polyetheretherketone) is one such high performance thermoplastic engineering polymer. It is marketed by I.C.I. in a range of unreinforced and fibre reinforced grades, one of which forms the basis of this study.

APC-2 is a PEEK / carbon fibre composite comprising 61% by volume (68% by weight) continuous carbon fibre impregnated with PEEK to form a pre-impregnated tape or 'prepreg'. The 'prepreg' tapes are laid up and moulded to form sheets suitable for processing by a variety of procedures.

Scrap is generated from these processes, and it is an economic assessment of the possibility of reclaiming and

utilising this scrap that is undertaken here.

Work already performed on the reclamation of APC-2 scrap has indicated that the scrap can be granulated, diluted with additional resin and used as an injection moulding compound of high value. Furthermore, it has been shown that preconsolidated sheet stock with good properties can be obtained by compression moulding 12.7mm square offcuts of APC-2 'prepreg' (1).

With the cost of virgin APC-2 'prepreg' being high (Jan 1988 price - £150 / Kg for quantities over 10Kg) it is likely that considerable savings may be made by reusing scrap material.

A recent study by Neale et al on the economics of recycling industrial scrap plastic in new products considered different recycling routes and how the incorporation of granulate affects unit cost of product manufactured to a particular design specification (2). An investment appraisal was made of machine side situations using Net Present Value (N.P.V.) analysis, for three commercially available granulators and a mathematical model established and used to predict cost relationships in products incorporating different amounts of scrap. They concluded that the opportunities for the profitable purchase of granulators for regrinding industrial scrap thermoplastics were considerable even at very low load factors.

Further to this work, Neale and Hilyard developed an investment appraisal model and computer program which was more applicable than the standard N.P.V. equation used in the above-mentioned study (3). This provided for the incorporation of more complete information and the ability to perform simple sensitivity analyses. The model was designed to cater for the

U.K. taxation system as amended in Chancellor Lawson's 1984 Budget. Inbuilt flexibility allowed it to cope with different tax rates, different rates of tax-allowable depreciation and different tax delay periods, these parameters being incorporated as input variables. This model was later refined and extended (4) and it is this most recent model that is employed in this case study.

OBJECTIVE

To assess the economic worth of investing in a compression moulding machine for the purpose of converting scrap APC-2 composite material into useful preconsolidated sheet.

PROCEDURE

Three compression moulding machines were identified which were suitable for producing preconsolidated sheet of dimensions 304.8mm x 304.8mm and minimum thickness 1.0mm from 12.7mm square pieces of scrap APC-2 'prepreg' under the recommended consolidation pressure of 5.5MPa and temperature of 390°C (1). These conditions required that the presses were capable of applying a minimum force of 52,103 Kg or 52.1 tonnes to the material.

Details of the first of these presses, a Daniels 75 tons (76.2 tonnes) Upstroke Moulding Press, marketed by John Brown Plastics Machinery Ltd. are contained in figures 1-3.

The remaining two presses are marketed by Bipel Ltd. as semi-automatic and fully automatic versions of the same 80 ton (81.3 tonnes) Compression Press (fig 4).

The extended computer model of Neale and Hilyard, originally written for the BBC B microcomputer, was taken and modified for

use on an Epson HX-20 Portable Computer. The resultant program is detailed in figure 5.

The model requires the quantification of a number of parameters. The values assigned to these parameters are listed below with comments where appropriate.

a) Year in which investment made = 1988

b) Name of machine = Daniels, Bipel Semi-Auto or Bipel Auto as appropriate.

c) Initial capital expenditure including allowance for installation cost - Daniels = £20,396, Bipel Semi-Auto £26,500 and Bipel Auto £35,000 (allowance for installation £1,000 in all cases).

d) Starting Corporation Tax rate = 35% (this is the current tax rate for a medium sized company).

e) Yearly decrement in Corporation Tax rate = 0%, number of years over which it occurs = 0 years (it is assumed that the Corporation Tax rate will remain constant at 35% for the duration of the project).

f) Rate of investment grant = 0% (no assistance assumed).

g) Required rate of return - three values used i.e. 10%, 20% and 30% (fixed load factor of 50%) in order to perform sensitivity analysis on the effect of rate of return on project viability.

h) Working capital investment = £0

i) Lifetime of project = 5 years (a conservative estimate of the lifetime of the compression moulding machine), delay in tax payment = 1 year (usual in the U.K.).

j) Maximum design output rating = 0.4 Kg / hr (it has been suggested that a realistic cycle time for the production of a

304.8mm x 304.8mm x 1.0mm sheet of APC-2 is 45 minutes. Using a value of 1.6g / cm^3 for the density of APC-2 (5) this equates to the production of 148.6g APC-2 per 45 minutes or approx. 200g per hour. However, it is believed that this cycle time can be substantially reduced, indeed halved, by the simple modification of the mould and the adoption of the pressing cycle recommended by I.C.I. (6). Thus a maximum design output rating of 400g / hr is considered reasonable.

k) Wage cost = £5 / hr (a reasonable rate for a semi-skilled operator).

l) Running cost, Daniels = £0.30 / hr, Bipel Semi-Auto = £1.09 / hr and Bipel Auto = £1.09 / hr (these values are based on the power requirements of the respective presses, assuming an electricity cost to industry of 3.85p / unit [1 unit = 1KW / hr]).

m) Material cost = £0 / Kg (it is assumed that scrap APC-2 'prepreg' is readily available and has no resale value).

n) Load factor - three values used i.e. 25%, 50% and 75% (fixed rate of return of 20%) to enable sensitivity analysis to be performed on the effect of load factor on project viability.

o) Scrap value of equipment = £0

p) Upper, lower value of unit price = £150 / Kg and £10 / Kg respectively (this range chosen since the price of virgin APC-2 is £150 / Kg).

q) Required increment in unit price = £10/ Kg.

r) Rate of first year depreciation allowance = 0% (as proposed in the 1984 Finance Act).

s) Writing down allowance = 25% (also as proposed in the 1984

Finance Act).

The computer program was run for each of the three compression presses using the above-mentioned parameters. Sensitivity analyses were performed by varying load factor (fixed rate of return) and rate of return (fixed load factor). In each case, the break-even price (i.e. the price at which the resultant preconsolidated sheet would have to be sold in order to cover the cost of the investment) was determined. The results are contained in TABLES 1-6.

DISCUSSION

It became clear from the results contained in TABLES 1-6 that the selling price of preconsolidated sheet manufactured from scrap APC-2 'prepreg' would not be low if the cost of investment in a new compression moulding press was to be offset. Nevertheless, it was noted that the projected break-even prices did represent significant reductions on the cost of virgin APC-2 material (£150 / Kg).

Not surprisingly, the lowest break-even prices were obtained for the press in which the lowest initial capital expenditure and, coincidentally, the lowest running costs were incurred i.e. the Daniels press. At a load factor of 50% and a required rate of return of 20%, the break-even selling price was £32.46 / Kg. The comparative break-even prices for the Bipel Semi-Auto and Auto presses were £40.18 / Kg and £48.18 / Kg respectively.

Analysing the data, it was observed that the break-even price was moderately sensitive to changes in required rate of return. For a fixed load factor of 50%, an increase in rate of return from 10% to 30% resulted in the following increase in

break-even price:- Daniels press 28.2%, Bipel Semi-Auto press 29.8% and Bipel Auto press 33.3%.

The break-even price was also shown to be substantially affected by changes in load factor. For a fixed required rate of return of 20%, a decrease in load factor from 75% to 25% resulted in the following break-even price increases:- Daniels press 98.3% Bipel Semi-Auto press 104.4% and Bipel Auto press 118.1%.

Clearly the price that can be commanded for preconsolidated sheet manufactured from scrap APC-2 'prepreg' is dependent upon the product's physical and mechanical properties and its availability. Sheets prepared by compression moulding scrap APC-2 'prepreg' squares possess random in-plane reinforcement. Typical properties as determined by I.C.I. (7) are contained in TABLE 7.

Because the recycled material possesses many of the selling features of virgin APC-2, it would be reasonable to expect the market price to be closely linked to that of the commercial composite material. The revolutionary and exclusive nature of APC-2, coupled with I.C.I.'s requirements to recoup research and development costs, is likely to ensure a high price for the material for some years to come. Opportunities exist, therefore, for recycled material to be marketed at a correspondingly favourable price.

CONCLUSION

Assuming a favourable market survey, and provided load factors can be maintained at or above 50%, opportunities exist for reasonable profits to accrue through the purchasing of a Daniels compression moulding press to manufacture preconsolidated sheet from scrap APC-2 'prepreg' - the sheet to be marketed at prices as low as £50 / Kg (one third that of virgin APC-2).

REFERENCES

1) G.C. McGRATH, private communication.

2) C.W. NEALE, N.C. HILYARD and P.BARBER, J. Conservation and Recycling, 6 (3), 91-105 (1983).

3) N.C. HILYARD and C.W. NEALE, J. Plastics and Rubber Processing and Applications, 5 (3), 285-288 (1985).

4) C.W. NEALE and N.C.HILYARD, Omega - Int. J. of Mgmt. Sci., 14 (6), 483-492 (1986).

5) I.C.I. FIBERITE, Data Sheet 3a (1986).

6) I.C.I. FIBERITE, Data Sheet 2 (1986).

7) I.C.I. FIBERITE, Data Sheet 7 (1986).

DANIELS

High speed upstroke moulding presses

Daniels high speed upstroke column presses incorporate proven features which enable the moulder to maximise his production using either loose or fixed tooling. The presses are supplied in either single acting gravity opening or double acting hydraulically opening versions. Hydraulic power units are available to operate either one press or several presses connected in series. The daylight specified can be modified to suit individual requirements and multi-daylight configurations can be supplied.

The Daniels process timer eliminates the variables associated with manual operation. With this equipment the operator simply loads the press and starts the cycle. Breathes, cure etc. then follow according to the predetermined settings of the timer. Every cycle is therefore identical and the operator, not being responsible for accurate press control, is free to perform other ancilliary operations.

Guards are normally fitted as standard which comply with the latest health and safety requirements.

Special presses other than the ones shown can be supplied to meet customers requests when the need arises.

Daniels Engineering Ltd.
Bath Road, Stroud,
Gloucestershire GL5 3TL, England.
Tel: 04536 2261 Telex: 43143

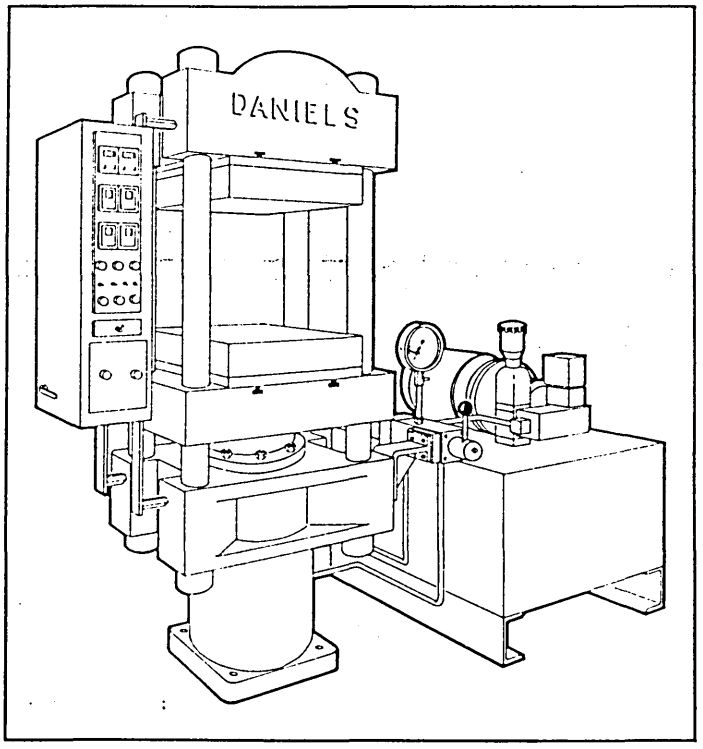

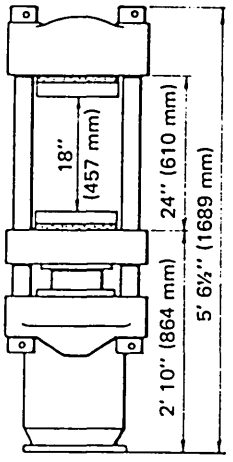

75 Ton

DANIELS
LEESONA CORPORATION
Division of John Brown

Figure 1 Daniels Compression Moulding Presses – General Information

The Daniels Column Type Single Acting Upstroke Press is constructed in accordance with the following specification.

BASIC PRESS

Of four column design; having a cast iron cylinder. The ram is of cast iron and is single acting. It is guided in a bushed gland ring which is assembled with shims for packing adjustment.

The tables also are iron castings, the moving table being guided by pads which bear on the four columns.

The cylinder casting is extended to form the press base, and is provided with four holes to accept 3/4" diameter fixing bolts.

ELECTRICALLY HEATED PLATENS

Two electrically heated platens are fitted to the press, suitable for operation at 390 degrees C having strip type resistance elements.

High density insulation material 1" thick is fitted to the press tables to reduce heat transfer from the platens.

TEMPERATURE CONTROLLERS

The operating temperature of the platens is regulated by indicating controllers (one per platen); housed in a panel attached to the left-hand side of the press and complete with contactors fuses and switchgear.

DIRECTIONAL CONTROL

Of the press is by Daniels three-position piston type valve, mounted at the right-hand side of the press and with lever for manual operation.

PRESSURE GAUGE

Indicates hydraulic pressure in pounds per square inch and bars. A conveniently situated chart permits ready conversion of these readings to indicate the force exerted in tons on the ram.

GUARDS

When a motorised pump is fitted, the latest health and safety regulations demand that guards are fitted. We can supply these, comprising fixed side and rear mesh screens, with a front manually operated mesh screen, mechanically interlocked with the main control valve.

MOTORISED PUMP

Of Vickers manufacture which is situated at floor level adjacent to the right-hand side of the press. The unit is complete with pressure relief and unloading valves, motor, starter and oil supply tank.

PROCESS CONTROLLER

A simple timer is fitted, arranged to control the duration of the cure period, at the end of which the press opens automatically.

The instrument has a range of 0-30 minutes, and is housed in the panel with the temperature controllers, etc.

When this process controller is fitted, the directional control valve is amended to incorporate an air cylinder assembly, with push buttons for cycle initiation or manual operation when required.

Figure 2. Daniels Compression Moulding Presses – Specification

PRESS DATA

Main Ram Diameter	8"
Main Ram Stroke	14"
Daylight between Tables	24"
Daylight between platens	18"
Platen size	14" square x 2" thick
Electric Loading	2.1 kw
Maximum hydraulic pressure	3,360.00 p.s.i.
Pump Motor H.P.	7.5 HP (5.6 kw)
Approximate press closing speed	1.2" per second

SERVICES REQUIRED

Electricity: 415 volts, 3 phase and neutral, 50 cycles, 4 wire.

Air: Small volume at approximately 80 p.s.i.(5.62 kg/cm2) for valve operation.

Hydraulic Oil: No Hydraulic Oil is supplied with the press, but a list of recommendations is given in the Machine Handbook.

Figure 3. Daniels 75 Ton Compression Moulding Press — Data

80 ton Compression Press

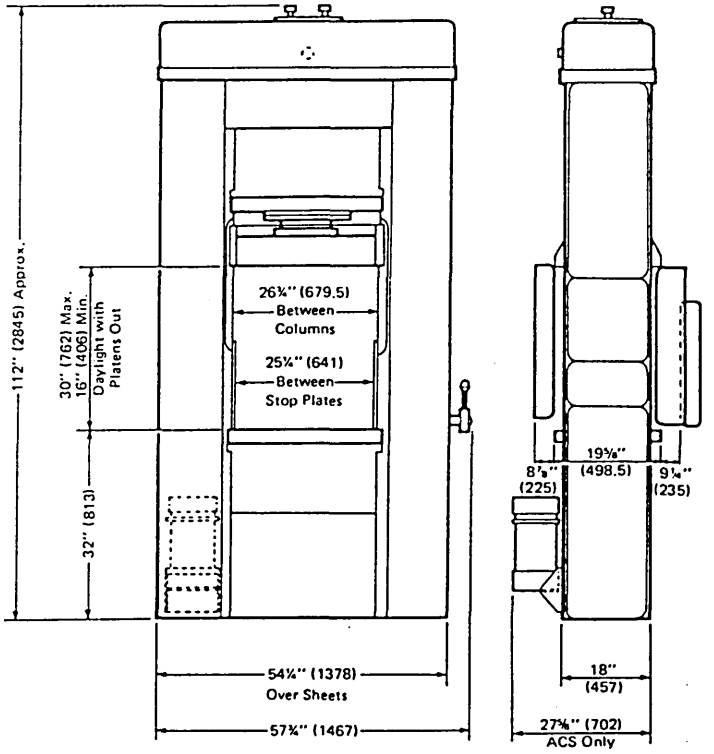

Dimension induction heated platens

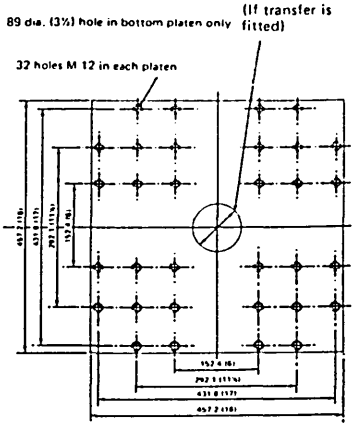

Dimensions in millimetres (equivalents in inches in bracket)

Table size left to right between sideplates	25¼ in	641 mm
Table size front to back	19⅝ in	498 mm
*Standard heated platen size (9.7 kVA per pair)	18 in x 18 in	457 mm x 457 mm
Daylight between tables	30 in	762 mm
Daylight between heated platens	21⅜ in	543 mm
Main ram stroke	14 in	355 mm
Hydraulic Circuit Pressure	1000 psi	68.97 Bars
Max. pressing force (Main ram pressure intensified to 3000 psi)	81 ton	82.4 t
Main ram pull back force at circuit pressure	3.2 ton	3.2 t
Transfer ram force	12.6 ton	12.8 t
Transfer ram stroke	3 in	76 mm
Maximum pummel diameter	2 in	50 mm
Approximate weight of maximum shot (based on 12g/in^3)	4 oz	113 g
Ejection force (top and bottom ejector)	2 ton	2.0 t
Ejector return force	1 ton	1.0 t
Ejector stroke (top and bottom)	3.5 in	89 mm
Total kVA self contained press.	28.3	28.3
Weight of press. nett. semi-auto self contained	3.62 ton	3963 Kg.

*20" platens can be fitted.

Metric units are a direct conversion of nominal imperial values.

BIPEL LIMITED
Aldridge Road Streetly
Sutton Coldfield West Midlands B74 2DZ
telephone 021-353 2480 telex 337741

BIPEL

Figure 4. Bipel 80 Ton Compression Moulding Press – Data

```
160 PRINT "ENTER YEAR IN WHICH INVESTMENT IS TO BE MADE"
170 INPUT B$
190 PRINT "ENTER MACHINE NAME"
200 INPUT A$
220 PRINT "ENTER INITIAL CAPITAL EXPENDITURE INCLUDING  ALLOWANCE
    FOR INSTALLATION COST (£)"
230 INPUT C
250 PRINT "ENTER STARTING CORPORATION TAX RATE (%)"
260 INPUT T
270 T=T/100
290 PRINT  "ENTER YEARLY DECREMENT IN  CORPORATION  TAX RATE (%),
    NUMBER OF YEARS OVER WHICH IT OCCURS (YEARS)"
300 INPUT DCT,NN
310 DCT=DCT/100
330 PRINT "ENTER RATE OF INVESTMENT GRANT (%)"
340 INPUT G
350 G=G/100
370 PRINT "ENTER REQUIRED RATE OF RETURN (%)"
380 INPUT K
390 K=K/100
410 PRINT "ENTER WORKING CAPITAL INVESTMENT (£)"
420 INPUT W
440 PRINT  "ENTER  LIFETIME  OF  PROJECT, DELAY IN PAYMENT OF TAX
    (YEARS)"
450 INPUT NM,D
470 PRINT "ENTER MAXIMUM DESIGN OUTPUT RATING (UNIT/HOUR)"
480 INPUT QM
500 PRINT "ENTER WAGE COST (£/HOUR)"
510 INPUT F
520 F=F/QM
540 PRINT "ENTER RUNNING COST (£/HOUR)"
550 INPUT E
560 E=E/QM
580 PRINT "ENTER MATERIAL COST (£/HOUR)"
590 INPUT M
610 PRINT "ENTER LOAD FACTOR (%)"
620 INPUT L
630 L=L/100
650 PRINT "ENTER SCRAP VALUE OF EQUIPMENT (£)"
660 INPUT S
680 PRINT "ENTER UPPER, LOWER VALUE OF UNIT PRICE (£/UNIT)"
690 INPUT PU,PL
710 PRINT "ENTER REQUIRED INCREMENT IN UNIT PRICE (£/UNIT)"
720 INPUT IP
740 PRINT "ENTER THE RATE OF FIRST YEAR DEPRECIATION ALLOWANCE
    (%)"
750 INPUT YU
760 YU=YU/100
780 PRINT "ENTER WRITING DOWN ALLOWANCE (%)"
790 INPUT WDA
800 WDA=WDA/100
810 'CALCULATION SECTION
820 '--------------------'
840 GOSUB 900
860 PRINT
```

Figure 5. Investment Appraisal Program (modified for Epson HX-20 Portable Computer).

```
865 Y=Y-0.25
870 IF Y<YL THEN 880 ELSE 820
880 END
890 '---------------------'
900 'SUB 1
910 Y=YU
920 Q=QM*L*35*48
930 AVC=F+M+E
940 AVC=AVC*1000
950 AVC=INT(AVC)
960 AVC=AVC/1000
970 V=AVC*Q
990 PRINT "---------------------------"
1000 PRINT TAB(0);"YEAR OF INVESTMENT =";TAB(20);B$
1020 PRINT TAB(0);"MACHINE=";TAB(11);A$
1040 PRINT  TAB(0);"WAGE  COST=";TAB(12) ; F ;TAB(16);"£/UNIT  OF
     OUTPUT"
1060 PRINT "P=OUTPUT PRICE"
1090 PRINT
1100 PRINT TAB(3);"P £/UNIT";TAB(15);"NPV £"
1110 P=PL
1120 TP=T-DCT*NN
1130 'FIRST REPEAT
1140 TT=T
1150 GOSUB 3000
1160 R=P*Q
1170 SU1=0
1180 N=1
1190 TT=T-DCT
1200 IF TT<TP THEN TT=TP
1210 'SECOND REPEAT
1220 GOSUB 3000
1230 KS=KS*10000
1240 KS=INT(KS)
1250 KS=KS/100
1260 KS=KS/100
1270 XX=1/((1+KS)^N)
1280 SU1=SU1+XX
1290 N=N+1
1300 TT=TT-DCT
1310 IF TT<TP THEN TT=TP
1320 IF N>NM THEN 1330 ELSE 1210
1330 P1=(R-V)*SU1
1340 SU2=0
1350 N=1+D
1360 TT=T-2*DCT
1370 IF TT<TP THEN TT=TP
1380 TQ=TQ-DCT
1390 IF TQ<TP THEN TQ=TP
1400 'THIRD REPEAT
1410 GOSUB 3000
1420 YY=TQ/((1+KS)^N)
1430 SU2=SU2+YY
1440 N=N+1
1450 TT=TT-DCT
```

Figure 5. (cont.)

```
1460 IF TT<TP THEN TT=TP
1470 TQ=TQ-DCT
1480 IF TQ<TP THEN TQ=TP
1490 IF N>NM+D THEN 1500 ELSE 1400
1500 P2=(R-V)*SU2
1510 SU3=0
1520 N=D
1530 TT=T-(N*DCT)
1540 IF TT<TP THEN TT=TP
1550 TI=T-DCT
1560 IF TI<TP THEN TI=TP
1570 'FOURTH REPEAT
1580 GOSUB 3000
1590 ZZ=((1-WDA)Δ(N-1))*TI/((1+KS)Δ(N))
1600 SU3=SU3+ZZ
1610 N=N+1
1620 TT=TT-DCT
1630 IF TT<TP THEN TT=TP
1640 TI=TI-DCT
1650 IF TT<TP THEN TI=TP
1660 IF N>NM+D THEN 1670 ELSE 1570
1670 P3=(C*(1-G)*(1-Y)*(WDA))*SU3
1680 TT=T-D*DCT
1690 IF TT<TP THEN TT=TP
1700 GOSUB 3000
1710 CC=-C+(Y*T*C)*(1-G)/((1+KS)ΔD)+(G*C)/((1+KS)ΔD)-W
1720 TT=T-NM*DCT
1730 IF TT<TP THEN TT=TP
1740 GOSUB 3000
1750 WS=(W+S)/((1+KS)ΔNM)
1760 SU4=0
1770 N=1
1780 TT=T
1790 'FIFTH REPEAT
1800 WD=WDA*((1-WDA)Δ(N-1))
1810 SU4=SU4+WD
1820 N=N+1
1830 IF N>NM THEN 1840 ELSE 1790
1840 WW=1-SU4
1850 WDV=(C*(1-Y)*(1-G))*WW
1860 TN=T-NM*DCT
1870 IF TN<TP THEN TN=TP
1880 TT=T-(NM+1)*DCT
1890 IF TT<TP THEN TT=TP
1900 GOSUB 3000
1910 WWV=TN*(S-WDV)/((1+KS)Δ(NM+1))
1920 NPP=CC+WS-WWV
1930 VVV=NPP+P1-P2+P3
1940 VVV=INT(VVV)
1950 PRINT TAB(5);P;TAB(15);VVV
1960 P=P+IP
1970 IF P>PU THEN 1980 ELSE 1130
1980 PRINT
1990 PRINT"-----------------------"
2020 PRINT
```

Figure 5. (cont.)

```
2030 RETURN
2040 '********************
3000 'SUB
3010 KO=K
3020 Z=1
3030 'SIXTH AND FINAL REPEAT
3040 KS=K*(1-TT/((1+KO)^D))
3050 KO=KS
3060 Z=Z+1
3070 IF Z>3 THEN 3080 ELSE 3030
3080 RETURN
```

Figure 5. (cont.)

OUTPUT PRICE (£ / Kg)	NET PRESENT VALUE (£)		
	R.O.R. 10%	R.O.R. 20%	R.O.R. 30%
10	-17333	-18007	-18487
20	-8005	-9988	-11544
30	1324	-1970	-4601
40	10652	6048	2342
50	19980	14066	9285
60	29309	22084	16228
70	38637	30102	23171
80	47965	38121	30114
90	57294	46139	37057
100	66622	54157	44000
110	75951	62175	50943
120	85279	70193	57886
130	94607	78212	64829
140	103936	86230	71772
150	113264	94248	78715
BREAK-EVEN PRICE	£28.58	£32.46	£36.63

TABLE 1. Daniels Press - Relationship between N.P.V. and Output Price for various Rates of Return (Load Factor 50%).

OUTPUT PRICE (£ / Kg)	NET PRESENT VALUE (£)	
	LOAD FACTOR 25%	LOAD FACTOR 75%
10	-16704	-19310
20	-12695	-7282
30	-8685	4745
40	-4676	16772
50	-667	28800
60	3342	40827
70	7351	52854
80	11360	64881
90	15369	76909
100	19378	88936
110	23387	100963
120	27396	112990
130	31405	125018
140	35415	137045
150	39424	149072
BREAK-EVEN PRICE	£51.66	£26.05

TABLE 2. Daniels Press - Relationship between N.P.V. and Output Price for various Load Factors (Rate of Return 20%).

OUTPUT PRICE (£ / Kg)	NET PRESENT VALUE (£)		
	R.O.R. 10%	R.O.R. 20%	R.O.R. 30%
10	-23455	-24198	-24714
20	-14126	-16180	-17771
30	-4798	-8162	-10828
40	4531	-144	-3885
50	13859	7874	3057
60	23187	15893	10000
70	32516	23911	16943
80	41844	31929	23886
90	51172	39947	30829
100	60501	47965	37772
110	69829	55984	44715
120	79158	64002	51658
130	88486	72020	58601
140	97814	80038	65544
150	107143	88056	72487
BREAK-EVEN PRICE	£35.14	£40.18	£45.60

TABLE 3. Bipel Semi-Auto Press - Relationship between N.P.V. and Output Price for various Rates of Return (Load Factor 50%).

OUTPUT PRICE (£ / Kg)	NET PRESENT VALUE (£)	
	LOAD FACTOR 25%	LOAD FACTOR 75%
10	-22104	-26293
20	-18095	-14265
30	-14086	-2238
40	-10077	9789
50	-6068	21816
60	-2058	33844
70	1951	45871
80	5960	57898
90	9969	69926
100	13978	81953
110	17987	93980
120	21996	106007
130	26005	118035
140	30014	130062
150	34023	142089
BREAK-EVEN PRICE	£65.13	£31.86

TABLE 4. Bipel Semi-Auto Press - Relationship between N.P.V. and Output Price for various Load Factors (Rate of Return 20%).

OUTPUT PRICE (£ / Kg)	NET PRESENT VALUE (£)		
	R.O.R. 10%	R.O.R. 20%	R.O.R. 30%
10	-29414	-30616	-31478
20	-20086	-22598	-24535
30	-10758	-14580	-17592
40	-1429	-6562	-10649
50	7899	1456	-3706
60	17227	9475	3237
70	26556	17493	10180
80	35884	25511	17123
90	45213	33529	24066
100	54541	41547	31009
110	63869	49566	37952
120	73198	57584	44895
130	82526	65602	51837
140	91854	73620	58780
150	101183	81638	65723
BREAK-EVEN PRICE	£41.53	£48.18	£55.34

TABLE 5. Bipel Auto Press - Relationship between N.P.V. and Output Price for various Rates of Return (Load Factor 50%).

OUTPUT PRICE (£ / Kg)	NET PRESENT VALUE (£)	
	LOAD FACTOR 25%	LOAD FACTOR 75%
10	-28522	-32711
20	-24513	-20683
30	-20504	-8656
40	-16495	3371
50	-12486	15398
60	-8476	27426
70	-4467	39453
80	-458	51480
90	3551	63508
100	7560	75535
110	11569	87562
120	15578	99589
130	19587	111617
140	23596	123644
150	27605	135671
BREAK-EVEN PRICE	£81.14	£37.20

TABLE 6. Bipel Auto Press - Relationship between N.P.V. and Output Price for various Load Factors (Rate of Return 20%).

MECHANICAL PROPERTIES

Property	Units	3 mm APC-2 Moulded Scrap	12.7 mm APC-2 Moulded Scrap	'Victrex' PEEK 450CA30 Standard Resin
Carbon fibre content w/w	%	68	68	30
Flexural modulus	GN/m^2 lb/in^2	26 3.8×10^6	38 5.5×10^6	13.1 -
Flexural strength	MN/m^2 lb/in^2	220 32×10^3	343 50×10^3	- -
Tensile strength	MN/m^2 lb/in^2	157 23×10^3	366 53×10^3	210 -
Impact-Initiation Energy*	J in lb f	3.2 28	9 80	2 -
Impact-Total energy*	J in lb f	7.4 65.5	29 257	9 -

* All impact results equalised for 3.2 mm thickness. Standard deviation in parenthesis.

TABLE 7. Typical Properties for Compression Moulded scrap APC-2 'prepreg'

APPENDIX 2

Proc. IX Intl. Congress on Rheology, Mexico, 1984.

RHEOLOGY OF POLYETHERSULPHONE (PES)/POLYDIMETHYL-SILOXANE (PDMS) BLENDS

A.A. Collyer*, D.W. Clegg**, G.H. France*, M. Morris**,
K. Blake*, D.J. Groves*** and M.K. Cox***

*Department of Applied Physics
**Department of Metallurgy
Sheffield City Polytechnic, Pond St., Sheffield, England, U.K.
***ICI Petrochemicals and Plastics Division,
Wilton Centre, Wilton, Middlesbrough, England, U.K.

ABSTRACT

Results obtained on PES/PDMS blends using a Davenport Extrusion Rheometer show that an addition of only 2% PDMS reduces the shear viscosity, the degree of non-Newtonian behaviour and the shear modulus of the blend over the PES melt, but causes an increase in the tensile viscosity.

Scanning electron micrographs show the complexity of the microstructure of the blends due to the degradation of PDMS, which gives rise to voiding and a lamellar structure. The observed rheological behaviour is attributed to the combination of this complex microstructure and the probable breakdown of the continuum rheological equations used to calculate the results.

KEYWORDS

Polyethersulphone; polydimethyl siloxane; extrusion rheometry; polymer blends; thermogravimetric analysis.

INTRODUCTION

Polyethersulphone (PES) is a high-temperature engineering thermoplastic that has an upper service temperature of 180°C. Although tough, it is, like most thermoplastics, notch sensitive. To extend its applications in the aerospace industry a better notched behaviour is necessary, but there must be no loss of thermal stability or of low toxic gas and smoke emission properties, which for PES are well within the specification given by Boeing.

A successful method of achieving improved notched behaviour is by adding a dispersed rubber phase to the thermoplastic matrix. However, the choice of rubber for use in PES is made difficult because of the high processing temperatures (320 - 390°C) of this thermoplastics. Elastomers that may withstand these temperatures would probably be silicone or fluorocarbon based, but the latter may ruin the good low toxic gas and smoke emission properties of PES.

Noshay and co-workers (1971, 1973, 1974) faced similar problems in the rubber toughening of polysulphone: these workers elected to use polydimethyl siloxane (PDMS) as the dispersed elastomeric phase. For this reason the present authors made the same choice.

As the PES and PDMS phases are grossly incompatible, with solubility parameters of 22.6 and 14.0 $MJ^{\frac{1}{2}} m^{-3/2}$ respectively, a simple blend would have poor mechanical properties owing to the poor adhesion between the two phases. In order to combine toughening with good adhesion between the phases, the difference in their solubility parameters must lie between 0.4 and 0.8 (Stehling and co-workers, 1981). Noshay and co-workers achieved this by making a block copolymer of polysulphone and PDMS, which was used as the dispersed rubber phase. This seemed successful on a laboratory scale, but nevertheless the present authors' initial intention was to use PDMS as the dispersed phase in the PES, and to use a PES/PDMS block copolymer as an interfacial agent to improve the adhesion between the two phases. This would reduce the cost of the new material.

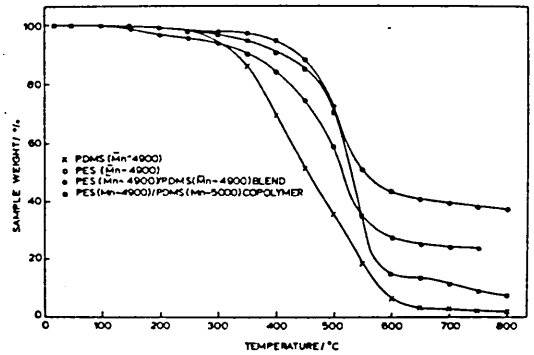

Fig. 1. Thermogravimetric analyses of PES, PDMS, a blend and a block copolymer of PES/PDMS

A thermogravimetric analysis of the materials was carried out to ascertain whether this initial proposal was realistic. From fig. 1, it can be seen that in the processing range of PES, the PDMS shows a noticeable weight loss, more so than either the blend or the block copolymer. For this reason the block copolymer would probably be used as the dispersed rubber phase.

For an introduction to the rheology of blends of thermoplastics with elastomers, the work of Munstedt (1981) was studied. The results revealed the following:-

(1) The temperature dependence of the viscosity functions is independent of the rubber or its concentration.

(2) There is a yield stress at the high rubber loadings or for smaller particle size.

(3) The blends have slightly higher shear viscosity than the thermoplastic in the higher shear stress range.

(4) The tensile viscosity of the blends is more sensitive to microstructure than the shear viscosity, and has higher values than for the matrix material.

(5) The extrudate swell is reduced by the rubber additive but the entrance pressure is independent of rubber concentration.

The above work was carried out with polybutadiene (PB) and polyacrylic ester in styrene acrylonitrile and PB in PVC. The main differences in the present work is that the above materials have overlapping process temperature ranges and the above experiments were carried out at lower shear stresses.

The present report covers the initial rheological measurements on PES/PDMS blends, calculating the results assuming a continuous fluid; and some initial examination of the microstructure of the extrudates is made.

EXPERIMENTAL

The materials used in the current experiments are defined in Table 1. The blends were initially mixed by hand and then passed twice through a single-screw extruder at 360°C. The final granules were pre-dried at 150°C for five hours before being extruded through a Davenport Extrusion Rheometer. The PDMS was not crosslinked.

TABLE 1 Materials Used in the Present Experiments

Material	Grade	Supplier
PES	300 P	ICI, Wilton, U.K.
PDMS	Polymer 26	Dow Corning, Swansea, UK.

The rheological parameters were obtained from pressure measurements at the entrances to a long die and an orifice die. The latter was used to determine the tensile viscosities of the melts using the theory of Cogswell (1978, 1981), and die swell measurements were related to recoverable shear strain using Tanner's equation (1970). All the shear rates were corrected using the Rabinowitsch correction.

RESULTS AND DISCUSSION

Figure 2 shows that the shear viscosity of the melts is reduced by the PDMS additive, that the blend becomes more Newtonian and that the critical shear stresses and shear rates at the onset of melt fracture are reduced. (See arrows in fig. 2.)

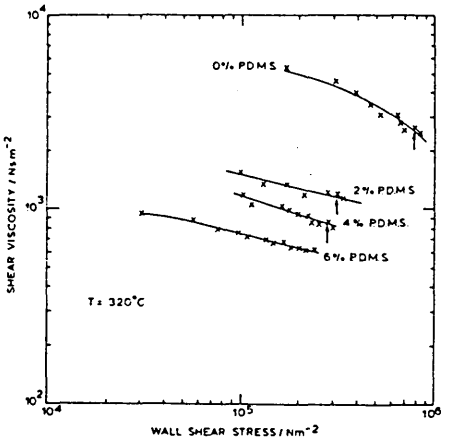

Fig. 2 Variation of shear viscosity with wall shear stress and PDMS concentration

The injection spiral moulding results shown in fig. 3 confirm the extrusion results by giving longer spiral lengths for blends with the higher PDMS concentration. These results are in direct contrast to the findings of Munstedt (1981) and this is partly attributed to the fact that the PDMS is very fluid at these temperatures. The morphologies of the blends, described below, indicate another possible explanation.

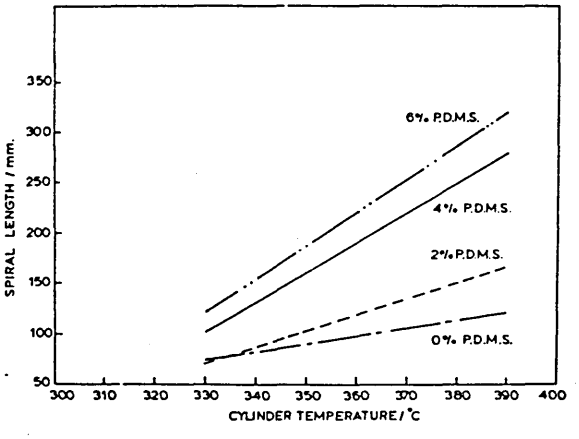

Fig. 3 Spiral lengths as a function of barrel temperature and PDMS concentration in injection spiral moulding

The two sets of results above indicate that the very fluid PDMS phase is profoundly affecting the flow by migrating to regions of high shear rate. Certainly, the extrudates and spiral mouldings obtained show gross delamination in the blends for PDMS concentrations greater than 1%.

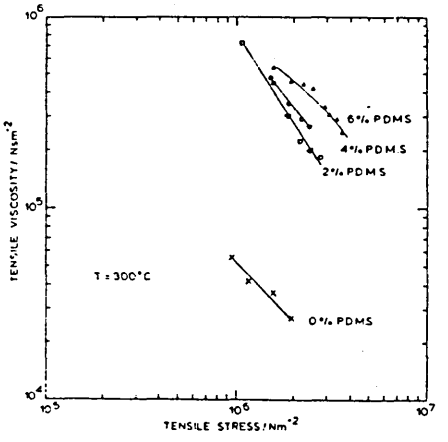

Fig. 4 Variation of tensile viscosity as a function of tensile stress and PDMS concentration

Figure 4 shows an increase in tensile viscosity of the blends over the PES melt, the greatest change being between 0 and 2% PDMS. This is in agreement with Munstedt (1981), who made measurements using an extensional rheometer. The authors, however, are uncertain of the effect on the measured values of the entrance pressure caused by the following effects at the die inlet:-

(1) the change in size and shape of the dispersed particles;

(2) the orientation of the dispersed particles;

(3) the possible rotation of the particles;

(4) the change in the distribution of the particles in a radial direction.

The authors believe that a proportion of the entrance pressure is taken up in causing these phenomena and that an overestimate of the tensile viscosity occurs. Some of the above effects are considered in much of the work on the mathematical modelling of two-phase flows, and it is felt that the work of Barthes-Biesel and co-workers (1980, 1981) may be applicable to the present results.

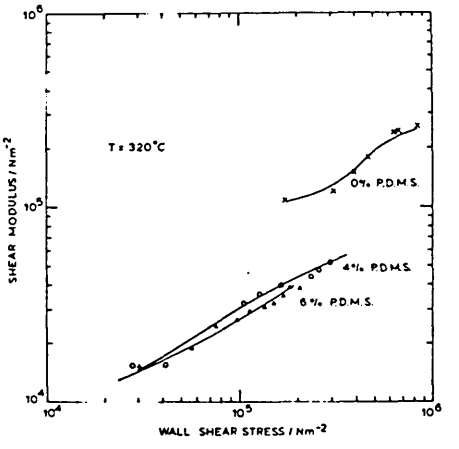

Fig. 5 The variation of shear modulus with wall shear stress and PDMS concentration

Shear modulus results obtained from extrude swell measurements are shown in fig. 5. The PDMS additive reduces the swelling ratio, in agreement with Munstedt (1981). These values of swelling ratio are used to calculate the shear moduli, which are thus reduced. This result seems consistent with poor adhesion between the phases. The authors however are quite aware that the change in morphology of the dispersed phase at the die exit may cause spurious results, as already indicated for the measurement of tensile viscosity. Clearly, some mathematical modelling of the kind already mentioned is necessary.

Figure 6 shows the microstructure of the extrudate from a 4% PDMS/PES blend and an EDAX silicon map of the same area. The microstructure is much more complex than at first believed. In many of the microstructures examined, the deformation and agglomeration of the PDMS particles give rise to a lamellar structure, and the decomposition of the PDMS gives rise to voiding and delamination. Some of the sites are filled with PDMS, but even here the adhesion between the two phases may be considerably reduced by volatiles released from the PDMS on partially decomposing. This voiding may enhance the toughening but causes the delamination.

From the above, it is clear that future work will have to be directed to a study of the blend morphology and how it is influenced by flow changes at the inlet and exit regions of the die. This must continue before any mathematical modelling of the system is attempted.

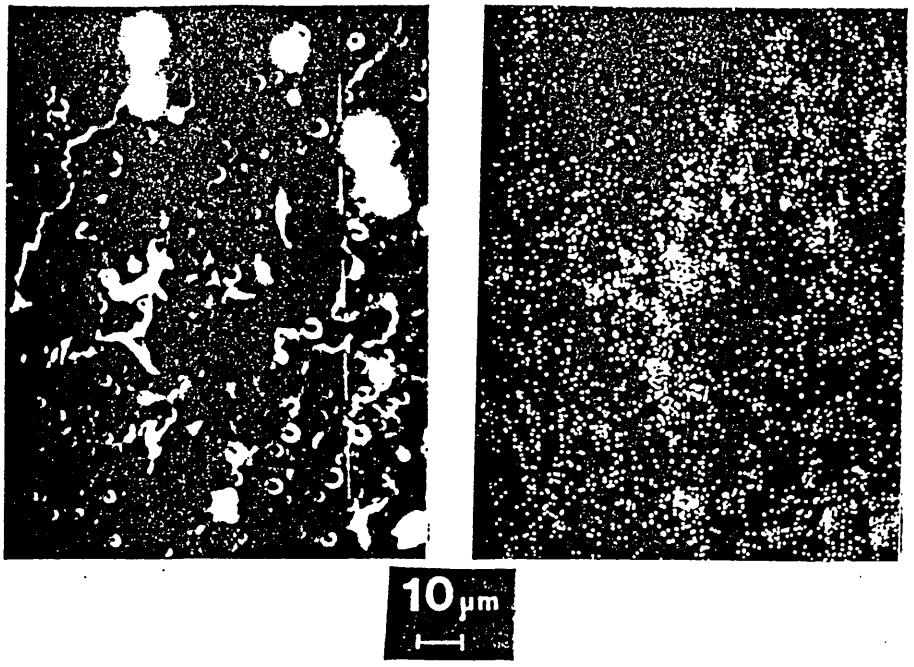

(a) (b)

Fig. 6 A scanning electron micrograph of a 4% PDMS/PES blend (a) and the equivalent EDAX map of the areas of silicon (b). The fracture surface is across the extrudate

A possible method of freezing the microstructure in the state found at the inlet region and in the die might employ a computer-controlled haul-off system. The inlet microstructure may be frozen in by pulling away extrudates from short or zero length dies at such a rate that the swelling ratio is unity. A linescan camera could be used to monitor the diameter of the extrudate, which is pulled away from the die at an increasing rate. When the swelling ratio is unity, the linescan camera triggers the haul-off to maintain a constant rate. Experiments would be carried out at different shear rates and the frozen in microstructures studied. The change in the stress field at the exit could present some challenging analysis.

CONCLUSIONS

Table 2 summarises the effect of a small addition of PDMS to the gross rheological behaviour of PES/PDMS blends.

TABLE 2 The Effect on the Gross Rheological Behaviour of PES/PDMS Blends by the Addition of PDMS

Shear Viscosity	Shear Thinning Index	Critical Shear Stress	Critical Shear Rate	Tensile Viscosity	Shear Modulus
↓	↑	↓	↑	↑	↓

The results, however, have been calculated assuming the fluid is a continuum. A study of the microstructure is of paramount importance prior to attempting to model the flow of the blends. It is hoped that the block copolymer when used instead of the PDMS will give rise to a more stable material and an easier system to model.

ACKNOWLEDGEMENTS

The authors would like to thank Owen Williams for the injection spiral moulding results and ICI and Dow Corning for the provision of the materials.

REFERENCES

Barthes-Biesel, D. (1980), J Fluid Mech., 100, 4, 831-853.

Bartles-Biesel, D. and Chkim, V. (1981). Int. J Multiphase Flow, 7, 5, 493-505.

Cogswell, F. N. (1978). J Non-Newtonian Fluid Mech., 4, 23-38.

Cogswell, F. N. (1981). Polymer Melt Rheology. George Goodwin Ltd, London.

Han, C. D. (1981). Polym. Engng. Rev., 1, 364.

Munstedt, H. (1981). Polym. Eng. and Sci., 21, 259-270.

Noshay, A., Matzner, M. and Merriam, C. N. (1971). Polym. Preprints, 12, 1.

Noshay, A., Matzner, M., Barth, B. P. and Walton, R. K. (1974). Amer. Chem. Soc. Div. Org. Coatings Plast. Chem. Preprint, Sept., 217.

Robeson, L. M., Noshay, A., Matzner, M. and Merriam, C. N., (1973), Die Agnew Mak. Chem., 29/30, 47-62.

Stehling, F. C. Huff, T., Speed, C. S. and Wissler, G. (1981), J. App. Polym. Sci., 26, 2693.

Tanner, R. I. (1970). J Polym. Sci., A-2, 8, 2067.

APPENDIX 3

THE RHEOLOGICAL BEHAVIOUR OR ENGINEERING THERMOPLASTICS AND SILICONE RUBBER BLENDS

KEYWORDS: polymer blends, polydimethylsiloxane, polyethersulphone, polybutyleneterephthalate, rheology.

ABSTRACT: Rheological studies were made using capillary and oscillatory rheometry on blends between (a) PES and PDMS, (b) PBT and PDMS and (c) PES and an $-(AB)_n$ block copolymer of PES and PDMS.. The capillary rheometry results indicated a limited compatibility between the physical blends and this was corroborated for PBT blends only by oscillatory experiments. The blends involving the block copolymer showed no limited compatibility and interfacial adhesion was poor. EDX and SIMS analysis indicated particle sizes of the order of 1 μ and a tendency for particle agglomeration.

REFERENCE: FRANCE, G.H., COLLYER, A.A., BLACKMORE, D.L., BLAKE, K., CLEGG, D.W., MORRIS, M., GROVES, D.J., BOOTSMA, J.P.C., KAMPSCHREUR, J.H., The rheologocial behaviour of engineering thermoplastics and silicone rubber blends.
Proc. Xth Internat. Congr. Rheol., 1988, Sydney, Aug. 14-19.

INTRODUCTION

The development of rubber toughened grades of most high temperature engineering thermoplastics such as polysulphone and polyethersulphone has been retarded because of problems associated with interfacial adhesion between the two components. A method of overcoming this problem is to use a block copolymer of the toughening rubber and the matrix polymer as a dispersed elastomeric phase. This has led to an interest in the processing behaviour of polymer blends involving a thermoplastic and an elastomer polydimethylsiloxane (PDMS) has been tried as a rubber toughening agent for polysulphone and polyethersulphone (PES), and the work described in this paper involves blends of PDMS with PES, with polybutyleneterephthalate (PBT) and with an $-\{AB\}_n$ block copolymer of PES/PDMS with an S_i-O-C linkage.

Several observers [1-8], studying the rheological behaviour of blends of incompatible polymers, have noted peaks and troughs in the viscosity-concentration curves for low concentrations of either one of the components. The peaks are attributed to a limited compatibility between the two components, which occurs below a limiting concentration, above which a two-phase blend exists.

In the work reported above the Hildebrand solubility parameters of the polymers studied are not as vastly different, which is not true of those used in the present work; PES (22.6), PBT (21.5) and PDMS (14.9), where the units are $(MJm^{-3})^{\frac{1}{2}}$. There may, therefore, be little limited compatibility between the silicone elastomer and PES or PBT.

EXPERIMENTAL

The PDMS was supplied by Dow Corning, the PES (Victrex 4800 P) is a standard ICI moulding grade and the PBT (Arnite T06 200) is a standard Akzo moulding grade. The $-\{AB\}_n$ PES/PDMS block copolymer with an S_i-O-C linkage was synthesised by M. Morris.

The capillary rheometry was carried out on a computer-controlled Davenport Extrusion Rheometer at Sheffield City Polytechnic. Oscillatory rheometry was carried out on two Rheometrics Dynamic Spectrometers, one at ICI Wilton (PES blends) by D.J. Groves and the other at Akzo Research Laboratories, Arnhem (PBT blends), by J.P.C. Bootsma and J.H. Kampschreur.

RESULTS AND DISCUSSION

(a) PES/PDMS Blends

The variation of blend viscosity with PDMS concentration is shown in Figure 1. This figure shows a viscosity minimum at 2% PDMS and a maximum at 4%, for a wall shear stress of 10^5 Nm^{-2}. The results from the oscillatory shear experiments (ICI) for a shear stress of 10^4 Nm^{-2} do not show the above variation, but, as seen in Figure 2, the viscosity decreases as the PDMS concentration increases and shear stress increases. The discrepancy between the two sets of results is attributed to the small size of the effect at 360°C.

Figure 3 shows the effect of blending a small amount of block copolymer to the PES. Table 1 gives the codes for the blends in this figure. The graphs show a steady decrease in viscosity with block copolymer concentration and shear stress, and oscillatory shear results back up this finding. A decrease in viscosity would be expected on adding more of the low molecular weight block copolymer. This suggests that there is no chemical linkage provided by the block copolymer at the PES/PDMS interface. Injection moulded products show gross delamination [6].

(b) PBT/PDMS Blends

Figure 4 shows the capillary rheometry results for PBT/PDMS blends. The trough at 4% PDMS and the maximum at 6% PDMS may not be more significant than the errors, but as seen in Figure 5, the Rheometrics results from Akzo show a similar trough at 2% PDMS. Interpretation of the results is difficult because of oxidative and hydrolytical degradation of the PBT during the course of the experiment [9,10].

(c) Morphological Results

The peaks and troughs in the viscosity-concentration curves for various polymer blends have been attributed to changes in morphology with concentration of the species. Some preliminary examinations

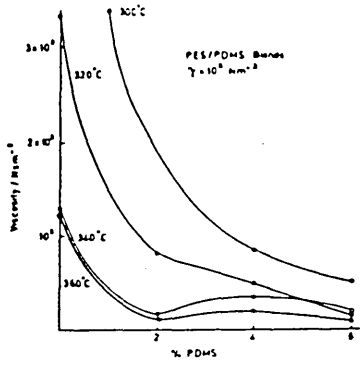

Figure 1 The variation of the viscosity of PES/PDMS blends with PDMS concentration and temperature in the capillary rheometer ($\tau = 10^5$ Nm^{-2}).

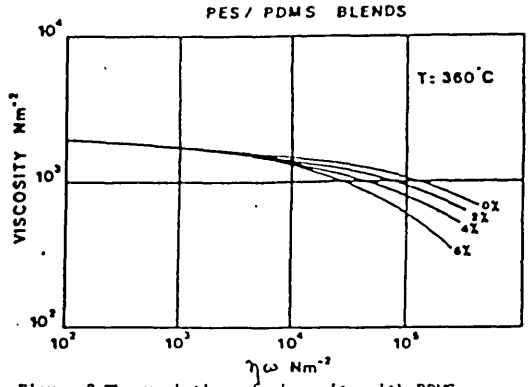

Figure 2 The variation of viscosity with PDMS concentration for a value of $\eta\omega$ of 10^4 Nm^{-2} and temperature (Rheometrics results from ICI).

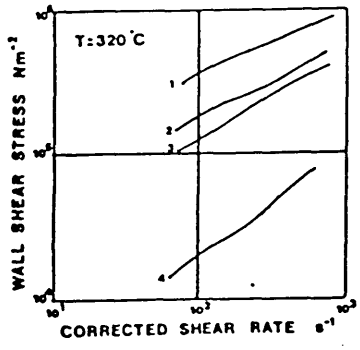

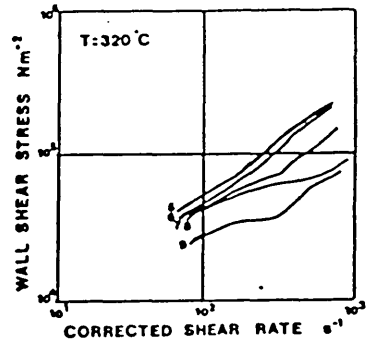

Figure 3 Capillary rheometry results at 320°C for PES/block copolymer blends.

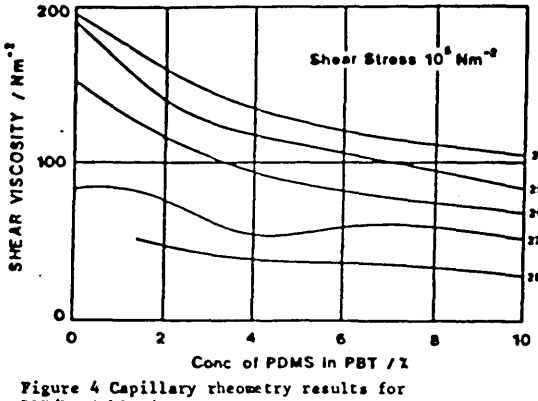

Figure 4 Capillary rheometry results for PBT/PDMS blends.

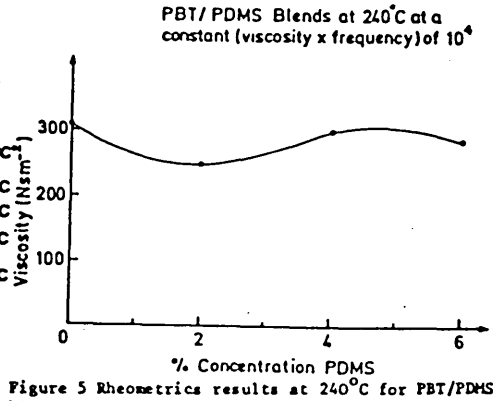

Figure 5 Rheometrics results at 240°C for PBT/PDMS blends.

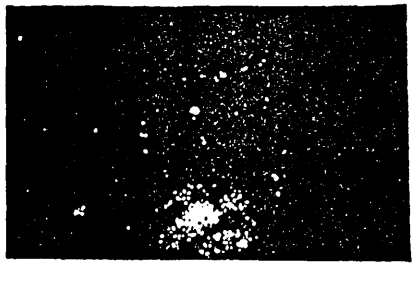

Figure 6 An EDX picture from the fracture surface of a PBT/PDMS extrudate (6% PDMS) showing silicon rich areas.

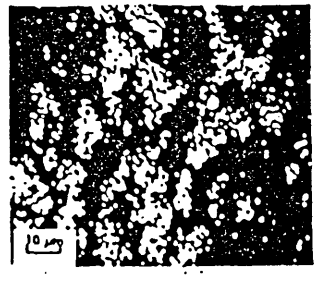

Figure 7 Secondary ion image of the fracture surface of a PES/PDMS extrudate using positive ions and 10 keV C_6^+ from a liquid metal ion source (0.5 μ dia. beam [11]).

of the blends of PES/PDMS (6% PDMS) and PBT/PDMS (6% PDMS) were made using SIMS and EDX. Figure 6 shows an EDX picture from the fracture surface of a PBT/PDMS extrudate. Two silicon rich areas are clearly visible of diameters 7 and 40 μ respectively.

Figure 7 shows a silicon map from the fracture surface of a PES/PDMS extrudate using SIMS. The better resolution shows 1 μ particles of PDMS, which tend to agglomerate [11]. The information from the SIMS result suggests that the 7 μ and 40 μ silicon rich areas in the EDX picture may be due to the agglomeration of small particles.

CONCLUSIONS

The fluctuations in the viscosity-concentration curves for both PES/PDMS and PBT/PDMS blends are small. This is attributed to the large differences in solubility parameters between the PDMS and the thermoplastics. Some observers, [4,12,13] have noted wall slip in melt blends that gave minima in viscosity-concentration graphs. Slip manifests itself by lowering the shear thinning index. On adding PDMS the shear thinning index increases over that value for PES. It is felt that there is no slip of the lower shear rates, but may occur at higher shear rates at higher temperatures. Slip may be investigated by the method of [14].

Further studies are to be made of PES/silicone elastomer blends using a slit die, which is theoretically more acceptable. This will be carried concurrently with shear heating measurements using an IR pyrometer. Moreover it is hoped to perfect the SIMS technique for investigating the size, shape and distribution of the dispersed phase.

The results for the PES/block copolymer blends show that interfacial adhesion is as poor as in the physical blends. This may be due to (1) the breaking of the S_i-O-C linkage at 320°C or (2) PDMS migration to the extremities of the block copolymer. There is evidence for both of these phenomena.

ACKNOWLEDGEMENT

The authors would like to thank Dow Corning for the provision of the silicone elastomer.

REFERENCES

[1] Lipatov, Y.S., Labedev, E.V.; Makromol. Chem., 12, 51 (1979).

[2] Lipatov, Y.S., Nesterov, A.Y., Ignatova, T.D., Shumskij, V.F., Gorbatenko, A.N.; Polym. Sci. USSR, 24, 607 (1982).

[3] Clegg, D.W., Collyer, A.A., Morton, K.; Polym. Commun., 24, 10-13 (1983).

[4] Utracki, L.A., Catani, A.M., Bata, G.L.; J. App. Polym. Sci., 27, 1913-1931 (1982).

[5] Wisniewski,C., Marin, G., Monge, Ph.; Eur. Polym. J., 21, 5, 479-484 (1985).

[6] Collyer, A.A., Clegg, D.W., France, G.H., Morris, M., Blake, K., Groves, D.J., Cox, M.K.; IX th Int. Congress Rheol., Acapulco, Oct. 8-13, 1984, 3, 543-550, Elsevier Applied Science (1985).

[7] Utracki, L.A., Kamal, N.R.; Polym. Eng. and Sci., 22, 2, 96-111 (1982).

[8] Utracki, L.A.; Polym. Eng. and Sci., 23, 11, 602-608 (1983).

[9] Passalacqua, V., Pilati, F., Zamboni, V., Fortunato, B., Maneresi, P.; Polymer, 17, 1044-1048 (1976).

[10] Lunn, R.M.; J. Polym. Sci: Polym. Chem.; 17, 203-213 (1979).

[11] Wirth, A.; in press.

[12] Kann, R., Shaw, M.T.; Paper D8 at 52nd Ann. Meeting of Soc. Rheol., Williamsburgh, Virginia, Feb. 23-28 (1981).

[13] Shih, C.K.; Polym. Eng. and Sci.; 16, 11 (1976).

[14] Jiang, T.Q., Young, A.C., Metzner, A.B.; Rheol. Acta, 25, 397-404 (1986).

Table 1 Codes for the blends in Figure 3

Sample No	Additive Block M_N PES	PDMS	Additive Conc. /%	PDMS Conc. /%
1	Pure Victrex PES		—	--
2	4900	5100	0.87	0.5
3	4900	5100	1.73	1.0
4	4900	5100	4.33	2.5
5	Linear	PDMS	2.5	2.5
6	9600	53000	3.0	2.5
7	9600	5100	6.44	2.5
8	1300	800	5.75	2.5
9	1300	5100	3.11	2.5